Addendum

p. 26: Comment: The average thickness of the S1 palaeosol in the region is between 3 and 4m (Liu et al, 1986)*. It is likely that there is lateral variation in the thickness of this palaeosol, which may lead to heterogeneity in the level of vertical connectivity between the aquifer units, although this is difficult to determine without detailed stratigraphic information. The vertical distributions of nitrate concentrations (discussed later in the chapter) give a broad indication of the degree of connectivity between the shallow and deep units. These show that substantial vertical mixing occurs near the Linyi fault, however, in the rest of the basin there is a clear difference between high nitrate concentrations in shallow samples (> 10 mg/L) and low concentrations in deep samples (< 1 mg/l), suggesting more limited vertical connectivity.

p. 26: Add to line 4: 'which has a thickness of 3-4 m', after 'palaeosol'.

p. 27: Comment: Rainfall data (monthly totals from 1980 to 2004) was supplied in the supplementary data CD under (E:\Appendix B\Supplementary data\Climate data 1980 to 2004.xls). Plots of yearly rainfall and pan evaporation are included.

p. 28: Comment: Total estimated drawdown since groundwater usage commenced (c.1965) varies across the basin. The estimated total drawdown in the centre of the cone of depression is ~125 m; as the total drawdown from 1961 to 2000 was 90 m (Cao, 2005), and the rate of drawdown in 2000 was ~3.5 m/year [90 m + (3.5 m/yr x 10 years) = 125m]. The distribution of groundwater heads shows that shape of the cone of depression is an ellipsoid, with greatest drawdown near Yuncheng City, and lesser drawdown with increasing distance from the city.

p. 28: Add to line 18: 'The shape of this cone is an ellipsoid, with highest drawdown near Yuncheng City, and lesser drawdown with increasing distance from the city' after '(Cao, 2005).'

p. 29: Comment: The salt lakes sit within local topographic depressions (normal fault blocks) on the southern margin of the basin. While some induced migration of saline water from the lake area has occurred recently due to intensive pumping near Yuncheng City (Gao et al, 2007), the lakes are groundwater discharge features, and are part of shallow flow systems that are not expected to contribute substantially to groundwater recharge across the basin. Given that the lakes are rich in evaporite minerals including halite, substantially elevated molar Cl/Br ratios (e.g. > 3000) would be expected to be observed if dissolution of minerals from the lakes and subsequent recharge of the aquifer was a major process. In general Cl/Br ratios (median of 1070) are slightly elevated in comparison to rainfall/seawater (~500), indicating that evaporite minerals (e.g. from lake deposits) do contribute some salinity (see chapter 3), although there is no correlation between Cl/Br and overall TDS concentrations, as would be expected if this was a major salinisation mechanism.

p. 45: Comment: A value of approximately 70 pmc was considered to indicate modern recharge on the basis that the age correction models yielded modern ages in all groundwater with > 70 pmc (while all samples with < 70 pmc had model residence times of at least 2000 years). Later, it is stated that a number of the residence times are considered to be 'mixing ages' on the basis of elevated nitrate concentrations.

p. 46: Comment: Soil water tritium contents were reported for a 15.5m-long soil profile collected in Pingding County (Shanxi Province), in loess that is similar to the Yuncheng area, ~ 300 km to the northeast (Lin and Wei, 2006). In 1998, a tritium peak (235 TU, corresponding to the peak atmospheric fallout in 1963) was identified at 10.5m depth, corresponding to an infiltration rate of ~0.3m/year and a recharge rate of 68mm/year over the last 35 years. Comparison was made with tritium profiles measured nearby in 1988 and 1990, showing that the peak had progressed downwards via piston flow. Large-scale land clearance in this region of China began approximately 2.5 to 3.5 ka BP; this is likely to have significantly increased

*All references in this addendum are present in the reference list of relevant thesis chapters

recharge rates in the modern era compared to the preceding period (as was the case with pre- and post- European settlement recharge rates in Australia). This may be responsible for the disparity between modern and historic recharge rates.

p. 51: Comment: The only location where substantial evaporative enrichment is indicated by the groundwater stable isotopes is in shallow groundwater adjacent to the Yellow River. In this area, irrigation water is sourced exclusively from the river. This water may either undergo evaporation in the river channel, or en-route to the farms (via canals). Irrigation may also be less efficient in this region, as farmers are not concerned about the costs of well construction and electricity used for groundwater pumping. Hence, pooling of water and inefficient irrigation may be more widespread, leading to a greater amount of direct evaporation.

p. 52: Comment: Regarding well screen intervals, we were unable to obtain precise data for the sampled wells. However, according to our information from the Yuncheng Regional Water Bureau, screens of shallow and intermediate production wells (e.g. < 120m depth) are generally 10 to 20 m long, while for deep production wells (160 to 350 m depth), the screens are generally ~40 m long. While this does mean that water from a relatively wide section of the aquifer is sampled (and hence there is added uncertainty in the residence time estimation), the wells do target particular formations to some degree, in order to extract water of particular qualities (particularly the domestic supply wells). Due to the large vertical stratification in quality (e.g. salinity and nitrate concentrations), the screens of deeper wells are restricted in length (e.g. to ~40m), so that shallow and intermediate water (of poor quality) is not intercepted.

p. 52: Add to line 22: 'Screens of shallow and intermediate production wells (e.g. < 120m depth) are generally 10 to 20 m long, while for deep production wells (160 to 350 m depth), the screens are generally ~40 m long' after '160m depth (Table 1).'

p. 57: Comment: Groundwater potassium concentrations were measured, ranging from 1.02 to 16.2 mg/L. Overall, potassium is a minor component of the groundwater – making up between 0.07% and 1.95% of the total cations (median of 0.46% of total cations). We neglected to include the K data, largely due to the format of the thesis (the data were not considered essential to any of the publications submitted).

p. 62: Comment: The K content was initially incorporated into the Fontes and Garnier CMB method, but was later excluded, as K is a minor component of the water. Its inclusion or exclusion has very little effect on the model q values (< 1% in all cases).

p. 62: line 14: Delete "+ K"

p. 64: Comment: *:* The $\delta^{13}C$ data were not incorporated in the CMB model (e.g. we did not use the 'improved CMB model' of Fontes and Garnier, 1979), rather we used their two previous models, one of which uses field alkalinity, and the other which uses the ionic balance of major ion species. The $\delta^{13}C$ data were used in the other model described, as presented in Clark and Fritz, (1997) (modified from Pearson, 1965). There is overall good agreement between the q values (proportions of C derived from dead carbon) derived using the models based on major ion chemistry, field alkalinity and $\delta^{13}C$.

p. 65: Comment: Unfortunately, no fertilizer was sampled, and we do not have details of the manufacturing process for the ammonium carbonate used in the region (e.g. whether atmospheric CO_2 is involved in the manufacturing process)

p. 69: Comment: The point regarding effective recharge was definitely considered. The similarity of $\delta^{2}H$ and $\delta^{18}O$ values for (non-evaporated) shallow water and monsoon rainfall was already discussed– leading to the stated conclusion that recharge (ie: effective recharge) only occurs during heavy rain events (e.g. during the monsoon). If the rainfall from non-monsoon

periods is excluded from the LMWL, the equation becomes $\delta^2H = 8.4\ \delta^{18}O + 15.5$, while the equation for the shallow groundwater (excluding evaporated samples) is $\delta^2H = 4.3\ \delta^{18}O - 24.6$. The difference in slope indicates that some minor evaporative enrichment prior to recharge may indeed be important in shallow groundwater, although most samples are relatively close to the LMWL.

p. 96: Comment: Unfortunately we did not analyse the ^{14}C activity of any soil carbonate. Given that some of the secondary carbonates in shallow horizons have precipitated from recent rainfall, there is a possibility that they are ^{14}C active.

p. 106: Comment: Given that the $^{87}Sr/^{86}Sr$ ratios of rainfall and terrestrial carbonates are so similar (including in areas to the west of the region, cf. Yokoo et al, 2004; Edmunds et al, 2006), and the prevalence of westerly aeolian transport (dust storms), it is inferred that a large component of the Sr in rainfall is derived from windblown terrestrial carbonate from western China.

p. 106: Add to line 14: 'derived', after 'predominantly'

p. 109: Comment: This point has been considered during the revision of this chapter for publication in Hydrogeology Journal (accepted in its final format 02.03.2011). While thenardite and mirabilite dissolution may be sources of Na in the groundwater, these minerals tend to be deposited along with halite in the saline lakes in the region (Gao et al, 2007). The molar Cl/Br ratios (predominantly < 1200) indicate that halite dissolution is not a major process (from mass balance, accounting for <5% of the total Na or Cl in groundwater). While this does not rule out sodium sulphate minerals being a source of Na, it suggests that dissolution of Na-evaporites from the salt lakes is not a dominant source of the Na. As you point out, this possibility cannot be ruled out without more detailed information about the mineralogy of the sediments throughout the study area, and sulphur isotope analysis may help to resolve this.

p. 134: Comment: The discussion of ICP-MS methods was kept brief in order to meet the requirements for publication length. The interference on mass 75 was taken into account in the following way:

- Mass 83Kr was monitored, and using the natural abundance ratio of $^{83}Kr/^{82}Kr$, the expected counts per second of ^{82}Kr were determined. The excess counts from this estimate on mass 82 were assumed to be due to ^{82}Se.
- Using the natural abundance of $^{82}Se/^{77}Se$, the contribution of ^{77}Se on mass 77 was estimated. Excess counts per second on mass 77 were assumed to be due to 40Ar37Cl. Using the natural abundance of $^{35}Cl/^{37}Cl = 75.77/24.22$, the contribution of 40Ar35Cl on mass ^{75}As was estimated, and the counts per second on mass 77 corrected accordingly for the final determination of As.
- As we worked with argon plasma, we considered that the Ar-based interference would overwhelm any Ca based interference (e.g. 40Ca35Cl).

As was noted in the methods section, there was good agreement between arsenic concentrations measured using ICP-MS and atomic absorption spectroscopy, which provided an independent check on the validity of the ICP-MS results.

p. 134: Add to line 10, after '$^{40}Ar^{37}Cl$ mass': 'The contribution of ^{77}Se on mass 77 was estimated by monitoring mass 83Kr, and using the natural abundances of $^{83}Kr/^{82}Kr$ and $^{82}Se/^{77}Se$'.

p. 142: Comment: There is a positive correlation between As and F concentrations, and As/Cl and F/Cl ratios in the intermediate groundwater ($r^2 = 0.721$ and 0.841, respectively), although As was only measured in 7 intermediate samples.

p. 154-155: Comment: Groundwater with Na-rich, Ca-poor chemistry is commonly found in the northern Sushui River Basin, along with high As and F concentrations. The Cambrian-Ordovician limestones are not intersected by the wells in the E'mei plateau; these wells target poorly consolidated loess and fine sand beds between ~180 and ~280 m depth. Given the high concentrations of As and F found in many areas of the basin (which is predominantly composed of loess), and the prevalence of groundwater with elevated As and F concentrations in other semi-arid basins containing loess globally (e.g. Smedley et al, 2005; Gomez et al, 2009; Scanlon et al, 2009), this is considered to be the most likely source of F and As.

p. 176: Comment: We did not collect a dedicated sample for iodine, we used the anion samples. We did not consider plastic from the sample bottles to be a source of iodine contamination. This is a potential issue for future consideration; however, at the time of sampling we simply used what bottles were available. The detection limit for I using the standard IC anion column was 30 to 40 ppb, hence IC was not suitable for analysing our unknowns. We did compare Br concentrations derived using both IC and ICP-MS, and there was good agreement (< 10% difference) with the Br concentrations determined using both methods. Given that I and Br are both halogens with very similar first ionization potential, this is an indication (although not definitive) that the ICPMS method was accurate in determining iodine concentrations. High RF power conditions (1450W) were used to facilitate ionisation of iodine, given its high first ionisation potential. The in-house standard was spiked with different amounts of I, so that 3 external standards were analysed; a 'no iodine' standard and standards containing 42 µg/L and 105 µg/L I, respectively.

p. 176: Add at the end of para 1: 'The in-house standard was spiked with different amounts of I, so that 3 external standards were analysed; a 'no iodine' standard and standards containing 42 µg/L and 105 µg/L I, respectively.'

p. 180: Comment: There is no correlation between K and I concentrations that would suggest a common source (e.g. fertilizer) in the contaminated shallow groundwater. Neither I nor K concentrations show any positive relationship with nitrate concentrations (e.g. they are not elevated in samples with high nitrate concentrations and $\delta^{15}N$ values close to 0‰); which relate to fertilizer contamination. The I/Cl and I/Br ratios tend to be similar in the shallow (more saline) and deep (less saline) groundwater (e.g. Figure 3), indicating that high Iodine concentrations are likely a function of relatively high overall salinity (related to evapotranspiration) in the shallow samples (both Cl and Br correlate strongly with overall TDS).

Copyright Notices

Notice 1

Notice 2

Geochemical and isotopic investigation of groundwater in the Yuncheng Basin, China: Implications for groundwater quality and quantity in semi-arid agricultural regions

Matthew J. Currell *BA/BSc(Hons)*

A thesis submitted for the degree of Doctor of Philosophy

School of Geosciences, Monash University

July 2010

Photo: Irrigation of a fruit orchard using groundwater near Linyi, in the Yuncheng Basin, China

Photo: Grave next to irrigated farmland in Yongji County, in the Yuncheng Basin

好雨知时节，
当春乃发生。
随风潜入夜，
润物细无声。

Good rain knows the seasons,
It arrives in Spring when needed most.
Carried on the wind it enters the night,
Finely wetting all things without sound.

-杜甫 Dufu 712– 770 A.D.

Table of Contents

Chapter 2

Recharge history and controls on groundwater quality in the Yuncheng Basin, north China

Chapter 3

Major ion chemistry, $\delta^{13}C$ and $^{87}Sr/^{86}Sr$ as indicators of hydrochemical evolution and sources of salinity in groundwater, the Yuncheng Basin, China

Chapter 5

Groundwater iodine content and its relationship to palaeoclimatic variability: Evidence from palaeowaters in a semi-arid basin, northern China

Chapter 6

Conclusions

Abstract

This thesis examines chemical and isotopic characteristics of groundwater from the Yuncheng Basin in north-central China, in order to understand the timing and mechanisms of recharge, controls on groundwater quality and the influence of climate and anthropogenic processes on groundwater quality and quantity. Groundwater radiocarbon activities range from 5.93 to 88.2 pmC, decreasing with depth in the Quaternary aquifer. Estimated groundwater residence times range from modern in the shallow unconfined aquifer unit (Q3 and Q4), to >20 k.a. in the semi-confined deep unit (Q1 and Q2). Residence times in deep groundwater increase from west to east, following the historic regional groundwater flow direction; this direction has been altered by pumping and groundwater now flows towards a cone of depression near Yuncheng City. The vertical recharge rate, calculated using age vs. depth relationships is ~1-10 mm/yr; this is lower than previous estimates using tritium in the soil zone nearby, indicating that vertical infiltration may have increased in modern times compared to historic times.

$\delta^{18}O$ and $\delta^{2}H$ values in shallow modern groundwater are similar to rainfall during the summer monsoon, indicating recharge via direct infiltration. The $\delta^{18}O$ and $\delta^{2}H$ values in deep groundwater are significantly lower than modern rainfall, indicating recharge under a cooler climate than the present, during the late Pleistocene and early Holocene. The $\delta^{18}O$ values increase from old to young groundwater, reflecting a broad temperature increase through the period of deep groundwater recharge. I/Cl and I/Br ratios correlate positively with $\delta^{18}O$ values in the deep palaeowaters ($r^2 = 0.48$ and 0.55), indicating

greater delivery of I to the basin in rainfall during warm periods. This may be due to increased biological I production in warmer oceans.

Shallow groundwater contains high nitrate concentrations (up to 630 mg/L); $\delta^{15}N$ and $\delta^{18}O$ values of nitrate are both generally between 0‰ and 5‰, indicating that synthetic fertilizers are the major source. Elevated nitrate concentrations (>20 mg/L) locally occur in deep groundwater, particularly near the Linyi fault, due to downwards vertical leakage. High TDS (up to 8450 mg/L), Br and Cl concentrations in shallow groundwater relative to rainfall indicate high levels of evapotranspiration in this water, due to flood irrigation and shallow water tables.

Groundwater $^{87}Sr/^{86}Sr$ values are similar to those in local rainfall and carbonate minerals (0.7110 to 0.7120); trends in HCO_3, pH and $\delta^{13}C$ values indicate that carbonate weathering is a substantial source of groundwater DIC. However, groundwater is generally Na-rich and Ca-poor, and Na/Ca ratios increase along horizontal flow paths due to cation exchange, probably in clay lenses. Groundwater with high Na/Ca ratios also has high concentrations of F and As (up to 6.6 mg/L and 27 ug/L, respectively), that are a health risk. The F and As are likely enriched due to desorption of F^- and $HAsO_4^{2-}$ from hydrous metal oxides in the aquifer sediments. Experiments conducted with sediments and synthetic water solutions indicate that greater mobilization of F and As occurs in Na-rich, Ca-poor water, hence, cation composition is an important control on F and As mobilization.

General Declaration

I hereby declare that this thesis contains no material which has been accepted for the award of any other degree or diploma at any university or equivalent institution and that, to the best of my knowledge and belief, this thesis contains no material previously published or written by another person, except where due reference is made in the text of the thesis.

This thesis includes 1 original paper published in peer reviewed journals and 3 unpublished publications. The core theme of the thesis is hydrogeochemistry and isotope hydrology of groundwater in the Yuncheng Basin, China. The ideas, development and writing up of all the papers in the thesis were the principal responsibility of myself, the candidate, working within the Monash University School of Geosciences under the supervision of Prof. Ian Cartwright and A/Prof. Deli Chen.

The inclusion of co-authors reflects the fact that the work came from active collaboration between researchers and acknowledges input into team-based research.

In the case of Chapters 2 to 5 my contribution to the work involved the following:

Thesis chapter	Publication title	Publication status*	Nature and extent of candidate's contribution
2	Recharge history and controls on groundwater quality in the Yuncheng Basin, China	Published in Journal of Hydrology	90%
3	Major ion chemistry, $\delta^{13}C$ and $^{87}Sr/^{86}Sr$ as indicators of hydrochemical evolution and sources of salinity in groundwater, the Yuncheng Basin, China	Submitted to Hydrogeology Journal	95%
4	Controls on elevated fluoride and arsenic concentrations in groundwater from the Yuncheng Basin, China	*	90%
5	Groundwater iodine content and its relationship to palaeoclimatic variability: Evidence from palaeowaters in a semi-arid basin, northern China	In preparation	95%

[* For example, 'published'/ 'in press'/ 'accepted'/ 'returned for revision']

I have renumbered sections of submitted or published papers in order to generate a consistent presentation within the thesis.

Signed: ……

Date: ……

Declaration for Thesis Chapter 2

Declaration by candidate

In the case of Chapter 2, the nature and extent of my contribution to the work was the following:

Nature of contribution	Extent of contribution (%)
Collection of data, analysis and interpretation, writing	90

The following co-authors contributed to the work:

Name	Nature of contribution	Extent of contribution (%) for student co-authors only
Ian Cartwright	Supervisory role, manuscript review	5%
Dean Bradley	Assistance in collection of data	2.5%
Dongmei Han	Assistance in collection of data	2.5%

Candidate's Signature		Date

Declaration by co-authors

The undersigned hereby certify that:

(1) the above declaration correctly reflects the nature and extent of the candidate's contribution to this work, and the nature of the contribution of each of the co-authors.
(2) they meet the criteria for authorship in that they have participated in the conception, execution, or interpretation, of at least that part of the publication in their field of expertise;
(3) they take public responsibility for their part of the publication, except for the responsible author who accepts overall responsibility for the publication;
(4) there are no other authors of the publication according to these criteria;
(5) potential conflicts of interest have been disclosed to (a) granting bodies, (b) the editor or publisher of journals or other publications, and (c) the head of the responsible academic unit;
(6) the original data are stored at the following location(s) and will be held for at least five years from the date indicated below:

Location(s)	

Signature 1		Date
Signature 2		
Signature 3	[redacted]	Jun. 15, 2010.

Declaration for Thesis Chapter 3

Declaration by candidate

In the case of Chapter 3, the nature and extent of my contribution to the work was the following:

Nature of contribution	**Extent of contribution (%)**
Collection of data; analysis; writing	95

The following co-authors contributed to the work:

Name	**Nature of contribution**	**Extent of contribution (%) for student co-authors only**
Ian Cartwright	Manuscript review; supervisory role	5

Candidate's Signature		**Date**

Declaration by co-authors

The undersigned hereby certify that:

(1) the above declaration correctly reflects the nature and extent of the candidate's contribution to this work, and the nature of the contribution of each of the co-authors.
(2) they meet the criteria for authorship in that they have participated in the conception, execution, or interpretation, of at least that part of the publication in their field of expertise;
(3) they take public responsibility for their part of the publication, except for the responsible author who accepts overall responsibility for the publication;
(4) there are no other authors of the publication according to these criteria;
(5) potential conflicts of interest have been disclosed to (a) granting bodies, (b) the editor or publisher of journals or other publications, and (c) the head of the responsible academic unit; and
(6) the original data are stored at the following location(s) and will be held for at least five years from the date indicated below:

Location(s)	

[Please note that the location(s) must be institutional in nature, and should be indicated here as a department, centre or institute, with specific campus identification where relevant.]

Signature 1		**Date**

Declaration for Thesis Chapter 4

Declaration by candidate

In the case of Chapter 4, the nature and extent of my contribution to the work was the following:

Nature of contribution	Extent of contribution (%)
Collection of data, analysis and interpretation, writing	90

The following co-authors contributed to the work:

Name	Nature of contribution	Extent of contribution (%) for student co-authors only
Ian Cartwright	Supervisory role, manuscript review	5%
Massimo Raveggi	Assistance in data collection & analytical method	2.5%
Dongmei Han	Assistance in data collection; manuscript review	2.5%

Candidate's Signature		Date

Declaration by co-authors

The undersigned hereby certify that:

(1) the above declaration correctly reflects the nature and extent of the candidate's contribution to this work, and the nature of the contribution of each of the co-authors.
(2) they meet the criteria for authorship in that they have participated in the conception, execution, or interpretation, of at least that part of the publication in their field of expertise;
(3) they take public responsibility for their part of the publication, except for the responsible author who accepts overall responsibility for the publication;
(4) there are no other authors of the publication according to these criteria;
(5) potential conflicts of interest have been disclosed to (a) granting bodies, (b) the editor or publisher of journals or other publications, and (c) the head of the responsible academic unit;
(6) the original data are stored at the following location(s) and will be held for at least five years from the date indicated below:

Location(s)	

		Date
Signature 1		
Signature 2		
Signature 3	[redacted]	Jun. 15, 2010.

Declaration for Thesis Chapter 5

Declaration by candidate

In the case of Chapter 5, the nature and extent of my contribution to the work was the following:

Nature of contribution	**Extent of contribution (%)**
Collection of data, analysis and interpretation, writing	95%

The following co-authors contributed to the work:

Name	**Nature of contribution**	**Extent of contribution (%) for student co-authors only**
Ian Cartwright	Manuscript review, supervisory role	2.5
Massimo Raveggi	Help with analytical method; data collection	2.5

Candidate's Signature		**Date**

Declaration by co-authors

The undersigned hereby certify that:

(7) the above declaration correctly reflects the nature and extent of the candidate's contribution to this work, and the nature of the contribution of each of the co-authors.
(8) they meet the criteria for authorship in that they have participated in the conception, execution, or interpretation, of at least that part of the publication in their field of expertise;
(9) they take public responsibility for their part of the publication, except for the responsible author who accepts overall responsibility for the publication;
(10) there are no other authors of the publication according to these criteria;
(11) potential conflicts of interest have been disclosed to (a) granting bodies, (b) the editor or publisher of journals or other publications, and (c) the head of the responsible academic unit; and
(12) the original data are stored at the following location(s) and will be held for at least five years from the date indicated below:

Location(s)	

[Please note that the location(s) must be institutional in nature, and should be indicated here as a department, centre or institute, with specific campus identification where relevant.]

Signature 1		**Date**
Signature 2		

Acknowledgements

Many people provided great support to me during the preparation of this thesis, without which it would never have been possible; my gratitude and warm thanks to all of you. Firstly, thanks to my supervisor Ian Cartwright, who supervised with a wonderful balance of hands-on guidance and allowing me to explore ideas with independence; thanks also to my co-supervisor Deli Chen, for helping to organize the project and teaching us what a real Chinese banquet involves. Thanks to Massimo Raveggi for working tirelessly with me in the labs at Monash, always with good humour and great patience.

Many thanks to those who helped me in the field in China, in particular Mr. Sun Xinzhong of the Yuncheng City Water Service Bureau, Dr. Dongmei Han, of the China Institute for Geographic Sciences and Natural Resources Research, and Dean Bradley of Monash University. Thanks also to those involved in the Australia-China Centre for Water Resource Research, without which this research could not have taken place, in particular Yongping Wei, Li Baoguo, Song Xianfang, Wang Zhimin, Angela Cassar and John Langford.

Thanks to the great friends who have made life at Monash University so much fun, and who have helped out and supported me in so many ways. In particular, thanks to Benny, Pat, Sahereh, Lucy, Michiel, Maxime, Henning, Agustin, Leonor, Chris F., Chris M., Chris C., Mazey, Crazy, Lucas, Heather, Jon, Harald, Alan, Mark, Jess, Simone, Roland, Joz, Deano, Islay, Shirin and all the rest of you who've made it such a great place to work each

day. Thanks to Steg for rocking-out with me when I needed time away from the PhD, and to Tom, Jonno, Mal, Cam and Ang for your support from the Unimelb side of town.

Lastly, thanks to Anne for your great support, all your smiles and good humour, and to my family who've supported me all the way, without necessarily knowing what on earth I've been doing at Monash and in China for the past 3-and-a-half years ☺

[This page is intentionally left blank]

Chapter 1

Introduction, background and thesis aims

1.1 Context and motivation for this research

China's economy has grown at an unprecedented rate over the past 15 years and its population is continuing to grow by ~0.5% per year (World Bank, 2008). Starting in the 1980s during the Opening and Reform period, the Chinese Central Government implemented policies aimed at rapidly raising living standards, including a major expansion of the scale and intensity of agriculture that is still continuing (Organisation for Economic Co-operation and Development, 2005; National Bureau of Statistics of China, 2010). Agriculture is a major sector of the economy, and China is committed to a longstanding policy of being self-sufficient in its food production. Hence, high agricultural outputs are required both in order to underpin economic growth and provide food for the large and growing population. Most agriculture in China consists of grain and other crops that depend on irrigation, so freshwater is required to support this production, as well as supplying drinking water. Rapid urbanization of rural populations, growth in industrial production and increasing consumption of water intensive agricultural products have also added significantly to water demand in recent years (Peng et al., 2009). In northern China, the climate is largely semi-arid or arid, and rainfall and surface water are severely limited (Li, 2003). Groundwater is therefore a crucial resource that supplies a large proportion of the agricultural and domestic water in the region (Gleik, 2009).

While major infrastructure projects like the south-north water transfer and desalination plants in coastal cities offer potential relief to water shortage problems in northern China in coming decades, there is severe immediate stress on groundwater resources, particularly in rural areas. Rates of groundwater extraction are high throughout the North China Plain and the inland provinces of the north such as Shanxi, Shaanxi, Gansu and Inner Mongolia and in some cases the extraction rates are increasing, in spite of looming shortages (Li, 2003; Foster et al., 2004; Cao, 2005; Edmunds et al., 2006; Fang et al., 2010). Groundwater quality is also commonly compromised and/or deteriorating in areas of intensive agriculture, posing a threat to the viability of using groundwater for domestic and agricultural supplies (e.g. Chen et al., 2004; Zhu et al., 2007; Gleik 2009).

In this context it is important that the groundwater resources of the region are assessed scientifically in order to understand issues such as the timescales and mechanisms of recharge, controls on groundwater quality, and the impacts of climate and anthropogenic practices on water quality and availability. Such data can form a basis for sustainable usage of groundwater resources (Gleeson et al., 2010). Many aquifers in arid and semiarid areas of China have been under exploitation for decades without widespread understanding of these issues or collection of geochemical data, and such data has only begun to emerge in the last five to ten years (e.g. Chen et al., 2003; Chen et al., 2004; Edmunds et al., 2006; Zhu et al., 2007; Gates et al., 2008). Research of this kind would ideally be carried out prior to or during groundwater resource development, however this has not been the case in much of China and regulation, informed by scientific knowledge, has been unable to keep pace with rapid development (Gleik, 2009). Geochemistry plays a vital role in understanding the long-term behaviour of groundwater systems and in understanding

groundwater flow paths, recharge and the evolution of water quality in systems that have been perturbed by groundwater extraction (Edmunds, 2009).

This geochemical investigation of groundwater in the Yuncheng Basin, which has served as a major groundwater supply in Shanxi province in northern China since the 1980s, is thus both warranted and overdue. The data and findings from this study provide information that is not only important for understanding groundwater recharge, flow and controls on groundwater quality in the Yuncheng Basin, but also has broader implications in terms of understanding the regional palaeoclimatic and groundwater recharge history, and processes that affect groundwater quality in similar environments in China and globally.

1.2 Geological setting and background

The Yuncheng Basin is a typical area in semi-arid northern China where groundwater is intensively used for irrigation and domestic supply (Cao, 2005; China Geological Survey, 2006). Approximately 60% of grain production and 80% of cotton production in Shanxi Province (total population ~31 million) occurs in the Yuncheng Basin, which has a population of ~5 million (Yuncheng City Water Bureau, pers. comm., 2008). Much of this production relies on irrigation using groundwater that is pumped from 15 m to 350 m depth from unconsolidated Quaternary sediments (Yuncheng Regional Water Bureau, 1982; Cao, 2005). Groundwater also supplies domestic water in the region.

1.2.1 Geology

The Yuncheng Basin is located along the middle reaches of the Yellow River (Fig. 1a) in the south of the Shanxi Rift; a series of trans-tensional basins that have been subsiding since the early Pliocene in response to transmitted stresses from the India-Eurasia collision (Xu and Ma, 1992). The basin is located within the belt of loess that covers large areas of north-central China (Fig 1a; Liu, 1988). The Yuncheng Basin comprises two major geographic zones; the Sushui River Basin and the E'mei Plateau (Fig. 1b). The Sushui River Basin is a graben that ranges in elevation from 320 to 420 m above sea level (a.s.l.) and which contains a ~500m thick sequence of Quaternary sediments that form the major aquifer in the Yuncheng Basin. The Zhongtiao fault and Linyi fault are the southern and northern margins of the Sushui River Basin, respectively (Fig 1b); these are ENE-trending normal faults that are typical of the basin margin faults in the Shanxi Rift (Xu and Ma, 1992). These two faults are linked in the east by a zone of transform faulting, which forms the eastern margin of the Yuncheng Basin (Fig. 1b). To the south of the Zhongtiao fault are the Zhongtiao Mountains (~800 to 1500 m a.s.l.), which comprise fractured Archean metamorphic rocks (Fig 1b). To the north of the Linyi fault is the E'mei Plateau, a horst block ranging in elevation from ~450 to 600 m a.s.l. that is blanketed by Quaternary loess. The northern Boundary of the Yuncheng Basin is the fault at the northern limit of the E'mei Plateau, which is the southern margin of another graben - the Fen River Basin (Fig 1b; China Geological Survey, 2006). To the west of the Yuncheng Basin in Shaanxi Province is the Wei River Basin, which likely connects with the Sushui River basin below the Yellow River (Fig 1b; Sun, 1988).

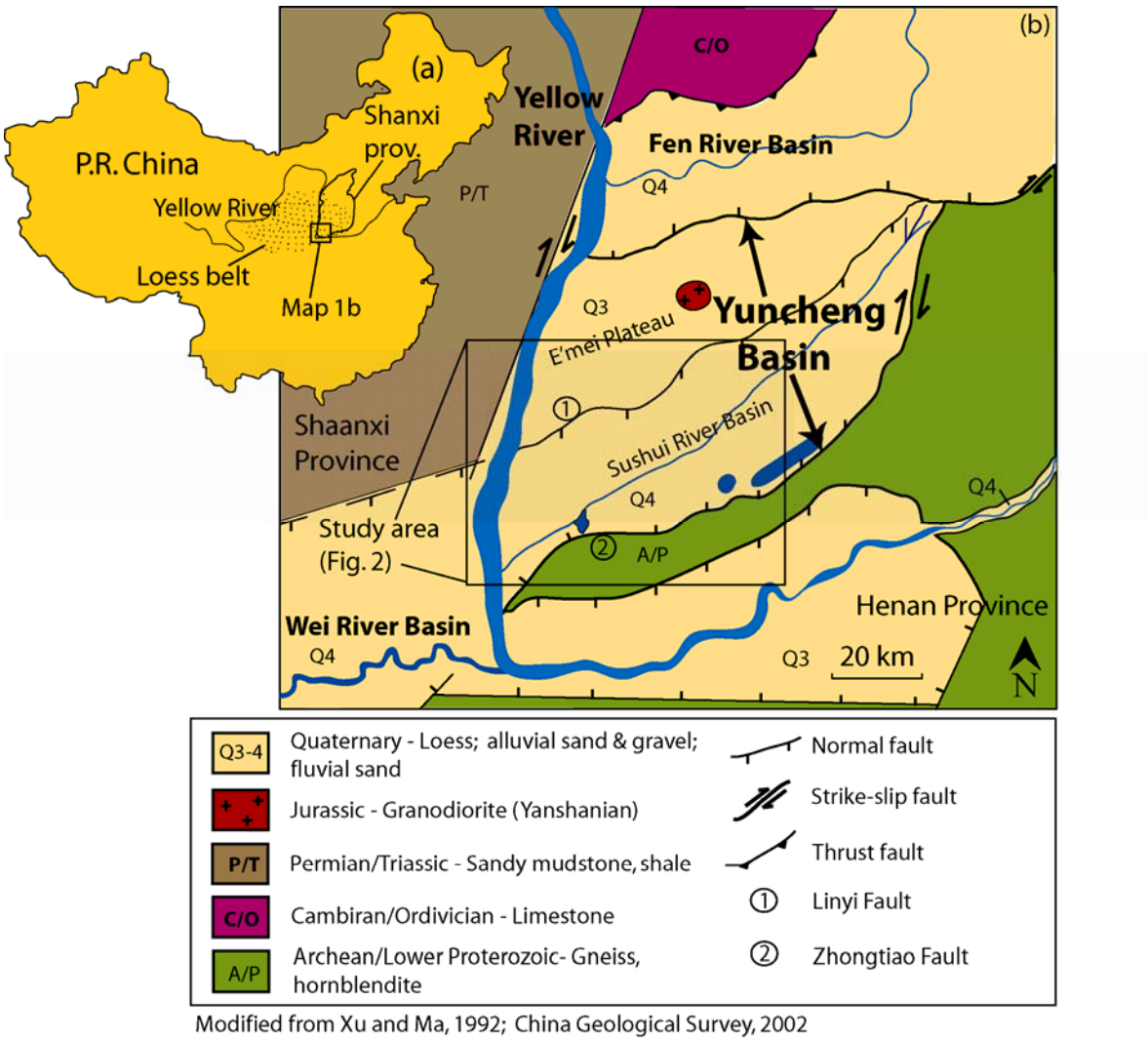

Fig. 1a. Location of the Yuncheng basin in north-central China; **1b.** Geological map of the Yuncheng Basin and surrounding area.

The Quaternary sediments of the Yuncheng Basin contain four chronostratigraphic units (Q1-Q4: Table 1) that can be broadly correlated throughout most of northern China (e.g. Chen et al., 2003). The Pleistocene sediments (Q1-Q3) are predominantly loess-palaeosol sequences. Holocene sediments (Q4) include alluvial sand and gravel in the piedmont of the Zhongtiao Mountains, fluvial sands, lacustrine clays and minor loess deposits (Huang et al., 2007). The Quaternary loess is composed of 0.005 to 0.05 mm-sized dust particles, transported from deserts in northwest China and central Asia by dust

storms, predominantly during arid periods in the Pleistocene (Liu, 1988). The loess in the Yuncheng Basin is relatively fine-grained compared with much of the loess in China, as the basin is close to the eastern limit of aeolian sediment transport from western China (Fig 1a; Sun, 1988). The loess is interlayered with clay-rich palaeosols that formed during relatively warm, wet periods between loess deposition events plus fluvial deposits from ephemeral streams and lacustrine clays that were deposited in saline lakes (Liu, 1988; Wang et al., 2002; Huang et al., 2007).

This study focuses on a 50 km by 70 km area of the Yuncheng Basin, including most of the Sushui River Basin and part of the E'mei Plateau (Fig 2a). Major geological units in the study area are shown in Table 1 and Figure 2b.

Unit	Age	Name	Major sediment type(s)	Thickness (m)
Q4	Holocene		Alluvial gravel & sand; Lacustrine clay	10-20m
Q3	Upper Pleistocene	Malaan Loess	Loess-Palaeosol sequence; fluvial sand	50-70m
Q2	Middle Pleistocene	Lishi loess	Loess-Palaeosol sequences; lacustrine clay; fluvial sand	100-200m
Q1	Lower Pleistocene	Wucheng Loess	Loess-Palaeosol sequences; lacustrine clay	100-200m
N	Neogene		Mudstone	~200m
C-O	Cambrian - Ordovician		Limestone	~500m
Arsm	Archean – Lower Proterozoic	Zhongtiao Group	Gneiss; Amphibolite; Hornblendite; Quartzite; Migmatite	> 1000m

Table 1. Major Geologic units in the study area (Yuncheng Regional Water Bureau, 1982; China Geological Survey, 2002)

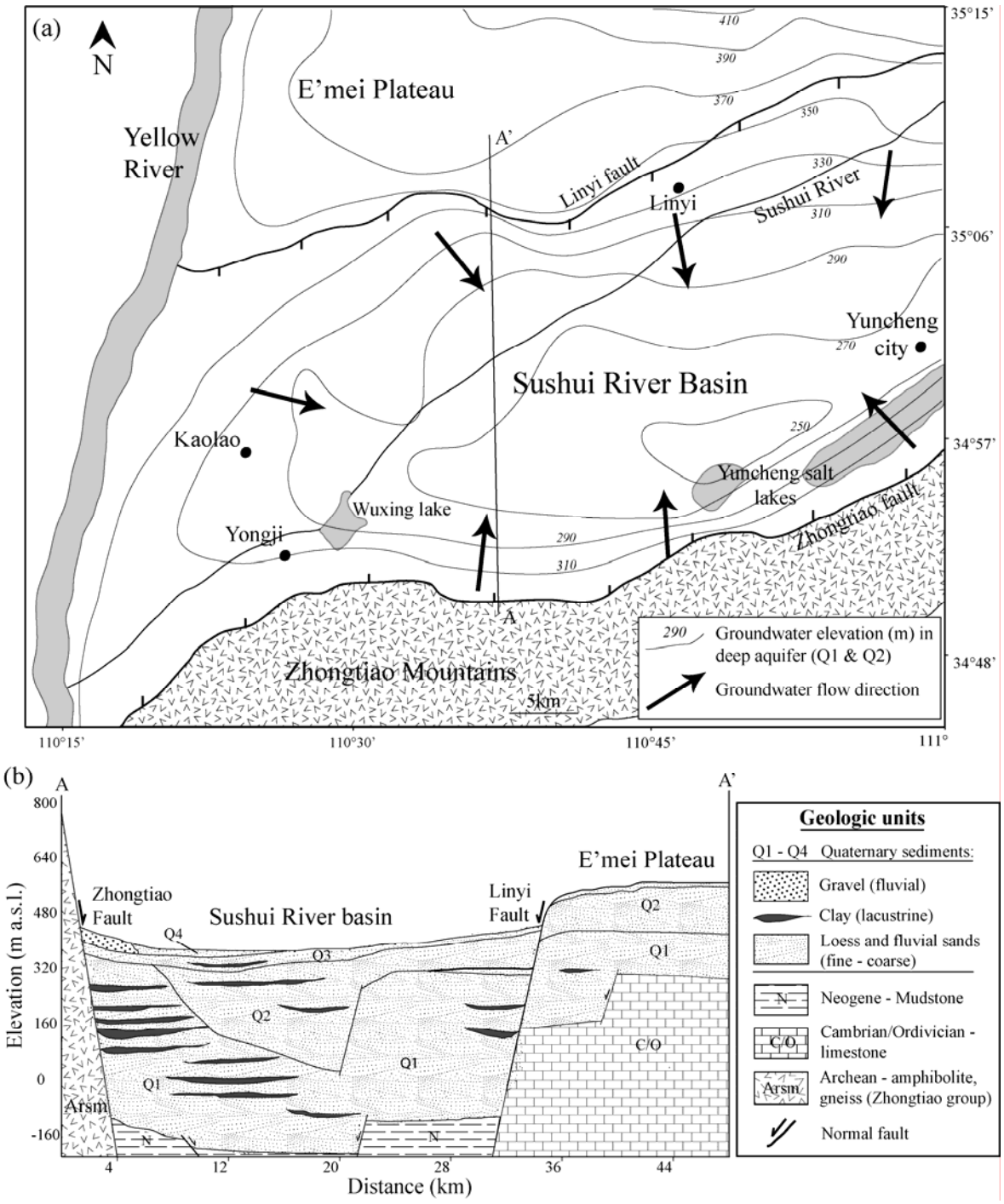

Fig. 2a. The study area, deep groundwater elevation contours and groundwater flow directions. **2b**. Schematic cross section of the Yuncheng Basin in the study area. Data from China Geological Survey (2006)

1.2.2 Hydrogeology

The Quaternary aquifer of the Sushui River Basin consists of two major aquifer units – a shallow unconfined unit (Q3 and locally Q4) and a semi-confined deep unit (Q1 and locally Q2) (Yuncheng Regional Water Bureau, 1982; Cao, 2005). These are separated by the S_1 palaeosol (Liu et al., 1986), which extends laterally throughout much of the basin and is a partial barrier to vertical mixing between the units (Cao, 2005). A distinct hydrostratigraphic unit may also occur in the upper ~50m of the Q2 sediments; however, this unit is essentially part of the deep (Q1 & Q2) unit (Cao, 2005). In the E'mei Plateau there is no shallow unconfined aquifer but groundwater is present in semi-confined Q1 sand and loess below ~120m of low porosity Q2 & Q3 loess (Fig 2b). This groundwater connects with deep groundwater in the Sushui River Basin (Yuncheng Regional Water Bureau, 1982). Groundwater also occurs in the fractured metamorphic basement below the southern Sushui River Basin (Fig. 2). This water has limited volume, but is used for local domestic supply in the vicinity of the Zhongtiao Mountains (Yuncheng Regional Water Bureau, 1982).

Based on groundwater elevations measured in 2004 (China Geological Survey, 2006), shallow groundwater flows from the southern and northern margins of the Sushui River Basin towards its centre, with an additional westerly component of flow towards the Yellow River. Shallow groundwater discharges into Yuncheng salt lake and Wuxing Lake; these lakes are in topographic depressions formed by local faulting and subsidence (Wang et al., 2002; China Geological Survey, 2006). In the deep aquifer, present day groundwater flows converge on a groundwater depression in the central Sushui River Basin, to the west of Yuncheng city (Fig 2a).

1.2.3 Climate

The climate in the Yuncheng Basin is semiarid, with annual rainfall ranging from ~300 to 800 mm/year, potential evapotranspiration from ~1500 to 2500 mm/yr, and mean annual temperatures of 12.5 to 13.5°C (Yuncheng Regional Water Bureau, 1982; China Geological Survey, 2006; Huang et al., 2007). Most rainfall occurs during the East Asian summer monsoon between July and September. In general, potential evaporation exceeds rainfall (e.g. Fig. 3); however, rainfall during heavy monsoonal rain events can exceed evaporation, allowing groundwater recharge (e.g. Fig 3a). Rainfall in the Yuncheng basin has broadly decreased over the past ~25 years from an average of 615 mm/yr between 1980 to 1985 to an average of 485 mm/yr between 1999 to 2004 (China Geological Survey, 2006). This is generally consistent with decreasing rainfall throughout the Yellow River Basin since records began in 1956, while temperatures have increased by ~1°C (Huang et al., 2009).

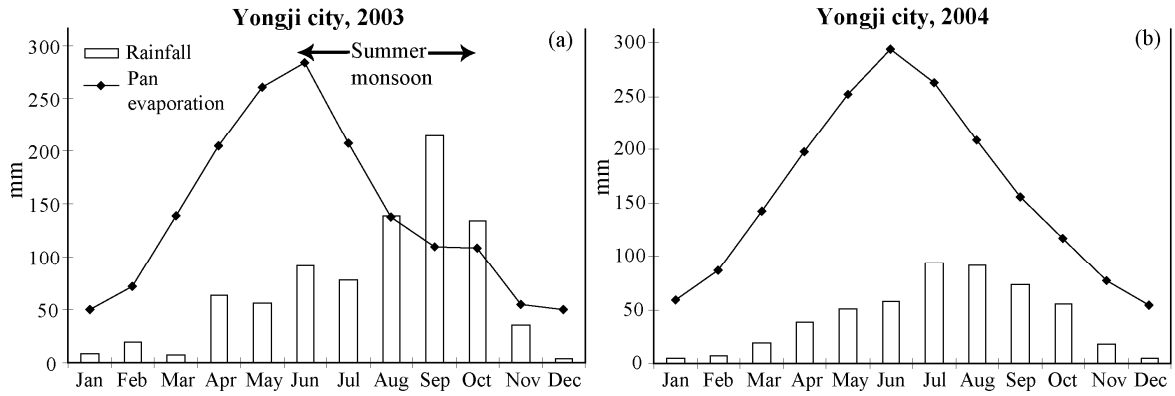

Fig 3. Monthly rainfall and pan evaporation measured in Yongji city during 2003 **(a)** and 2004 **(b)**. Monthly rainfall is exceeded by evaporation in most months, except during heavy monsoon rains. Data from China Geological Survey, 2006.

1.2.4 Groundwater usage and associated issues

The first wells in the Yuncheng Basin were drilled in the Sushui River Basin in 1960s, mainly to supply domestic water (Gao, 2005). Drilling of thousands of irrigation wells took place in the 1980s with the development of large-scale intensive irrigated agriculture, mostly summer maize and winter wheat cropping (Gao, 2005). In the last 10 to 15 years, agriculture has diversified into planting of cash-crops such as cotton and fruit orchards, and the number of wells and rates of groundwater use again increased substantially compared to the 1980s (Cao, 2005; Gao, 2005).

1.2.4.1 Groundwater quantity

Between the 1960s and 1990s, the amount of groundwater pumped in the Yuncheng Basin increased ~40-fold (Gao, 2005). The estimated total extraction of groundwater from the basin in 2000 was $8*10^8$ m^3. This is ~4 times the estimated sustainable yield of ~$2*10^8$ m^3/yr proposed by Cao (2005). Groundwater in the deep unit (Q1 & Q2) is generally less saline than in the shallow unit; hence, the majority of pumping since the late 1980s has been from wells >120 m depth (Cao, 2005). The intensive pumping has led to high rates of drawdown in the deep aquifer that have increased from 2.7 m/yr in 1987 to 3.3 m/yr in 2000 (Cao, 2005). A cone of depression has developed in the deep aquifer to the west of Yuncheng city (Fig 2a) and has increased in area from ~700 km^2 in 1986 to ~1600 km^2 in 2000 (Cao, 2005). The high levels of drawdown threaten to reduce bore yields and potentially deplete the groundwater resources in the future.

1.2.4.2 Groundwater quality

Since the mid-1980s, groundwater quality in the shallow unit (Q3 & Q4) has deteriorated; groundwater TDS concentrations have increased and in many locations this water has become unsuitable for irrigation (Yuncheng Regional Water Bureau, pers. comm. 2008). Salinisation likely occurs due to the widespread practice of flood irrigation, which facilitates evapotranspiration of irrigation water in the soil zone, prior to its re-infiltration into the unconfined aquifer. The use of nitrogen-based chemical fertilizer (mostly ammonium nitrate) is also widespread in the Yuncheng Basin (Yuncheng Regional Water Bureau, pers. comm., 2008), resulting in nitrate contamination of the shallow groundwater, as occurs in a number of areas in northern China (e.g. Hu et al., 2005; Chen et al., 2006). Due to the high rates of pumping in the deep aquifer, downwards vertical hydraulic gradients are ~0.1 to ~0.45 in most of the basin (China Geological Survey, 2006); hence, vertical leakage may be occurring, leading to deterioration of deep groundwater quality. Additionally, high fluoride concentrations have been reported in groundwater from some parts of the basin, notably in the Kaolao area, where groundwater F concentrations are up to 6 mg/L (Gao 2005; Gao et al., 2007).

In spite of these issues related to groundwater quantity and quality, and the great dependence of the region on groundwater, the groundwater resources of the Yuncheng Basin have been sparsely studied from a geochemical viewpoint in the Chinese scientific literature and little if at all in English scientific literature; this thesis aims to address this deficiency. Further background information on the geology, hydrogeology, climate and geography of the Yuncheng Basin is provided within the individual chapters of this thesis as it relates to the specific topic areas.

1.3 Research aims, scope & approach

This thesis aims to address issues related to groundwater quality and quantity in the Yuncheng Basin using environmental isotopes, major ion chemistry and other geochemical data from groundwater, rainfall and sediments collected between 2007 and 2009. There are three primary areas on which the research is focused, within which there are several research questions that this thesis examines. The specific research aims are:

1.3.1 Research aim 1: Characterise the age and recharge history of groundwater in the Yuncheng Basin using stable and radiogenic isotopes.

Reliable data on groundwater residence time and recharge rates and mechanisms is crucially important in assessing the sustainability of groundwater use (Edmunds, 2009); this is particularly important in arid and semi-arid regions, where recharge is generally limited (Scanlon et al., 2006). When extraction of groundwater far exceeds the natural recharge rate, a groundwater resource can be defined as 'non-renewable' (Jacobson et al., 1989; Edmunds 2003). In recent years it has emerged that groundwater that is being intensively pumped in the north China plain (e.g. Chen et al., 2003; Kreuzer et al., 2009) and northwest China (Edmunds et al., 2006; Gates et al., 2008) is palaeowater, recharged thousands or tens of thousands of years ago. Given the high levels of pumping in the Yuncheng Basin, particularly from the deep aquifer (Cao, 2005), there is a pressing need to determine the age of this groundwater, understand the mechanism(s) of recharge and estimate historic and modern recharge rates.

Recharge in arid and semi-arid areas can be complex (Wood and Sandford 1995; Scanlon et al., 2006). Many factors, including the intensity of rain events, rates of

evapotranspiration, soil type, vegetation and influence of surface water bodies combine to determine whether and how much recharge can occur in such regions (Scanlon et al., 2002; 2006). Isotopic techniques provide useful information on recharge in these settings; for example, the stable isotopes of hydrogen and oxygen (δ^2H and $\delta^{18}O$) in groundwater and rainfall can be used to evaluate timing and sources of recharge, and the relationships between recharge and climate (Clark and Fritz, 1997). Radiocarbon (^{14}C) activities are also now widely used to estimate groundwater residence time, as many deep aquifers contain water recharged from 1000s to 10000s of years, within the range of ~0.5 to 5 half-lives of ^{14}C (e.g. Vogel and Ehhalt, 1963; Kazemi et al., 2006). There is complexity in constraining carbon sources and determining accurate initial ^{14}C activities in groundwater samples (e.g. Fontes and Garnier 1979; Kalin, 2000; Coetsiers and Walraevens 2009; Cartwright., 2010; Blaser et al., 2010), so the combined use of radiocarbon and other isotope and geochemical indicators (e.g. major ion chemistry, $\delta^{13}C$, δ^2H and $\delta^{18}O$) is crucial in accurate age estimation (Edmunds, 2009).

1.3.2 Research aim 2: *Understand the processes that control groundwater quality in the Yuncheng Basin, using hydrogeochemical data.*

Declining groundwater quality is at least an equally pressing concern as declining quantity in many regions of the world (Tefrey and ul-Haque, 2010). Collection and discussion of water quality data either in Chinese or English is scarce in China, despite acknowledgement by the Central Government that water quality is a pressing issue (Gleik, 2009). It was estimated in 2007 that 100s of millions of Chinese people, mostly in rural areas, do not have access to safe drinking water and many of these people drink water

contaminated with nitrate, arsenic, fluoride and other toxins related to agriculture, industrial wastewater and/or natural enrichment (Organisation for Economic Co-operation and Development, 2007).

Understanding the controls on the quality of groundwater used for irrigation and domestic supplies is a vital concern for the Yuncheng Basin and other basins in the region (China Geological Survey, 2006). The intensive irrigation and use of fertilizer leave groundwater vulnerable to nitrate contamination and salinisation, while high fluoride and arsenic concentrations have already been documented in the basin and/or in nearby regions (Gao et al., 2007; Guo et al., 2007a, 2007b). The source(s) and behaviour of nitrate in groundwater can be investigated using $\delta^{15}N$ and $\delta^{18}O$ data (e.g. Kendall, 1998), while salinisation processes can be examined using major ion chemistry, (e.g. molar ion ratios) and stable isotopes ($\delta^{2}H$ and $\delta^{18}O$) (e.g. Herczeg and Edmunds, 2000; Cartwright et al., 2004; Zhu et al., 2007). Isotope tracers, such as $^{87}Sr/^{86}Sr$ and $\delta^{13}C$, can also be used in conjunction with major ion chemistry data to characterise water-rock interaction processes, particularly mineral weathering and exchange reactions, that are commonly important in controlling the chemical evolution of groundwater (Faure, 1991; Armstrong et al., 1998; Dogramaci and Herczeg, 2002).

Mechanisms of F and As enrichment in groundwater from semiarid regions are still relatively poorly understood (Smedley and Kinniburgh, 2002; Bhattacharya et al., 2006; Gomez et al., 2009). However, groundwater major ion chemistry, sediment mineralogy and geochemistry, together with geochemical modeling are shedding light on the factors and mechanisms that cause F and As enrichment in these settings (e.g. Smedley et al., 2005; Scanlon et al., 2009). Using these approaches will allow characterization of the natural and

anthropogenic processes that are involved in controlling groundwater quality in the Yuncheng Basin.

1.3.3 Research aim 3: *Investigate palaeoclimate and further characterize past environments in northern China using geochemical techniques.*

There is continued and growing interest in understanding past climatic variation on global and regional scales (e.g. Intergovernmental Panel on Climate Change, 2007). The East Asia region, including the Yuncheng Basin, is affected by the East Asian summer monsoon, and has been influenced both by global climatic phenomena (e.g., large temperature changes over 1000s of years), as well as local effects (e.g., changes in rainfall amounts and monsoon intensity: An et al., 2000; Huang et al., 2007; Kreuzer et al., 2009). Groundwater is a potential source of information that can be used to better understand palaeoclimatic variations on these spatial and temporal scales (e.g. Kreuzer et al., 2009).

$\delta^{2}H$, $\delta^{18}O$ and $\delta^{14}C$ data are commonly used to characterize the age and recharge history of groundwater and hence provide information on changes in temperature and rainfall amounts over the period of groundwater recharge (e.g. Dutton, 1995; Clark and Fritz, 1997; Kreuzer et al., 2009). Additionally, further insight can potentially be gained using novel techniques – such as groundwater iodine concentrations. Iodine displays complex behaviour during transport from marine to terrestrial environments, and is sensitive to a number of factors such as temperature, rainfall intensity and soil characteristics (e.g. Lloyd et al., 1982; Fuge and Johnson, 1986; Truesdale and Jones 1996; Neal et al., 2007). Biological production of I by marine organisms is known to be a major source of I in the atmosphere and possibly rainfall, and may play an important role in

regulating climate, particularly in tropical and sub-tropical regions (e.g. O'Dowd et al., 2002; Carpenter, 2003; Saiz-Lopez and Plane, 2004; Smythe-Wright et al., 2006). In spite of this, iodine has only rarely been studied in groundwater, and never before in the context of investigating palaeoclimate. By examining groundwater iodine concentrations in conjunction with other palaeoclimatic indicators in the Yuncheng Basin (e.g. $\delta^{2}H$, $\delta^{18}O$ and $\delta^{14}C$), the palaeoclimatic and palaeoenvironmental history of Northern China can potentially be further characterised and the geochemical relationships between the oceans, atmosphere and terrestrial hydrosphere can be better understood.

1.4 Thesis outline

This thesis consists of four manuscript-style chapters that examine different aspects of the geochemistry and isotopic composition of groundwater in the Yuncheng Basin. These chapters have either been published, submitted or are in preparation for submission to international hydrology or geochemistry journals, hence, each stands alone with an abstract, introduction, methods, results, discussion, conclusions and references. Because of this format, some background information is inevitably repeated.

Chapter 2 uses $a^{14}C$ data, along with $\delta^{13}C$ and major ion chemistry, to estimate groundwater residence times throughout the Yuncheng Basin. The residence times are examined in the context of the modern flow regime in the basin. Estimates of the vertical recharge rate are made, and these are compared with recharge rates calculated in a nearby region using ^{3}H data. $\delta^{2}H$ and $\delta^{18}O$ values are examined along with the $a^{14}C$ data and other published data from northern China in order to characterize the recharge history in the

basin, and understand the relationship palaeoclimate and groundwater recharge. Sources of salinisation and nitrate contamination are also investigated, using TDS, $\delta^{15}N$ and $\delta^{18}O$, and these quality indicators are examined in conjunction with hydraulic head data in order to characterize vertical mixing in the aquifer.

Chapter 3 examines the major ion chemistry in groundwater, rainfall and sediments from the basin in conjunction with $\delta^{13}C$ and $^{87}Sr/^{86}Sr$ values, in order to further characterise the processes that control groundwater chemistry at different stages (e.g. during recharge and flow) and in different parts of the aquifer (e.g. shallow vs. deep groundwater). The degree of evapotranspiration that shallow and deep groundwater has been subject to is estimated using mass balance, while the roles of carbonate weathering, silicate weathering and cation exchange reactions are examined using the $\delta^{13}C$, $^{87}Sr/^{86}Sr$ and major ion ratios. Trends in these data are examined along groundwater flow paths, allowing characterisation of the hydrochemical evolution of groundwater.

Chapter 4 examines the geochemical characteristics of groundwater with elevated fluoride and arsenic concentrations in the Yuncheng basin, and proposes a mechanism to explain the mobilization of F and As from the aquifer matrix into groundwater. This is achieved through examining the major ion chemistry of groundwater samples, geochemical modelling with PHREEQC, and a series of experiments using sediments collected from the basin and synthetic water solutions prepared in the laboratory.

Chapter 5 explores the relationship between groundwater Iodine concentrations and palaeoclimate in the north China region. These relationships are investigated with the aid of $\delta^{18}O$ and $a^{14}C$ data, which were used to characterize palaeoclimate and its relationship to groundwater recharge in Chapter 2. The iodine data are also compared to other published groundwater iodine data, and are placed in the context of the differing palaeoclimatic histories of northern China and other parts of the world.

Chapter 6 presents a summary of the major findings of each chapter and the overall conclusions arising from this research.

References:

An, Z., Porter, S.C., Kutzbach, J.E., Wu, X., Wang, S., Liu, X., Li, X., Zhou, W., 2000. Asynchronous Holocene optimum of the East Asian monsoon. Quaternary Science Reviews 19, 743-762.

Armstrong, S.C., Sturchio, N.C., 1998. Strontium isotopic evidence on the chemical evolution of pore waters in the Milk River Aquifer, Alberta, Canada. Applied Geochemistry 13(4), 463-475.

Bhattacharya, P., Claesson, M., Bundschuh, J., Sracek, O., Fagerberg, J., Jacks, G., Martin, R.A., Stoniolo, A.R., Thir, J.M., 2006. Distribution and mobility of arsenic in the Rio Dulce alluvial aquifers in Santiago del Estero Province, Argentina. Science of the Total Environment 358, 97-120.

Blaser, P.C., Coetsiers, M., Aeschbach-Hertig, W., Kipfer, R., Van Camp, M., Loosli, H.H., Walraevens, K., 2010. A new groundwater radiocarbon correction approach

accounting for palaeoclimate conditions during recharge and hydrochemical evolution: The Ledo-Paniselian Aquifer, Belgium. Applied Geochemistry 25, 437-455.

Cao, X.H., 2005. Study of the Confined Groundwater System of Middle-deep Layers in Sushui Catchment. In: Shanxi Hydrotechnics Bulletin No. 3. China Academic Journal Electronic Publishing House. pp 41-43. (in Chinese)

Carpenter, L.J., 2003. Iodine in the marine boundary layer. Chemistry Reviews 103, 4953-4962.

Cartwright, I., Weaver, T., Fulton, S., Nichol, C., Reid, M., Cheng, X., 2004. Hydrogeochemical and isotopic constraints on the origins of dryland salinity, Murray Basin, Victoria, Australia. Applied Geochemistry 19, 1233-1254.

Cartwright, I. 2010. Using groundwater geochemistry and environmental isotopes to assess the correction of ^{14}C ages in a silicate-dominated aquifer system. Journal of Hydrology 382, 174-187.

Chen, J.Y., Tang, C., Sakura, Y., Kondoh, A., Yu, J., Shimada, J., Tanaka, T., 2004. Spatial geochemical and isotopic characteristics associated with groundwater flow in the North China Plain. Hydrological Processes 18, 3133-3146.

Chen, J.Y., Tang, C.Y., Yu, J.J., 2006. Use of ^{18}O, ^{2}H and ^{15}N to identify nitrate contamination of groundwater in a wastewater irrigated field near the city of Shijiazhuang, China. Journal of Hydrology 326, 367-378.

Chen, Z.Y., Qi, J.X., Xu, J.M., Xu, J.M., Ye, H., Nan, Y.J., 2003. Palaeoclimatic interpretation of the past 30 ka from isotopic studies of the deep confined aquifer of the North China plain. Applied Geochemistry 18, 997 – 1009.

China Geological Survey, 2006. Groundwater resources and environmental issues assessment in the six major basins of Shanxi (in Chinese). China Geological Survey Special publication, Beijing. 98p.

Clark, I., Fritz, P., 1997. Environmental Isotopes in Hydrogeology. Lewis Publishing, New York. 328p.

Coetsiers, M., Walraevens, K., 2009. A new correction model for ^{14}C ages in aquifers with complex geochemistry – application to the Neogene Aquifer, Belgium. Applied Geochemistry 24, 768-776.

Dogramaci, S.S., Herczeg, A.L., 2002. Strontium and carbon isotope constraints on carbonate-solution interactions and inter-aquifer mixing in groundwaters of the semi-arid Murray Basin, Australia. Journal of Hydrology 262, 50-67.

Dutton, A.R., 1995. Groundwater isotopic evidence for paleorecharge in U.S. High Plains aquifers. Quaternary Research 43, 221-231.

Edmunds, W.M., 2003. Renewable and non-renewable groundwater in semi-arid regions. Developments in Water Science 50, 265-280.

Edmunds, W. M., Ma, J., Aeschbach-Hertig, W., Kipfer, R., Darbyshire, D. P. F., 2006. Groundwater recharge history and hydrogeochemical evolution in the Minqin Basin, North West China. Applied Geochemistry 21(12), 2148-2170.

Edmunds, W. M., 2009. Geochemistry's vital contribution to solving water resource problems. Applied Geochemistry 24(6): 1058-1073

Fang, Q.X., Ma, L., Green, T.R., Wang, T.D., Ahuja, L.R., 2010. Water resources and water use efficiency in the North China Plain: Current status and agronomic management. Agricultural Water Management 97(8), 1102-1116.

Faure, G., 1991. Principles and Applications of Inorganic Geochemistry. Prentice-Hall, New Jersey. 626 pp.

Fontes, J.-C., Garnier, J.M., 1979. Determination of the initial ^{14}C activity of the total dissolved carbon: a review of the existing models and a new approach. Water Resources Research 15(2), 399-413.

Foster, S., Garduno, H., Evans, R., Olson, D., Tian, Y., Zhang, W., Han, Z. 2004. Quaternary Aquifer of the North China Plain - assessing and achieving groundwater resource sustainability. Hydrogeology Journal 12, 81-93.

Fuge, R., Johnson, C.C., 1986. The geochemistry of iodine – a review. Environmental Geochemistry and Health 8(2), 31-54.

Gates, J.B., Edmunds, W.M., Darling, W.G., Ma, J., Pang, Z., Young, A.A., 2008. Conceptual model of recharge to southeastern Badain Jaran Desert groundwater and lakes from environmental tracers. Applied Geochemistry 23, 3519 - 3534.

Gao, X., 2005. The distribution of fluoride in groundwater and nature of the processes causing high fluoride concentrations in groundwater in theYuncheng Basin. Msc Thesis, China Geological University, Wuhan. 61p. (in Chinese)

Gao, X., Wang, Y., Li, Y., Guo, Q., 2007. Enrichment of fluoride in groundwater under the impact of saline water intrusion at the salt lake area of Yuncheng basin, northern China. Environmental Geology 53(4), 795 – 803.

Gleeson, T., VanderSteen, J., Sopohocleous, M.A., Taniguchi, M., Alley, W.M., Allen, D.M., Zhao, Y., 2010. Groundwater sustainability strategies. Nature Geoscience 3, 378-379.

Gleik, P.H., 2009. China and Water (Chapter 5). In: Gleik, P.H., Cooley, H., Cohen, M.J., Morikawa, M., Morrison, J., Palaniappan, M. (eds), *The world's water 2008-2009. The Biennial report on freshwater resources.* Island Press, Washington, pp. 79-97.

Gomez, M.L., Blarasin, M.T., Martinez, D.E., 2009. Arsenic and fluoride in a loess aquifer in the central area of Argentina. Environmental Geology 57, 143-155.

Guo Q., Wang Y., Ma T., Ma R., 2007(a). Geochemical processes controlling the elevated fluoride concentrations in groundwaters of the Taiyuan Basin, Northern China. Journal of Geochemical Exploration 93(1): 1-12.

Guo, Q., Wang, Y., Gao, X., Ma, T., 2007(b). A new model (DRARCH) for assessing groundwater vulnerability to arsenic contamination at basin scale: a case study in Taiyuan basin, northern China. Environmental Geology 52, 923-932.

Herczeg, A.L., Edmunds, W.M., 2000. Inorganic ions as tracers. In: Cook, P., Herczeg, A., (eds). *Environmental Tracers in Subsurface Hydrology*, Kluwer Academic Publishiers, Boston, pp. 31-77.

Hu, K.L., Huang, Y.F., Li, H., Li, B.G., Chen, D., White, R.E., 2005. Spatial variability of shallow groundwater level, electrical conductivity and nitrate concentration, and

risk assessment of nitrate contamination in North China Plain. Environment International 31, 896-903.

Huang C.C., Pang J., Zha X., Su H., Jia Y., Zhu Y., 2007. Impact of monsoonal climatic change on Holocene overbank flooding along Sushui River, middle reach of the Yellow River, China. Quaternary Science Reviews 26: 2247-2264.

Intergovernmental Panel on Climate Change, 2007. Palaeoclimate (Chapter 6). In: Solomon, S., Qin, M., Manning, Z., Chen, Z., Marquis, M., Averyt, K.B., Tignor, M., Miller, H.L. (eds), *Climate Change 2007: The Physical Science Basis. Contribution of Working Group I to the Fourth Assessment Report of the Intergovernmental Panel on Climate Change.* Cambridge University Press, Cambridge, UK, pp 433-498.

Jacobson, G., Calf, G.E., Jankowski, J., 1989. Groundwater chemistry and palaeorecharge in the Amadeus Basin, Central Australia. Journal of Hydrology 109, 237-266.

Kalin, R.M., 2000. Radiocarbon dating of groundwater systems. In: Cook, P.G., Herczeg, A. (Eds.), Environmental Tracers in Subsurface hydrology. Kluwer, New York, pp. 111-144.

Kazemi, G.A., Lehr, J.H., Perrochet, P., 2006. Groundwater Age. John Wiley & Sons, N.J. 325p.

Kendall, C., 1998. Tracing Nitrogen Sources and Cycling in Catchments *in:* C. Kendall & J.J., McDonnell (ed) Isotope Tracers in Catchment hydrology. Elsevier Science B.V., Amsterdam. pp. 519-576.

Kreuzer, A.M., Rohden, C.V., Friedrich, R., Chen, Z., Shi, J., Hajdas, I., Aeschbach-Hertig, W., 2009. A record of temperature and monsoon intensity over the past 40 kyr from groundwater in the North China Plain. Chemical Geology 259, 168-180.

Li, X., 2003. Pressure of water shortage on agriculture in arid region of China. Chinese Geographical Science, 13(2), 124-129.

National Bureau of Statistics of China, 2010. Statistical Communiqué of the People's Republic of China on the 2009 National Economic and Social Development. Electronic resource: http://www.stats.gov.cn/was40/gjtjj_en_detail.jsp ?searchword=agriculture& channelid=9528&record=3. Accessed March, 2010.

Neal, C., Neal, M., Wickham, H., Hill, L., Harman, S. 2007. Dissolved iodine in rainfall, cloud, stream and groundwater in the Plynlimon area of mid-Wales. Hydrology and Earth System Sciences 11(1), 283-293.

O'Dowd, C.D., Jimenez, J.L., Bahreini, R., Flagan, R.C., Seinfeld, J.H., Hameri, H., Pirjola, L., Kulmala, K., Jennings, S.G., Hoffmann, T., 2002. Marine aerosol formation from biogenic iodine emissions. Nature 417, 632-636.

Organisation for Economic Co-operation and Development, 2005. OECD review of agricultural policies: China. Paris : Organisation for Economic Co-operation and Development, 235p.

Organisation for Economic Co-operation and Development, 2007. OECD environmental performance review of China. Paris: Organisation for Economic Co-operation and Development, 336p.

Oram, D.E., Penkett, S.A., 1994. Observations in Eastern England of elevated methyl iodide concentrations in air of Atlantic origin. Atmospheric Environment 28, 1159-1174.

Peng, Z., Lu, C., Zhang, L., Cheng, X., 2009. Urban fresh water resources consumption of China. China Geographical Science 19, 219-224.

Saiz-Lopez A., Plane, J.M.C., 2004. Novel iodine chemistry in the marine boundary layer. Geophysical Research Letters 31, L04112.

Scanlon, B.R., Healey, R.W., Cook, P.G., 2002. Choosing appropriate techniques for quantifying groundwater recharge. Hydrogeology Journal 10, 18-39

Scanlon, B.R., Keese, K.E., Flint, A.L., Flint, L.E., Gaye, C.B., Edmunds, W.M., Simmers, I., 2006. Global synthesis of groundwater recharge in semiarid and arid regions. Hydrological Processes 20, 3335-3370.

Scanlon, B.R., Nicot, J.P., Reedy, R.C., Kurtzman, D., Mukherjee, A., Nordstrom, D.K., 2009. Elevated naturally occurring arsenic in a semiarid oxidizing system, Southern High Plains aquifer, Texas, USA. Applied Geochemistry 24, 2061-2071.

Smedley, P.L., Kinniburgh, D.G., 2002. A review of the source, behaviour and distribution of arsenic in natural waters. Applied Geochemistry 17, 517-568.

Smedley, P.L., Kinniburgh, D.G., Macdonald, D.M.J., Nicolli, H.B., Barros, A.J., Tullio, J.O., Pearce, J.M., Alonso, M.S., 2005. Arsenic associations in sediments from the loess aquifer of La Pampa, Argentina. Applied Geochemistry 20, 989-1016.

Smythe-Wright, D., Boswell, S.M., Breithaupt, P., Davidson, R.D., Dimmer, C.H., Diaz, L.B.E., 2006. Methyl iodide production in the ocean: Implications for climate change. Global Biogeochemical Cycles 20, GB3003.

Tefrey, M.G., ul-Haque, I., 2010. Clean groundwater underpins the developing world. Ground Water 48(2), 170.

Truesdale, V.W., Jones, S.D., 1996. The variation of iodate and total iodine in some UK rainwaters during 1980-1981. Journal of Hydrology 179, 67-86.

Vogel, J.C., Ehhalt, D.H., 1963. The use of C isotopes in groundwater studies. In: Radioisotopes in Hydrology, IAEA, Vienna, pp. 383-396.

Wood, W.W., Sanford, W.E., 1995. Chemical and isotopic methods for quantifying ground-water recharge in a regional, semiarid environment. Ground Water 33, 458-468.

World Bank, 2008. World Development Indicators: Total Population. Electronic resource: http://datafinder.worldbank.org/population-total, accessed March, 2010.

Yuncheng Regional Water Bureau & Shanxi province Geological Survey, 1982. Hydrological and Geological maps and explanations for the Yuncheng region, 1:100000. Shanxi Geological Survey Special Report (In Chinese). 80p.

Zhu, G.F., Li, Z.Z., Su, Y.H., Ma, J.Z., Zhang, Y.Y., 2007. Hydrogeochemical and isotope evidence of groundwater evolution and recharge in Minqin basin, Northwest China. Journal of Hydrology 333, 239-251.

Chapter 2

Recharge history and controls on groundwater quality in the Yuncheng Basin, north China

Matthew J. Currell[1] , Ian Cartwright [1], Dean C. Bradley[1], Dongmei Han[2]

[1] School of Geosciences, Monash University, Clayton VIC 3800, Australia
[2] Institute of Geographic Sciences and Natural Resources Research, China Academy of Sciences, Beijing, 100101, China

-----Published in Journal of Hydrology (*J. Hydrol* ***385,* *216-229*)-----**

ABSTRACT

Environmental isotopes and water quality indicators (e.g. TDS and NO_3 contents) were used to characterize the age, recharge history and controls on the quality of groundwater resources in the Yuncheng Basin, north China, where extensive extraction occurs for agriculture and domestic supply. $\delta^{18}O$ and $\delta^{2}H$ values as low as -10.6‰ and -73‰, respectively, together with low radiocarbon activities (<20 pmC) show that deep groundwater comprises palaeowaters largely recharged in the late Pleistocene (~10 to 22ka B.P.) under a cooler climate than the present. Shallow groundwater has higher radiocarbon activities (>70 pmC), indicating a significant component of modern (post-1950s) recharge. The shallow groundwater has higher $\delta^{18}O$ and $\delta^{2}H$ values (up to -8.1‰ and -54‰) that are similar to those in modern summer monsoon rainfall, indicating that current recharge is via direct infiltration and/or leakage of ephemeral streams during heavy rain events. Historic recharge rates estimated using radiocarbon ages are between 1 and 10mm/yr, corresponding to <2% of local rainfall, which is lower than estimates of modern recharge

nearby based on tritium data. The relationship between groundwater $\delta^{18}O$ values and ^{14}C ages is similar to that observed in groundwater from other basins in northern China, confirming that much deep groundwater in the region is palaeowater, and suggesting that a broad scale assessment of groundwater residence times may be made from $\delta^{18}O$ and $\delta^{2}H$ values. Most deep groundwater has low TDS and nitrate concentrations (median 1090 mg/L and 1.8 mg/L, respectively), while shallow groundwater has TDS contents of up to 8450 mg/L (median 1980 mg/L) and NO_3 concentrations up to 630 mg/L (median 31 mg/L). A lack of enrichment in $\delta^{18}O$ values in the high salinity shallow groundwater indicates that transpiration by crops and possibly minor mineral dissolution are the major salinisation processes, rather than evaporation or leakage from salt lakes. The majority of nitrate in groundwater has $\delta^{15}N_{NO3}$ values between 0.8 - 5.0‰ and $\delta^{18}O_{NO3}$ values between 1.8 - 4.1‰, indicating that synthetic fertilizers are the main source of elevated NO_3 concentrations. Increasing residence times from east to west in deep groundwaters reflect the historic regional flow pattern in the basin. However, present-day flow is now dictated by a large cone of depression that has formed due to intensive deep groundwater pumping since the 1980s. High downward vertical hydraulic gradients (up to 0.45) have also developed as a result of this pumping, promoting downwards leakage of shallow water, indicated by high nitrate concentrations (>20 mg/L) in some deep wells (>180m). Preferential leakage has occurred near the Linyi fault, in the northern Sushui River Basin. Salinisation, nitrate contamination and excessive drawdown of deep groundwater are major concerns for the future of the groundwater resources in this region.

Keywords: Groundwater, Sustainability, Environmental Isotopes, China, Nitrate, Palaeowaters

2.1 INTRODUCTION

Groundwater is a vital source of clean drinking and irrigation water in many of the world's semi-arid regions. This is increasingly the case due to the effects of population growth and climate change, which are causing severe stress to surface water supplies in these areas (Edmunds, 2003). One of the most water-stressed parts of the world is northern China, which is a semi-arid region supporting a large population and major agricultural activity (Foster et al., 2004). In recent decades many shallow aquifers in northern China have become salinised and contaminated by nitrate and other pollutants due to human activities, particularly agriculture (e.g. Hu et al., 2005; Chen et al., 2006; Zhu et al., 2008). As a result, deep groundwater (>120m), which has generally been immune to these effects, is being increasingly utilized for both agriculture and domestic supply. Recent studies indicate that locally, deep groundwater supplies in northern China are palaeowaters that were recharged under different climatic conditions to the present and which may not be being replenished by modern recharge (e.g. Edmunds et al., 2006; Zhu et al., 2007; Gates et al., 2008a; Kreuzer et al., 2009). Determining whether this is generally the case throughout northern China is crucial in assessing the sustainability of deep groundwater use. There is also the potential for deep groundwater that is not fully confined to become contaminated due to downward leakage of overlying shallow groundwater if intensive pumping of the deep groundwater is occurring. Understanding the controls, timescales and impacts of such leakage is vital to the protection of deep groundwater quality.

This study examines groundwater from the Quaternary aquifer in the Yuncheng Basin, in southwest Shanxi Province, along the middle reaches of the Yellow River (Fig.

1). The Yuncheng Basin contributes up to 60% of total grain and 80% of cotton production in Shanxi province (Yuncheng City Water Bureau, pers. comm., 2008), which has a population of over 31 million. However, despite the reliance on groundwater for agriculture and domestic supply, few studies have been carried out to assess the age and recharge history of the basin's groundwater resources. These issues are addressed here using environmental isotopes ($\delta^{18}O$, $\delta^{2}H$, ^{14}C). An assessment of controls on groundwater quality, particularly sources of salinity and nitrate in the aquifer are also examined using TDS and NO_3 concentrations and $\delta^{15}N_{NO3}$ and $\delta^{18}O_{NO3}$ values. These data are combined with physical hydrogeology to determine where and to what extent vertical mixing is occurring. This research provides information that is vital for assessing the sustainability of groundwater extraction practices in a major agricultural region experiencing severe water stress. The results of this research add to the growing body of work on the paleoclimatic and groundwater recharge history of northern China (An et al., 2000; Chen et al., 2003; Edmunds et al., 2006; Huang et al., 2007; Gates et al. 2008a, 2008b; Kreuzer et al., 2009) and have relevance to many arid and semi-arid regions in the world that are dependent on deep groundwater.

2.2 STUDY AREA

2.2.1 Geological setting

The Yuncheng Basin, located between 34°50' and 35°30'N and 110°15' and 111°20'E, comprises two major geographic zones, the 5770 km^2 Sushui River Basin (elevation 350 to 500 m), and the E'mei Plateau (elevation 460 to 650 m) (Fig. 1). The Sushui River Basin occupies a subsiding graben enclosed by the frontier fault of the

Zhongtiao Mountains to the south and the Linyi Fault to the north. These faults are oriented ENE-WSW and are linked by a zone of transform faulting to the east (Xu and Ma, 1992) (Fig. 1). The Sushui River Basin contains a 300 - 500 m thick Quaternary aquifer that consists of interlayered sediments, primarily aeolian loess, along with lacustrine clays and fluvial sands and gravels (Yuncheng Regional Water Bureau, 1982; Huang et al., 2007). The loess was deposited during the Pleistocene by dust storms that carried weathered material from deserts in northwest China and central Asia to the region (Liu et al., 1982). Based on palaeosol horizons and fossil assemblages, there are four major stratigraphic divisions in the Quaternary sediments (Q1 – Q4) (Liu et al., 1982; 1986), which can be broadly correlated across much of northern China (China Geological Survey, 2002).

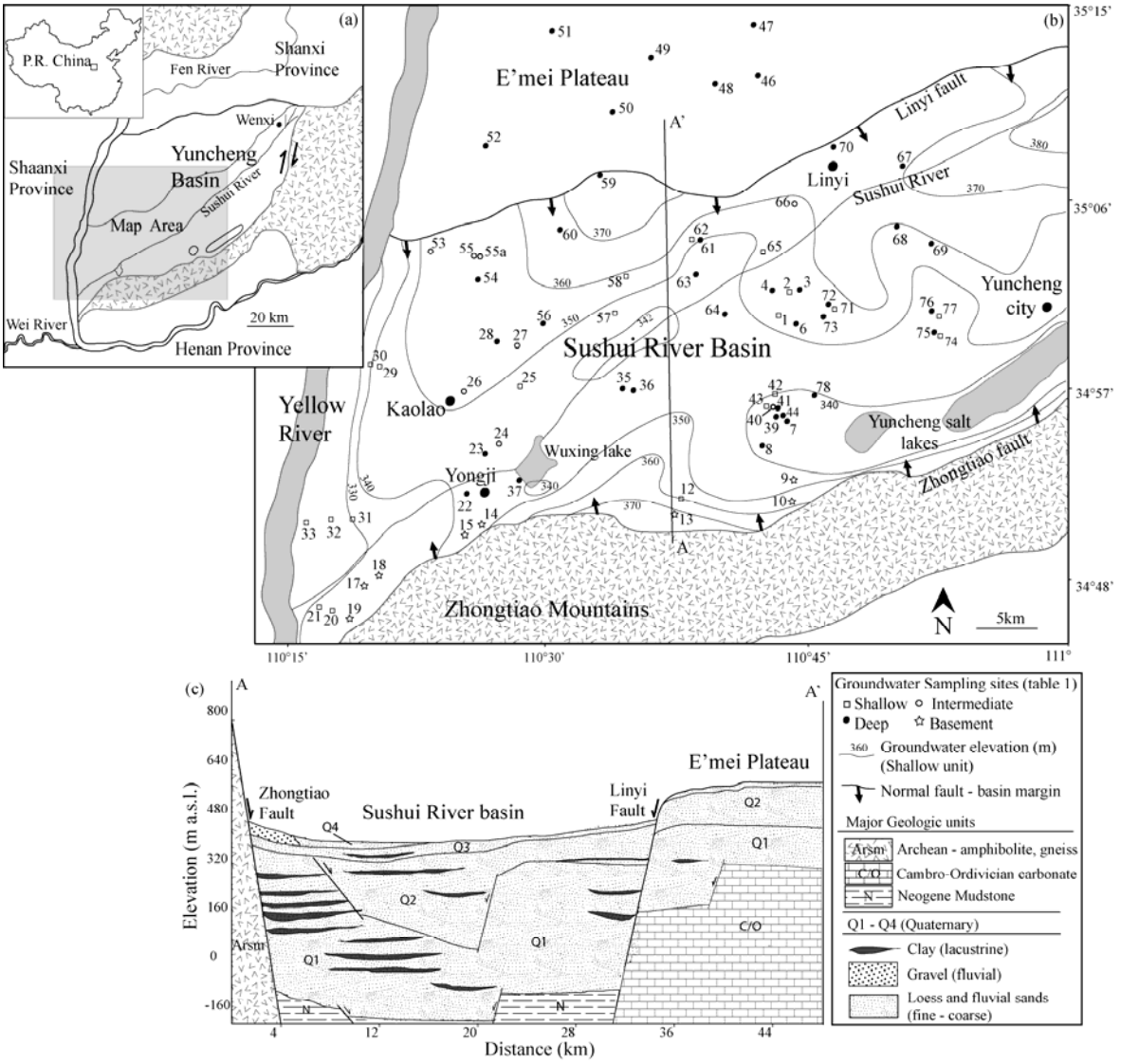

Fig. 1a. Location of the Yuncheng Basin in Shanxi province, China, with the study area highlighted and sample localities marked. **1b** Schematic cross-section of the basin, showing the Quaternary Aquifer and major hydrostratigraphic units. Data from Yuncheng Regional Water Bureau, (1982) and China Geological Survey, (2006).

The Quaternary aquifer comprises a shallow, unconfined unit (Q3 and locally Q4) with a total thickness ranging from 15 to 70m, and a semi-confined deep unit (Q1 and locally Q2) that is 250 to 500 m thick (China Geological Survey, 2006; Fig. 1). The two units are separated by a major non-depositional horizon with a well-developed palaeosol layer (referred to as the S1 palaeosol by Liu et al., 1986). It has been suggested that a

separate intermediate unit exists between ~80 and 120m, although this unit is probably part of and/or connected with the deep unit (Cao 2005). In the E'mei Plateau region there is no shallow aquifer but groundwater is present in confined sand layers below 120m depth, under a thick accumulation of massive, low porosity Q3 and Q2 loess. Deep groundwater below the E'mei Plateau probably connects with deep groundwater in the Sushui River Basin (Yuncheng Regional Water Bureau, 1982). In the south of the area adjacent to the Zhongtiao Mountains, the Quaternary aquifer sits above fractured Archaean metamorphic rocks (Arsm), which include hornblendite, amphibolite and quartzite that also make up the Zhongtiao Mountains. The basement hosts groundwater in fractures, and this water is used as a limited drinking supply. Elsewhere, the Quaternary sediments are underlain by sedimentary rocks, mainly Neogene mudstone and Cambro-Ordivician limestone (Fig. 1; Yuncheng Regional Water Bureau, 1982).

2.2.2 Climate and groundwater use

The climate in the basin is semi-arid with average rainfall of ~550mm/year, approximately 70% of which occurs during the East-Asian summer monsoon between June and October (China Geological Survey, 2006). Groundwater supplies both domestic and irrigation water. Low intensity irrigated agriculture began in the 1960s, mostly using surface water diverted from the Yellow river, while large-scale groundwater extraction for irrigation and domestic supply commenced in the 1980s, along with planting of cash crops such as cotton and fruit orchards. In recent years, the bulk of groundwater pumping has been from deep wells (>120m) due to the poor quality of much of the shallow groundwater (Cao, 2005).

2.2.3 Groundwater flow

Based on groundwater elevations in 2004, horizontal groundwater flow is from the basin margins towards its centre (Fig. 1) (China Geological Survey, 2006). The Yuncheng salt lakes and Wuxing Lake occupy topographic lows and act as local discharge areas. Horizontal hydraulic gradients in the shallow unit (Q3 & Q4) are relatively low (0.01 to 0.001) particularly in the centre of the basin (Fig. 1). Horizontal hydraulic gradients in the deep unit (Q1 & Q2) are higher (up to 0.015), which probably results in faster horizontal flow than in the shallow unit. Vertical groundwater flow is downwards throughout the basin, and is now likely more rapid than horizontal flow due to high vertical hydraulic gradients (0.01 to 0.45) caused by deep groundwater pumping.

2.3 SAMPLING AND ANALYSIS

Groundwater wells ranging from 15 to 350m in depth have been drilled throughout the Quaternary aquifer. Sampling of wells was conducted in three counties – Yongji, Linyi and Yuncheng, covering the western Sushui River Basin, and a small part of the E'mei Plateau (Fig. 1). 73 groundwater samples were collected from irrigation and domestic supply wells, most of which were being continuously pumped. Some of the irrigation wells have long screened intervals (several meters), and therefore water samples are from a relatively wide section of the aquifer. 20 samples were collected from shallow wells (17 to 70 m) screened in the Q3 and Q4 layers (Fig. 1), while 45 samples were from deep wells (80 to 320m), in the Q1 and Q2 layers. Among these, eight samples were from wells in the top of the Q1 and Q2 unit between 80 and 120m depth ('intermediate' samples), while 37 are from wells greater than 160m depth (Table 1). Eight samples were also collected from

wells screened in the basement in the far south of the region. Electrical conductivity and pH were measured during sample collection using Extech Instruments portable meters. Alkalinity was determined with a Hach digital titrator, by addition of bromocresol-green methyl red indicator and titration with 1.5N H_2SO_4 on the day of sample collection. Dissolved oxygen was measured immediately after sample collection either using drop-wise titration of $Na_2S_2O_3$ after addition of $MnSO_4$, KI and H_2NSO_3H or with an Extech Instruments DO meter. Samples for isotope and major ion analysis were collected in HDPE bottles, filled to overflowing and capped.

$\delta^{18}O$, $\delta^{2}H$ and $\delta^{13}C$ values were measured using a Finnigan MAT 252 mass spectrometer at Monash University. $\delta^{18}O$ values were determined via equilibration with He-CO_2 at 25°C for 24 hours and analysed by continuous flow using a ThermoFinnigan Gas Bench. $\delta^{2}H$ was measured by reaction with Cr at 850°C, using an automated Finnigan MAT H/Device. $\delta^{18}O$ and $\delta^{2}H$ values were measured relative to internal standards calibrated using IAEA VSMOW, GISP and SLAP. Data were normalized following Coplen, (1988) and are expressed relative to VSMOW, where $\delta^{18}O$ and $\delta^{2}H$ of SLAP are -55.5‰ and -428‰, respectively. $\delta^{13}C$ values of dissolved inorganic carbon (DIC) were measured by acidification with H_3PO_4 in a He atmosphere and analysed by continuous flow. Precision (1σ) is: $\delta^{18}O = \pm 0.1$‰; $\delta^{2}H = \pm 1$‰. $\delta^{13}C = \pm 0.2$‰. $\delta^{15}N$ values were determined on total N using a Carlo Erba 1110 Flash EA and a ThermoFinnigan DeltaPlus Advantage mass spectrometer. Precision (1σ) is ±0.2‰. It was assumed that all N was present as NO_3, given the oxygen-rich nature of the samples. $\delta^{18}O$ of nitrates were measured following McIlvin and Altabet (2005) using a GVI Isoprime mass spectrometer. Radiocarbon (^{14}C) activities were measured using accelerator mass spectrometry (AMS) at

Australian National University, Canberra. The activities were expressed as percent modern carbon (pmC) values, with standard errors ranging between ±0.08 to 0.53 PMC. Nitrate concentrations (along with other major anion contents) were measured on filtered samples using a Metrohm ion chromatograph at Monash University.

2.4 RESULTS AND DISCUSSION

2.4.1 Groundwater quality

Groundwater total dissolved solids (TDS) concentrations range between 261 mg/L and 8450 mg/L (Table 1). The freshest groundwater is from the basement (TDS 261 to 504 mg/L, median 370 mg/L) followed by deep groundwater (TDS 526 to 1810 mg/L, median 1090 mg/L) and the intermediate wells (765 to 5150 mg/L, median 1060), while shallow groundwater (<70 m depth) is the most saline (700 to 8450 mg/L, median 1980 mg/L) (Fig. 2). TDS contents are generally lower at the basin margins and higher in the center (Fig. 2). This increase is likely due to a combination of evapotranspiration and mineral dissolution along groundwater flow paths.

Sample no.	Unit*	Depth (m)	Latitude	Longitude	TDS (mg/L)	pH	O_2 (mg/L)	HCO_3 (mg/L)	NO_3 (mg/L)	δ^2H ‰	$\delta^{18}O$ ‰	Pre - evaporation δ^2H‰	Pre - evaporation $\delta^{18}O$‰	$\delta^{13}C$ ‰	$\delta^{15}N$ ‰	$\delta^{18}O_{NO3}$ ‰	D-excess d
1	S	34	350029.8	1104326.8	5290	7.60	4	740	633	-63	-8.9			-11.2	2.2		8.1
2	S	20	350139.2	1104405.1	3100	7.86	6	730	36.2	-66	-8.7			-11.2	1.5	2.57	3.6
12	S	20	345153.5	1103748.1	713	7.20	1	448	0.08	-64	-9.6			-14.4			13
20	S	30	344630.5	1101738.2	2160	7.66	3	460	56.8	-44	-5.2	-56	-8.2	-14.0	12.0		9.6
21	S	70	344641.6	1101653.9	838	7.80	2	332	24.5	-60	-9.0			-15.6	7.1		12
25	S	58.5	345709.6	1102823.7	1490	8.65	2	596	0.13	-56	-8.2			-9.9			9.6
29	S	35	345802.1	1102022.3	700	8.22	2	792	1.15	-46	-5.7	-56	-8.2	-9.9			9.6
30	S	40	345814.5	1101948.8	858	8.25	3	864	1.17	-41	-3.5	-63	-9.1	-9.3	2.2		10
31	S	50	345050.9	1101846.8	1950	7.78	4	424	1.27	-51	-7.2	-54	-8.1	-12.1			11
32	S	50	345046.4	1101727.6	2010	8.24	3	336	0.13	-65	-10.0			-13.2	3.1		15
33	S	70	345037.8	1101536	5290	8.17	4	312	0.11	-60	-9.1			-14.6			13
42	S	17	345649.4	1104309	6090	7.36	5	463	69.4	-63	-8.5			-10.8	8.8	6.82	5.3
43	S	20	345612.9	1104240.5	8450	7.94	6	269	54.5	-61	-8.1				15.1	6.60	3.8
57	S	55	350036.6	1103355.4	879	8.65	5	547	36.5	-61	-8.3			-9.5	4.1	3.11	5.6
58	S	30	350223.3	1103435	1480	8.60	6	680	105	-65	-9.4			-10.1			11
62	S	40	350412.2	1103826.7	1540	8.18	5	520	24.4	-66	-9.0			-11.1	2.0	2.34	5.4
65	S	40	350337.4	1104233.7	2590	7.64	6	648	63.0	-64	-8.6			-11.0	6.3		4.8
71	S	27	350058.6	1104616.9	2010	8.27	6	558	27.0	-65	-8.6			-11.3	4.4		3.6
74	S	30	345934.5	1105241	2490	7.83	4	644	103	-65	-8.8			-12.8	7.6	4.14	5.4
77	S	40	350029.4	1105233.2	2530	8.11	5	630	192	-60	-8.7				12.1	11.40	9.4
24	I	120	345488.9	1102713.5	1120	8.33	3	340	0.66	-68	-10.0			-13.0	3.0		12
26	I	110	345655.8	1102513.4	845	8.55	3	389	0.11	-64	-8.9			-10.4	3.5		7.3
27	I	117	345909.1	1102819	865	8.79	4	148	0.08	-62	-8.5			-9.8			6.1
40	I	80	345610.2	1104258.7	4670	7.76	5	415	21.2	-57	-7.5				1.9		3.3
53	I	120	350334.7	1102309.7	765	8.12	6	312	13.5	-70	-9.81						8.6
55	I	120	350319.2	1102930.3	5150	7.75	2	648	33.9	-74	-10.3						8.7
55a	I	120	350319.2	1102930.3	1010	7.9	2	605	23.1		-10.0						8.4
66	I	100	350548.4	1104421.7	3070	7.98	6	500	22.3	-66	-9.3			-9.8	5.0	1.80	6.7
3	D	240	350144.1	1104435.2	1090	8.20	3	448	2.16	-67	-9.0			-9.7			5.4
4	D	270	350140.5	1104301	1310	8.13	4	308	1.43	-71	-9.9			-10.8			7.9
6	D	220	350008.8	1104426	957	8.03	7	444	0.39	-65	-9.0			-10.2			7.3
7	D	300	345540.2	1104336.5	1110	7.84	1	264	1.31	-72	-10.3			-12.4			10
8	D	230	345421.3	1104226.4	774	8.06	4	332	0.94	-73	-10.3			-16.4			9.3
22	D	240	345205.2	1102527.1	733	8.13	2	224	0.27	-72	-10.8			-14.2	1.0		14
23	D	150	345400.6	1102629.6	601	8.28	4	268	0.21	-66	-10.3			-14.6			17
28	D	210	345913.7	1102713.8	1810	8.35	5	556	0.88	-66	-8.6			-10.3			2.9

*S = Shallow, D = Deep, I = Intermediate, B = Basement

Continued..

Sample no.	Unit*	Depth (m)	Northing	Easting	TDS (mg/L)	pH	O_2 (mg/L)	HCO_3 (mg/L)	NO_3 (mg/L)	δ^2H ‰	$\delta^{18}O$ ‰	$\delta^{13}C$ ‰	$\delta^{15}N$ ‰	$\delta^{18}O_{NO3}$ ‰	D-excess d
35	D	210	345701.4	1103426.2	1630	8.26	2	208	2.29	-69	-10.0	-13.7			11
36	D	250	345700.5	1103504.3	1630	8.16	2	356	0.60	-69	-9.9	-11.3			10
37	D	200	345235.6	1102832.6	1040	8.42	3	220	0.22	-73	-10.6	-13.3			12
39	D	220	345550.4	1104301.7	1090	7.93	6	262	2.41	-71	-10.2	-12.0	1.7		11
41	D	270	345610.2	1104258.7	1060	8.05	4	282	1.69	-73	-9.9	-13.4	4.6		6.4
44	D	300	345552.9	1104324.1	1110	8.15	6	255	2.47	-73	-10.3	-11.3	3.6		9.5
46	D	210	351152.4	1104613.9	667	7.80	6	344	29.5	-69	-9.5	-10.0			7.4
47	D	200	351412.9	1104157.2	526	7.83	6	358	11.3	-69	-9.7	-10.3	1.9		9.2
48	D	260	351129.2	1103943.3	608	8.14	7	421	21.3	-64	-8.8	-8.9	4.3		6.0
49	D	260	351238.6	1103559.4	579	7.90	6	316	39.7	-70	-10.1	-8.3	3.8	3.03	10
50	D	230	351008.8	1103346.9	634	8.30	6	420	22.9	-66	-9.1	-8.2	3.8		7.0
51	D	224	351353.5	1103018.6	561	8.32	7	360	24.2	-66	-9.2	-8.3	4.2		7.9
52	D	280	350830.8	1102630.3	623	8.15	6	430	18.0	-65	-9.2	-9.3			9.1
54	D	160	350211.5	1102601.5	1290	7.94	2	615	43.5	-64	-8.7	-9.2	1.6	2.12	5.4
56	D	220	350006.5	1102946.9	1020	8.61	5	685	7.09	-64	-8.6	-9.9	2.4		4.6
59	D	230	350710.5	1103303.4	1290	7.80	6	272	12.2	-73	-10.4		7.9		9.8
60	D	178	350435.9	1103049.3	1270	8.57	6	566	211	-67	-9.5	-8.9	2.5	2.97	8.8
61	D	180	350409.8	1103804.7	1240	8.04	6	456	11.0	-66	-9.0				6.0
63	D	220	350227.4	1103837.8	1820	8.13	3	186	3.89	-80	-10.7		3.5		5.4
64	D	180	350029.2	1104016.1	1100	8.10	5	434	0.457	-73	-9.7	-9.5	2.8		4.8
67	D	202	350731.4	1105031	748	7.97	4	398	0.295	-65	-9.2	-8.9			8.3
68	D	180	350540.1	1105145.9	1270	7.93	6	448	0.989	-64	-9.4				11
69	D	200	350442.7	1105012.4	1110	7.69	2	422	1.27	-67	-9.2	-10.3	0.8		6.4
70	D	230	350829.2	1104633.9	994	7.57	6	356	20.5	-72	-9.5		8.5	3.91	4.1
72	D	240	350058.6	1104616.9	1090	7.89	3	396	0.227	-70	-9.6	-9.6	3.1		6.5
73	D	180	350026.7	1104557.5	1160	7.84	3	384	0.783	-72	-9.7				5.3
75	D	320	345941.8	1105225.8	821	8.17	6	336	0.877	-68	-9.5	-9.5	2.5		8.0
76	D	230	350041.4	1105214	1250	7.86	4	352	1.76	-74	-9.9	-11.8			5.4
78	D	230	345645.5	1104529.3	868	8.06	4	334	1.27	-66	-9.6				11
9	B	347	345421.3	1104423.4	406	7.55	6	276	7.41	-64	-9.3	-13.6			11
10	B	100	345143.5	1104404.4	380	7.62	4	248	0.01	-63	-10.4	-12.7			11
13	B	160	345109.3	1103719.8	329	7.42	5	208	0.01	-62	-9.7	-12.7			15
14	B	190	345041.6	1102620.1	360	7.42	5	164	12.1	-65	-10.1	-13.9			16
15	B	254	345001	1102513.4	261	7.52	2	148	2.55	-62	-9.3	-13.8			16
17	B	75	344740.3	1101930	504	7.80	5	304	14.6	-62	-9.3	-12.2			13
18	B	130	344812.4	1102019.9	335	7.75	6	208	4.41	-58	-9.2	-13.8			15
19	B	115	344607.1	1101834.8	440	7.86	5	280	11.9	-61	-9.0	-12.2			11

Table 1. Grounwater sample numbers, locations and depths; results of groundwater chemical and isotopic analyses

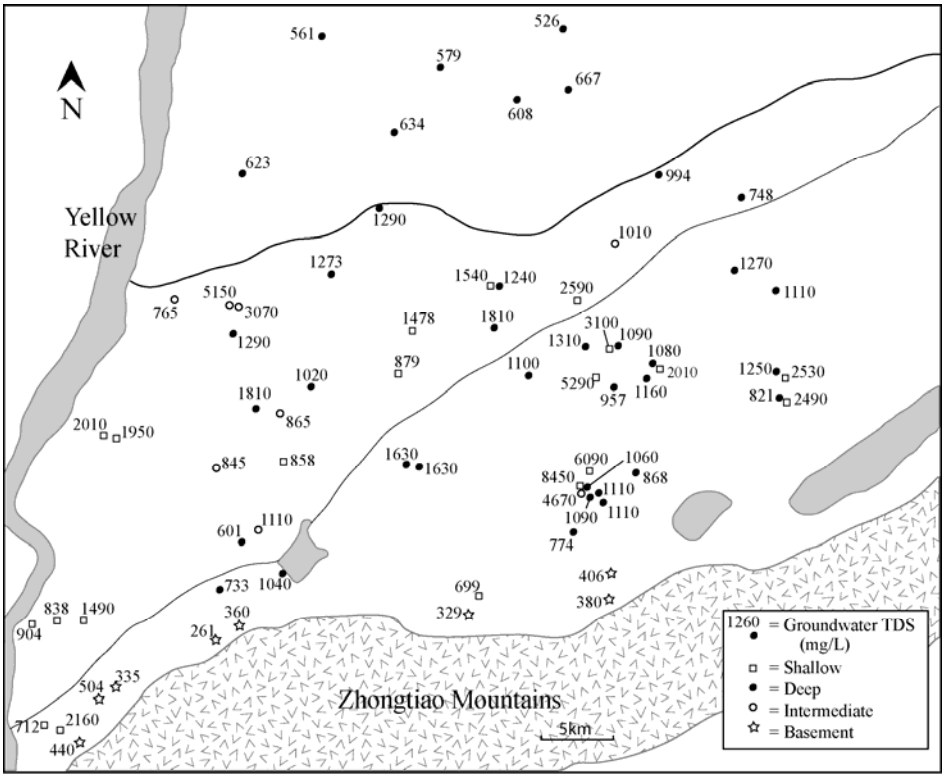

Fig. 2. Groundwater TDS concentrations in shallow, intermediate, deep and basement wells. High concentrations in shallow groundwater, particularly at the center of the basin, are primarily due to transpiration. (Data from Table 1.)

High nitrate (NO_3) concentrations occur locally, particularly in shallow groundwater (range 0.08 to 630 mg/L, median 31.6 mg/L; Fig. 3, Fig. 4). Due to the lack of natural nitrate in most geologic formations, NO_3 concentrations >5 mg/L generally indicate contamination by fertilizers, animal wastes and/or effluents (Heaton, 1986). $\delta^{15}N_{NO3}$ and $\delta^{18}O_{NO3}$ values in ~75% of groundwater samples are between 0.8 - 5.0‰ and 1.8 - 4.1‰, respectively (Table 1), indicating that a large proportion of nitrate is derived from synthetic fertilizers (c.f. Fogg et al., 1998). Ammonium carbonate $(NH_4)_2CO_3$ and urea NH_4NO_3 are both used extensively in the region to fertilize crops, and as they are manufactured using atmospheric N_2 they would add N with $\delta^{15}N$ values close to 0‰ to groundwater. Seven shallow groundwater samples have nitrate concentrations >10 mg/L and higher $\delta^{15}N_{NO3}$ values (> 6‰). Increasing $\delta^{18}O_{NO3}$ with increasing $\delta^{15}N$ values in these

samples indicate that these waters have probably undergone de-nitrification (Kendall, 1998; Fig 3).

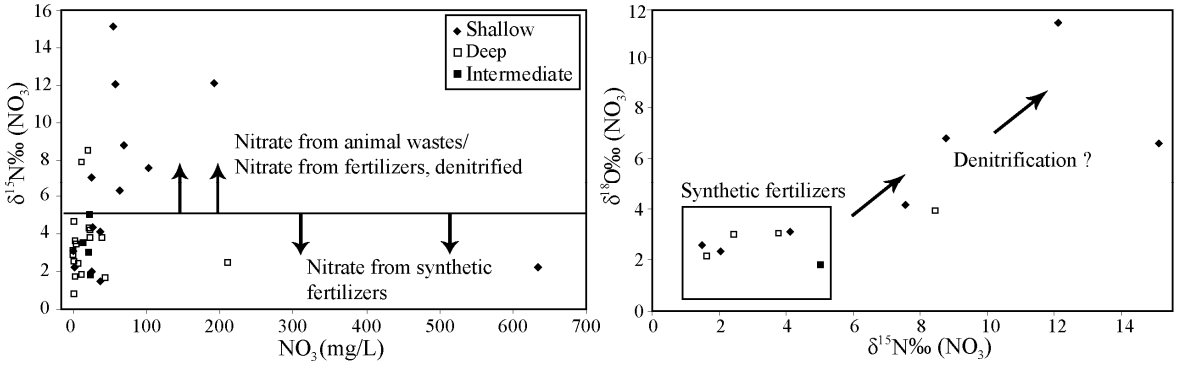

Fig. 3a. $\delta^{15}N_{NO3}$ values and NO_3 concentrations. Most nitrate in groundwater appears to come from synthetic fertilizers. **3b**. $\delta^{15}N_{NO3}$ and $\delta^{18}O_{NO3}$ values, indicating de-nitrification has occurred in some shallow samples with high nitrate concentrations (Data from Table 1).

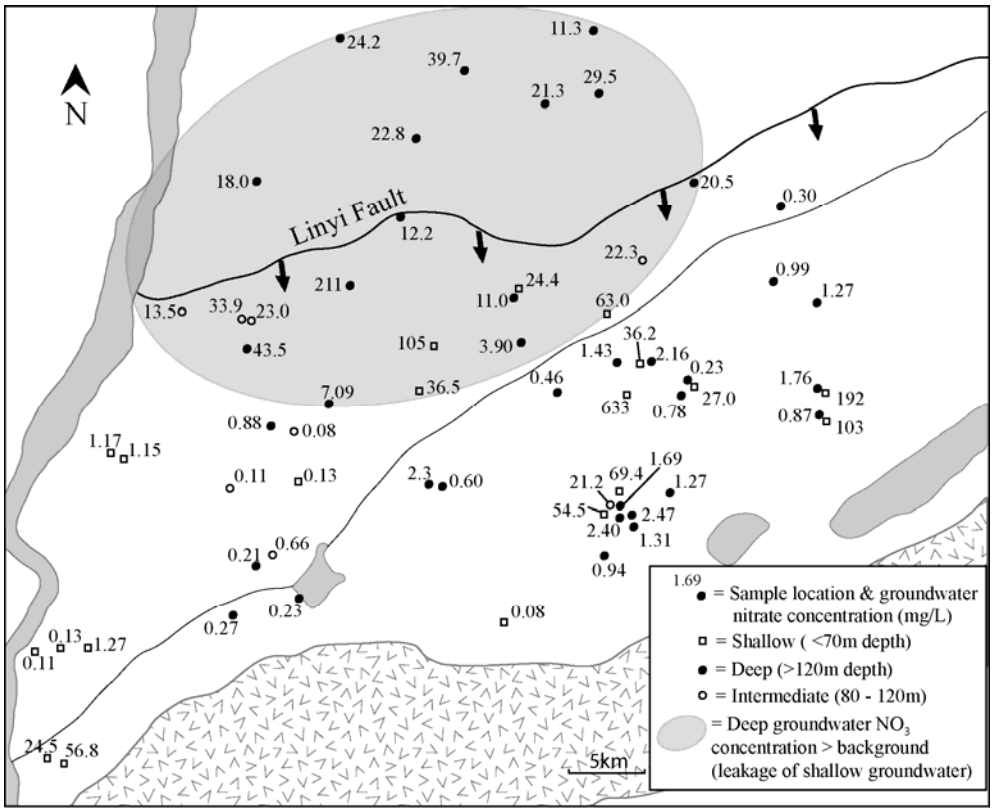

Fig. 4. Groundwater Nitrate concentrations in shallow, intermediate and deep wells (data from Table 1).The highest concentrations are found in shallow groundwater samples; however elevated concentrations also occur in deep wells (highlighted), particularly near the Linyi fault, indicating downwards leakage of shallow water.

2.4.2 Vertical mixing

Due to the increased extraction of groundwater from deep wells over the last 25 years (currently ~80% of extraction comes from wells deeper than 120m); the hydraulic head in the deep aquifer has steadily declined. This is particularly true within the cone of depression west of Yuncheng City, where the rate of drawdown has been ~3m/year since 1986 (Cao, 2005). In contrast, low pumping rates of shallow groundwater and addition of irrigation returns have resulted in steady or rising head levels in shallow wells (Cao, 2005). The difference in hydraulic head between the shallow (Q3 & Q4) and deep (Q1 & Q2) units in 2004 is shown on Fig. 5. Under natural conditions, there was probably little difference in head between the units (Cao, 2005). However currently in the cone of depression the difference in head exceeds 90m, translating to downward hydraulic gradients of up to 0.45.

Given the relatively low background nitrate concentrations in deep groundwater samples (<2 mg/L, Fig. 4) and that the major N source is modern agriculture, high NO_3 concentrations in deep groundwater are a strong indication of downwards vertical leakage of shallow groundwater. The majority of deep groundwater samples have low nitrate concentrations (median 1.8 mg/L); however 13 of the 37 samples have NO_3 concentrations >7 mg/L and 5 of 7 intermediate samples have concentrations >13.5 mg/L, indicating that vertical leakage has occurred. All but one of these samples are in the north of the study area, either in the E'mei plateau or to the immediate south of the Linyi Fault in the northern Sushui River Basin (Fig. 4). The Linyi Fault thus appears to be acting as a pathway for downward leakage. This is consistent with higher dissolved oxygen values in these samples compared to the rest of the deep groundwater (median 5.7 vs. 3.9 mg/L,

considered to be from different populations at the 95% level using a Mann-Whitney U-test). There is also evidence of more gradual vertical mixing occurring throughout the whole basin; for example, in addition to having elevated NO_3 concentrations a number of samples from intermediate wells (80 to 120m) have elevated TDS contents, and TDS and NO_3 contents generally decrease and homogenize with depth (Fig. 5b & c). These data are consistent with gradual vertical mixing between saline shallow groundwater and lower salinity deep groundwater throughout the basin.

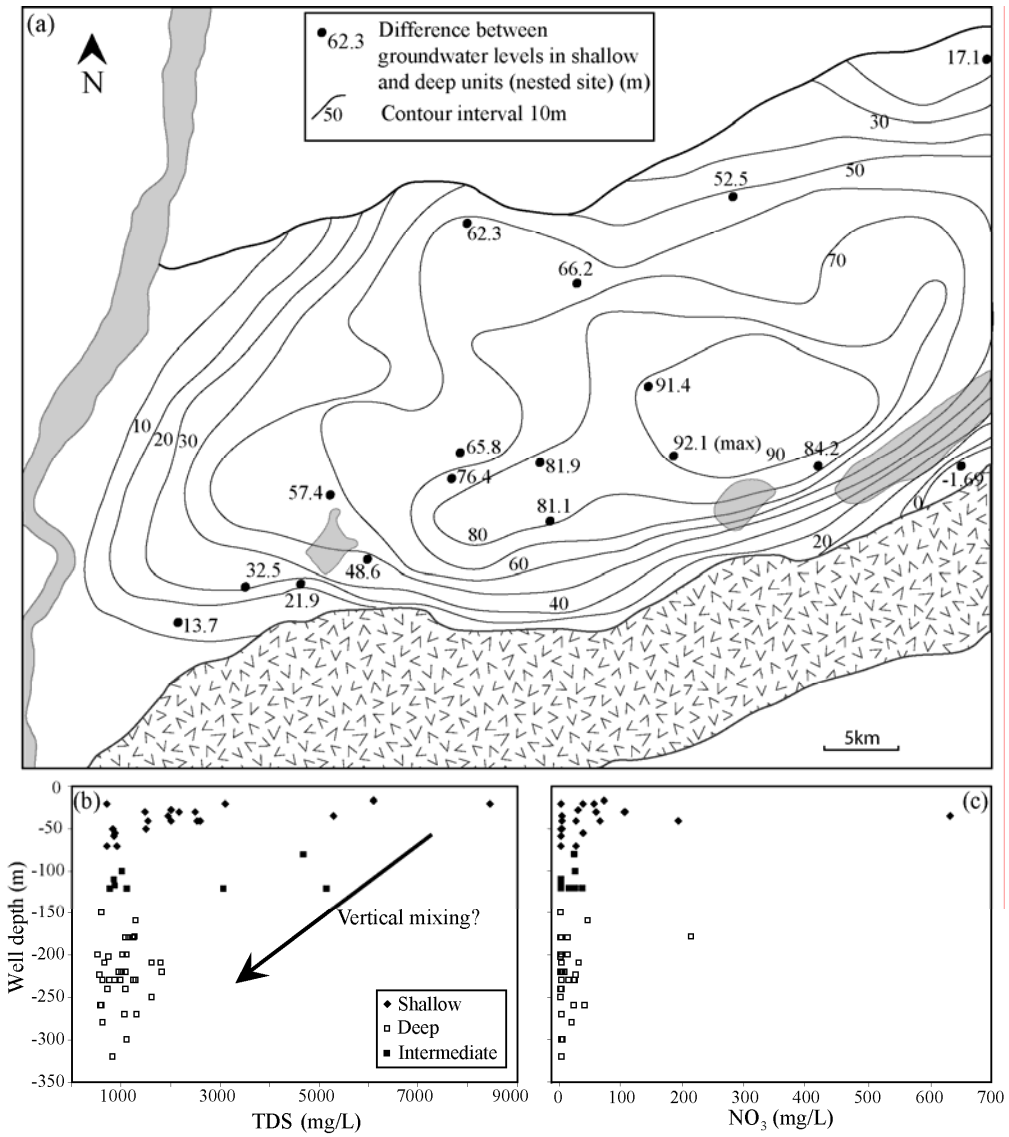

Fig. 5a. Difference in hydraulic head (in meters) between shallow and deep aquifer units (data from China Geological Survey, 2006). The difference is largest in the cone of depression, where agriculture and deep groundwater extraction have been very intensive since the 1980s. TDS contents vs. depth (**5b**) and nitrate concentrations vs. depth (**5c**), show patterns consistent with vertical mixing (data from Table 1)

2.4.3 Estimation of groundwater residence times

Groundwater radiocarbon activities range from 5.93 to 88.15 percent modern carbon (pmC) (Table 2). These values indicate a range of groundwater residence times, spanning the Holocene and late Pleistocene. Based on previous study of groundwater ^{14}C

activities and noble gas temperatures, ^{14}C activities of ~20pmC in groundwater from northern China are thought to broadly correspond to the Pleistocene/Holocene transition (Edmunds et al. 2006; Kreuzer et al. 2009). Two models were applied to convert pmC values into residence times, correcting for dissolution of ^{14}C–free carbon from carbonate in the aquifer. A broad positive correlation between groundwater HCO_3 concentrations and $\delta^{13}C$ values (Fig. 6) indicates that dissolution of carbonate minerals contributes substantially to groundwater DIC. Hence, the chemical mass balance (CMB) method of Fontes and Garnier, (1979) and a $\delta^{13}C$ mixing model (Pearson, 1965; Clark and Fritz, 1997) were considered applicable. A range of input parameters were applied, allowing a mean age for each sample to be calculated (Table 2).

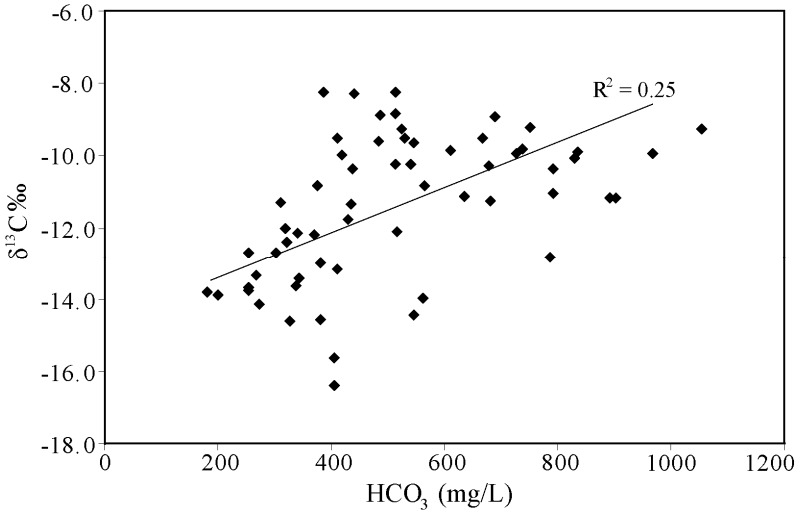

Fig. 6. Groundwater DIC concentrations and $\delta^{13}C$ values. The positive correlation indicates that groundwater derives substantial DIC from dissolution of matrix carbon, with relatively high $\delta^{13}C$ values (Data in Table 1.)

For the chemical mass balance model q (the fraction of ^{14}C-active C) = $m\text{DIC}_{rech}/m\text{DIC}_{final}$, where $m\text{DIC}_{rech}$ is the molar concentration of DIC in recharging water and $m\text{DIC}_{final}$ the final groundwater DIC concentration. $m\text{DIC}_{final}$ was estimated using: $m\text{DIC}_{final} = m\text{DIC}_{rech} + [m\text{Ca} + \text{Mg} – \text{SO}_4 + 0.5(\text{Na} + \text{K} - \text{Cl})]$, which accounts for major

water-rock interaction processes in typical aquifers (Fontes and Garnier 1979). $m\text{DIC}_{\text{RECH}}$ was estimated using two approaches, firstly by assuming the pH and temperature dependant DIC concentration of recharging water (e.g. at pH = 6, T = 15°C; $m\text{DIC}_{\text{RECH}}$ = 10 mmol/L). Secondly, one shallow groundwater (sample 12) from the piedmont of the Zhongtiao mountains was taken as being the best representative of groundwater in a recharge area, as it is from a shallow depth (20m) and has relatively low TDS (700 mg/L) and pH (7.2). The DIC concentration from this sample (7.34 mmol/L) was also used as $\text{mDIC}_{\text{rech}}$ (Table 2).

The $\delta^{13}C$ mixing model assumes open-system equilibration between soil DIC and dissolved atmospheric CO_2 during recharge, followed by closed-system carbonate dissolution in the aquifer. From mass balance q (the proportion of total C derived from recharging water) is given by:

$$q = \frac{\delta^{13}C_{DIC} - \delta^{13}C_{CARB}}{\delta^{13}C_{RECH} - \delta^{13}C_{CARB}}$$ (Clark and Fritz, 1997)

$\delta^{13}C_{DIC}$ is the measured $\delta^{13}C$ of DIC in groundwater; $\delta^{13}C_{CARB}$ is that from the aquifer sediment (loess), taken as -4‰ (e.g. Cao et al. 2008) and $\delta^{13}C_{RECH}$ is the $\delta^{13}C$ of the water when it reaches the saturated zone. Using a $\delta^{13}C_{RECH}$ of -18‰, which has been suggested as appropriate for soils in northwestern China dominated by C_3 plants (Gates et al. 2008), yields a set of relatively low q values, including a number of values < 0.5. Using a value of -15‰ produced a more realistic set of q values (Table 2), which may suggest a greater component of C_4 vegetation in the Yuncheng region compared to northwest China (e.g. Yu et al. 2000).

Sample	Unit	$a^{14}C$ pmC	±	Uncorrected age (yr)	$\delta^{13}C$ ‰ (PDB)	$\delta^{13}C$ mixing model q	Residence time	Fontes & Garnier (1979) model q(I)	q(II)	Residence time I,II	Mean residence time (yr)
30	S	88.2	0.4	1000	-9.3	0.58	Modern	0.46	0.39	Modern	Modern
31	S	71.3	0.3	2700	-12.1	0.75	500	0.67	0.60	Modern	Modern
57	S	37.2	0.2	7900	-9.5	0.59	3800	0.64	0.57	3500, 4500	3900± 600
40	D(I)	88.7	0.3	1000	-10	0.62	Modern	0.66	0.59	Modern	Modern
66	D(I)	34.0	0.1	8600	-9.8	0.61	4800	0.66	0.59	4600, 5500	5000± 500
27	D(I)	34.0	0.2	8700	-9.7	0.60	4800	0.61	0.53	3800, 4900	4500± 700
23	D*	18.7	0.1	13400	-14.6	0.91	13100	0.77	0.71	11000, 11700	12200± 1200
54	D*	5.9	0.1	22700	-9.2	0.57	18800	0.60	0.53	18200, 19300	18800±600
60	D*	15.6	0.1	14900	-8.9	0.55	10500	0.58	0.51	9700, 10900	10400± 700
64	D	12.4	0.1	16800	-9.5	0.59	13000	0.71	0.64	13600, 14400	13500± 900
37	D	5.9	0.1	22700	-13.3	0.83	21900	0.81	0.76	21100, 21600	21600±500
67	D	36.4	0.2	8100	-8.9	0.55	3500	0.70	0.63	4500, 5400	4200±1200
35	D	19.7	0.1	13000	-13.7	0.85	12100	0.89	0.86	12200, 12500	12200±300
56	D*	21.1	0.1	12500	-9.9	0.62	8900	0.61	0.53	7700, 8800	8600± 900
8	D	11.3	0.1	17500	-16.4	1.02	18000	0.78	0.73	15400, 16000	17000± 1600
3	D	25.0	0.2	11100	-9.8	0.61	7400	0.69	0.62	7600, 8500	7700± 800
72	D	29.9	0.1	9700	-9.6	0.60	5700	0.70	0.63	6300, 7100	6200±900
49	D*	22.3	0.1	12100	-8.3	0.52	7000	0.81	0.76	10100, 10700	8700± 2000
4	D	13.1	0.1	16400	-10.8	0.68	13600	0.77	0.71	14000, 14700	14000± 700
44	D	20.3	0.2	12800	-11.3	0.70	10300	0.79	0.74	10700, 11200	10600± 600
75	D	38.4	0.2	7700	-9.5	0.59	3600	0.72	0.65	4400, 5200	4200± 1000
9	B	63.1	0.3	3700	-13.6	0.85	2500	0.78	0.72	1100, 1800	2000± 900
10	B	78.7	0.5	1900	-12.7	0.79	100	0.80	0.74	Modern, 100	Modern
18	B	84.9	0.3	1300	-13.8	0.86	100	0.83	0.78	Modern	Modern

*Samples with high NO_3 concentration (imply mixing with young groundwater)

Table 2. Groundwater radiocarbon activities and $\delta^{13}C$ data; groundwater residence time estimates based on various correction schemes.

Many of the q values calculated using both models are below the range generally quoted for loess (0.75 – 0.9: Vogel, 1970), which is consistent with the calcite-rich mineralogy of loess in the region (Liu 1988). A mean residence time was calculated giving equal weight to the $\delta^{13}C$ mixing model and the CMB model. The residence times are broadly consistent with groundwater in other major aquifers in northern China and show similar relationships with $\delta^{18}O$ values to other groundwater in the region (discussed below in *2.4.7 - Regional context*).

2.4.4 Groundwater residence times, recharge, and flow paths

The range of groundwater residence times spans over 20,000 years (Table 2). Five groundwater samples, including two of three shallow groundwater samples, two basement

samples and one intermediate sample yield modern ages (corrected initial ^{14}C activities >100 pmC), indicating that they were either recharged since the 1950s atmospheric nuclear tests, or contain a significant component of water from this time (Clark and Fritz, 1997). The high nitrate concentrations (>20 mg/L) in many shallow samples (Table 1) also signify that shallow groundwater has a considerable modern component. Basement groundwater is also relatively young, including water from a very deep well (350m) that has a residence time of ~2000 years (Fig. 7). This is probably due to water moving quickly through fracture networks, allowing recently recharged water to reach much greater depths than in the Quaternary aquifer. Five deep groundwater samples dated using radiocarbon also had high nitrate concentrations (> 5 mg/L), indicating probable mixing with shallow water affected by agriculture. Hence, these residence times are interpreted as mixing ages (c.f. Kazemi et al., 2006; Table 2). Residence times generally increase with depth in the Quaternary aquifer (Fig. 7). Most deep groundwater (>180m) has residence times of between 7000 and 22000 years, while intermediate groundwater has residence times from modern to ~5000 years.

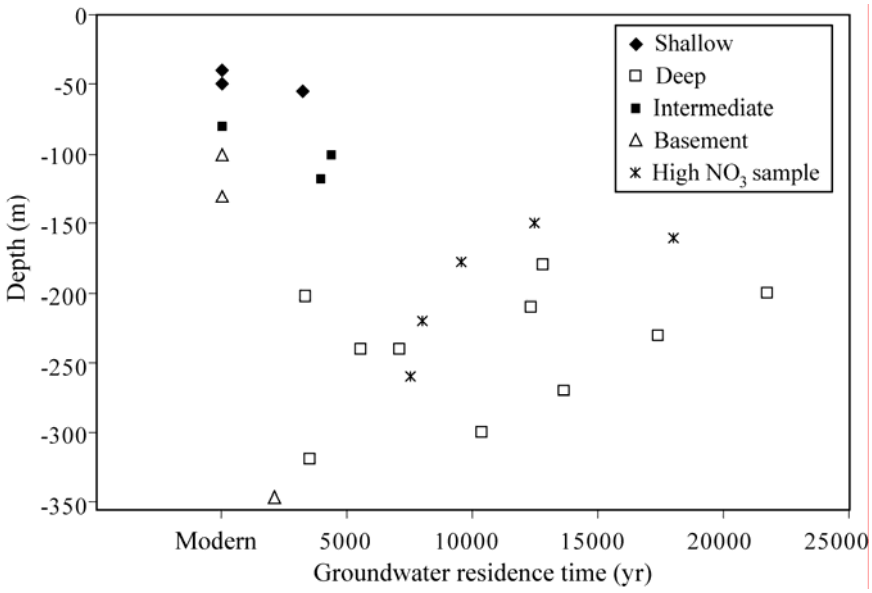

Fig. 7. Groundwater residence times and well depths in the Yuncheng Basin. The broad increase in ages with depth signifies the importance of vertical flow and recharge.

The overall increase in groundwater ages with depth signifies the historic importance of downwards vertical flow and recharge. Both direct infiltration of precipitation and leakage from surface water bodies are likely important recharge sources, indicated by numerous overbank/flood deposits in the sediments deposited by ephemeral streams which flow(ed) after heavy rains (Huang et al., 2007). Lin and Wei, (2006) estimated modern direct recharge through similar loess in central Shanxi province to be ~68mm/year, or 12.5% of local annual rainfall, based on tritium profiles in the unsaturated zone. This recharge rate is large compared to other arid and semi-arid regions of the world (e.g. Allison et al., 1985; Edmunds, 2003; Cartwright et al., 2007; Gates et al., 2008b), which may be due to the high intensity rainfall during the monsoon. The residence time vs. depth profiles in the shallow and intermediate wells (Fig. 7) imply vertical groundwater velocities of between ~0.005 and 0.02 m/year, which for an aquifer with porosity between 0.2 and 0.5 (appropriate for loess, Fetter, 2001) yield recharge rates between 1 and 10

mm/year, or ~0.2 to 2% of local rainfall. These rates are basin-wide and assume vertical piston flow, which is potentially problematic as the loess is known to contain some fractures and joints (Liu et al., 1982). Regardless of whether preferential flow occurs, the rates appear significantly lower than those estimated using tritium by Lin and Wei, (2006). The different recharge estimates may represent the differences between historic and modern recharge rates. Recharge rates based on radiocarbon ages in groundwater are representative of recharge over 1000s of years over a wide area, while those based on tritium correspond to recharge in the last few decades on a local scale (Scanlon et al., 2002). Elsewhere, for example in southeast Australia, differences between the two methods have been shown to reflect recent changes in recharge due to clearing of native vegetation and development of agriculture (Allison et al., 1985; Calf et al., 1986; Cartwright et al., 2007). Clearing of forest and grassland in the Chinese Loess Plateau on larges scales began in the last ~500 years, in conjunction with major population increases and expansion of agriculture in the Ming Dynasty (1368 – 1644). Major land-clearing events also occurred during the 1950s and early 1960s (Fu 1989). Hence, a major increase in recharge facilitated by vegetation change may explain the difference in the calculated recharge rates.

In the deep unit there is only a general correlation between groundwater age and depth (Fig. 7); however, residence times also increase from the east (<5ka) to west (>15ka) (Fig. 8). This indicates that regional horizontal flow of deep groundwater has been important historically. Land elevation decreases from east to west in the Yuncheng Basin from the mountainous area surrounding the town of Wenxi (Fig. 1) where the headwaters of the Sushui River occur, to the broader, lower elevation plains of the central and western

Yuncheng Basin. The Wenxi region is also rich in alluvial sediments, which facilitate high recharge rates; hence this area has likely been the historic regional recharge zone (Yuncheng Regional Water Bureau, 1982; China Geological Survey, 2006). Regional east-to-west flow with additional input from vertical infiltration and horizontal flow from the basin margins (e.g. the Zhongtiao Mountains) is thus likely the basin's natural flow condition. However, flow in the deep unit (Q1 & Q2) has now been completely changed due to pumping. All horizontal deep groundwater flow is now towards the cone of depression, west of Yuncheng city (Cao, 2005; Fig. 8).

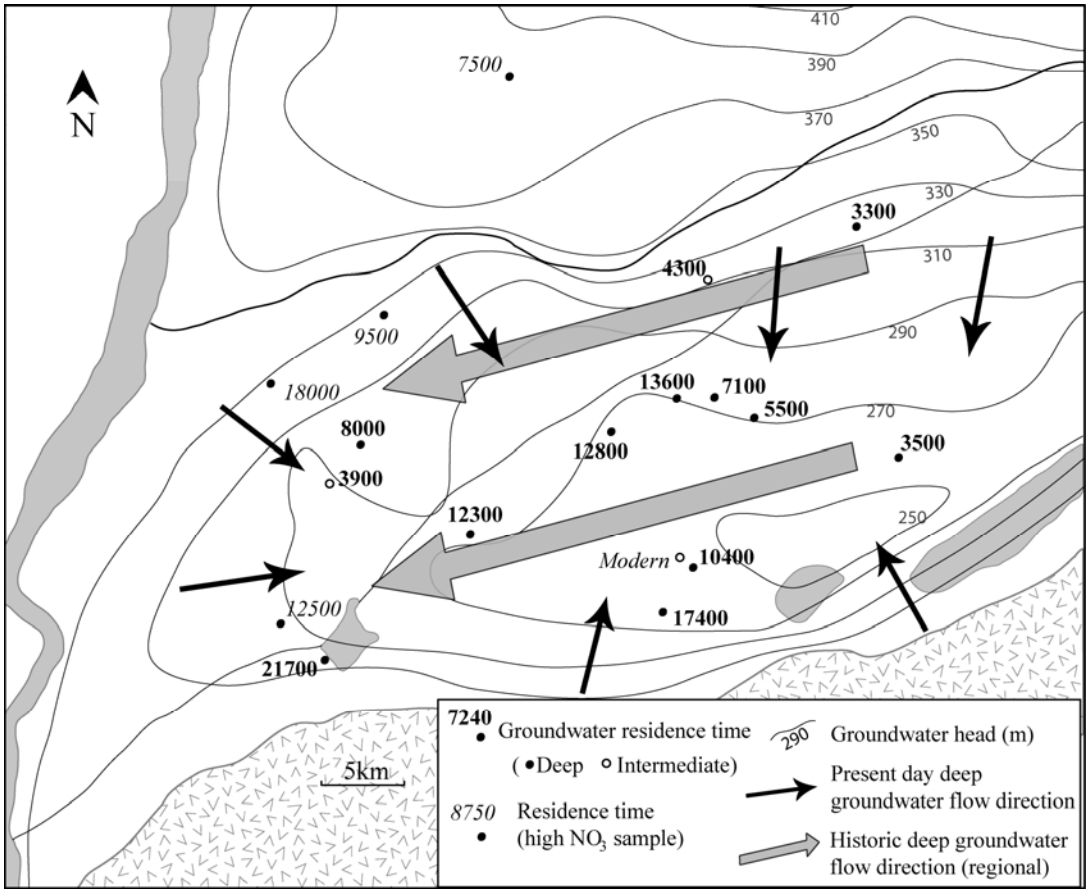

Fig. 8. Comparison between modern and historic deep groundwater flow directions in groundwater, as indicated by residence times and head values

2.4.5 Stable isotopes and recharge environments

Groundwater $\delta^{18}O$ and $\delta^{2}H$ values mostly plot close to the global meteoric water line (GMWL) (Rozanski et al. 1993) and local meteoric water line (LMWL) derived from the weighted mean monthly rainfall $\delta^{18}O$ and $\delta^{2}H$ values for 1985-1992 at Xi'an, 150km southwest of Yongji city (International Atomic Energy Agency/World Meteorological Organisation, 2007, Fig. 9).

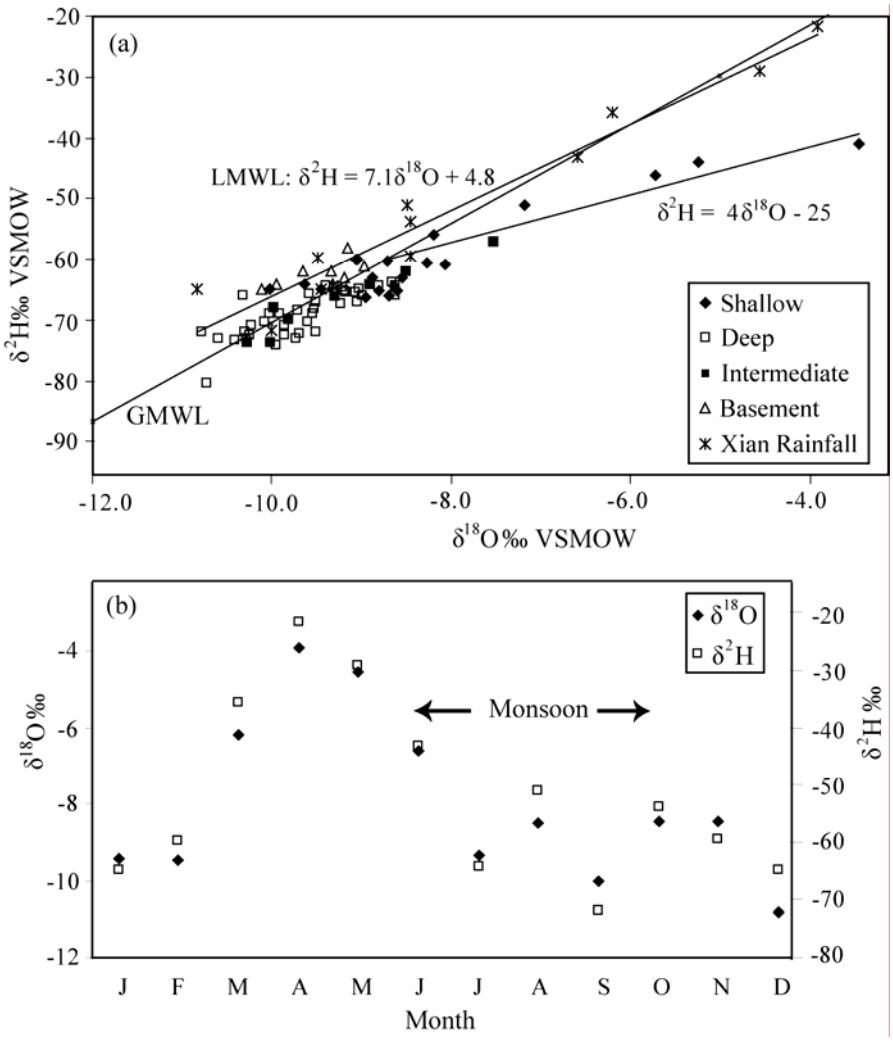

Fig. 9a. Groundwater $\delta^{18}O$ and $\delta^{2}H$ data (Table 1), relative to the GMWL (Rozanski et al., 1993) and LMWL. **9b.** Monthly weighted mean $\delta^{18}O$ and $\delta^{2}H$ in rainfall from Xi'an (1985 – 1992) (International Atomic Energy Agency/World Meteorological Organisation, 2007).

This includes most of the shallow samples with high TDS concentrations, suggesting that the main salinity source in these waters is transpiration (e.g. by crops), which causes negligible fractionation of $\delta^{18}O$ and $\delta^{2}H$ values (e.g. Herczeg et al., 2001; Cartwright et al., 2006). Evaporation (either during recharge or from shallow water tables) or leakage of saline water from nearby salt lakes should cause systematic displacement from the meteoric water lines (Clark and Fritz, 1997; Cartwright et al., 2009), increasing $\delta^{18}O$ values as Cl concentrations increase, which is not observed (Fig. 9a & Fig. 10). Dissolution of minerals (e.g. calcite, gypsum etc.) may also contribute to the high TDS contents; however, if mineral weathering was a major salinity source then high TDS values would also be expected to occur in deep groundwater, where residence times are longer. The fact that samples with high TDS values (>2000mg/L) are confined to shallow levels (<40m) suggests that the salinity is linked to surface agriculture. The 4 highest TDS samples (>3000 mg/L) are located in areas where shallow groundwater head levels measured during the spring irrigation season of 2004 were within 1m of the ground surface (China Geological Survey 2006), and cation/Cl ratios in these waters are similar to rainfall (Currell, unpublished data). These data are consistent with transpiration as the major salinity source, facilitated by the dense cropping of grain and cotton and intensive irrigation. A few shallow samples fall along a linear trend to the right of the GMWL with a slope of 4‰ (Fig. 9a), indicating evaporative concentration at ~55% humidity (Clark and Fritz, 1997). These samples all occur in the far west of the region adjacent to the Yellow River, and the evaporated $\delta^{18}O$ signature may indicate local recharge of evaporated surface water from the river. Projecting these samples back to the meteoric water line along this

trend allows estimation of pre-evaporation $\delta^{18}O$ and $\delta^{2}H$ values, which are listed alongside the original values in Table 1.

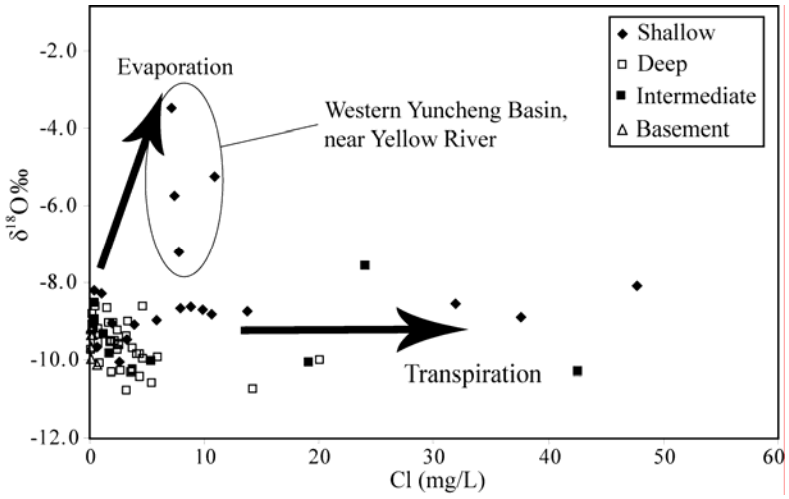

Fig. 10. Relationship between groundwater Cl concentrations and $\delta^{18}O$ values, indicating that transpiration is a more important salinity source than evaporation in groundwater with high TDS contents.

Including these corrected values, shallow groundwater has mean $\delta^{18}O$ and $\delta^{2}H$ values of -8.8‰ and -62‰ respectively, similar to the weighted mean $\delta^{18}O$ and $\delta^{2}H$ values in modern precipitation at Xi'an during the monsoon season (June–October) (-8.5‰ and -57‰ respectively, Fig. 9b). This is consistent with recharge of shallow groundwater primarily occurring during the monsoon period. Deep groundwater has mean $\delta^{2}H$ and $\delta^{18}O$ values of -9.6‰ and -69‰ respectively, which are lower than those in shallow groundwater and modern precipitation (Fig. 9a; Table 1). These values, combined with the estimated residence times, indicate that deep groundwater is palaeowater recharged during a colder and/or wetter climate than presently experienced (c.f. Dansgaard, 1964; Clark and Fritz, 1997; Kreuzer et al., 2009). Basement groundwater $\delta^{18}O$ values are 1-2‰ lower than in shallow groundwater with similar residence times, and also lie slightly to the left of the meteoric water lines (Fig. 9a). This may be a result of an altitude effect (e.g. Clark and

Fritz, 1997), as recharge of this unit occurs in the Zhongtiao mountains (750 – 1800m elevation). The basement groundwater is hosted within fractures in low porosity metamorphic rocks and relatively small volume of water that can be contained in this porosity means that basement water is unlikely to be a major source of recharge to the deep unit in the Quaternary aquifer. The distribution of residence times is also inconsistent with significant recharge to deep groundwater from the basement (Fig. 8), hence altitude cannot account for the depleted δ^2H and $\delta^{18}O$ values in deep groundwater generally.

$\delta^{18}O$ values increase with decreasing groundwater residence times in the Quaternary aquifer (Fig. 11). This may reflect increasing temperatures since the initial cool climate of the late Pleistocene, followed by warming into the Holocene, or a lessening of the intensity of the East Asian monsoon over this period, or a combination of both effects (e.g. Kreuzer et al., 2009). In much of China the temperature and amount effects compete, because most rainfall occurs during the East Asian summer monsoon when warm temperatures cause enrichment of ^{18}O and ^{2}H but the large amount of rain causes depletion in ^{18}O and ^{2}H (Yamanaka et al., 2004; Johnson and Ingram, 2004). This is evident in modern monthly rainfall δ^2H and $\delta^{18}O$ values, which increase from December to May with increasing temperatures, then fall during the monsoon period (Fig 9b). The sedimentary record also indicates significant changes both in temperature and monsoon intensity over the late Pleistocene and Holocene in the Yuncheng Basin, and throughout northern China (e.g. An et al., 1991, 2000; Huang et al., 2007; Li et al., 2008), which are expected to have affected groundwater δ^2H and $\delta^{18}O$ values. Sample 37 with a residence time of ~21,700 years, corresponding approximately to the last glacial maximum, has the lowest $\delta^{18}O$ and δ^2H values (-10.6‰ & -73‰, Table 1). Edmunds et al. (2006) and Gates et al. (2008)

showed that noble gas recharge temperatures in late Pleistocene aged groundwater in northwest China to be 2 to 9°C cooler than modern or late Holocene groundwater, while Kreuzer et al., (2009) estimated Pleistocene groundwater with residence times up to 40kyr to have noble gas recharge temperatures 4-5°C cooler than Holocene groundwater. Temperature may thus be able to account for the increasing groundwater δ^2H and $\delta^{18}O$ values between the late Pleistocene and early Holocene. Kreuzer et al., (2009) reported that little groundwater had residence times of approximately 20,000 years in the North China Plain, which they attribute to an arid climate and a weak summer monsoon during this period, preventing groundwater recharge. The fact that groundwater with residence times around 20,000 years is found in the Yuncheng Basin may indicate the area was still affected by the monsoon while the North China Plain, located to the northeast, was not.

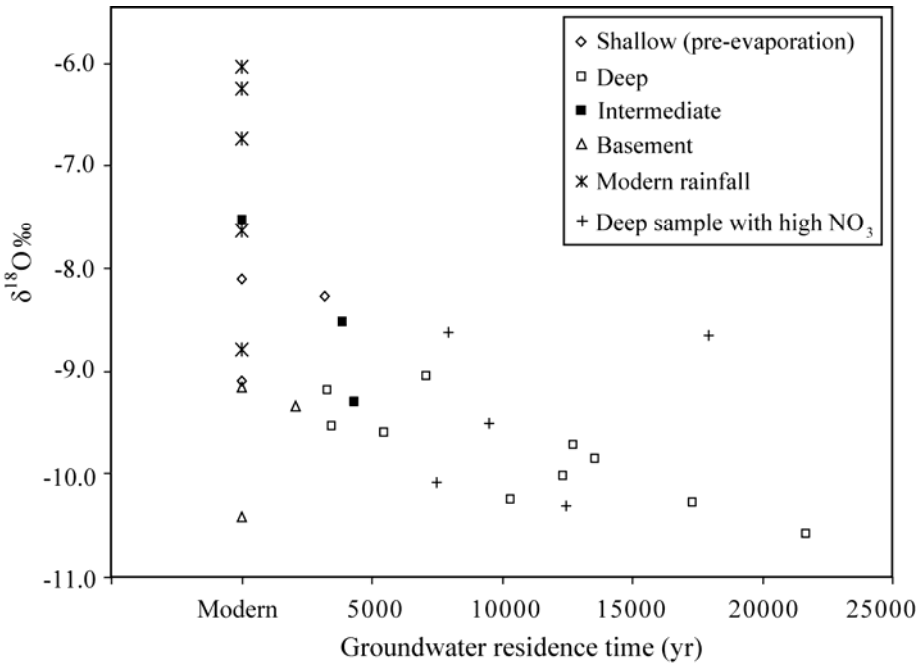

Fig. 11. Groundwater residence times and $\delta^{18}O$ values (Data from Table 1; Table 2). Shallow samples include estimated pre-evaporation values (Table 1). Deep groundwater samples with high nitrate concentrations are interpreted as having input from shallow groundwater, and are marked distinct from other deep samples.

Deep groundwater samples with residence times between 4,000 and 8,000 years have higher $\delta^{18}O$ values than both Pleistocene and early Holocene groundwater (> -9.6‰) (Fig. 11). This may be due to a continuation of increasing temperatures through the early to mid Holocene. Analysis of loess profiles from the Yuncheng Basin and wider region have previously identified a warm and wet period between c.9000 and 3500 years B.P., referred to as the mid-Holocene climatic optimum (An et al., 2000; Huang et al., 2007). The high $\delta^{18}O$ values in groundwater from this period suggests that temperature was still the dominant control on groundwater $\delta^{2}H$ and $\delta^{18}O$ values, as increased monsoon intensity would be expected to cause a decrease in rainfall (and hence groundwater) $\delta^{18}O$ values due to the amount effect. This explanation again contrasts with the data of Kreuzer et al., (2009), who found that noble gas recharge temperatures in groundwater from the North China Plain showed little variation during the Holocene, indicating that increasing groundwater $\delta^{18}O$ values over the period were a result of decreasing monsoon strength, rather than increasing temperatures. This difference may again be a function of the geographic location of the two study areas – the Yuncheng Basin is located south of the North China Plain, and may have continued to experience a stronger monsoon throughout the early and mid-Holocene periods. Previous studies suggest that the climatic optimum was experienced later in north-central China than in northeastern China (An et al., 2000).

Shallow groundwater has the highest $\delta^{18}O$ and $\delta^{2}H$ values, even after correction for the effects of evaporation. The depositional patterns (e.g. high dust storm frequency) and composition (e.g. high carbonate content) of the loess in the area indicate that temperatures decreased in the late Holocene (last ~3000 years) and that climate became increasingly arid (Huang et al., 2007). Hence, the high $\delta^{18}O$ values may be due to the relative aridity in

recent times, which has had a larger effect on $\delta^{18}O$ and $\delta^{2}H$ values via the amount effect than the slight temperature decrease. Deuterium excess (d) values (Table 1) show relatively little variation over the full range of groundwater residence times, with most values between 5 and 10 (median = 8.7), indicating that the humidity of the source regions of precipitation throughout the period of recharge was relatively constant and around 85% (Clark and Fritz 1997). While the aridity in the region has varied over time, the bulk of rainfall has consistently been derived from the East Asian summer monsoon, for which the source regions have been unchanged over the period of recharge, and possibly as far back as the end of the Pliocene (An et al. 1991, Han et al. 1997, An et al. 2000). This rainfall appears to have been the source of much of the groundwater recharge to basins in northern China, even to the west of the study area (e.g. Gates et al. 2008).

2.4.6 Modern groundwater recharge and irrigation returns

Given that shallow groundwater has a significant modern component and that irrigated agriculture has been practiced in the region for at least the last 50 years, a large proportion of shallow groundwater would have recharged since large-scale planting of shallow rooted crops, irrigation and fertilization began. The high groundwater TDS and NO_3 concentrations in this water (Table 1; Fig. 2) may indicate a component of irrigation returns that have undergone transpiration and dissolution of N from fertilizers. Irrigation returns might be expected to have low $\delta^{2}H$ and $\delta^{18}O$ values, as deep groundwater is the primary irrigation source, although the historic composition of irrigation water has varied (e.g. surface water was used during the 1960s and 1970s). Shallow groundwater may also be composed of precipitation from the monsoon, which has interacted with soils containing

high N contents from fertilizers and undergone transpiration via crops before reaching the saturated zone. The δ^2H and $\delta^{18}O$ values in shallow water being similar to modern precipitation during the monsoon are more consistent with this mechanism.

2.4.7 Regional context

Similar δ^2H and $\delta^{18}O$ values from Late Pleistocene and Holocene aged groundwater have been reported in other studies of deep groundwater in northern China and there is significant overlap between the data collected in the Yuncheng Basin and previous published data from the Minqin Basin, the North China Plain, and the Badain Jaran Desert (Chen et al., 2003; Edmunds et al., 2006; Gates et al., 2008; Kreuzer et al. 2009; Fig. 12). The overlap in these data sets indicates that groundwater δ^2H and $\delta^{18}O$ values act as a broad proxy for groundwater age throughout northern China. Groundwater with $\delta^{18}O$ values between approximately -9.5 and -12.0‰ were generally recharged during the late Pleistocene, while groundwater with residence times younger than 5000 years mostly have $\delta^{18}O$ values of -7.0 to -9.0‰ (Fig. 12). δ^2H and $\delta^{18}O$ can thus potentially be used as a first estimate of groundwater residence times throughout north China, allowing identification of groundwater recharged during the late Pleistocene as opposed to the late Holocene or recent times.

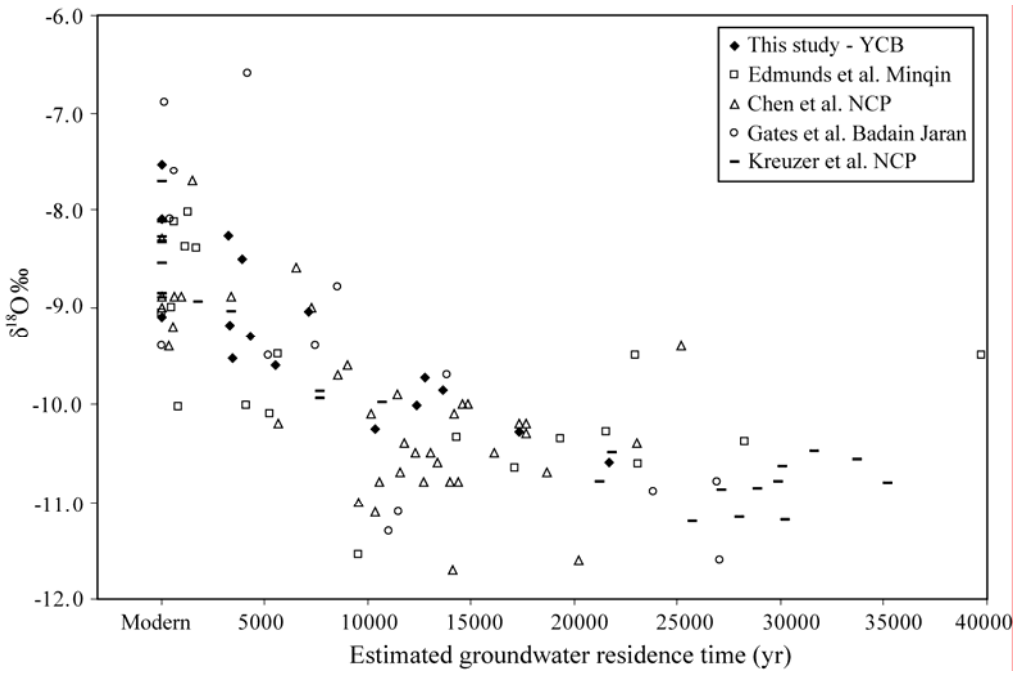

Fig. 12. Groundwater $\delta^{18}O$ and residence time data from groundwater basins in northern China. Residence times from Gates et al. (2008); Chen et al. (2003) as reported using $\delta^{13}C$ mixing model, from Kreuzer et al. (2009) as reported mean ages, and from Edmunds et al. (2006) using reported pmc values, and basic age model based on Vogel (1970), with q = 0.85. NCP = North China Plain, YCB = Yuncheng Basin (data from Table 2). Excludes basement groundwater and deep groundwater with high NO_3 concentrations. Shallow groundwater data include estimated pre-evaporation $\delta^{18}O$ values

2.4.8 Sustainability of groundwater usage

The stable isotope and radiocarbon data indicate that groundwater in the Yuncheng Basin was recharged over many thousands of years over periods characterized by different climatic conditions. Given the long residence times of deep groundwater (Fig. 8; Table 2), any modern recharge or replenishment of this resource must be negligible compared to the volumes currently extracted. This is evident in the rapid fall in deep groundwater head levels in the last 25 years (Cao, 2005). The drawdown in deep groundwater is inevitably causing a decrease in groundwater bore yields, which will intensify if pumping continues at, or increases from, present levels.

Deep groundwater quality is also deteriorating due to downward leakage of shallow groundwater with high nitrate and TDS concentrations. The area where mixing and

contamination is most severe (near the Linyi fault) is not near the center of the cone of depression, where downwards hydraulic gradients are the highest (Fig. 5). This highlights that the presence of faults exerts a strong control on leakage. However, the high TDS and NO_3 concentrations in the intermediate groundwater throughout the basin indicate that widespread gradual leakage is occurring. The NO_3 and TDS concentrations in deep groundwater will thus probably rise steadily in coming years if downward hydraulic gradients facilitated by pumping remain high. The deterioration of deep groundwater quality in the cone of depression region will potentially be more severe than in the area where leakage has already reached deep wells (Fig. 4), as TDS and NO_3 concentrations are higher in the shallow groundwater here than in the northern Sushui River Basin (Table 1).

Rapidly declining deep groundwater levels in response to intensive extraction for irrigation is occurring in many other areas in northern China (e.g. Foster et al., 2004). Declining groundwater quality due to leakage of contaminated shallow groundwater is also likely to impact these basins in the near future. Areas such as the North China Plain and Alashan region of Inner Mongolia have locally more widespread and severe shallow nitrate contamination problems than the Yuncheng basin and similarly high rates of deep groundwater usage (e.g. Hu et al., 2005). Development of many areas in arid and semi-arid northern China since the 1980s has been underpinned by irrigated agriculture, dependant on groundwater pumping. A large amount of drinking water has also been supplied by these wells. While deep groundwater is a potentially large, high quality and valuable resource to these densely populated areas, it is imperative that groundwater usage takes into account the age, recharge history and controls on groundwater quality in these basins. Community water management practices need to be considered in this context to ensure

the life of these groundwater resources is maximized, both from a quality and quantity point of view.

2.5 CONCLUSIONS

Deep groundwater in the Yuncheng basin is palaeowater, mostly recharged between c.7000 and 22000 years ago during the cooler climate of the late Pleistocene, and the early Holocene. Groundwater δ^2H and $\delta^{18}O$ values increase from older to younger waters, reflecting warming temperatures from the late Pleistocene into and throughout the Holocene, and changes in the intensity of the East Asian monsoon. A similar relationship has been observed in other groundwater basins in the region, indicating that δ^2H and $\delta^{18}O$ values can potentially be used as a broad first estimate of groundwater ages throughout northern China.

Shallow groundwater contains a significant component of modern water and has δ^2H and $\delta^{18}O$ values similar to rainfall during the summer monsoon. Groundwater recharge thus probably occurs mainly during the monsoon when rains are heaviest, via direct infiltration and leakage of surface water bodies, and some irrigation returns. Historical recharge rates are estimated to be between 1 and 10mm/year, which is much lower than previous estimates of modern recharge in loess from northern China. This may reflect an increase in vertical infiltration between historic and modern times due to development of agriculture and/or land clearing.

Under natural conditions, recharge to the Quaternary aquifer came from a combination of vertical infiltration and regional horizontal flow, indicated by increasing groundwater residence times with depth, and from east to west in deep groundwater. However, recharge of deep groundwater is minimal in comparison with groundwater

extraction, which has led to rapid drawdown, and the regional flow path has been altered fundamentally by pumping. All deep groundwater now flows towards a large groundwater depression west of Yuncheng city.

Shallow groundwater has high nitrate and TDS concentrations. $\delta^{15}N_{NO3}$ and $\delta^{18}O_{NO3}$ values between 0‰ and 5.0‰ in most samples indicate that the source of NO_3 is synthetic fertilizers. Most samples with high TDS contents have $\delta^{2}H$ and $\delta^{18}O$ values that lie on the global and local meteoric water lines, suggesting transpiration rather than evaporation has caused the high salinity. Deep groundwater is mostly of better quality, with relatively low TDS and nitrate concentrations. However, locally high nitrate concentrations occur in the vicinity of the Linyi fault, indicating downwards leakage of shallow groundwater facilitated by pumping and the presence of fractures in this area. Elsewhere, elevated nitrate and TDS concentrations in groundwater from intermediate wells at the top of the deep aquifer (80 – 120m) indicate broad scale downwards vertical mixing throughout the basin.

Declining well yields and increasing nitrate and TDS contents in deep groundwater are to be expected if rates of extraction continue at present levels or increase. Given that the area depends heavily on deep groundwater for irrigation and drinking supply, and the long time-scales involved in recharge to the unit, these are major concerns for the future prosperity of the region.

Acknowledgements

This research was partly initiated and greatly supported by the Australia-China Water Resources Research Centre, including Dr. Deli Chen, Dr. Yongping Wei, Prof. Song Xianfang and Prof. Li Baoguo. Special thanks also to the Yuncheng City Water Resources Service Bureau, in particular Mr. Sun Xinzhong. Logistical support was also given by the Yongji, Linyi and Yuncheng county Water Resource Bureaus, and Dr. Wang Zhimin. Thanks also to Massimo Raveggi for invaluable support during the analysis of samples.

References

Allison, G.B., Stone, W.J., Hughes, W.M., 1985. Recharge in karst and dune elements of a semi-arid landscape by natural isotopes and chloride (Murray Basin, Australia). Journal of Hydrology 76(1-2), 1-25.

An, Z., Kukla, G.J., Porter, S.C., Xiao, J., 1991. Magnetic susceptibility evidence of monsoon variation on the Loess Plateau of central China during the last 130,000 years. Quaternary Research 36, 29-36.

An, Z., Porter, S.C., Kutzbach, J.E., Wu, X., Wang, S., Liu, X., Li, X., Zhou, W., 2000. Asynchronous Holocene optimum of the East Asian monsoon. Quaternary Science Reviews 19, 743-762.

Calf, G.E., Ife, D., Tickell, S., Smith, L.W., 1986. Hydrogeology and isotope hydrology of Upper Tertiary and Quaternary aquifers in northern Victoria. Australian Journal of Earth Science 33, 19-26.

Cao, J.J., Zhu, C.S., Chow, J.C., Liu, W.G., Han, Y.M., Watson, J.G., 2008. Stable carbon and oxygen isotopic composition of carbonate in fugitive dust in the Chinese Loess Plateau. Atmospheric Environment 42, 9118-9122.

Cao, X.H., 2005. Study of the intermediate and deep layers of the Sushui River Basin confined groundwater system. In: *Shanxi Hydrotechnics Bulletin No. 3.* China Academic Journal Electronic Publishing House. pp 41-43. (In Chinese)

Cartwright, I. Weaver, T.R., Finfield, L.K., 2006. Cl/Br ratios and environmental isotopes as indicators of recharge variability and groundwater flow: an example from the southeast Murray Basin, Australia. Chemical Geology 231, 38-56.

Cartwright, I., Weaver, T.R., Stone, D., Reid, M., 2007. Constraining modern and historical recharge from bore hydrographs, ^{3}H, ^{14}C, and chloride concentrations: Applications to dual-porosity aquifers in dryland salinity areas, Murray Basin, Australia. Journal of Hydrology 332, 69-92.

Cartwright, I., Hall, S., Tweed, S., Leblanc, M., 2009. Geochemical and isotopic constraints on the interaction between saline lakes and groundwater in southeast Australia. Hydrogeology Journal 17(8), 1991-2004.

Chen, J.Y., Tang, C.Y., Yu, J.J., 2006. Use of ^{18}O, ^{2}H and ^{15}N to identify nitrate contamination of groundwater in a wastewater irrigated field near the city of Shijiazhuang, China. Journal of Hydrology 326, 367-378.

Chen, Z.Y., Qi, J.X., Xu, J.M., Xu, J.M., Ye, H., Nan, Y.J., 2003. Palaeoclimatic interpretation of the past 30 ka from isotopic studies of the deep confined aquifer of the North China plain. Applied Geochemistry 18, 997 – 1009.

China Geological Survey, 2002. Geological Atlas of China [English version] Beijing Geological publishing house, 348p.

China Geological Survey, 2006. Groundwater resources and environmental issues assessment in the six major basins of Shanxi (in Chinese), China Geological Survey Special publication, Beijing. 98p.

Clark, I., Fritz, P., 1997. Environmental Isotopes in Hydrogeology. Lewis Publishing, New York. 328p.

Coplen, T.B., 1988. Normalization of oxygen and hydrogen isotope data. Chemical Geology 72, 293-297.

Dansgaard, W., 1964. Stable isotopes in precipitation. Tellus 16, 436-438.

Edmunds, W.M., 2003. Renewable and non-renewable groundwater in semi-arid regions. Developments in Water Science 50, 265-280.

Edmunds, W. M., Ma, J., Aeschbach-Hertig, W., Kipfer, R., Darbyshire, D. P. F., 2006. Groundwater recharge history and hydrogeochemical evolution in the Minqin Basin, North West China. Applied Geochemistry 21(12), 2148-2170.

Fetter, C.W., 2001. Applied Hydrogeology (4^{th} edition). Prentice-Hill, New Jersey. 598p.

Fogg, G.E., Rolston, D.E., Decker, D.L., Louie, D.T., Grismer, M.E., 1998. Spatial variation in nitrogen isotopic values beneath nitrate contamination sources. Ground Water 36, 418-426.

Fontes, J.-C., Garnier, J.M., 1979. Determination of the initial ^{14}C activity of the total dissolved carbon: a review of the existing models and a new approach. Water Resources Research 15(2), 399-413.

Foster, S., Garduno, H., Evans, R., Olson, D., Tian, Y., Zhang, W., Han, Z. 2004. Quaternary Aquifer of the North China Plain - assessing and achieving groundwater resource sustainability. Hydrogeology Journal 12, 81-93.

Fu, B., 1989. Soil erosion and its control in the loess plateau of China. Soil Use and Management 5(2), 76-82.

Gates, J.B., Edmunds, W.M., Darling, W.G., Ma, J., Pang, Z., Young, A.A., 2008a. Conceptual model of recharge to southeastern Badain Jaran Desert groundwater and lakes from environmental tracers. Applied Geochemistry 23, 3519 - 3534.

Gates, J.B., Edmunds, W.M., Ma, J., Scanlon, B.R., 2008b. Estimating groundwater recharge in a cold desert environment in northern China using chloride. Hydrogeology Journal 16, 893-910.

Han J.M., Keppens E., Liu T.S., Paepe R. and Jiang W.Y., 1997. Stable isotope composition of the carbonate concretion in loess and climate change. Quaternary International 37: 37-43.

Heaton, T.H.E., 1986. Isotopic studies of nitrogen pollution in the hydrosphere and atmosphere: A review. Chemical Geology 59, 87-109.

Herczeg, A.L., Dogramaci, S.S., Leany, F.W., 2001. Origin of dissolved salts in a large, semi-arid groundwater system: Murray Basin, Australia. Marine and Freshwater Research 52, 41-52.

Hu, K.L., Huang, Y.F., Li, H., Li, B.G., Chen, D., White, R.E., 2005. Spatial variability of shallow groundwater level, electrical conductivity and nitrate concentration, and

risk assessment of nitrate contamination in North China Plain. Environment International 31, 896-903.

Huang, C.C., Pang, J., Zha, X., Su, H., Jia, Y., Zhu, Y., 2007. Impact of monsoonal climatic change on Holocene overbank flooding along Sushui River, middle reach of the Yellow River, China. Quaternary Science Reviews 26, 2247-2264.

IAEA/WMO, 2007. Global Network of Isotopes in Precipitation. The GNIP database. Accessible at http://isohis.iaea.org.

Johnson, K.R., Ingram, B.L., 2004. Spatial and temporal variability in the stable isotope systematics of modern precipitation in China: implications for paleoclimatic reconstructions. Earth and Planetary Science Letters 220, 365-377.

Kazemi, G.A., Lehr, J.H., Perrochet, P., 2006. Groundwater Age. John Wiley & Sons, N.J. 325p.

Kendall, C., 1998. Tracing Nitrogen Sources and Cycling in Catchments *in:* C. Kendall & J.J., McDonnell (ed) Isotope Tracers in Catchment hydrology. Elsevier Science B.V., Amsterdam. pp. 519-576.

Kreuzer, A.M., Rohden, C.V., Friedrich, R., Chen, Z., Shi, J., Hajdas, I., Aeschbach-Hertig, W., 2009. A record of temperature and monsoon intensity over the past 40 kyr from groundwater in the North China Plain. Chemical Geology 259, 168-180.

Li G.J., Ji J.F, Zhao L., Mao C.P., Chen J., 2008. Response of silicate weathering to monsoon changes on the Chinese Loess Plateau. Catena 72, 405-412.

Lin, R., Wei, K., 2006. Tritium profiles of pore water in the Chinese loess unsaturated zone: Implications for estimation of groundwater recharge. Journal of Hydrology 328, 192-199.

Liu, T.S., An, Z. S., Yuan, B.Y., 1982. Aeolian processes and dust mantles (loess) in China. In: Quaternary Dust Mantles of China, New Zealand and Australia. Proceedings of a workshop. Australian National University. pp 1-19.

Liu, T.S., Zhang, S.X., Han, J.M., 1986. Stratigraphy and palaeoenvironmental changes in the loess of central China. Quaternary Science Reviews 5, 489-495.

McIlvin, M.R, Altabet, M.A., 2005. Chemical conversion of nitrate and nitrite to nitrous oxide for nitrogen and oxygen isotopic analysis in freshwater and seawater. Analytical Chemistry 77**,** 5589–5595

Pearson, F.J., 1965. Use of C-13/C-12 ratios to correct radiocarbon ages of material initially diluted by limestone. In: Proceedings of the 6th International conference on Radiocarbon and Tritium dating, Pulman, WA, p.357

Rozanski, K., Araguas-Araguas, L., Gonfiantini, R., 1993. Isotopic patterns in modern global precipitation. In: Swart, P.K., Lohmann, K.C., McKenzie, J., Savin, S. (Eds.), Climate Change in Continental Isotopic Records. AGU Geophysical Monograph Series. American Geophysical Union, Washington, DC, pp.1-36.

Scanlon, B.R., Healey, R.W., Cook, P.G., 2002. Choosing appropriate techniques for quantifying groundwater recharge. Hydrogeology Journal 10, 18-39

Vogel, J.C., 1970. Groningen radiocarbon dates IX. Radiocarbon 12, 444-471.

Xu, X., Ma, X., 1992. Geodynamics of the Shanxi Rift system, China. Tectonophysics 208, 325-340.

Yamanaka, T., Shimada, J., Hamada, Y., Tanaka, T., Yang, Y., Zhang, W., Hu, C.S., 2004. Hydrogen and oxygen isotopes in precipitation in the northern part of the North China Plain: climatology and inter-storm variability. Hydrological Processes 18, 2211-2222.

Yu, G., Chen, X., Ni, J., Cheddadi, R., Guiot, J., Han, H., Harrison, S.P., Huang, C., Ke, M., Kong, Z., Li, S., Li, W., Liew, P., Liu G., Liu, J., Liu, Q., Liu, K-B., Prentice, I.C., Qui, W., Ren, G., Song, C., Sugita, S., Sun, X., Tang, L., Van Campo, E., Xia, Y., Xu, Q., Yan, S., Yang, X., Zhao, J., Zheng, Z., 2000. Palaeovegetation of China: a pollen data-based synthesis for the mid-Holocene and last glacial maximum. Journal of Biogeography 27, 635-664.

Yuncheng Regional Water Bureau & Shanxi Geological Survey, 1982. Hydrological and Geological maps and explanations for the Yuncheng region, 1:100000, Shanxi Geological Survey Special Report (In Chinese). 80p.

Zhu, G.F., Li, Z.Z., Su, Y.H., Ma, J.Z., Zhang, Y.Y., 2007. Hydrogeochemical and isotope evidence of groundwater evolution and recharge in Minqin basin, Northwest China. Journal of Hydrology 333, 239-251.

Zhu, G.F., Su, Y.H., Feng, Q., 2008. The hydrochemical characteristics and evolution of groundwater and surface water in the Heihe River Basin, northwest China. Hydrogeology Journal 16, 167-182.

[This page is intentionally left blank]

Chapter 3

Major ion chemistry, $\delta^{13}C$ and $^{87}Sr/^{86}Sr$ as indicators of hydrochemical evolution and sources of salinity in groundwater, the Yuncheng Basin, China

Matthew J. CURRELL[1], Ian CARTWRIGHT[1,2]

1. School of Geosciences, Monash University, Clayton VIC, Australia 3800
2. National Centre for Groundwater Research and Training, Flinders University, Adelaide SA 5001, Australia

----Submitted to Hydrogeology Journal (28/06/10) **----**

ABSTRACT

Processes controlling groundwater chemistry during recharge and flow in the Yuncheng Basin, China, were characterised using major ion chemistry, $^{87}Sr/^{86}Sr$ ratios and $\delta^{13}C$ values. Evapotranspiration during recharge increased solute concentrations by a factor of ~5 to 50 in deep groundwater with residence times of up to 20 ka, while much higher degrees of evapotranspiration have occurred in shallow modern groundwater due to irrigation. Elevated total molar cation/Cl ratios (up to 48) in deep and intermediate groundwater compared to rainfall (~4.6) indicate that mineral dissolution has also occurred. The aquifer sediments contain up to 20 weight% calcite, and trends in HCO_3 concentrations, pH, and $\delta^{13}C$ values indicate that carbonate weathering is a significant source of DIC during recharge and flow within the aquifer. $^{87}Sr/^{86}Sr$ ratios of groundwater from the Quaternary aquifer (0.7110 to 0.7162, median of 0.7116) are similar to those of carbonate in the loess aquifer sediments (0.7111 ±0.0005) and local rainfall (0.7112 ±0.0004) and are significantly lower than those of silicates from the loess (0.7200

±0.0015), again consistent with carbonate weathering. However, despite the evidence for substantial carbonate dissolution, the groundwater is generally Ca-poor (<10% of total cations) and Na-rich (> 80% of total cations) due to cation exchange.

Key words: Hydrochemistry, Environmental isotopes, China, Loess, Semi-arid

3.1 INTRODUCTION

Continuing economic growth and food security in China are underpinned by high agricultural outputs that have been achieved since the 1980s (Organisation for Economic Co-operation and Development, 2005). Much of this agriculture in arid and semiarid regions of northern China is heavily dependant on groundwater resources, which often also supply domestic water (Gleik, 2009). Characterizing the processes that control groundwater chemistry (and therefore its quality) is a vital part of managing groundwater and agricultural practices in northern China, where the arid climate and large population have led to severe stress on potable water supplies (e.g. Li, 2003; Edmunds et al., 2006; Zhu et al., 2007; Fang et al., 2010). In general, the processes that control chemical evolution of groundwater in the aquifers of the Loess Plateau of northern China such as the Yuncheng Basin, which supply groundwater to large populations, have been sparsely studied (China Geological Survey, 2006). The sources of salinity, including evapotranspiration and weathering of different mineral types, and the role of exchange reactions in controlling groundwater chemistry in these loess aquifers are poorly understood. Understanding these processes is important not only because they control the groundwater quality but also because aspects of groundwater chemistry (e.g. pH, cation composition) can have a major effect on the mobilization of toxic elements (e.g. F and As) (e.g. Smedley et al., 2005; Scanlon et al., 2009) that are found in locally high concentrations in groundwater from the region (e.g. Gao et al., 2007; Guo et al., 2007).

This study uses groundwater, rainfall and sediment major ion geochemistry along with $^{87}Sr/^{86}Sr$ and $\delta^{13}C$ data to characterize geochemical processes during recharge and

flow of groundwater in the Yuncheng Basin, northern China. Major ion chemistry, in particular molar ion ratios, are useful in assessing sources of solutes and characterising hydrogeochemical evolution in aquifers (e.g. Edmunds et al., 1982; Herczeg and Edmunds, 2000; Cartwright et al., 2004). Sr isotopes are a sensitive indicator of water-rock interaction (e.g. Dogramaci and Herczeg, 2002; Harrington and Herczeg, 2003; Gosselin et al., 2004, Cartwright, 2010), while $\delta^{13}C$ values are an effective tracer of carbon sources and the evolution of DIC in aquifers (Clark and Fritz, 1997). Constraining the geochemical processes in the Yuncheng Basin aquifer is important for understanding and managing the groundwater resources in this region and similar loess-dominated basins.

3.2 GEOLOGICAL SETTING & BACKGROUND

3.2.1 The Yuncheng Basin

The Yuncheng Basin in Shanxi Province, shown in Figure 1, has a population of > 5 million and is a significant area of agricultural production that is experiencing severe water stress and water quality issues (Cao, 2005; China Geological Survey, 2006). The basin comprises a semi-confined aquifer composed of interlayered Quaternary sediments (Q1-Q4), including loess, fluvial sands and gravels, and lacustrine clays (Yuncheng City Regional Water Bureau, 1982; China Geological Survey, 2006). The loess is composed of dust particles, mostly 0.005 – 0.01mm diameter, sourced from arid deserts of central Asia and western China, and transported via dust storms; palaeosols within the loess were formed during warm, wet periods during which clay-rich soils developed in between loess accumulation events (e.g. Liu et al., 1986; An et al., 1991; Gallet et al., 1996; Yokoo et al., 2004).

The Quaternary aquifer can be divided into shallow (0 to ~70 m; Q3 & Q4), and deep (70 to ~500 m; Q1 & Q2) units, which are separated by the major S1 palaeosol (Liu et al., 1986). A distinct intermediate hydrostratigraphic unit may also occur in the top ~50 m of the Q2 sediments (70 to 120 m depth); however, this layer essentially forms part of the deep unit (Cao, 2005). Groundwater exists in fractures in the underlying/adjacent Archean metamorphic basement rocks in the south of the area and this is used as a local drinking water source (Fig. 1; Yuncheng Regional Water Bureau, 1982). This rock formation (Arsm) comprises gneiss, hornblendite/hornblende-rich amphibolite, quartzite and migmatite; the major minerals include hornblende, biotite, garnet, diopside, chlorite, quartz, plagioclase and magnetite (Yuncheng Regional Water Bureau, 1982).

Yearly rainfall averages 550mm/year and is far less than potential evapotranspiration (~2000mm/yr). Most rainfall occurs in the East Asian summer monsoon during which time rainfall can exceed evapotranspiration, facilitating groundwater recharge. Historically, groundwater has predominantly flowed from the elevated southern and northern margins of the basin to its lower interior (China Geological Survey, 2006); while the distribution of ^{14}C residence times indicates long-term basin-scale flow from the eastern Yuncheng Basin to the west (Currell et al., 2010). However, these flow paths have been altered due to pumping; groundwater now flows towards a cone of depression to the west of Yuncheng city (Cao 2005; Currell et al., 2010).

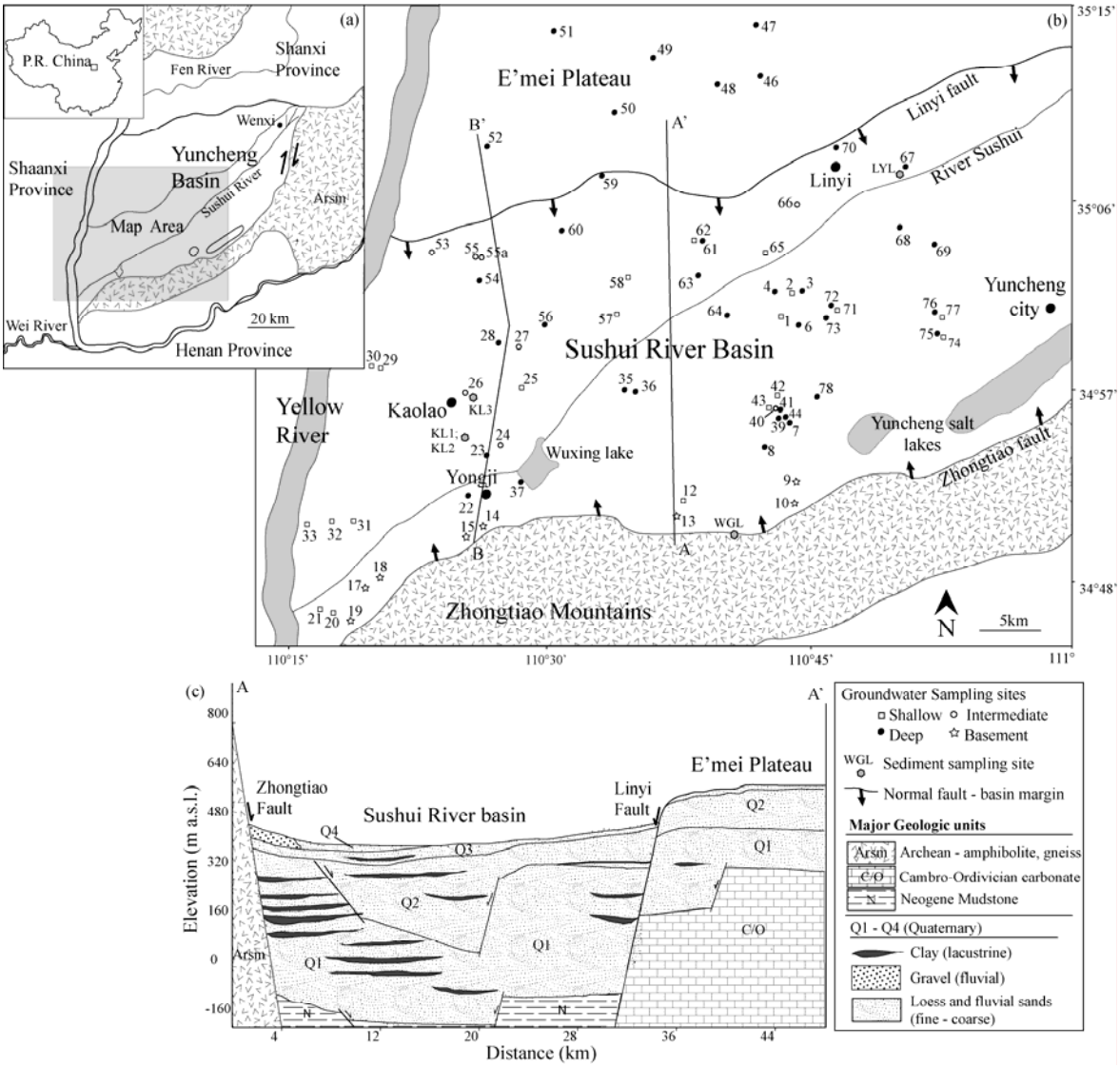

Fig. 1 Location of the Yuncheng Basin **(a)**; groundwater and sediment sampling sites **(b)**; schematic cross section of the Yuncheng Basin **(c)**.

3.2.2 Groundwater age and quality

^{14}C activities, TDS contents and $\delta^{15}N$ and NO_3 values indicate that groundwater in the basin has a residence time of up to 22 ka and that anthropogenic processes have had a significant impact on groundwater quality in parts of the aquifer (Currell et al., 2010). Shallow groundwater in many locations has high total dissolved solids (TDS) contents (up to 8450 mg/L) and/or high nitrate concentrations (up to 630 mg/L); most of the nitrate is

from chemical fertilizers (Currell et al., 2010). Hence, deep groundwater is now a particularly important water source. $\delta^{18}O$ values and ^{14}C activities indicate that the deep groundwater was largely recharged during the late Pleistocene. This deeper groundwater has lower TDS contents (median 1090 mg/L; maximum 1810 mg/L) and is generally unaffected by contamination from agriculture, although high nitrate concentrations occur near the Linyi fault (up to 210 mg/L), indicating leakage of shallow groundwater into the deep aquifer (Currell et al., 2010).

3.3 METHODS & ANALYTICAL TECHNIQUES

Groundwater sampling methods and analytical techniques for pH, EC, dissolved oxygen, alkalinity and $\delta^{13}C$ are described in Currell et al., (2010). Samples for major cation analysis were filtered through 0.45 μm cellulose acetate filters and acidified with 16 N distilled HNO_3 to pH < 2, and were analysed on a Varian Vista ICP-AES at the Australian National University, Canberra. Major anions (Cl, Br, NO_3, SO_4 and F) were determined on filtered samples using a Metrohm ion chromatograph at Monash University, Melbourne. The maximum error in charge balance was 16%, while 63 of the 73 samples had charge balance errors of less than 10%. PHREEQC version 2.14.2 (Parkhurst and Apello, 1999) was used to determine saturation indices for calcite, dolomite and amorphous silica.

$^{87}Sr/^{86}Sr$ ratios in groundwater and sediments were measured at the University of Adelaide. For water samples, sufficient water to yield 2 μg of Sr was evaporated to dryness, then the residue was dissolved in 2 ml of 6M HCl, evaporated again to dryness and re-dissolved in 2M HCl. Sr was extracted from centrifuged supernatant using cation exchange columns and Biorad AG50W X8 200-400 mesh resin. Isotope analyses were

carried out on a Finnigan MAT 262 thermal ionization mass spectrometer in static mode. $^{88}Sr/^{86}Sr$ values were normalized to 8.375209. Analysis of the standard SRM gave $^{87}Sr/^{86}Sr$ ratios of 0.710238 ± 0.000012 (2se). The analytical uncertainty range for water samples was ± 0.000009 to 0.000017 (2se). For the sediments, carbonate minerals were dissolved by leaching powdered sample with 1M HCl, while silicate minerals were extracted by digesting the residual powder with concentrated HF and HNO_3 at 150°C. Dissolution of chlorite and Fe-oxides would also occur during leaching with HCl, however these are not expected to contribute substantial Sr. Four samples of loess were analysed using X-ray diffraction, at Ballarat University. X-ray diffraction traces were obtained from the samples after fine milling, with a Siemens D500 diffractometer, using Fe-filtered CoK_α radiation. Operating conditions were 35kV/25mA, step scan 0.03θ 2θ at 1^o/2θ/min, range 4^o to 76.0^o 2θ, fixed 1^o divergence and receiving slits and a 0.15^o scatter slit. Quantitative XRD results were obtained using SiroQuant™ ver 3.0. Sediment mineralogy, $^{87}Sr/^{86}Sr$ ratios, and $\delta^{13}C$ values are shown in Table 1, Table 2 shows the major ion composition of rainfall samples, and Table 3 summarizes the groundwater geochemistry.

3.4 RESULTS

3.4.1 Sediment composition

Loess samples were collected from 2-3m below the ground surface, from the L_1 layer of the Q3 Malaan loess, which was deposited at ~12.5 ka B.P. (Liu et al. 1986; Fig. 1; Table 1). The samples are dominated by quartz (>40%), Na-feldspar (~20%), carbonate minerals (mostly calcite ~8 - 20%), and clay minerals (mostly illite and kaolin ~15%). Both primary and secondary carbonate is present, including detrital carbonate, fossil

gastropod shells, calcrete nodules and carbonate grain coatings. One clay sample from a drill hole at 53m depth was also collected. Clay lenses are interlayered throughout the Quaternary aquifer and were deposited in palaeo-lakes that formed in areas of high subsidence (Wang et al. 2002). The Yuncheng salt lake (Fig. 1) is a modern example of one such lake, it is hyper-saline with Na-Cl-SO_4 type chemistry (Wang et al., 2002). The clays contain abundant evaporite minerals including gypsum, thenardite and up to 13% halite, indicating similar hyper-saline lake chemistry (Wang et al., 2002). The $\delta^{13}C$ values of carbonate in the loess range between -3.5‰ and -7.5‰ (Table 1), which is typical of carbonate throughout the Chinese Loess Plateau (Han et al., 1997; Rao et al., 2006; Cao et al., 2008). $^{87}Sr/^{86}Sr$ ratios of the carbonate (acid soluble) and silicate (acid insoluble) fractions of the loess range from 0.71086 to 0.71165 and 0.71837 to 0.72513, respectively. These ratios are similar to carbonate and silicate components of the Quaternary sediments elsewhere in northern China (Gallet et al., 1996; Yokoo et al., 2004; Edmunds et al., 2006).

Mineral	**LYL**[1]	**KL1**	**KL3**	**WGL**
Quartz (%)	42.1[2]	39.3	41.4	43.3
Albite	19.6	19.6	18.5	17.5
Orthoclase	-	3.1	2.3	3
Calcite	15.4	20.6	16	7.7
Dolomite	2.1	1.3	2.5	6.4
Aragonite	0.5	-	-	-
Low Mg Calcite	0.7	-	-	-
Gypsum	-	0.3	0.5	2.9
Chlorite	0.3	3.3	3.7	3.3
Illite/Muscovite	12.5	12.2	14.6	15.7
Kaolin	6.1	0.3	0.4	0.3
$\delta^{13}C$ (‰)	-3.9	-4.3	-3.5	-7.5
$^{87}Sr/^{86}Sr$ Acid soluble	0.71128	0.71086	0.71093	0.71165
$^{87}Sr/^{86}Sr$ Acid insol.	0.71837	0.71891	0.71843	0.72513

[1]Sample name, as shown on Fig. 1.
[2]Mineral proportions determined by XRD

Table 1. Proportions of minerals, $\delta^{13}C$ values and $^{87}Sr/^{86}Sr$ ratios of loess samples from the Yuncheng Basin

3.4.2 Rainfall chemistry

Recharge of groundwater in the Yuncheng Basin primarily occurs during the East Asian summer monsoon (Currell et al., 2010). The monsoon has affected the region for at least 2.5Ma (An et al. 2000) and is the major source of recharge to most groundwater basins in northern China (e.g. Gates et al., 2008; Kreuzer et al., 2009). Rainfall chemistry was estimated from two rain samples collected in Yuncheng City in May and June 2009 and data from 1992-93 rainfall from Jinan and Beijing, 550km and 700km northeast of Yuncheng City, respectively (Fujita et al. 2000: Table 2). Major ion concentrations in rainfall are variable due to rainout, incorporation of sea spray and natural aerosols, and anthropogenic inputs (e.g. from coal burning). Elevated SO_4 and NO_3 concentrations of up to 9.6 & 2.0 mg/L, respectively (Table 2) in the rain from Yuncheng City reflect anthropogenic inputs (Okada, 1990; Fujita et al., 2000); concentrations of these ions are probably much higher than the pre-industrial era rainfall that recharged much of the deep groundwater. In general, the concentrations of other major ions in the rainfall are likely similar to those in the rain that recharged the Quaternary aquifer, as there are few anthropogenic sources of these elements in the region (Fujita et al., 2000), and the source regions for the monsoon have remained unchanged over this period (An et al., 1991; Huang et al., 2007). For this study an average rainfall composition based on the data in Table 2 is used. Sample YCRa contains high total cation/Cl ratios (~12.3) that may have resulted from anthropogenic sources (e.g. cement kiln emissions; Fujita et al., 2000) or dry deposition (e.g. windblown Na and Ca-sulfate). However, this does not have a large effect on the average cation/Cl ratios (Table 2).

Sample	Concentrations (mg/L)						Molar ratios			
Name	Na	Cl	SO4	Ca	Mg	NO3	Na/Cl	Ca/Cl	Mg/Cl	Total/Cl
YCRa	1.86	0.42	9.57	2.43	0.27	1.95	6.90	5.17	0.213	12.28
YCRb	0.34	0.45	2.25	1.70	0.12	0.98	1.17	3.37	0.139	4.68
JN (S)	0.37	0.78	9.36	3.74	0.21	3.04	0.727	4.25	0.386	5.36
JN (W)	0.90	2.13	13.1	5.14	0.35	4.46	0.650	2.14	0.242	3.03
BJ (S)	0.67	0.92	8.64	2.96	0.26	3.35	1.12	2.85	0.404	4.37
BJ (W)	1.27	2.55	20.0	9.18	0.86	7.63	0.764	3.19	0.493	4.44
Average	0.90	1.21	10.5	4.19	0.34	3.57	1.15	3.08	0.358	4.58

JN = Jinan, BJ = Beijing, (S) = Summer, (W) = Winter, From Fujita et al. (2000)

Table 2. Major ion concentrations in rainfall from samples collected in Yuncheng city, and published values for Beijing and Jinan (Fujita et al., 2000).

3.4.3 Groundwater major ion chemistry

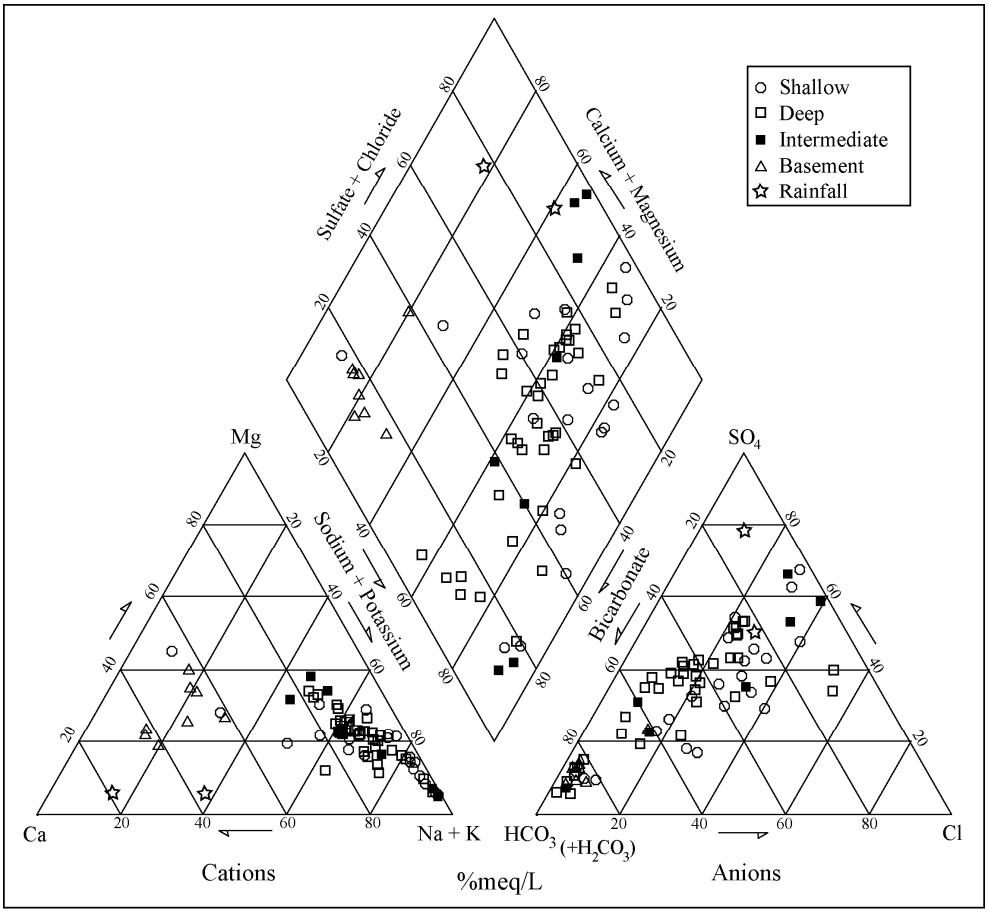

Fig. 2 Piper diagram showing proportions of major ions in groundwater from the Yuncheng Basin. The majority of groundwater in the Quaternary aquifer has high relative concentrations of Na and HCO_3 (data from Table 3).

As shown in Figure 2, most groundwater in the Quaternary aquifer is Na-HCO_3 type and differs substantially in major ion composition from rainfall, indicating that processes other than simple evapotranspiration are important in controlling groundwater chemistry. Na comprises 16 - 97% (median of 85%) and 62 - 97% (median of 79%) of the total cations on a molar basis in shallow and deep groundwater, respectively. Anion concentrations are more variable (Fig. 2), but HCO_3 is generally the dominant anion, comprising 4 - 90% (median of 42%) and 10 – 95% (median of 54%) of the total anions in shallow and deep groundwater, respectively. In the most saline groundwater (TDS > 2500 mg/L), Cl and SO_4 are the dominant anions (Cl + SO_4 > 80% of the total anions), probably due to removal of HCO_3 via calcite precipitation. The dominant water type in the basement is Ca-HCO_3 or Ca-Mg-HCO_3-type; Ca comprises 32 -56% and Mg 17% - 35% of the total cations and HCO_3 comprises 70 to 93% of the total anions (Fig. 2).

3.4.3.1 Major ion ratios

Cl/Br ratios in groundwater allow the distinction between halite dissolution and evapotranspiration as mechanisms to increase salinity (Davis et al., 1998; Cartwright et al., 2004; Alcala and Custodio, 2008). The molar Cl/Br ratio of rainfall from Yuncheng City is ~270 (Table 3), which is typical of inland rainfall (Davis et al., 1998). Basement groundwater that has low TDS contents and which was recharged relatively recently (Currell et al., 2010) has Cl/Br ratios from ~300 to 900 (Table 3), while Cl/Br ratios of most groundwater from the Quaternary aquifer are 302 to 1810 (median of 1070). The observation that groundwater has higher Cl/Br ratios than local rainfall or the oceans indicates minor addition of Cl from sources other than rain, most likely halite that is

locally present in loess in northern China (Yokoo et al., 2004). However, due to the exclusion of Br from the mineral lattice, halite commonly has Cl/Br ratios of >10,000 (Davis et al., 1998; Cartwright et al., 2004); hence the amount of halite dissolution must be minor. From mass balance, the amount of halite required to increase Cl/Br ratios from 300 to 1100 assuming Cl/Br of halite of 10,000 and an initial Cl concentration of 0.034 mmol/L (the average rainfall Cl concentration), is ~0.1 mmol/L. This represents < 5% of the total Cl and Na in most groundwater (Table 3).

Given that the Br in groundwater is derived from rainfall and that Br generally behaves conservatively in groundwater (Herczeg and Edmunds, 2000), the degree to which solutes in groundwater have been concentrated by evapotranspiration (the 'ET factor') can be derived from comparison of the Br concentration in groundwater and rainfall (Table 3). Estimates of this factor range from 3.8 - 890 (median of 45). Broadly similar, but slightly higher factors are reached using Cl data rather than Br (3.2 to 1400, median of 77), probably due to the minor addition of Cl from halite dissolution.

Sample Number	Unit*	Depth (m)	TDS (mg/L)	pH	HCO_3 (mg/L)	Cl	Br	NO_3	SO_4	Ca	Na	Mg	Si	Sr	$^{87}Sr/^{86}Sr$	$\delta^{13}C$	Cl/Br (molar)	ET Factor Br_{gw}/Br_{rain}	S.I. Calcite	S.I. Dolomite	S.I. Am Sil
1	S	-34	5290	7.6	740	1335	1.96	633	2165	47.7	1452	220	2.1	12.0	0.71154	-11.2	1530	561	0.09	1.13	-1.34
2	S	-20	3100	7.9	730	348	0.606	36.2	1238	23.2	966	98.7	2.2	3.96		-11.2	1290	173	0.15	1.20	-1.36
12	S	-20	700	7.2	448	20.8	0.055	0.079	42.2	117	26.0	70.6	7.4	0.44	0.71617	-14.4	850	15.8	0.30	0.66	-0.84
20	S	-30	2160	7.7	460	388	0.585	56.8	672	157	480	98.7	6.0	2.12		-14.0	1500	167	0.68	1.44	-0.94
21	S	-70	713	7.8	332	66.8	0.083	24.5	125	103	81.8	41.6	6.6	1.14	0.71185	-15.6	1810	23.7	0.55	0.98	-0.90
25	S	-59	858	8.7	596	15.4	0.115	0.13	64.0	7.64	305	14.9	5.7	0.28	0.71142	-9.9	302	32.8	0.60	1.79	-0.99
29	S	-35	1950	8.2	792	263	0.428	1.15	202	21.9	641	50.9	5.5	1.65		-9.9	1390	122	0.69	2.04	-0.99
30	S	-40	2010	8.3	864	251	0.499	1.17	224	19.1	696	44.8	6.0	3.89	0.71119	-9.3	1130	143	0.66	1.98	-0.95
31	S	-50	1490	7.8	424	274	0.640	1.27	363	152	289	59.7	9.0	1.25	0.71382	-12.1	965	183	0.82	1.52	-0.77
32	S	-50	838	8.2	336	90.1	0.066	0.13	187	40.8	207	35.5	6.4	1.16		-13.2	3070	18.9	0.68	1.60	-0.92
33	S	-70	904	8.2	312	137	0.171	0.11	186	49.8	178	54.5	6.0	1.26	0.71145	-14.6	1810	48.7	0.66	1.65	-0.95
42	S	-17	6090	7.4	463	1130	2.22	69.4	3170	269	1647	198	2.4	7.79	0.71152	-10.8	1150	634	0.34	0.82	-1.34
43	S	-20	8450	7.9	269	1690	3.13	54.5	5178	386	1807	258	0.2	8.20			1220	894	0.72	1.54	-1.24
57	S	-55	879	8.7	547	38.1	0.163	36.5	51.0	3.17	283	9.2	3.8	0.26	0.71129	-9.5	528	46.5	0.19	1.14	-1.16
58	S	-30	1480	8.6	680	115	0.301	105	204	5.37	477	13.1	3.6	0.39		-10.1	859	86.1	0.36	1.40	-1.19
62	S	-40	1540	8.2	520	207	0.283	24.4	388	22.1	410	66.5	4.8	2.26		-11.1	1650	80.8	0.44	1.64	-1.05
65	S	-40	2590	7.6	648	281	0.669	63.0	843	57.0	645	153	5.6	3.61	0.71211	-11.0	945	191	0.31	1.32	-0.98
71	S	-27	2010	8.3	558	314	0.433	27.0	534	14.4	577	53.2	4.0	1.78		-11.3	1630	124	0.32	1.50	-1.13
74	S	-30	2490	7.8	644	375	0.915	103	742	42.0	698	106	5.9	2.97	0.71175	-12.8	925	261	0.37	1.42	-0.96
77	S	-40	2530	8.1	630	487	1.36	192	479	22.0	739	66.7	4.3	1.44			809	388	0.39	1.55	-1.10
24	I	-120	1120	8.3	312	187	0.329	0.66	274	44.6	265	59.2	5.8	1.88		-13.0	1280	94.1	0.74	1.86	-0.96
26	I	-110	845	8.6	648	15.4	0.077	0.11	41.9	5.10	312	12.4	4.4	0.25	0.71114	-10.4	454	21.9	0.38	1.52	-1.09
27	I	-117	865	8.8	605	12.4	0.128	0.083	71.3	4.03	315	8.65	4.6	0.22	0.71114	-9.8	219	36.5	0.44	0.98	-1.08
40	I	-80	4670	7.8	340	850	1.51	21.2	2782	429	944	361	2.7	11.8	0.71160		1270	431	0.83	1.93	-1.30
53	I	-120	765	8.1	389	58.9	0.158	13.5	114	37.5	169	33.7	8.3	1.85			842	45.1	0.64	1.89	-0.80
55	I	-120	5150	7.8	148	1507	1.72	33.9	3095	289	1021	448	4.4	12.8	0.71155		1970	493	0.25	1.45	-1.09
66	I	-100	1010	8.0	500	42.5	0.118	22.3	205	28.2	266	31.8	8.5	1.51	0.71312	-9.8	812	33.7	0.44	1.54	-0.79
55a	I	-120	3070	7.9	415	676	0.831	23.1	1408	153	703	243	3.7	6.96			1830	237	0.73	1.22	-1.16
3	D	-240	1090	8.2	448	72.6	0.157	2.16	287	27.4	277	41.8	6.7	1.17	0.71246	-9.7	1040	44.9	0.57	1.60	-0.89
4	D	-270	1310	8.1	308	154	0.324	1.43	481	45.8	311	55.7	6.3	2.29	0.71230	-10.8	1070	92.6	0.50	1.36	-1.40
6	D	-220	957	8.0	444	59.2	0.145	0.39	228	39.1	226	43.2	6.9	1.12	0.71231	-10.2	922	41.3	0.56	1.45	-0.88
7	D	-300	1110	7.8	264	127	0.275	1.31	399	53.9	246	46.3	6.5	1.60		-12.4	1040	78.7	0.25	0.72	-0.91
8	D	-230	774	8.1	332	96.5	0.146	0.94	179	28.6	183	31.9	5.4	0.99	0.71130	-16.4	1490	41.7	0.35	1.04	-1.00
22	D	-240	733	8.1	224	116	0.216	0.27	162	57.5	167	16.8	8.1	0.57		-14.2	1210	61.6	0.59	0.94	-0.81
23	D	-150	601	8.3	268	68.7	0.150	0.21	84.9	30.0	138	26.6	5.9	0.89	0.71144	-14.6	1030	43.0	0.57	1.37	-0.95
28	D	-210	1810	8.4	556	164	0.280	0.88	376	22.6	566	56.0	4.9	1.24		-10.3	1320	80.0	0.65	1.99	-1.03
35	D	-210	1630	8.3	208	713	1.09	2.29	743	86.8	570	107	4.7	3.70	0.71162	-13.7	1480	310	0.65	1.67	-1.05
36	D	-250	1630	8.2	356	209	0.398	0.60	646	70.7	356	95.3	6.1	3.11	0.71232	-11.3	1180	114	0.73	1.88	-0.94

*S = Shallow, I = Intermediate, D = Deep, B = Basement, R = Rainfall

Continued..

37	D	-200	1040	8.4	220	193	0.349	0.22	254	34.9	265	25.4	6.6	0.80	0.71202	-13.3	1250	99.6	0.54	1.28	-0.91
39	D	-220	1090	7.9	262	131	0.238	2.41	378	54.3	242	46.8	6.6	1.71	0.71138	-12.0	1250	68.0	0.36	0.93	-0.89
41	D	-270	1060	8.1	282	148	0.246	1.69	321	47.2	226	47.6	5.4	1.52		-13.4	1350	70.2	0.46	1.21	-0.98
44	D	-300	1110	8.2	255	131	0.234	2.47	377	53.8	236	46.5	6.5	1.69		-11.3	1270	66.8	0.55	1.32	-0.91
46	D	-210	667	7.8	344	27.9	0.096	29.5	88.7	25.4	178	14.0	8.3	1.05		-10.0	653	27.5	0.13	0.29	-0.79
47	D	-200	526	7.8	358	4.96	0.020	11.3	18.3	22.0	112	31.7	7.7	1.09		-10.3	566	5.65	0.15	0.75	-0.83
48	D	-260	608	8.1	421	8.33	0.049	21.3	33.6	12.9	161	26.1	6.6	0.77	0.71104	-8.9	382	14.0	0.28	1.15	-0.90
49	D	-260	579	7.9	316	30.7	0.104	39.7	178	21.5	141	25.5	7.6	1.09		-8.3	664	29.8	0.10	0.55	-0.83
50	D	-230	634	8.3	420	10.8	0.052	22.9	49.9	11.4	178	22.3	6.3	0.66		-8.2	468	14.8	0.35	1.29	-0.92
51	D	-224	561	8.3	360	12.5	0.046	24.2	17.8	13.8	140	30.3	6.7	0.81		-8.3	616	13.1	0.43	1.48	-0.90
52	D	-280	623	8.2	430	11.4	0.050	18.0	42.3	16.9	162	28.3	7.1	0.92	0.71131	-9.3	515	14.3	0.41	1.32	-0.83
54	D	-160	1290	7.9	615	52.9	0.150	43.5	300	17.5	381	41.2	6.0	1.24		-9.2	795	42.8	0.23	1.11	-0.94
56	D	-220	1020	8.6	685	19.4	0.084	7.09	99.8	5.27	324	12.6	4.4	0.36		-9.9	520	24.0	0.44	1.57	-1.09
59	D	-230	1290	7.8	272	154	0.226	12.2	482	58.1	282	56.0	6.9	3.24			1540	64.5	0.24	0.74	-0.88
60	D	-178	1270	8.6	566	76.9	0.340	211	134	8.64	390	23.1	4.4	0.74	0.71139	-8.9	510	97.1	0.51	1.74	-1.10
61	D	-180	1236	8.0	456	119	0.183	11.0	320	34.7	314	44.3	7.0	2.09			1470	52.2	0.50	1.38	-0.88
63	D	-220	1820	8.1	186	506	0.713	3.89	433	68.0	425	56.4	4.8	3.80	0.71148		1600	204	0.43	1.06	-1.05
64	D	-180	1100	8.1	434	88.5	0.152	0.46	298	29.9	276	43.5	5.7	1.88		-9.5	1310	43.4	0.49	1.42	-0.96
67	D	-202	748	8.0	398	28.5	0.071	0.30	131	24.7	187	33.5	6.4	0.95		-8.9	909	20.2	0.32	1.07	-0.91
68	D	-180	1270	7.9	448	117	0.223	0.99	383	54.9	293	63.9	6.5	1.83			1180	63.8	0.59	1.53	-0.91
69	D	-200	1110	7.7	422	85.3	0.180	1.27	308	56.8	248	56.4	8.2	1.20	0.71256	-10.3	1070	51.5	0.34	0.96	-0.81
70	D	-230	990	7.6	356	68.1	0.134	20.5	268	38.4	251	30.3	8.5	1.98	0.71358		1140	38.3	0.01	0.20	-0.79
72	D	-240	1090	7.9	396	93.0	0.154	0.23	308	49.6	252	49.9	7.5	1.15	0.71224	-9.6	1360	43.9	0.46	1.21	-0.84
73	D	-180	1160	7.8	384	133	0.250	0.78	341	68.4	225	75.9	7.1	1.77	0.71203		1200	71.5	0.52	1.37	-0.87
75	D	-320	821	8.2	336	64.9	0.159	0.88	205	44.5	163	56.6	7.6	1.58	0.71142	-9.5	920	45.5	0.65	1.70	-0.88
76	D	-230	1250	7.9	352	164	0.289	1.76	382	56.4	277	62.9	6.8	1.86	0.71155	-11.8	1280	82.6	0.41	1.16	-0.88
78	D	-230	868	8.1	334	91.3	0.181	1.27	205	52.9	165	61.6	6.8	1.49			1140	51.8	0.62	1.59	-0.89
9	B	-347	406	7.6	276	5.35	0.040	7.41	20.6	56.0	29.1	25.9	0.2	0.43	0.71437	-13.6	304	11.3	0.19	0.33	-0.90
10	B	-100	380	7.6	248	3.80	0.021	0.007	29.7	53.4	23.7	25.0	0.2	0.24	0.71615	-12.7	402	6.08	0.19	0.34	-1.04
13	B	-160	329	7.4	208	4.41	0.020	0.011	30.1	44.8	18.0	25.1	0.2	0.25		-12.7	504	5.64	-0.15	-0.26	-0.94
14	B	-190	360	7.4	164	23.3	0.064	12.1	49.7	65.0	20.3	12.3	0.2	0.26		-13.9	822	18.3	-0.09	-0.63	-0.90
15	B	-254	261	7.5	148	4.12	0.016	2.55	18.0	50.1	12.3	10.6	0.2	0.23		-13.8	598	4.43	-0.21	-0.81	-0.88
17	B	-75	504	7.8	304	9.60	0.047	14.6	26.5	80.9	40.8	25.0	0.3	0.59	0.71336	-12.2	459	13.5	0.61	1.00	-0.79
18	B	-130	335	7.8	208	5.26	0.013	4.41	27.4	61.5	14.9	14.4	0.2	0.31	0.72031	-13.8	902	3.76	0.32	0.29	-0.93
19	B	-115	440	7.9	280	14.5	0.067	11.9	23.8	55.5	47.2	22.0	0.2	0.49		-12.2	487	19.1	0.49	0.86	-0.94
YCR(a)	R	NA	25.9	5.8		0.42	0.0035	1.95	9.58	2.43	1.86	0.27	nd	0.01			268	N/A			
YCR(b)	R	NA	12.4	6.2		0.45	ND	0.98	2.24	1.70	0.34	0.12	nd	nd			N/A	N/A			

Table 3. Sample locations, depths, major ion compositions, selected ion ratios and saturation index values calculated using PHREEQ

Figure 3 shows that in groundwater with TDS concentrations > 1200 mg/L, the majority of total cation/Cl ratios are relatively low (median of 3.0) and are similar to those in rainfall or seawater (~3.0 to 5.0), showing the dominant role of evapotranspiration in controlling the chemistry of this groundwater (Fig. 3a). Higher total cation/Cl ratios (5.0-50) in groundwater with TDS <1200 mg/L indicate that water-rock interaction is important in controlling the geochemistry of the lower salinity groundwater. The generally high concentrations of HCO_3 in deep and intermediate groundwater (median = 356 mg/L) and relatively high pH values (7.5 to 9) also indicate that mineral weathering is an important control on the chemistry of the lower salinity groundwater (e.g. Herczeg and Edmunds, 2000). Carbonate minerals make up ~20% of the loess (Table 1) and given their high dissolution rates relative to silicates (Lasaga, 1984), they would be expected to be dissolved by groundwater (Clark and Fritz, 1997). However, the relative proportions of Ca and Mg in the Quaternary aquifer groundwater are generally low (Ca = 0.7 - 42% of total cations, median of 7%; Mg = 2.5 - 42% of total cations, median of 13%). These cation compositions are not typical of groundwater that has predominantly weathered carbonates (e.g. Herczeg and Edmunds, 2000), indicating either that weathering of other mineral types (e.g. silicates) is more important, or that subsequent modification of groundwater cation composition (e.g. via ion exchange or carbonate precipitation) occurs in addition to carbonate weathering. Basement groundwater has total cation/Cl ratios of 3.0 - 21 (median of 12), including relatively high Ca/Cl and Mg/Cl ratios (> 3.0) (Fig 3c & 3d); these indicate that weathering is an important control on chemistry and that evapotranspiration is minimal.

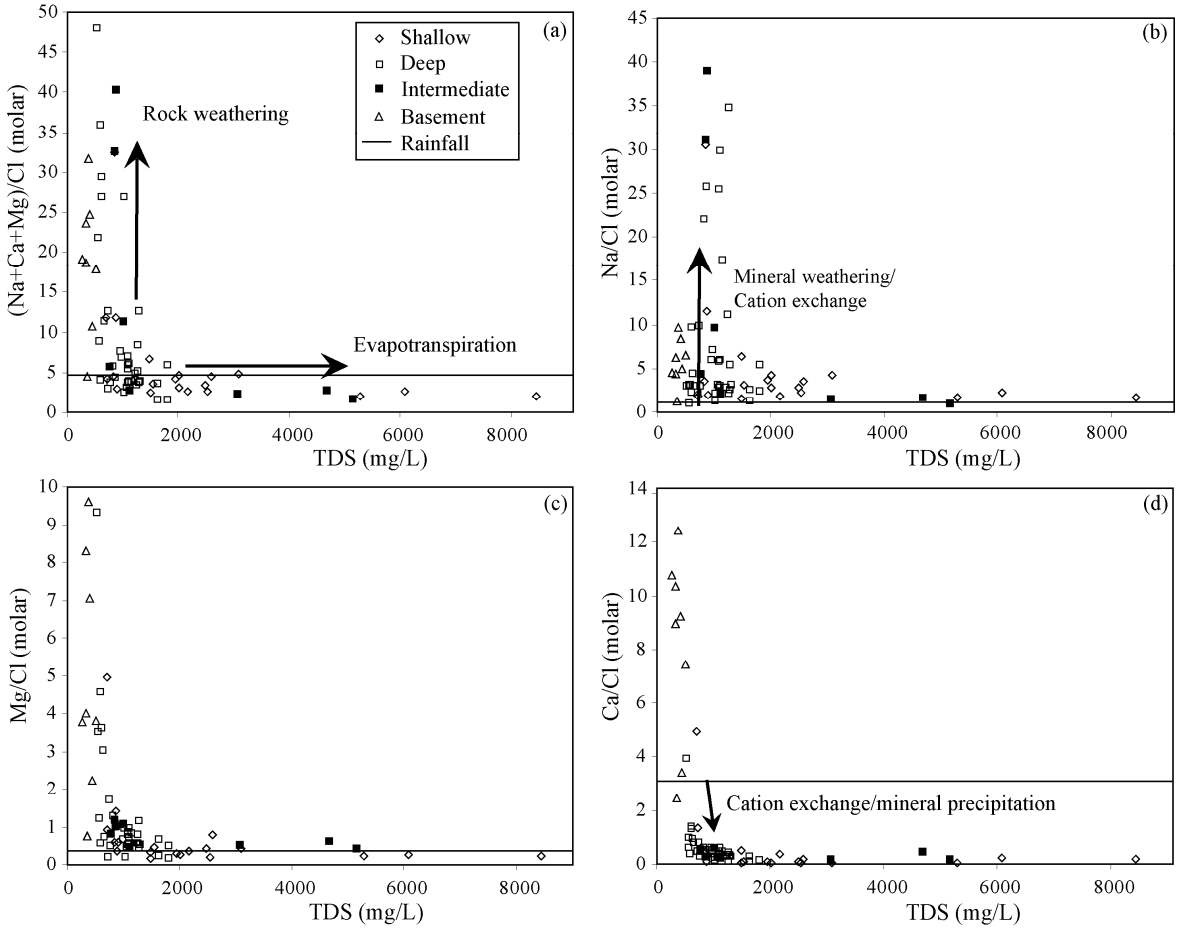

Fig. 3 Total molar cation/chloride ratios **(a)**; Na/Cl ratios **(b);** Mg/Cl ratios **(c);** Ca/Cl ratios **(d)** vs. TDS in groundwater, indicating the importance of evapotranspiration in high salinity groundwater and water-rock interaction in low salinity water. Data from Table 3

3.4.4 $\delta^{13}C$

As shown in Figure 4, groundwater $\delta^{13}C$ values in the Quaternary aquifer range between -16.4‰ and -8.2‰ (median of -10.6‰; Table 3) and are intermediate between $\delta^{13}C$ values expected for DIC in water recharged via soil dominated by C_3 vegetation ($\delta^{13}C$ ~ -15‰, Clark and Fritz, 1997) and carbonates in the loess ($\delta^{13}C$ ~ -4‰, Fig 4a). These values and the positive correlation between groundwater HCO_3 concentrations and $\delta^{13}C$ values ($r^2 = 0.25$) indicate that carbonate weathering is a major source of groundwater DIC

(c.f., Dogramaci and Herczeg, 2002). The $\delta^{13}C$ values increase from ~-15‰ in the recharge area in the south to ~-10‰ in the center of the Sushui River Basin (fig. 4b), indicating progressive carbonate dissolution along flow paths. Both congruent and incongruent carbonate weathering would cause $\delta^{13}C$ values to increase, approaching the values of carbonate in the aquifer (Clark and Fritz, 1997; Dogramaci and Herczeg, 2002).

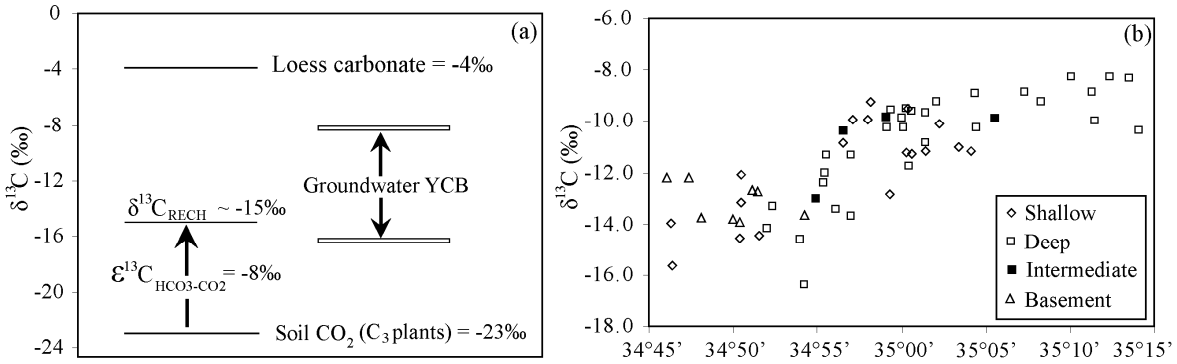

Fig. 4a. Estimated $\delta^{13}C$ fractionations during recharge and dissolution of carbonates; **4b.** $\delta^{13}C$ values vs. northing, indicating that carbonate dissolution occurs in the Quaternary aquifer.

3.4.5 Strontium and $^{87}Sr/^{86}Sr$

Sr concentrations range from 0.25 to 12.0 mg/L in shallow groundwater (median = 1.72 mg/L) and 0.22 to 12.8 mg/L in deep and intermediate groundwater (median = 1.48 mg/L), which is much higher than Sr concentrations in rainfall (e.g. YCRa has 0.011 mg/L Sr; Table 3). Despite the wide range of Sr concentrations, $^{87}Sr/^{86}Sr$ ratios from groundwater in the Quaternary aquifer are within a relatively narrow range (0.7110 to 0.7162, median of 0.7116, $\sigma = 0.001$). The ratios are similar to both rainfall (0.7110 to 0.7117) and the acid soluble (carbonate) fraction of the loess (0.7109 to 0.7116); these sources have similar $^{87}Sr/^{86}Sr$ ratios, as Sr in rain is predominantly from windblown terrestrial carbonate (Okada et al, 1990; Yokoo et al., 2004). Hence, evapotranspiration of rainfall and carbonate weathering are the major Sr sources in groundwater. As shown in

Figure 5, the relatively high molar Sr/Cl ratios (> 0.01) in groundwater with TDS <1200 implies carbonate weathering is likely the most important source of Sr in low salinity groundwater, By contrast, at higher salinities, Sr from evapotranspiration of rainfall far outweighs the Sr derived from weathering (Fig. 5a). $^{87}Sr/^{86}Sr$ ratios in ~30% of the groundwater samples are higher than in rainfall and carbonates (> 0.7120; Fig. 5b), indicating that a component of Sr also comes from weathering of silicates. The acid insoluble fraction of the loess has significantly higher $^{87}Sr/^{86}Sr$ values than rainfall or carbonates (0.7184 to 0.7251). If silicates in the loess (e.g. albite) were a major source of Sr, then significantly higher $^{87}Sr/^{86}Sr$ ratios than those observed would be expected (e.g. > 0.7150), hence they are likely a minor source.

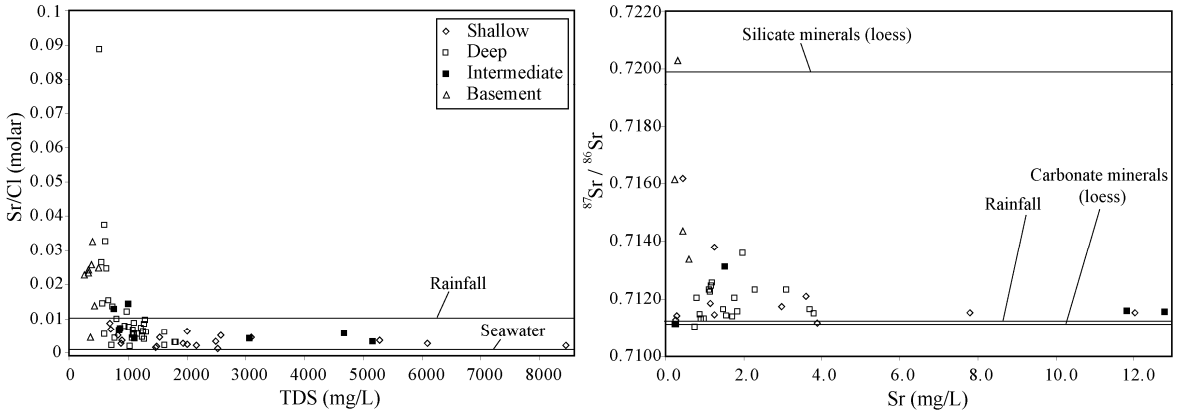

Fig. 5a. Sr/Cl ratios in groundwater vs. TDS values; **5b.** Sr concentrations and mean $^{87}Sr/^{86}Sr$ values in rain, carbonate minerals and silicate minerals, indicating that Sr from evapotranspiration of rainfall and weathering of carbonates are the dominant sources of groundwater Sr. Data from Table 3.

In comparison to the Quaternary aquifer, groundwater from the basement has low Sr concentrations (0.24 to 0.59 mg/L), but a wider range of $^{87}Sr/^{86}Sr$ values (0.7133 to 0.7203, median of 0.7152). Han et al., (2010) report bulk rock $^{87}Sr/^{86}Sr$ ratios of 0.71147-0.89504 for this formation in the Yunzhong Mountains, 350km north of the Yuncheng Basin, these values are typical of old silicate rocks globally (Dickin, 1995; Harrington and

Herczeg, 2003). The low Sr concentrations and higher $^{87}Sr/^{86}Sr$ ratios in the basement groundwater hence likely reflect addition of small amounts of Sr via incongruent weathering of silicate minerals (e.g. hornblende, diopside, feldspar, biotite) with high $^{87}Sr/^{86}Sr$ ratios.

3.4.6 Evolution of hydrogeochemistry during flow

The proportions of major ions in groundwater vary along horizontal flow paths from the basin margins to centre as illustrated by the south-north transect B-B' in Figure 6. Shallow, young groundwater in the recharge area in the piedmont of the Zhongtiao Mountains, (e.g. samples 12 and 21) has chemistry that is similar to evaporated rainfall, with Ca and Mg being the dominant cations (Ca + Mg > Na: Table 3). These samples have low TDS contents (~700mg/L) and have had relatively little interaction with the aquifer matrix. Apart from these samples, groundwater in the Quaternary aquifer is almost universally Na-dominated, and evolves towards increasingly Na and HCO_3 –rich compositions along flow paths, at the expense of the other major ions (Fig. 6). For example, between latitudes 345205.2, near the Zhongtiao Mountains, and 345655.8, in the central Sushui River Basin, the amount of Na as a proportion of the total molar cations increases from 77% to 95% and the amount of HCO_3 as a proportion of total anions increases from 48% to 94%. The observation that relative HCO_3 concentrations increase along flow directions precludes precipitation of carbonates as a mechanism to reduce relative Ca and Mg compositions.

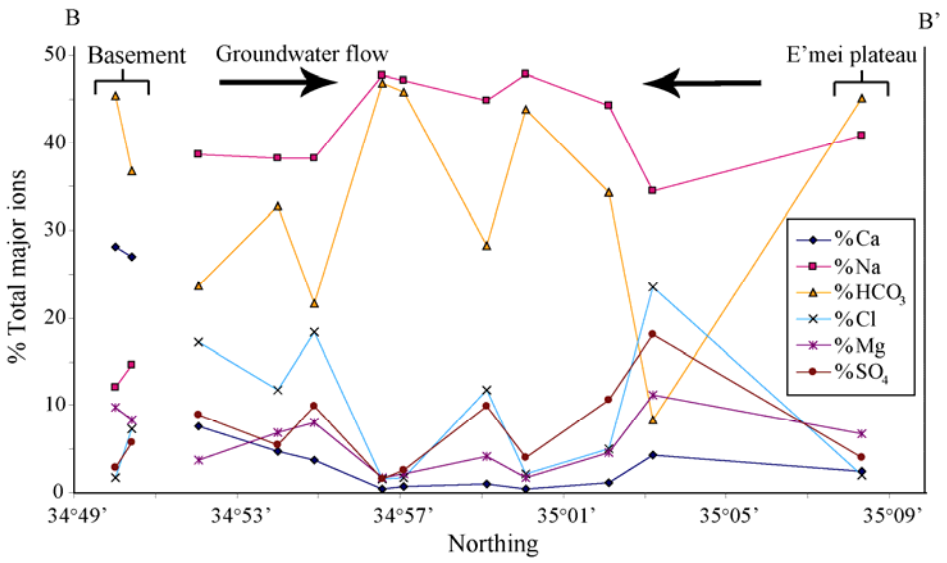

Fig. 6. Percentages of major ions on a molar basis in groundwater along a S-N transect (B-B', Fig. 1). Groundwater becomes increasingly dominated by Na and HCO_3 at the expense of Ca + Mg and Cl from the basin margins to its centre. Data from Table 3.

The possible sources of Na in groundwater are weathering of albite and Na-evaporite minerals in the aquifer; and cation exchange. As discussed earlier, halite dissolution only accounts for only a small amount of the Na in groundwater, while other Na-bearing evaporites such as thenardite and mirabilite were not detected in the loess samples and are only minor components of loess in the region (Liu, 1988; Yokoo, 2004). Albite makes up (~20%) of the loess and may be a source of Na, however, dissolved silica concentrations are generally lower (0.2 to 9.0 mg/L) than is typically the case in groundwater where feldspar weathering is a major process (~20 to > 100 mg/L: Harrington and Herczeg, 2003; Cartwright et al., 2004). Groundwater Na and Si concentrations do not correlate positively, as would be expected if albite was a major source of solutes, while the groundwater is undersaturated with respect to amorphous silica (SI = -0.79 to -1.36: Table 3), ruling out buffering of dissolved silica contents by amorphous silica precipitation. The conclusion that albite dissolution is only a minor source of Na is consistent with the

$^{87}Sr/^{86}Sr$ ratios, which indicate that silicate minerals are only a minor source of Sr in groundwater. This implies that much of the Na in groundwater instead derives from cation exchange between Ca (and possibly Mg and Sr) derived from rainfall and carbonate weathering, and Na^+ adsorbed by clays and/or hydrous metal oxides in the aquifer matrix (Wang et al., 2002). This is consistent with increasing Na/Ca ratios along groundwater flow paths (from basin margins to centre) that are not accompanied by increasing total equivalent cation/Cl ratios as shown in Figure 7.

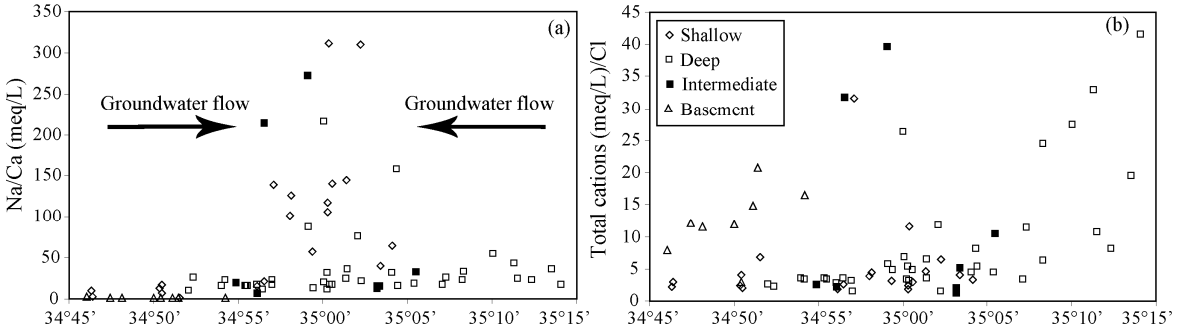

Fig 7a. Relationship between Na/Ca ratios and latitude, **7b**. Total equivalent cations/Cl vs. latitude. The increase in Na/Ca along flow paths isn't accompanied by an increase in total equivalent cation/Cl ratios, consistent with cation exchange between Na and Ca in the Quaternary aquifer.

Figure 8 shows that groundwater Sr/Ca and Mg/Ca ratios are also generally high relative to rainfall and carbonate minerals and increase along groundwater flow paths (fig. 8a & b). This may result due to progressive loss of Ca by cation exchange in the aquifer and/or addition of Mg and Sr via incongruent weathering of carbonates along flow paths, whereby impure forms of calcite (Mg or Sr-rich calcite) and dolomite are dissolved, and pure Ca-CO_3 is precipitated under dynamic equilibrium (e.g. Herczeg and Edmunds, 2000; Dogramaci and Herczeg, 2002). Groundwater Mg/Cl ratios are generally above rainfall ratios (Fig. 8c), and as there are few other Mg-bearing minerals in the loess (Table 1), incongruent dolomite dissolution is likely an important source of Mg. This is consistent

with increasing dolomite saturation index values along flow paths (Clark and Fritz, 1997; Fig. 8). However, the molar Sr/Cl ratios generally stay constant or decrease along flow paths, hence; the high Sr/Ca ratios largely reflect Ca loss via cation exchange rather than Sr gain from incongruent weathering. The Sr/Cl ratios decrease to values below rainfall ratios in the centre of the basin (fig 8c), and are accompanied by decreasing Sr/Na ratios (Fig. 8e), indicating that Sr likely also undergoes exchange with Na. Given the high groundwater Sr/Ca ratios, exchange between Sr and Na must still be significantly lesser than Na-Ca exchange.

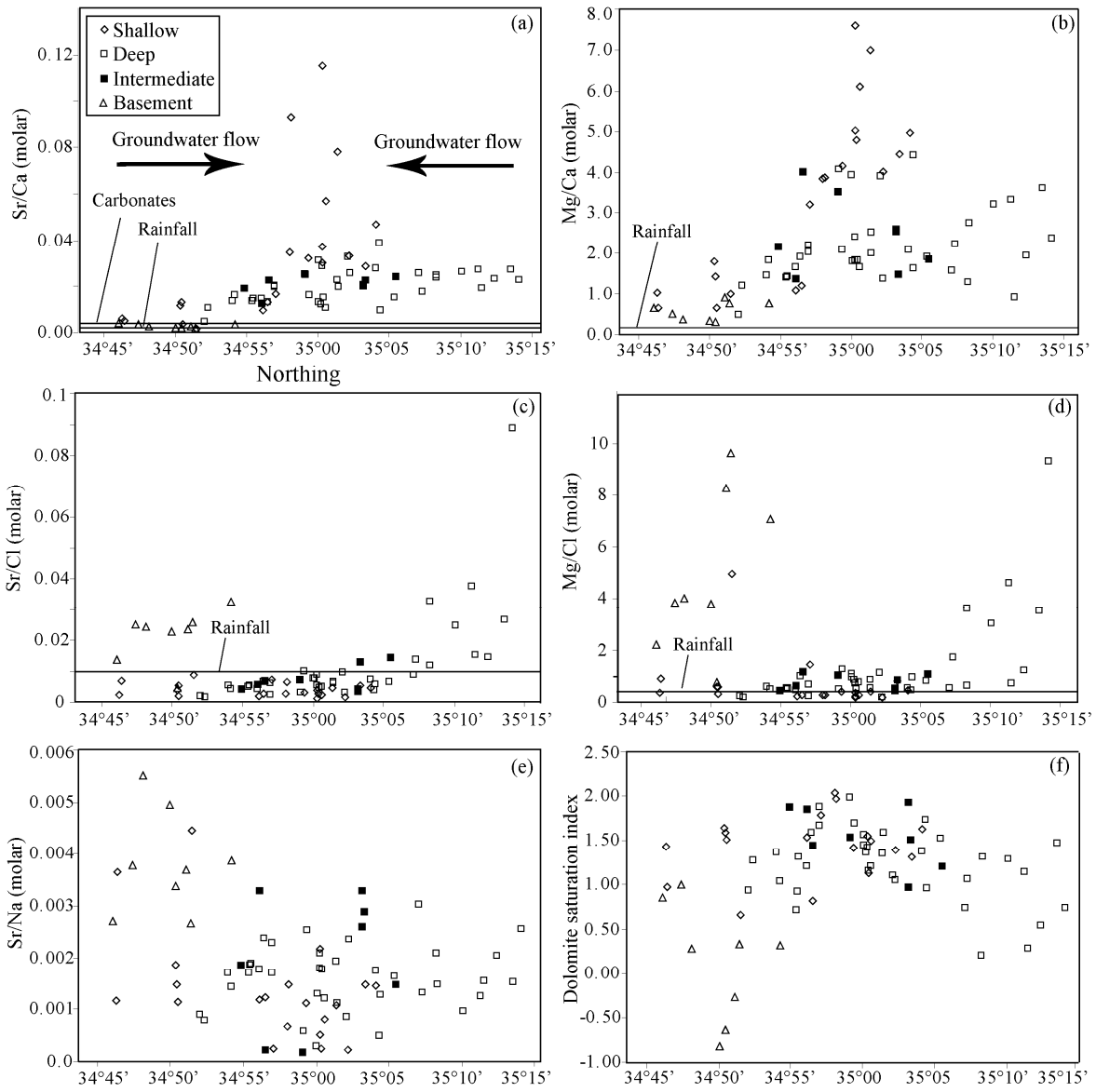

Fig 8. Trends in Sr/Ca **(a)**; Mg/Ca **(b)**; Sr/Cl **(c)**; Mg/Cl **(d)**; Sr/Na **(e)** and dolomite saturation indices **(f)** vs. latitude. These ratios indicate that incongruent weathering of carbonates and loss of Sr due to cation exchange with Na affect groundwater chemistry during flow.

3.5 DISCUSSION

The major ion chemistry, $\delta^{13}C$ and Sr data indicate that the major processes involved in the evolution of groundwater chemistry in the Yuncheng Basin are evapotranspiration, carbonate weathering (both congruent and incongruent) and cation exchange between Na and Ca.

3.5.1 Evapotranspiration

Evapotranspiration of rainwater in the unsaturated zone prior to recharge is promoted by the semi-arid climate and fine-grained soils (China Geological Survey, 2006) Shallow groundwater, much of which is affected by agriculture, has undergone the highest degree of evapotranspiration (e.g. ET factors > 100; Table 3). This is due to the large input of irrigation water that undergoes transpiration by crops, and the resulting high water tables (locally ~1m from the surface; China Geological Survey, 2006). Some deep groundwater samples that have high NO_3 concentrations due to mixing with shallow groundwater also have ET factors >100 (e.g. samples 60 and 63). Substantial, but lesser concentration of solutes by evapotranspiration (ET factors ~5 to 50) is also evident in deep groundwater with residence times of 1000s or 10000s of years and nitrate concentrations < 1 mg/L (Table 3), that has probably not mixed extensively with shallow groundwater (Currell et al., 2010). This indicates that natural evapotranspiration during recharge has always been an important process concentrating solutes prior to water reaching the saturated zone, and thus rainfall chemistry will always be an important control on groundwater composition.

In deep groundwater from the E'mei Plateau (Fig. 1, samples 46-52), the ET factor is relatively low (~5 to 25, Table 3). The relatively hard loess in this region contains more fractures than loess in the Sushui river basin (Yuncheng Regional Water Bureau, 1982); hence preferential flow likely occurs, limiting the degree of evapotranspiration. Mineral weathering is a more important source of solutes in this water, indicated by relatively high cation/Cl ratios (Fig. 3), while high nitrate concentrations also indicate that water from the surface (affected by agriculture) has reached depths of >150m in decades or years in this

region. Basement groundwater has also undergone a relatively low degree of evapotranspiration (ET factors ~3 to 20), due to rapid preferential recharge via fractures in the metamorphic rock. Hence, TDS values are low (< 500 mg/L) and mineral weathering is the dominant source of solutes, reflected by the high Cation/Cl ratios (Fig. 3). In general, the chemistry of the basement water (Mg and Ca-rich, low TDS concentrations) is distinctive compared to groundwater in the Quaternary aquifer (Fig. 2; Fig. 6); this is consistent with minimal horizontal input or mixing from the basement, which is a volumetrically minor groundwater source in comparison to the Quaternary sediments (Yuncheng Regional Water Bureau, 1982).

3.5.2 Carbonate weathering

The $\delta^{13}C$ and Sr data indicate that carbonate weathering is a major source of DIC and Sr in groundwater (section 3.4.4; 3.4.5). All groundwater from the Quaternary aquifer is saturated with respect to calcite (saturation index values +0.01 to +0.83) and dolomite (S.I. values +0.2 to +2.04), including shallow groundwater from the recharge area (Table 3). This implies that groundwater becomes saturated with respect to carbonate minerals soon after recharge. The amounts of calcite dissolution in groundwater that occur under open and closed system conditions can be qualitatively modelled based on DIC concentrations, pH values and $\delta^{13}C$ (e.g. Langmuir, 1971; Bishop and Lloyd, 1990; Clark and Fritz, 1997); Fig. 9a shows some theoretical evolution paths with respect to groundwater DIC during calcite dissolution. Assuming an initial pCO_2 of between $10^{-1.5}$ to $10^{-2.0}$ bars is appropriate for a semi-arid region with high potential ET (Brook et al., 1983). Taking this as a starting point for the evolution of DIC and pH during calcite dissolution

(Fig. 9a) suggests that while a large amount of calcite dissolution occurred under an open system (during recharge), some component of DIC is also derived from closed system dissolution. If dissolution occurred entirely under an open system, then $\delta^{13}C$ values would be controlled by soil CO_2, and remain at ~-15‰ (Clark and Fritz, 1997). Groundwater in the south of the basin generally has $\delta^{13}C$ values that are similar or slightly higher than this value (~-12 to -14‰), implying dissolution predominantly in an open system. However, groundwater in most of the Quaternary aquifer has higher $\delta^{13}C$ values (-12 to -8‰), that are consistent with substantial closed system carbonate dissolution (Table 3; Fig. 9b).

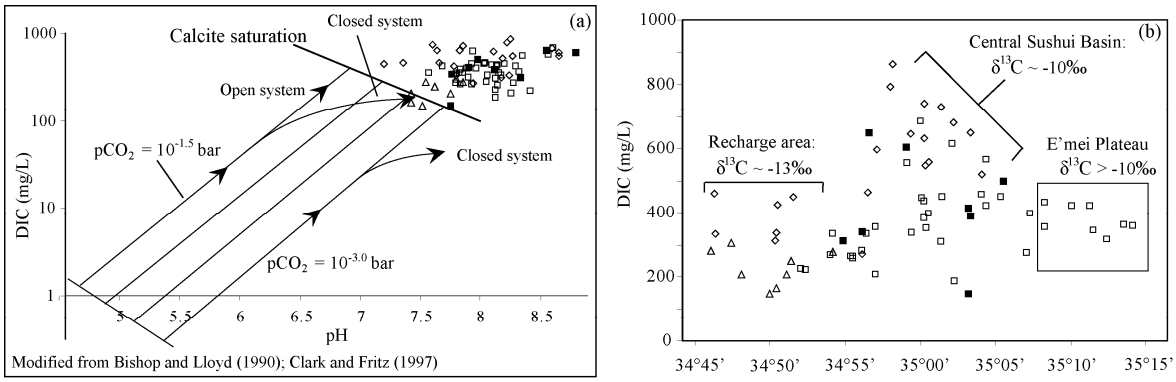

Fig. 9a. Groundwater DIC and pH values along with possible evolution paths during calcite dissolution under open and closed systems. **9b**. Groundwater DIC concentrations and $\delta^{13}C$ values in different sections of the basin indicating variable amounts of open and closed system carbonate dissolution

Relatively high DIC concentrations (> 500 mg/L), pH values (> 8.2) and $\delta^{13}C$ values (~ -10‰) occur in groundwater from the centre of the Sushui river basin (Fig 4; Fig 9b), implying that relatively large amounts of closed system carbonate dissolution have taken place. Given that groundwater likely becomes saturated with respect to carbonate minerals at an early stage of evolution, calcite dissolution in the mature waters at the centre of the basin likely occurs either as a second-stage process in response to cation exchange, so that groundwater maintains equilibrium with respect to calcite after loss of Ca (e.g.

Walraevens et al., 2007), and/or due to progressive incongruent weathering of Mg-rich calcite or dolomite along flow paths (e.g. Dogramaci and Herczeg, 2002).

Higher $\delta^{13}C$ values (-8 to -10‰) occur in groundwater from the E'mei plateau, despite these waters being relatively immature (they are at the beginning of horizontal flow paths) and having lower DIC concentrations (< 400 mg/L) than water in the central Sushui River Basin (Fig. 9b). The carbonate dissolution in this water has likely occurred almost entirely under a closed system, due to rapid infiltration/preferential flow in the hard, fractured loess in this region (see section 3.5.1); this would cause a greater increase in $\delta^{13}C$ values per unit DIC added to the groundwater (Clark and Fritz, 1997).

The high Ca/Cl and Mg/Cl ratios in the basement groundwater may also result from the weathering of carbonate in the soil and/or minor vein calcite in the metamorphic rocks. However, the $^{87}Sr/^{86}Sr$ ratios in this water indicate that the majority of Sr is derived from weathering of silicates, while relatively low $\delta^{13}C$ values (-12.2 to -13.9‰, median of -13.2‰) indicate minimal closed-system carbonate dissolution has occurred in this water. Incongruent dissolution of Ca and Mg-rich silicates (e.g. hornblende and diopside) are likely to be equally or more important sources of cations in this groundwater.

3.5.3 Cation Exchange

The observation that groundwater in the Quaternary aquifer is generally Na-rich and Ca-poor, and becomes increasingly Na-dominated along flow paths, despite the evidence of substantial carbonate dissolution (e.g. from trends in the $\delta^{13}C$, DIC and $^{87}Sr/^{86}Sr$ values), indicates that cation exchange between Na and Ca is a significant control on groundwater chemistry. Based on the major ion ratios, exchange largely involves Ca,

but also likely affects Sr and possibly Mg; although the relatively high Mg/Ca ratios and Mg/Cl ratios indicate that loss of Mg via exchange is significantly lesser than loss of Ca and/or is balanced by addition of Mg from incongruent dolomite dissolution (Fig. 8).

Cation exchange is favourable in relatively low ionic-strength waters (e.g. at [Na] <0.1M) where there is an abundance of negatively charged mineral surfaces, as these surfaces generally have greater affinity for divalent than monovalent cations (Stumm and Morgan, 1996). Exchange occurs in a wide variety of aquifer lithologies (e.g. Edmunds and Walton, 1983; Cerling et al., 1989; Walraevens et al., 2007; Blaser et al., 2010), including other basins filled with loess (e.g. Bhattacharya et al., 2006; Gomez et al. 2009). In the Yuncheng basin, the exchange likely occurs in lacustrine clay lenses interlayered throughout the Quaternary aquifer, as clays typically contain abundant exchange sites. The Yuncheng clays also have a large potential Na-source, as the hyper-saline lakes from which they were deposited had Na-rich chemistry (Wang et al., 2002).

Cation exchange may additionally/alternatively occur within the loess and palaeosols that make up the bulk of the aquifer matrix. Hydrous Fe, Mn and Al-oxides are a significant component of the loess and palaeosols (Liu, 1988) and these may provide suitable exchange sites. Exchange may also relate to large-scale disturbance and/or transient conditions in the aquifer (e.g. McNab et al., 2009); for example, high levels of pumping and/or mixing with irrigation water in recent decades may have mobilized Na that was otherwise relatively immobile in clay lenses. The wide occurrence of Cation exchange in the aquifer has important implications for the evolution of groundwater chemistry in the Yuncheng Basin, as mobilization As and F in groundwater has been shown to occur due to changes in Na/Ca ratios in similar aquifer settings in Argentina and the U.S. (Gomez et al.,

2009; Scanlon et al., 2009) and these elements locally occur in high concentrations in the region (Gao et al., 2007; Guo et al., 2007).

3.6 CONCLUSIONS

Groundwater in the Yuncheng Basin, a semi-arid aquifer in northern China that is composed of interlayered Quaternary loess, has evolved from meteoric recharge to its observed compositions via a combination of natural and anthropogenic processes, the most important being evapotranspiration, carbonate weathering and cation exchange.

The degree of evapotranspiration of infiltrating meteoric recharge is high throughout the Quaternary aquifer. Br and Cl data indicate that in pre-modern times, natural evapotranspiration during recharge concentrated solutes delivered in rainfall by a factor of ~5 to 50. This natural evapotranspiration is significantly lesser than the degree of modern evapotranspiration in shallow groundwater caused by irrigation, which has concentrated solutes by factors >100.

Major ion chemistry, $^{87}Sr/^{86}Sr$ and $\delta^{13}C$ data indicate that carbonate dissolution is a significant source of DIC and Sr in groundwater. However, in spite of the substantial carbonate weathering, groundwater in the Quaternary aquifer is generally Ca-poor and Na-rich. The major ion ratios indicate that this is due to cation exchange, removing Ca (and possibly Sr) and enriching groundwater Na contents during flow through the aquifer. The fact that most groundwater in the Quaternary aquifer, other than in recharge areas, is dominated by Na indicates that this is a widespread process and a significant control on groundwater cation compositions. Carbonate weathering occurs both as congruent and incongruent dissolution and under both open and closed system conditions.

Basement groundwater has much lower Sr concentrations than water in the Quaternary aquifer, but a wider range of $^{87}Sr/^{86}Sr$ ratios, that result from weathering of silicate minerals with high $^{87}Sr/^{86}Sr$ ratios in metamorphic rocks. The high groundwater $^{87}Sr/^{86}Sr$ values are accompanied high Ca/Cl and Mg/Cl ratios that are consistent with incongruent weathering of hornblende and diopside. Relatively slow weathering rates, due to the silicate lithology, and preferential flow through fractures (limiting evapotranspiration during recharge), result in relatively low salinities in this groundwater.

Acknowledgements

This research was partly initiated and greatly supported by the Australia-China Water Resources Research Centre, including Dr. Deli Chen, Dr. Yongping Wei, Prof. Song Xianfang and Prof. Li Baoguo. Special thanks also to the Yuncheng City Water Resources Service Bureau, in particular Mr. Sun Xinzhong.

REFERENCES

Alcala F.J., Custodio E., 2008. Using the Cl/Br ratio as a tracer to identify the origin of salinity in aquifers in Spain and Portugal. Journal of Hydrology 359, 189-207.

An, Z., Kukla G.J., Porter, S.C., Xiao J., 1991. Magnetic susceptibility evidence of monsoon variation on the Loess Plateau of central China during the last 130,000 years. Quaternary Research 36, 29-36.

An, Z., Porter, S.C., Kutzbach, J.E., Wu, X., Wang, S., Liu, X., Li, X., Zhou, W., 2000. Asynchronous Holocene optimum of the East Asian monsoon. Quaternary Science Reviews 19, 743-762.

Bhattacharya, P., Claesson, M., Bundschuh, J., Sracek, O., Fagerberg, J., Jacks, G., Martin, R.A., Stoniolo, A.R., Thir, J.M., 2006. Distribution and mobility of arsenic in the Rio Dulce alluvial aquifers in Santiago del Estero Province, Argentina. Science of the Total Environment 358, 97-120.

Blaser, P.C., Coetsiers, M., Aeschbach-Hertig, W., Kipfer, R., Van Camp, M., Loosli, H.H., Walraevens, K., 2010. A new groundwater radiocarbon correction approach accounting for palaeoclimate conditions during recharge and hydrochemical evolution: The Ledo-Paniselian Aquifer, Belgium. Applied Geochemistry 25, 437-455.

Bishop, P.K., Lloyd, J.W., 1990. Chemical and isotopic evidence for Hydrogeochemical processes occurring in the Licolnshire Limestone. Journal of Hydrology 121, 293-320

Brook, G.A., Folkoff, M.E., Box, E.O., 1983. A world model of soil carbon dioxide. Earth Surface Landforms 8, 79–88.

Cao, X.H., 2005. Study of the intermediate and deep layers of the Sushui River Basin confined groundwater system. In: *Shanxi Hydrotechnics Bulletin No. 3.* China Academic Journal Electronic Publishing House. pp 41-43. (In Chinese)

Cao, J.J., Zhu, C.S., Chow, J.C., Liu, W.G., Han, Y.M., Watson, J.G., 2008. Stable carbon and oxygen isotopic composition of carbonate in fugitive dust in the Chinese Loess Plateau. Atmospheric Environment 42, 9118-9122.

Cartwright, I., Weaver, T., Fulton, S., Nichol, C., Reid, M., Cheng, X., 2004. Hydrogeochemical and isotopic constraints on the origins of dryland salinity, Murray Basin, Victoria, Australia. Applied Geochemistry 19, 1233-1254.

Cartwright, I., 2010. Using groundwater geochemistry and environmental isotopes to assess the correction of ^{14}C ages in a silicate-dominated aquifer system. Journal of Hydrology, 382, 174-187.

Cerling, T.E., Pederson, B.L., Von Damm, K.L., 1989. Sodium-calcium ion exchange in the weathering of shales: Implications for global weathering budgets. Geology 17, 552-554.

China Geological Survey, 2006. Groundwater resources and environmental issues assessment in the six major basins of Shanxi (in Chinese), China Geological Survey Special publication, Beijing. 98p.

Clark, I., Fritz, P., 1997. Environmental Isotopes in Hydrogeology. Lewis Publishing, New York. 328p.

Currell, M.J., Cartwright, I., Bradley, D.C., Han, D.M., 2010. Recharge history and controls on groundwater quality in the Yuncheng Basin, north China. Journal of Hydrology 385, 216-229.

Davis, S.N., Whittemore, D.O., Fabryka-Martin, J., 1998. Uses of chloride/bromide ratios in studies of potable water. Ground Water 36(2), 328-350

Dickin, A.P., 1995. Radiogenic Isotope Geology. Cambridge University Press, Cambridge. 452p.

Dogramaci, S.S., Herczeg, A.L., 2002. Strontium and carbon isotope constraints on carbonate-solution interactions and inter-aquifer mixing in groundwaters of the semi-arid Murray Basin, Australia. Journal of Hydrology 262, 50-67.

Edmunds, W.M., Bath, A.H., Miles, D.L., 1982. Hydrochemical evolution of the East Midlands Triassic sandstone aquifer, England. Geochimica et Cosmochimica Acta 46, 2069-81.

Edmunds, W.M.**,** Walton, N.R.G., 1983. The Lincolnshire Limestone—Hydrogeochemical evolution over a ten-year period. Journal of Hydrology 61, 201-211

Edmunds, W. M., Ma, J., Aeschbach-Hertig, W., Kipfer, R., Darbyshire, D. P. F., 2006. Groundwater recharge history and hydrogeochemical evolution in the Minqin Basin, North West China. Applied Geochemistry 21(12), 2148-2170.

Fang, Q.X, Ma, L., Green, T.R., Yu, Q., Wang, T.D., Ahuja, L.R., 2010. Water resources and water use efficiency in the North China Plain: Current status and agronomic management options. Agricultural Water Management 97, 1102-1116.

Faure, G., 1991. Principles and Applications of Inorganic Geochemistry. Prentice-Hall, New Jersey. 626 pp.

Fujita, S., Takahashi, A., Weng, J, Huang, L., Kim, H., Li, C., Huang, F.T.C., Jeng, F. 2000. Precipitation chemistry in East Asia. Atmospheric Environment 34, 525-537.

Gallet S., Jahn B. and Torii M., 1996. Geochemical characterization of the Luochuan loess-paleosol sequence, China, and paleoclimatic implications. Chemical Geology 133, 67-88.

Gao, X., Wang, Y., Li, Y., Guo, Q., 2007. Enrichment of fluoride in groundwater under the impact of saline water intrusion at the salt lake area of Yuncheng basin, northern China. Environ. Geol. 53(4), 795 – 803.

Gates, J.B., Edmunds, W.M., Darling, W.G., Ma, J., Pang, Z., Young, A.A., 2008. Conceptual model of recharge to southeastern Badain Jaran Desert groundwater and lakes from environmental tracers. Applied Geochemistry 23, 3519 - 3534.

Gleik, P.H., 2009. China and Water (Chapter 5). In: Gleik, P.H., Cooley, H., Cohen, M.J., Morikawa, M., Morrison, J., Palaniappan, M. (eds), *The world's water 2008-2009. The Biennial report on freshwater resources.* Island Press, Washington, pp. 79-97.

Gomez M.L., Blarasin M.T. and Martinez D.E., 2009. Arsenic and fluoride in a loess aquifer in the central area of Argentina. Environmental Geology 57, 143-155.

Gosselin, D.C., Harvey, F.E., Frost, C., Stotler, R., Macfarlane, P.A., 2004. Strontium isotope geochemistry of groundwater in the central part of the Dakota (Great Plains) aquifer, USA. Applied Geochemistry 19, 359-377.

Guo, Q., Wang, Y., Gao, X., Ma, T., 2007. A new model (DRARCH) for assessing groundwater vulnerability to arsenic contamination at basin scale: a case study in Taiyuan basin, northern China. Environmental Geology 52, 923-932.

Han, D.M., Liang, X., Currell, M.J., Jin, M.G., Zhong, W.J., Liu C.M., Song, X.F. Environmental isotopic and hydrochemical characteristics of groundwater systems in Daying and Qicun geothermal fields, Xinzhou Basin, Shanxi, China. Hydrological Processes, In Press (accepted manuscript) doi: http://dx.doi.org/10.1002/hyp.7742

Han, J.M., Keppens, E., Liu, T.S., Paepe, R., Jiang, W.Y., 1997. Stable isotope composition of the carbonate concretion in loess and climate change. Quaternary International 37, 37-43.

Harrington, G.A., Herczeg, A.L., 2003. The importance of silicate weathering of a sedimentary aquifer in arid Central Australia indicated by very high $^{87}Sr/^{86}Sr$ ratios. Chemical Geology 199, 281-292.

Herczeg, A.L., Edmunds, W.M., 2000. Inorganic ions as tracers. In: Cook, P., Herczeg, A., (eds). *Environmental Tracers in Subsurface Hydrology*, Kluwer Academic Publishiers, Boston, pp. 31-77.

Huang C.C., Pang J., Zha X., Su H., Jia Y. and Zhu Y., 2007. Impact of monsoonal climatic change on Holocene overbank flooding along Sushui River, middle reach of the Yellow River, China. Quaternary Science Reviews 26, 2247-2264.

Kreuzer, A.M., Rohden, C.V., Friedrich, R., Chen, Z., Shi, J., Hajdas, I., Aeschbach-Hertig, W., 2009. A record of temperature and monsoon intensity over the past 40 kyr from groundwater in the North China Plain. Chemical Geology 259, 168-180.

Lasaga, A.C., 1984. Chemical kinetics of water-rock interaction. Journal of Geophysical Research 89, 4009-4025.

Langmuir, D.L., 1971. The geochemistry of some carbonate ground waters in central Pennsylvania. Geochimica et Cosmochimica Acta 35, 1023-1045.

Li, X., 2003. Pressure of water shortage on agriculture in arid region of China. Chinese Geographical Science 13(2), 124-129.

Liu, T.S., Zhang, S.X, Han, J.M., 1986. Stratigraphy and palaeoenvironmental changes in the loess of central China. Quaternary Science Reviews 5, 489-495.

Liu, T.S. 1988. Loess in China. 2nd Edition. China Ocean Press, Beijing, 224p.

McNab Jr., W.W., Singleton, M.J., Moran, J.E., Esser, B.K., 2009. Ion exchange and trace element surface complexation reactions associated with applied recharge of low-

TDS water in the San Joaquin Valley, California. Applied Geochemistry 24, 129-137.

Organisation for Economic Co-operation and Development, 2005. OECD review of agricultural policies: China. Paris: Organisation for Economic Co-operation and Development, 235p.

Okada, K., Naruse, H., Tanaka, T., Nemoto, O., Iwasaka, Y., Wa, P-M., Duce, R.A., Uematsu, M., Merrill, J.T., Arao, K., 1990. X-ray spectrometry of individual Asian dust-storm particles over the Japanese islands and the North Pacific Ocean. Atmospheric Environment 24A, 1369-1378.

Parkhurst, D.L., Apello, C.A.J., 1999. User's guide to PHREEQC (Version 2) – a computer program for speciation, batch-reaction, one-dimensional transport, and inverse geochemical calculations: USGS Water Resource Investigation Report 99-4259.

Rao, Z., Zhu, Z., Chen, F., Zhang J., 2006. Does $\delta^{13}C_{carb}$ of Chinese loess indicate past C_3/C_4 abundance? A review of research on stable carbon isotopes of the Chinese loess. Quaternary Science Reviews 25, 2251-2257.

Scanlon, B.R., Nicot, J.P., Reedy, R.C., Kurtzman, D., Mukherjee, A., Nordstrom, D.K., 2009. Elevated naturally occurring arsenic in a semiarid oxidizing system, Southern High Plains aquifer, Texas, USA. Applied Geochemistry 24, 2061-2071.

Smedley, P.L., Kinniburgh, D.G., Macdonald, D.M.J., Nicolli, H.B., Barros, A.J., Tullio, J.O., Pearce, J.M., Alonso, M.S., 2005. Arsenic associations in sediments from the loess aquifer of La Pampa, Argentina. Applied Geochemistry 20, 989-1016.

Stumm, W., Morgan, J.J., 1996. Aquatic Chemistry: Chemical Equilibria and Rates in Natural Water. John Wiley and Sons, New York. 1022p.

Walraevens, K., Cardenal-Escarcena, J., Van Camp, M., 2007. Reaction transport modelling of a freshening aquifer (Tertiary Ledo-Paniselian Aquifer, Flanders-Belgium). Applied Geochemistry 22, 289-305.

Wang, Q., Li C., Tian, G., Zhang, W., Liu, C., Ning, L., Yue, J., Cheng, Z., He C., 2002. Tremendous change of the earth surface system and tectonic setting of salt-lake formation in Yuncheng Basin since 7.1 Ma. Science in China Series D- Earth Sciences 45(2), 110-122.

Yokoo, Y., Nakano, T., Nishikawa, M., Quan, H., 2004. Mineralogical variation of Sr-Nd isotopic and elemental compositions in loess and desert sand from the central Loess Plateau in China as a provenance tracer of wet and dry deposition in the northwestern Pacific. Chemical Geology 204, 45-62.

Yuncheng Regional Water Bureau & Shanxi Geological Survey, 1982. Hydrological and Geological maps and explanations for the Yuncheng region, 1:100000, Shanxi Geological Survey Special Report (In Chinese). 80p.

Zhu, G.F., Li, Z.Z., Su, Y.H., Ma, J.Z., Zhang, Y.Y., 2007. Hydrogeochemical and isotope evidence of groundwater evolution and recharge in Minqin basin, Northwest China. Journal of Hydrology 333, 239-251.

Chapter 4

Controls on elevated fluoride and arsenic concentrations in groundwater from the Yuncheng Basin, China

Matthew J. Currell[1] , Ian Cartwright[1], Massimo Raveggi[1], Dongmei Han[2]

[1] School of Geosciences, Monash University, Clayton VIC 3800, Australia
[2] Institute of Geographic Sciences and Natural Resources Research, China Academy of Sciences, Beijing, 100101, China

-----Submitted to Applied Geochemistry (accepted pending minor revisions)-----

ABSTRACT

Analysis of groundwater chemistry and sediments was carried out to investigate causes of elevated fluoride (1.5 to 6.6 mg/L) and arsenic concentrations (10 to 27 μg/L; one sample affected by local contamination with 4870 μg/L As), in groundwater from the Yuncheng Basin, northern China. Groundwater from nine out of 73 wells contains both F and As concentrations above World Health Organisation safe drinking guidelines (>1.5 mg/L and >10 μg/L, respectively); fluoride concentrations above safe levels are more widespread than arsenic (27 vs. 12 wells). The elevated As and F concentrations represent a significant health risk, as groundwater is widely used to supply agricultural and domestic water in the region. High F and As concentrations occur in shallow groundwater affected by agriculture and deep groundwater with long residence times (> 13 ka) that shows little sign of anthropogenic influence. The strong positive correlation between groundwater F/Cl and As/Cl ratios (r^2 = 0.98 and 0.77 in shallow and deep groundwater, respectively) indicates that these elements are mobilized and enriched by common processes. Positive

correlations between F and As concentrations and Na/Ca ratios (r^2 = 0.67 and 0.46, respectively) indicate that groundwater major ion chemistry plays a significant role in mobilizing F and As. Mobilization likely occurs via de-sorption of As and F anions (e.g. $HAsO_4^{2-}$ and F^-) from hydrous metal oxides. Moderate positive correlations between pH and As and F concentrations (r^2 = 0.36 and 0.17, respectively) indicate that high pH may also favour de-sorption, while HCO_3 may act as a sorption competitor. High groundwater Na/Ca ratios likely result from cation exchange, while pH and HCO_3 contents are predominantly controlled by carbonate weathering reactions. Sediments from the area were reacted with various water solutions, producing F concentrations between 0.49 and 2.7 mg/L and As concentrations between 0.51 and 16.7 µg/L. Up to 45% more F and 35% more As were released when sediments were reacted with a Na-rich, Ca-poor solution compared to a Ca-rich solution; this is consistent with increased mobilization of F^- and $HAsO_4^{2-}$ by Na-rich, Ca-poor groundwater. Increasing F and As concentrations across a wide area caused by high levels of pumping is a potential future health concern.

Key Words

Fluoride, Arsenic, Groundwater, Semi-arid, Loess, China

4.1 INTRODUCTION

4.1.1 Fluoride and arsenic in groundwater

Groundwater in many developing regions such as China, India and East Africa has elevated fluoride (F^-) concentrations (Handa, 1975; Sun, 1988; Gaciri and Davies, 1993; Datta et al., 1996; Choubissa, 2001; Brunt et al., 2004; Edmunds and Smedley, 2005; Jacks et al., 2005; Tekle-Haimanot et al., 2006; Guo et al., 2007a). Use of groundwater with fluoride above the World Health Organisation standard of 1.5 mg/L for domestic supply is a serious health issue, as it causes endemic dental and skeletal fluorosis (World Health Organisation, 1984; 2004). Fluorosis causes discolouration and deterioration of teeth and bones and in serious cases can lead to loss of mobility. Groundwater with high As concentrations is also a widespread global health problem, including in many semi-arid basins that contain oxidized groundwater (e.g. Smedley and Kinniburgh, 2002; Smedley et al., 2005; Bhattacharya et al., 2006; Guo et al., 2007b; Gomez et al., 2009; Scanlon et al., 2009). These studies all show a link between enrichment of As and other elements that form anions and oxy-anion complexes, including F, Mo, B, U and V, that is likely due to sorption-desorption behaviour on metal oxides (particularly hydrous Fe, Mn and Al oxides).

Fluorosis is a widespread problem in the Yuncheng Basin, northern China (Fig. 1), with approximately 20% of people living in the basin being affected by the disease in the last two decades (Gao, 2005). During the last 10 years, drinking supply wells in villages affected by fluorosis have been abandoned. However, many domestic and irrigation wells are still in use, as the alternative water supply options for the >5 million people (notably

the Yellow and Sushui Rivers) are heavily allocated and/or polluted. High F concentrations in the Yuncheng Basin are an immediate and well known health concern warranting detailed investigation; and given the links between F and As enrichment, the potential for As contamination, which has not been studied in this area, also needs to be assessed. It is well documented that long-term intake of As from drinking water leads to a range of health problems ranging from skin disorders to increased incidences of many cancers (World Health Organisation, 2001). While groundwater with high As concentrations is presently not widespread in the basin, the high levels of pumping and anthropogenic disturbance of the natural flow system (cf. Cao, 2005; China Geological Survey, 2006) may cause increasing As concentrations in groundwater from a wider area in the future.

Intrusion of salt water from Yuncheng salt lake has been proposed as playing a role in increasing shallow groundwater F concentrations near Yuncheng City (Gao et al., 2007). However, leakage from the salt lake is a local process only affecting shallow groundwater in a small part of the basin (Gao et al., 2007). Both shallow and deep groundwater in the basin far removed from the salt lakes has high F and As concentrations, while high groundwater F and As concentrations (up to 6.2 mg/L and 115 μg/L, respectively), are also a problem in the Taiyuan Basin, located ~250km to the north of the Yuncheng Basin (Guo et al., 2007a; Guo et al., 2007b). These two basins formed over the same time period and contain similar sediments, mostly fine-grained aeolian loess that is interlayered with fluvial and lacustrine deposits (Sun, 1988; Xu and Ma, 1992); hence, it is likely that there are broad-scale processes in the region which cause elevated F and As concentrations in groundwater. This paper assesses the geochemical controls on the origins and mobilization mechanisms of F and As in the Yuncheng Basin. It is hoped that the results of this study

will allow better understanding of the causes of F and As contamination in similar loess-dominated basins globally. Understanding the causes of and controls on enrichment of F and As in groundwater is of great importance in northern China, given that groundwater is a major domestic and agricultural supply of water, and it is also important in many other hydrogeological settings, particularly arid and semi-arid regions where there is ongoing difficulty providing safe drinking water (e.g. Edmunds, 2003).

4.1.2 The Yuncheng Basin

The geology and hydrogeology of the Yuncheng Basin are summarised by Currell et al., (2010). The basin comprises a Quaternary aquifer of interlayered sediments that is up to 500 m thick, including a shallow unit (<70 m), a deep unit (>120 m), and an intermediate unit (70 to 120 m), although this unit is probably hydraulically connected to the deep unit (Cao 2005, China Geological Survey 2006). The sediment is mostly aeolian loess containing quartz, feldspar, calcite, clays and mica, that comprises a series of depositional layers, mostly 2 to 5 m thick, separated by thinner (<1 m) palaeosol layers (Liu et al., 1986, Liu 1988). The loess in the Yuncheng Basin is also interlayered with alluvial sands and lacustrine clay lenses (China Geological Survey, 2006). The region has a semi-arid climate with annual rainfall averaging ~550 mm and potential evapotranspiration of ~1900 mm. Most rainfall (>65%) occurs between June and September during the East Asian summer monsoon (China Geological Survey, 2006).

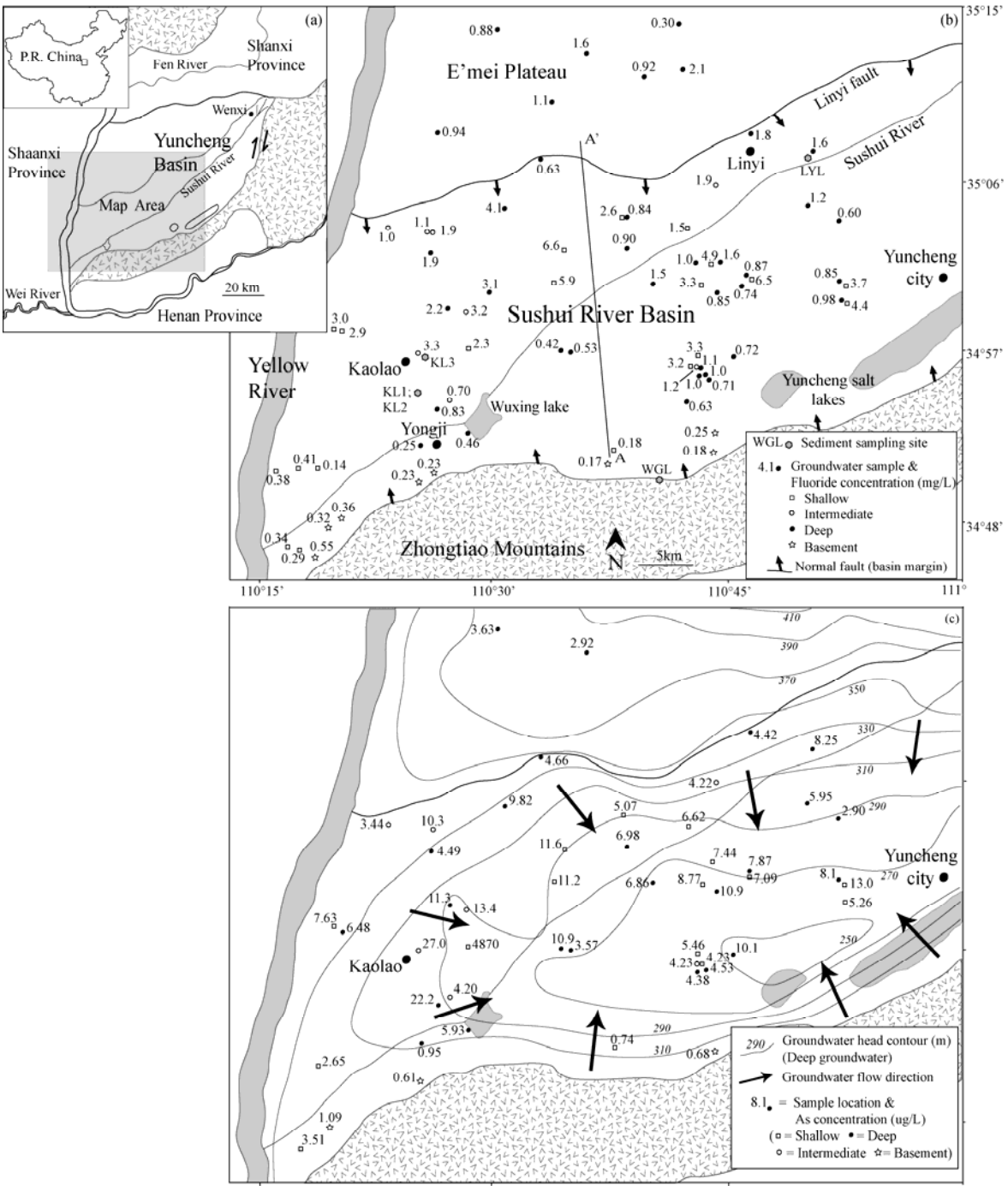

Fig. 1a. Location of the Yuncheng Basin **1b.** The study area, sample sites and groundwater fluoride concentrations **1c.** Groundwater arsenic concentrations and deep groundwater head contours and flow directions. Both F and As concentrations are highest in the northern Sushui River Basin. Data from Table 1; China Geological Survey, 2006.

Groundwater ^{14}C ages indicate that historically, regional groundwater flow was from the eastern Yuncheng Basin to the west, towards the Yellow River (Currell et al., 2010), while intermediate-scale flow also occurred from the sloping southern and northern margins of the basin to its flatter interior (China Geological Survey, 2006). However, due to the large amount of pumping of deep groundwater since the 1980s, horizontal groundwater flow is now mostly towards a cone of depression to the west of Yuncheng City (China Geological Survey, 2006). Shallow groundwater is pumped much less than deep groundwater, as the quality is generally too poor for irrigation or drinking. Hence, groundwater levels in the shallow aquifer are generally steady or rising, facilitating evapotranspiration and concentration of solutes. Leakage of shallow groundwater into the deep aquifer is occurring locally throughout the basin (Currell et al., 2010).

4.2 METHODS

A total of 73 groundwater samples were collected from 3 counties – Yongji, Linyi and Yuncheng, which cover much of the Sushui River Basin and a small part of the E'mei Plateau, during 2007 and 2008 (Fig. 1). Samples were obtained from shallow, intermediate and deep wells in the Quaternary sediments and from wells at a range of depths in the fractured metamorphic basement rock in the south of the basin (Fig. 1; Table 1). Groundwater EC, pH, dissolved oxygen and alkalinity were measured in the field as described in Currell et al., (2010). Major cations were analysed using a Varian Vista ICP-AES at Australian National University, Canberra. Major anions, including F^-, were measured using a Metrohm ion chromatograph at Monash University, Australia.

PHREEQC version 2.14.2 (Parkhurst and Apello, 1999) was used to determine saturation indices for fluorite and calcite along with the speciation of F and As in solution.

As concentrations were determined at Monash University using a Thermo Finnigan X series II, quadrupole ICP-MS. For calibration, the USGS standard reference material SGR-1 was dissolved and evaporated to form a sample cake, then re-dissolved and diluted with a 3% HNO_3 solution to make calibration standards of varying concentrations. Drift corrections were applied by the use of Te as an internal standard and by the repeated analysis of standards throughout the analytical sessions. The isobaric interference of $^{40}Ar^{35}Cl$ on ^{75}As was taken into account and corrected accordingly by quantifying the contribution of Cl using the $^{40}Ar^{37}Cl$ mass. Internal precision of the ICPMS measurements were of the order of 1.5% while the external precision from repeat analyses was within 10%. Accuracy of the As measurements was checked using three methods; firstly, by analysing an in-house groundwater standard with similar TDS to the unknowns spiked with a known concentration of As, secondly by analyzing the USGS standard reference material SCO-1 repeatedly throughout the sample runs, thirdly by analysis of three of the samples using Atomic Absorption Spectroscopy (which agreed to within 4% with the ICPMS data).

Five sediment samples from the Yuncheng Basin were reacted with de-ionized water and two synthetic groundwater solutions over different time periods to assess the influence of major ion chemistry on F and As mobilisation. The synthetic solutions have similar pH, TDS and major ion chemistry to local groundwater, however, Solution A has equal molar Na and Ca concentrations while Solution B is Na-rich and Ca-poor (Table 3). These solutions were added to the five sediment samples in 1:1 weight ratios, in clean

Petri-dishes and left at a constant temperature (20°C). The sediment-solution mixtures were left to react for either 5 minutes or 6 hours and were then filtered, and the resulting water was analysed for F concentrations using IC and As concentrations using ICPMS. Four samples of loess were analysed for mineral compositions using X-ray diffraction, at Ballarat University, Australia. X-ray diffraction traces were obtained from the samples after fine milling, with a Siemens D500 diffractometer, using Fe-filtered CoK_α radiation. Operating conditions were 35kV/25mA, step scan 0.03θ 2θ at 1^o/2θ/min, range 4^o to 76.0^o 2θ, fixed 1^o divergence and receiving slits and a 0.15^o scatter slit. Mineral phases present were identified by computer-aided (Panalytical X'Pert HighScore Plus, Bruker Diffrac Plus EVA) searches of the 2008 ICDD PDF4/Minerals relational database. Quantitative XRD results were obtained using SiroQuant™ ver 3.0.

4.3 RESULTS

4.3.1 Hydrogeochemistry

Field parameters (pH, dissolved oxygen concentrations, alkalinity) and some groundwater major ion chemistry (TDS, Cl and NO_3 concentrations) together with $\delta^{13}C$, $\delta^{18}O$, $\delta^{2}H$ values and ^{14}C activities are reported in Currell et al., (2010). Groundwater pH values range from 7.2 to 8.8 and all groundwater is oxidising, containing between 1 and 6.5 mg/L dissolved oxygen and considerable dissolved SO_4 and NO_3 (Table 1). Speciation calculations carried out using PHREEQC indicate that under these conditions (with pe calculated on the basis of dissolved oxygen concentrations and the O^{2-}/O redox couple); As is present as As(V), mostly $HAsO_4^{2-}$ (>99%), while F is largely present as F^- (>95%) with

minor amounts of MgF^+, NaF and CaF^+. As and F are typically present as these species in groundwater from oxidised, semi-arid aquifer settings (Smedley and Kinniburgh, 2002).

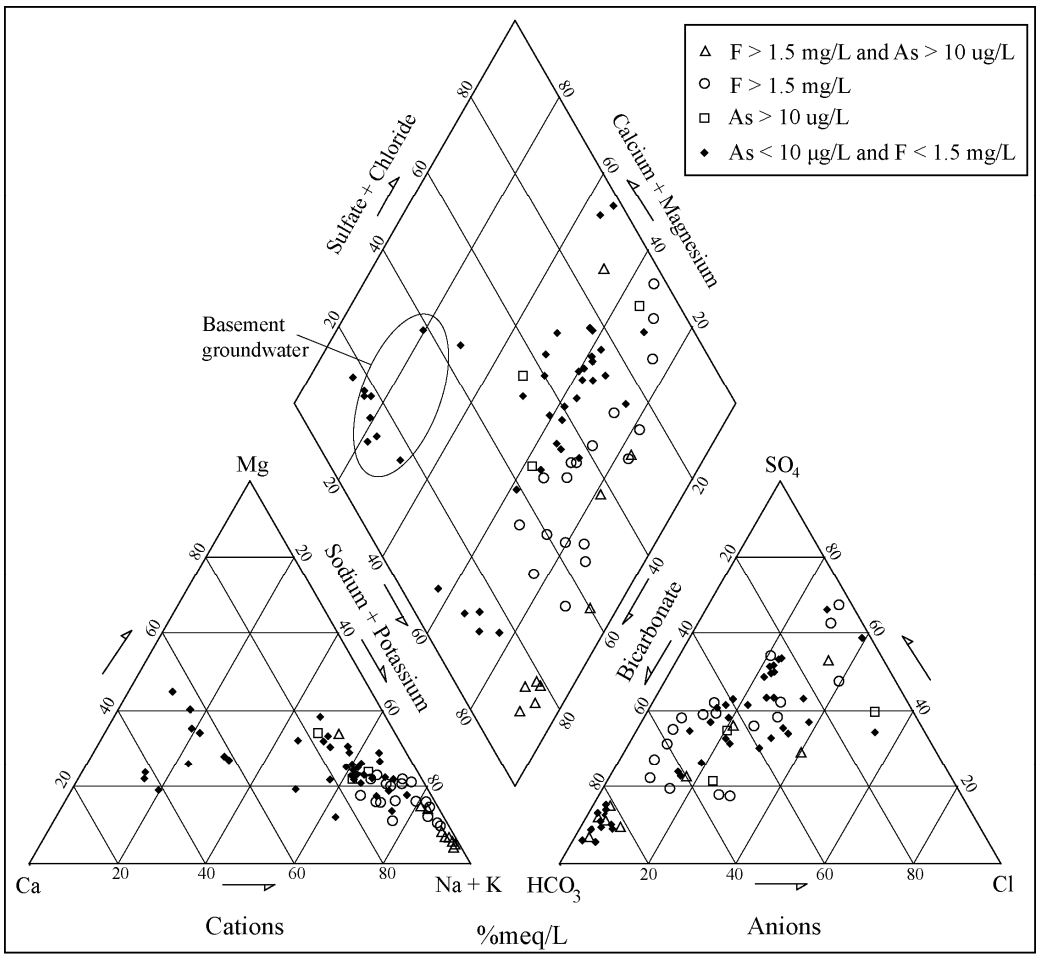

Fig. 2. Piper diagram showing the major ion composition of groundwater. Samples with F and As concentrations above recommended WHO safe drinking water standards (F > 1.5 mg/L; As > 10 µg/L) are marked separate from the other groundwater samples.

Groundwater total dissolved solids (TDS) contents range between 260 and 8450 mg/L (Table 1); shallow groundwater is generally more saline than deep and intermediate groundwater (median TDS = 1980 mg/L vs. 1090 mg/L), primarily due to evapotranspiration in agricultural areas with shallow water tables and return of irrigation water (Currell et al., 2010). Most groundwater in the Quaternary aquifer is Na-HCO_3 type (Na makes up > 70% of total cations; HCO_3 makes up > 40% of total anions, Fig. 2),

however, groundwater in recharge areas at the margin of the basin (e.g. Samples 12 & 21) has relatively high proportions of Ca and Mg (e.g. Ca + Mg > 50% of total cations, Fig. 3a & 3d). Na increases in relative abundance along groundwater flow paths towards the centre of the basin, where it comprises >90% of the total cations and Na/Ca equivalents ratios are locally > 100 (Table 1; Fig. 3a; 3d). This change in cation composition is generally not accompanied by an increase in total cation/Cl equivalents ratios (Table 1), suggesting that it is largely due to cation exchange between Na and Ca, rather than progressive dissolution of Na-bearing minerals (e.g. albite). Molar Cl/Br ratios in groundwater (300 to 1810; median 1070) are locally slightly elevated relative to typical oceanic/rainfall ratios (e.g. 300 – 800, Davis et al., 1998), indicating that some dissolution of halite has probably occurred; however, Cl/Br ratios of this magnitude indicate only minor amounts of halite dissolution (e.g. Cartwright et al., 2004). The lack of a positive correlation between Na and dissolved silica concentrations indicates that weathering of albite probably is not a major control on Na concentrations in the groundwater, given that all samples are undersaturated with respect to amorphous silica (SI values -0.79 to -1.36), which rules out buffering of dissolved Si concentrations by amorphous silica precipitation (Table 1). High molar Na/Cl ratios (e.g. >5) and low Ca/Cl ratios (<0.4) in groundwater from the centre of the basin in comparison to rainfall (Na/Cl ~0.8, Ca/Cl ~3.0: Fujita et al., 2000) are also consistent with cation exchange being a major control on Na and Ca concentrations (Table 1). The exchange probably takes place in the lacustrine clay lenses interlayered throughout the aquifer, which contain abundant exchange sites that may have sorbed large amounts of Na^+ when the clays were deposited, in hyper-saline inland lakes with ocean water-type chemistry (Wang et al., 2002).

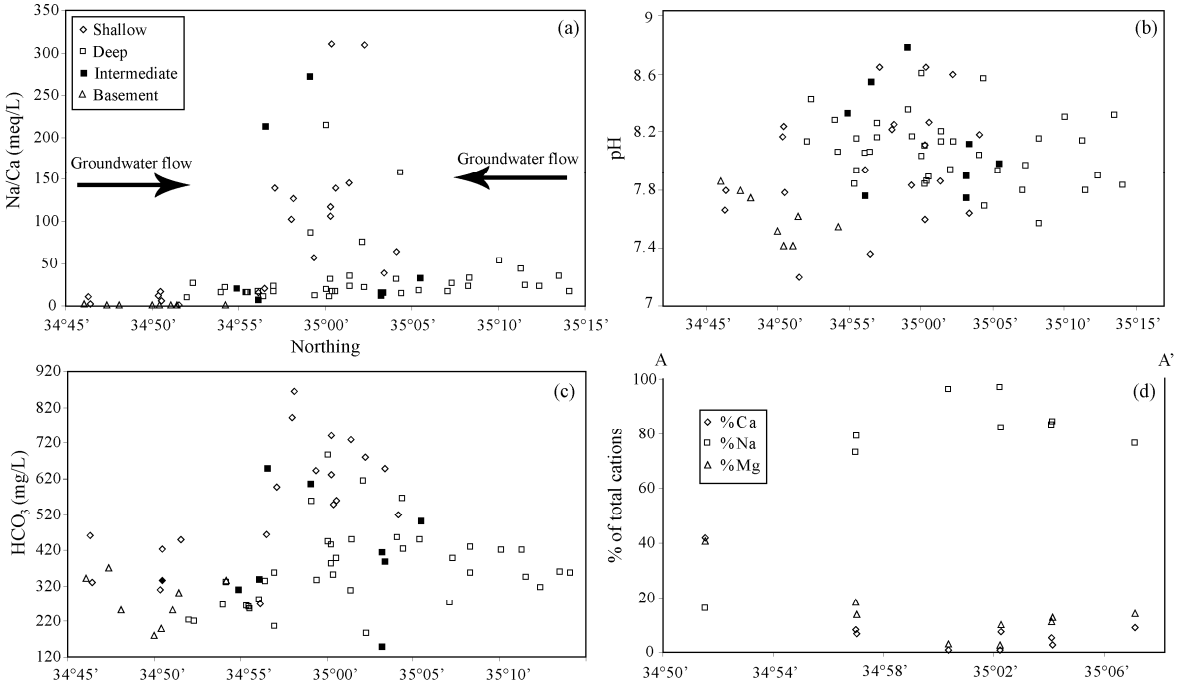

Fig. 3a. Groundwater equivalent Na/Ca ratios vs. latitude **3b.** Groundwater pH vs. latitude **3c.** Groundwater HCO_3 concentrations vs. latitude **3d.** Variation in the proportions of major cations along a south-north transect (marked A-A' on Fig. 1), showing the change in major cation composition in nine wells along a groundwater flow path. Data from Table 1.

The increasing Na/Ca ratios from the basin margins to its centre are accompanied by a slight increase in pH values (Fig 3b), which may relate directly to increasing Na^+ relative to Ca^{2+} and/or carbonate weathering. Much of the DIC in groundwater derives from weathering of carbonate minerals (predominantly calcite), which make up 15-20% of the loess, as indicated by positive correlation between DIC concentrations and $\delta^{13}C$ values ($r^2 = 0.25$, Currell et al., 2010). All samples in the Quaternary aquifer are saturated with respect to calcite (S.I. values from +0.01 to +0.83), indicating that dissolution probably largely occurs during recharge. However, bicarbonate concentrations also increase from ~350 mg/L at the basin margins to ~600 mg/L in its interior, along with increasing Na/Ca ratios and pH values (Fig 3c). This suggests that second-stage calcite dissolution may occur under closed system conditions, to maintain calcite equilibrium after cation

exchange lowers the Ca^{2+} content (e.g. Walraevens et al., 2007). The groundwater Ca content would still remain low under this scenario provided that there was still exchangeable Na^{+} to allow cation exchange to continue (Walraevens et al., 2007). Preliminary analysis of $^{87}Sr/^{86}Sr$ data from the sediments and groundwater from the area are consistent with these interpretations, the groundwater generally has $^{87}Sr/^{86}Sr$ values close to the values of the carbonate minerals and rainfall in the region (~0.7110; cf. Yokoo et al., 2004; Edmunds et al., 2006; Currell, unpublished data), while only minor amounts of Sr are derived from weathering of silicates (e.g. albite).

Sample Number	Unit*	Latitude	Longitutde	Depth (m)	DO (mg/L)	pH	F (mg/L)	As (µg/L)	Na (mg/L)	Ca	Mg	Cl	HCO_3	SO_4	Si	Na/Ca (meq/L)	Cations/Cl~ (meq/L)	S.I.^ Fluorite	S.I. Calcite	S.I. A. Sil	Residence time (years)#
20	S	344630.5	1101738.2	-30	3	7.7	0.3	3.51	480	157	98.7	388	460	672	5.99	11	2.27	-2.1	0.68	-0.94	
21	S	344641.6	1101653.9	-70	2	7.8	0.3		81.8	103	41.6	66.8	332	125	6.57	2.8	3.02	-2.0	0.55	-0.90	
33	S	345037.8	1101536	-70	4	8.2	0.4		178	49.8	54.5	137	312	186	6.03	12.5	2.45	-2.2	0.66	-0.95	
32	S	345046.4	1101727.6	-50	3	8.2	0.4		207	40.8	35.5	90.1	336	187	6.36	17.7	4.03	-2.2	0.68	-0.92	
31	S	345050.9	1101846.8	-50	4	7.8	0.1	2.65	289	152	59.7	274	424	363	9.02	6.6	2.03	-2.6	0.82	-0.77	Modern
12	S	345153.5	1103748.1	-20	1	7.2	0.2	0.74	26.0	117	70.6	20.8	448	42.2	7.39	0.8	6.88	-2.4	0.30	-0.84	
43	S	345612.9	1104240.5	-20	6	7.9	3.2		1810	386	258	1690	269	5180	0.2	16	1.86	-0.1	0.72	-1.24	
42	S	345649.4	1104309	-17	5	7.4	3.3	5.46	1650	269	198	1130	463	3170	2.4	21	2.48	-0.1	0.34	-1.34	
25	S	345709.6	1102823.7	-58.5	2	8.7	2.3	4870	305	7.64	14.9	15.4	596	64.0	5.68	139	31.52	-1.4	0.60	-0.99	
29	S	345802.1	1102022.3	-35	2	8.2	2.9	6.48	641	21.9	50.9	263	792	202	5.55	102	3.94	-0.8	0.69	-0.99	
30	S	345814.5	1101948.8	-40	3	8.3	3.0	7.63	696	19.1	44.8	251	864	224	6.04	127	4.44	-0.9	0.66	-0.95	Modern
74	S	345934.5	1105241	-30	4	7.8	4.4	5.26	698	42.0	106	375	644	742	5.9	58	3.12	-0.4	0.37	-0.96	
77	S	346029.4	1105233.2	-40	5	8.1	3.7	13.0	739	22.0	67	487	630	479	4.3	117	2.46	-0.7	0.39	-1.10	
1	S	346029.8	1104326.8	-34	4	7.6	3.3	8.77	1450	47.7	220	1335	740	2165	2.13	106	1.81	-0.8	0.09	-1.34	
57	S	346036.6	1103355.4	-55	5	8.7	5.9	11.2	283	3.17	9.2	38.1	547	51.0	3.8	311	11.65	-0.9	0.19	-1.16	3200± 1300
71	S	346058.6	1104616.9	-27	6	8.3	6.5	7.09	577	14.4	53	314	558	534	4.0	140	2.98	-0.4	0.32	-1.13	
2	S	346139.2	1104405.1	-20	6	7.9	4.9	7.44	966	23.2	98.7	348	730	1238	2.25	145	4.52	-0.6	0.15	-1.36	
58	S	346223.3	1103435	-30	6	8.6	6.6	11.6	477	5.37	13	115	680	204	3.6	310	6.51	-0.7	0.36	-1.19	
65	S	346337.4	1104233.7	-40	6	7.6	1.4	6.62	645	57.0	153	281	648	843	5.6	39	4.04	-1.3	0.31	-0.98	
62	S	346412.2	1103826.7	-40	5	8.2	2.6	5.08	410	22.1	66	207	520	388	4.8	65	3.34	-1.0	0.44	-1.05	
22	D	345205.2	1102527.1	-240	2	8.1	0.3	0.95	167	57.5	16.8	116	224	162	8.10	10.1	2.55	-2.3	0.59	-0.81	
37	D	345235.6	1102832.6	-200	3	8.4	0.5	5.93	265	34.9	25.4	193	220	254	6.55	26	2.29	-2.2	0.54	-0.91	21700±600
23	D	345400.6	1102629.6	-150	4	8.3	0.8	22.2	138	30.0	26.6	68.7	268	84.9	5.86	16.1	3.58	-1.6	0.57	-0.95	12500± 1100
8	D	345421.3	1104226.4	-230	4	8.1	0.6		183	28.6	31.9	96.5	332	179	5.36	22.3	3.29	-1.9	0.35	-1.00	17400± 2000
24	I	345488.9	1102713.5	-120	3	8.3	0.7	4.20	265	44.6	59.2	187	312	274	5.78	21	2.52	-1.7	0.74	-0.96	
7	D	345540.2	1104336.5	-300	1	7.8	0.7		246	53.9	46.3	127	264	399	6.54	15.9	3.44	-1.6	0.25	-0.91	
39	D	345550.4	1104301.7	-220	6	7.9	1.0	4.38	242	54.3	46.8	131	262	378	6.6	15.5	3.28	-1.3	0.36	-0.89	
44	D	345552.9	1104324.1	-300	6	8.2	1.0	4.53	236	53.8	46.5	131	255	377	6.5	15.3	3.22	-1.3	0.55	-0.91	10400± 800
40	I	345610.2	1104258.7	-80	5	7.8	1.2	4.23	944	429	361	850	340	2782	2.7	8	2.24	-0.8	0.83	-1.30	Modern
41	D	345610.2	1104258.7	-270	4	8.1	1.1		226	47.2	47.6	148	282	321	5.4	16.7	2.74	-1.2	0.46	-0.98	
78	D	345645.5	1104529.3	-230	4	8.1	0.7	10.1	165	52.9	61.6	91.3	334	205	6.8	10.9	3.53	-1.6	0.62	-0.89	
26	I	345655.8	1102513.4	-110	3	8.6	3.3	27.0	312	5.10	12.4	15.4	648	41.9	4.38	213	31.85	-1.2	0.38	-1.09	
36	D	345700.5	1103504.3	-250	2	8.2	0.5	3.57	356	70.7	95.3	209	356	646	6.07	18	3.10	-1.9	0.73	-0.94	
35	D	345701.4	1103426.2	-210	2	8.3	0.4	10.9	570	86.8	107	713	208	743	4.69	23	1.40	-2.0	0.65	-1.05	12300±200
27	I	345909.1	1102819	-117	4	8.8	3.2	13.4	315	4.03	8.65	12.4	605	71.3	4.60	272	39.75	-1.3	0.44	-1.08	3900± 1000
28	D	345913.7	1102713.8	-210	5	8.4	2.2	11.3	566	22.6	56.0	164	556	376	4.91	87	5.63	-1.1	0.65	-1.03	

*S = Shallow; I = Intermediate; D = Deep; B = Basement. Samples listed in order of increasing latitude in each unit

#Residence time, calculated using radiocarbon activities as described in Currell et al., (2010).

^S.I. = Saturation Index, calculated using PHREEQC (Parkhurst and Apello, 1999)

~ = Total cations/chloride (miliequivalents/L)

Continued...

75	D	345941.8	1105225.8	-320	6	8.2	1.0		163	44.5	56.6	64.9	336	205	7.6	12.8	4.81	-1.4	0.65	-0.88	3500± 1700
56	D	346006.5	1102946.9	-220	5	8.6	3.1	11.7	324	5.27	12.6	19.4	685	99.8	4.4	215	26.33	-1.3	0.44	-1.09	8000± 800
6	D	346008.8	1104426	-220	7	8.0	0.9		226	39.1	43.15	59.2	444	228	6.94	20.1	6.72	-1.6	0.56	-0.88	
73	D	346026.7	1104557.5	-180	3	7.8	0.7		225	68.4	75.9	133	384	341	7.1	11.5	3.25	-1.5	0.52	-0.87	
64	D	346029.2	1104016.1	-180	5	8.1	1.5	6.86	276	29.9	43.5	88.5	434	298	5.7	32	5.32	-1.2	0.49	-0.96	12800± 2000
76	D	346041.4	1105214	-230	4	7.9	0.8	8.10	277	56.4	62.9	164	352	382	6.8	17	3.04	-1.5	0.41	-0.88	
72	D	346058.6	1104616.9	-240	3	7.9	0.9	7.87	252	49.6	49.9	93.0	396	308	7.5	17.7	4.81	-1.5	0.46	-0.84	5500±1600
4	D	346140.5	1104301	-270	4	8.1	1.0		311	45.8	55.7	154	308	481	6.31	24	3.51	-1.4	0.50	-1.40	13600± 1100
3	D	346144.1	1104435.2	-240	3	8.2	1.6		277	27.4	41.8	72.6	448	287	6.73	35	6.46	-1.2	0.57	-0.89	7100± 1400
54	D	346211.5	1102601.5	-160	2	7.9	1.9	4.49	381	17.5	41.2	52.9	615	300	6.0	76	11.83	-1.2	0.23	-0.94	18000±1300
63	D	346227.4	1103837.8	-220	3	8.1	0.9	6.98	425	68.0	56.4	506	186	433	4.8	22	1.44	-1.3	0.43	-1.05	
55	I	346319.2	1102930.3	-120	2	7.8	1.1		1021	289	448	1510	148	3090	4.4	12	1.35	-1.1	0.25	-1.09	
55a	I	346319.2	1102930.3	-120	2	7.9	1.9	10.3	703	153	243	676	415	1410	3.7	16	1.97	-0.7	0.73	-1.16	
53	I	346334.7	1102309.7	-120	6	8.1	1.1	3.44	169	37.5	33.7	58.9	389	114	8.3	15.7	5.11	-1.3	0.64	-0.80	
61	D	346409.8	1103804.7	-180	6	8.0	0.8	4.79	314	34.7	44.3	119	456	320	7.0	31	4.47	-1.7	0.50	-0.88	
60	D	346435.9	1103049.3	-178	6	8.6	4.1	9.82	390	8.64	23.1	76.9	566	134	4.4	158	8.10	-0.9	0.51	-1.10	9500± 1200
69	D	346442.7	1105012.4	-200	2	7.7	0.6	2.90	248	56.8	56.4	85.3	422	308	8.2	15.2	5.25	-1.7	0.34	-0.81	
68	D	346540.1	1105145.9	-180	6	7.9	1.1	5.95	293	54.9	63.9	117	448	383	6.5	19	4.47	-1.2	0.59	-0.91	
66	I	346548.4	1104421.7	-100	6	8.0	1.9	4.22	266	28.2	31.8	42.5	500	205	8.5	33	10.52	-1.0	0.44	-0.79	4300± 1200
59	D	346710.5	1103303.4	-230	6	7.8	0.6	4.66	282	58.1	56.0	154	272	482	6.9	17	3.25	-1.7	0.24	-0.88	
67	D	346731.4	1105031	-202	4	8.0	1.6	8.25	187	24.7	33.5	28.5	398	131	6.4	26	11.39	-1.1	0.32	-0.91	3300±2100
70	D	346829.2	1104633.9	-230	6	7.6	1.8	4.42	251	38.4	30.3	68.1	356	268	8.5	23	6.27	-0.9	0.01	-0.79	
52	D	346830.8	1102630.3	-280	6	8.2	0.9		162	16.9	28.3	11.4	430	42.3	7.1	33	24.40	-1.7	0.41	-0.83	
50	D	347008.8	1103346.9	-230	6	8.3	1.1		178	11.4	22.3	10.8	420	49.9	6.3	54	27.42	-1.8	0.35	-0.92	
48	D	347129.2	1103943.3	-260	7	8.1	0.9		161	12.9	26.1	8.33	421	33.6	6.6	44	32.83	-1.8	0.28	-0.90	
46	D	347152.4	1104613.9	-210	6	7.8	2.1		178	25.4	14.0	27.9	344	88.7	8.3	24.5	10.63	-0.8	0.13	-0.79	
49	D	347238.6	1103559.4	-260	6	7.9	1.6	2.92	141	21.5	25.5	30.7	316	178	7.6	22.8	7.99	-1.2	0.10	-0.83	7500± 2800
51	D	347353.5	1103018.6	-224	7	8.3	0.9	3.63	140	13.8	30.3	12.5	360	17.8	6.7	36	19.53	-1.8	0.43	-0.90	
47	D	347412.9	1104157.2	-200	6	7.8	0.3		112	22.0	31.7	4.96	358	18.3	7.7	17.7	41.42	-2.6	0.15	-0.83	
19	B	344607.1	1101834.8	-115	6	7.9	0.5		29.1	56.0	25.9	5.35	280	20.6	5.95	3.0	7.85	-1.6	0.49	-0.94	
17	B	344740.3	1101930	-75	5	7.8	0.3	1.09	18.0	44.8	25.1	4.41	304	30.1	8.30	1.8	12.19	-1.9	0.61	-0.79	
18	B	344812.4	1102019.9	-130	4	7.8	0.4		23.7	53.4	25.0	3.80	208	29.7	6.00	0.8	11.53	-1.9	0.32	-0.93	Modern
15	B	345001	1102513.4	-254	5	7.5	0.2	0.61	20.3	65.0	12.3	23.3	148	49.7	6.68	0.9	11.86	-2.3	-0.21	-0.88	
14	B	345041.6	1102620.1	-190	2	7.4	0.2		12.3	50.1	10.6	4.12	164	18.0	6.45	1.1	2.96	-2.3	-0.09	-0.90	
13	B	345109.3	1103719.8	-160	6	7.4	0.2		14.9	61.5	14.4	5.26	208	27.4	5.96	1.4	14.92	-2.7	-0.15	-0.94	
10	B	345143.5	1104404.4	-100	5	7.6	0.2	0.68	40.8	80.9	25.0	9.60	248	26.5	4.66	1.5	20.67	-2.6	0.19	-1.04	Modern
9	B	345421.3	1104423.4	-347	5	7.6	0.3		47.2	55.5	22.0	14.5	276	23.8	6.51	1.8	16.55	-2.3	0.19	-0.90	2100± 1000

Table 1. Sample locations, depths and results of chemical analyses and geochemical modelling

4.3.2 Groundwater F and As concentrations

Twenty seven groundwater samples (37% of the total samples) have fluoride concentrations at or above the World Health Organisation safe drinking level of 1.5 mg/L, including thirteen from shallow wells and fourteen from deep and intermediate wells (Fig. 1, Table 1). Twelve groundwater samples (16% of the total samples) have arsenic concentrations above the WHO safe drinking guideline (10 μg/L), including four from shallow wells and eight from deep and intermediate wells. One groundwater sample (no. 25) from 58m depth near Kaolao contains 4870 μg/L of As (Fig.1c), which is probably too high to have resulted from natural processes, implying an anthropogenic source, such as leakage of stored pesticides (Fig. 1, Table 1). Two wells in the vicinity of this area with As concentrations above 10 μg/L (Samples 26 and 27) may also be affected by this source (e.g. Fig. 1c). Elevated F concentrations in the same samples (up to 3.3 mg/L, Fig. 1b) may be connected to the same source; however there are few anthropogenic sources of F related to agriculture and the F concentrations in these samples are within the range of high F groundwater elsewhere in the region (1.5 to 6.6 mg/L, Fig 1). F and As concentrations in the basement groundwater are <0.55 mg/L and <1.1 μg/L, respectively. The majority of groundwater with high F and As concentrations is from the central or northern part of the Sushui River Basin, approximately between latitudes 34°56' and 35°06' (Fig. 1). F and As concentrations correlate positively in shallow and deep groundwater (r^2 = 0.52 and 0.39, respectively), and are even more strongly correlated when normalized for salinity (As/Cl vs. F/Cl, $r^2_{shallow}$ = 0.98, r^2_{deep} = 0.77, Fig. 4). This indicates that these elements either have a common source or that a common mechanism mobilizes both elements.

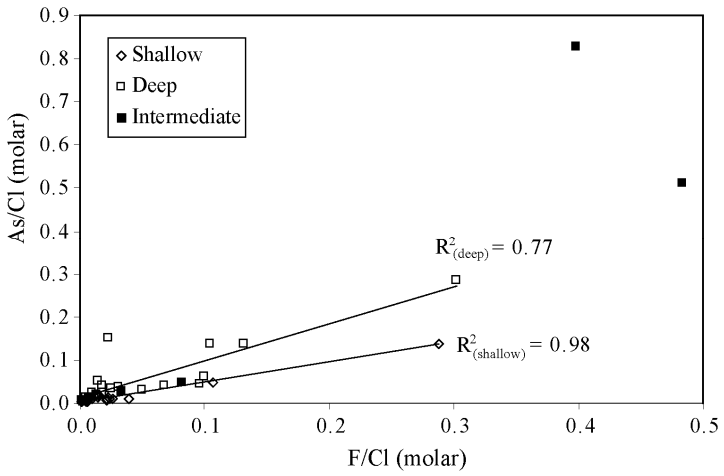

Fig. 4. F/Cl vs. As/Cl ratios in groundwater samples from the Yuncheng Basin. The strong correlations indicate that enrichment of these elements is governed by a common mechanism and/or set of aquifer conditions. Data from Table 1.

Groundwater residence time in the Yuncheng Basin increases with depth, from modern to 1000's of years in shallow groundwater, to between 5000 and ~22,000 years in deep groundwater (Table 1; Currell et al., 2010), and elevated F and As concentrations occur in groundwater with a wide range of residence times (Table 1). Notwithstanding the possible local anthropogenic source of As (near Kaolao), the widespread occurrence of high F and As concentrations in groundwater with a range of ages indicates that natural processes are likely responsible for much of the F and As enrichment. The lack of correlation between As or F and NO_3 concentrations, which are related to agriculture (Currell et al., 2010) also indicates that input from agricultural chemicals is unlikely to be a major F and As source on a regional scale (Fig. 5).

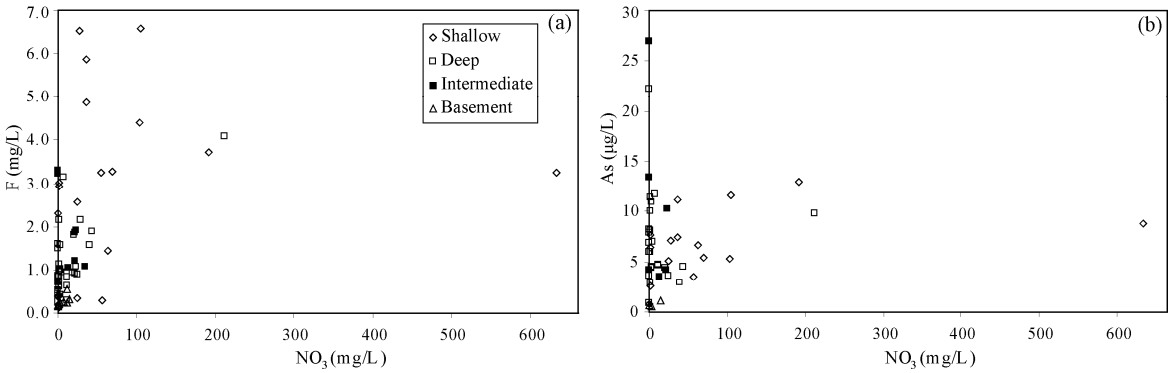

Fig. 5. Relationships between nitrate concentrations and groundwater F **(5a)** and As **(5b)** concentrations. The lack of any correlation between F and As with NO_3 indicates that enrichment is probably not linked to anthropogenic input (indicated by high NO_3 concentrations). Data from Table 1.

The groundwater molar F/Cl and As/Cl ratios are generally above those that are typical of unpolluted rainfall (e.g. As/Cl ~$2*10^{-5}$; F/Cl ~ 0.02, Andreae, 1980; Saether et al., 1995). While the groundwater with a modern component (e.g. shallow groundwater) may have received rainfall with elevated F/Cl ratios due to modern atmospheric emissions (e.g. Jacks et al., 2005), the majority of deep groundwater, which has residence times >5000 years, would be unaffected by such input. Groundwater with elevated F/Cl and As/Cl ratios occurs at nearly all depths in the aquifer (Fig. 6) and across a large geographic area (Fig 7), indicating that broad scale As and F enrichment has occurred in the aquifer. The high F/Cl and As/Cl ratios indicate that enrichment of these elements is independent of evapotranspiration, as no groundwater is saturated with respect to any major As or F bearing minerals, and therefore evapotranspiration should concentrate Cl, As and F equally. Some of the saline shallow samples (TDS > 2000 mg/L) with high F and As concentrations also have relatively low F/Cl and As/Cl ratios, indicating that evapotranspiration does contribute to the high F and As concentrations, but this is a local process confined to shallow depths (Fig. 6).

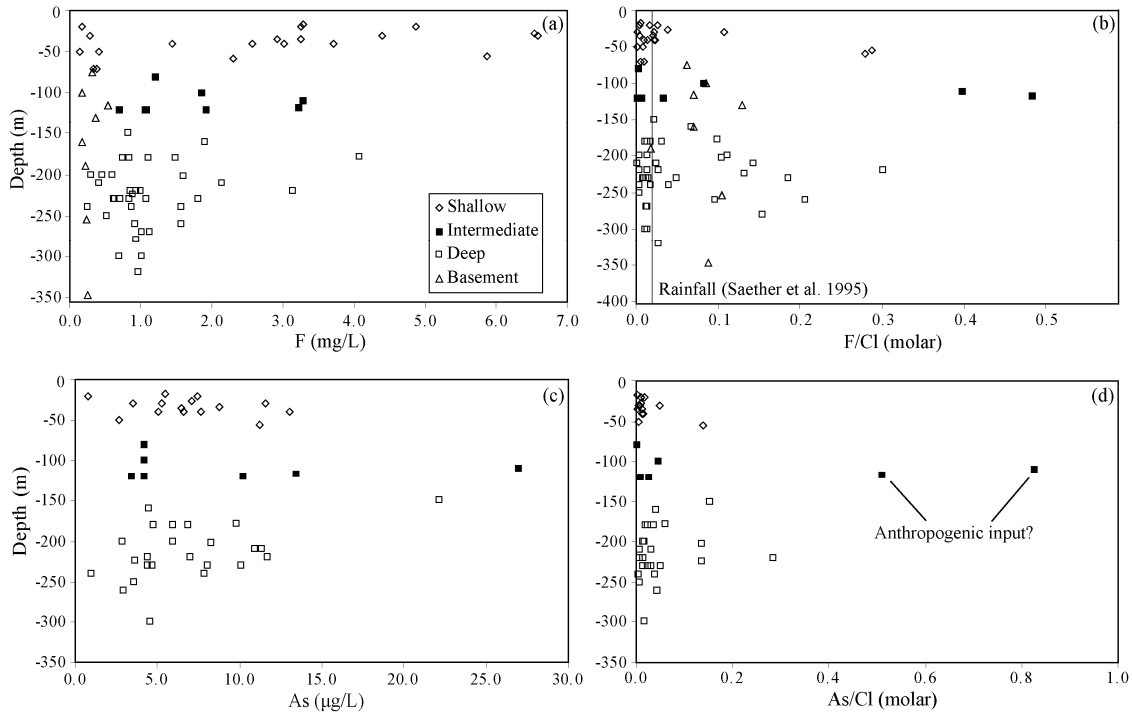

Fig. 6a. Distribution of F with depth **6b.** As vs. depth **6c.** F/Cl vs. depth **6d.** As/Cl vs. depth (Data from Table 1.)

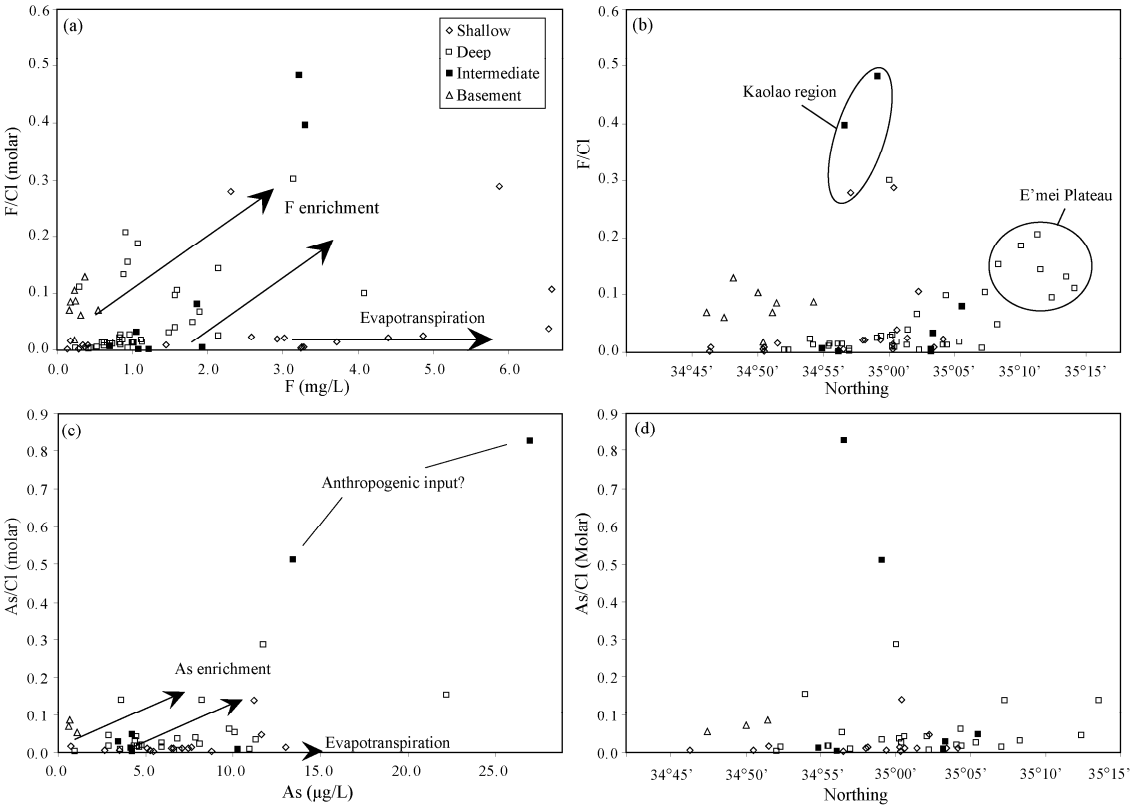

Fig. 7a. F/Cl vs. F concentrations **7b.** As/Cl vs. As concentrations **7c.** variation in F/Cl with latitude **7d.** As/Cl ratios vs. latitude. Rainfall F/Cl value from Saether et al., (1995). Data from Table 1.

4.3.3 Geochemistry of high F and As groundwater

Groundwater with high F and As concentrations has a distinctive major ion chemistry, being generally Na-rich, Ca-poor and having relatively high pH values (>7.8). There is a substantial positive correlation between F and As concentrations and Na/Ca ratios (r^2 = 0.67 & 0.46, respectively, Fig. 8a, 8b). As discussed in section 4.3.1, Na/Ca ratios in groundwater increase away from the basin margins, towards the central and northern Sushui River Basin, probably due to cation exchange. F and As concentrations also correlate positively with HCO_3 concentrations (r^2 = 0.49 & 0.20, respectively), while As, and to a lesser extent F concentrations correlate positively with pH values (R^2 = 0.36 & 0.17, respectively, Fig. 8). These data indicate that variations in the groundwater major ion chemistry and possibly pH, which are controlled by water-rock interaction processes in the aquifer (e.g. section 4.3.1), are important in mobilizing F and As.

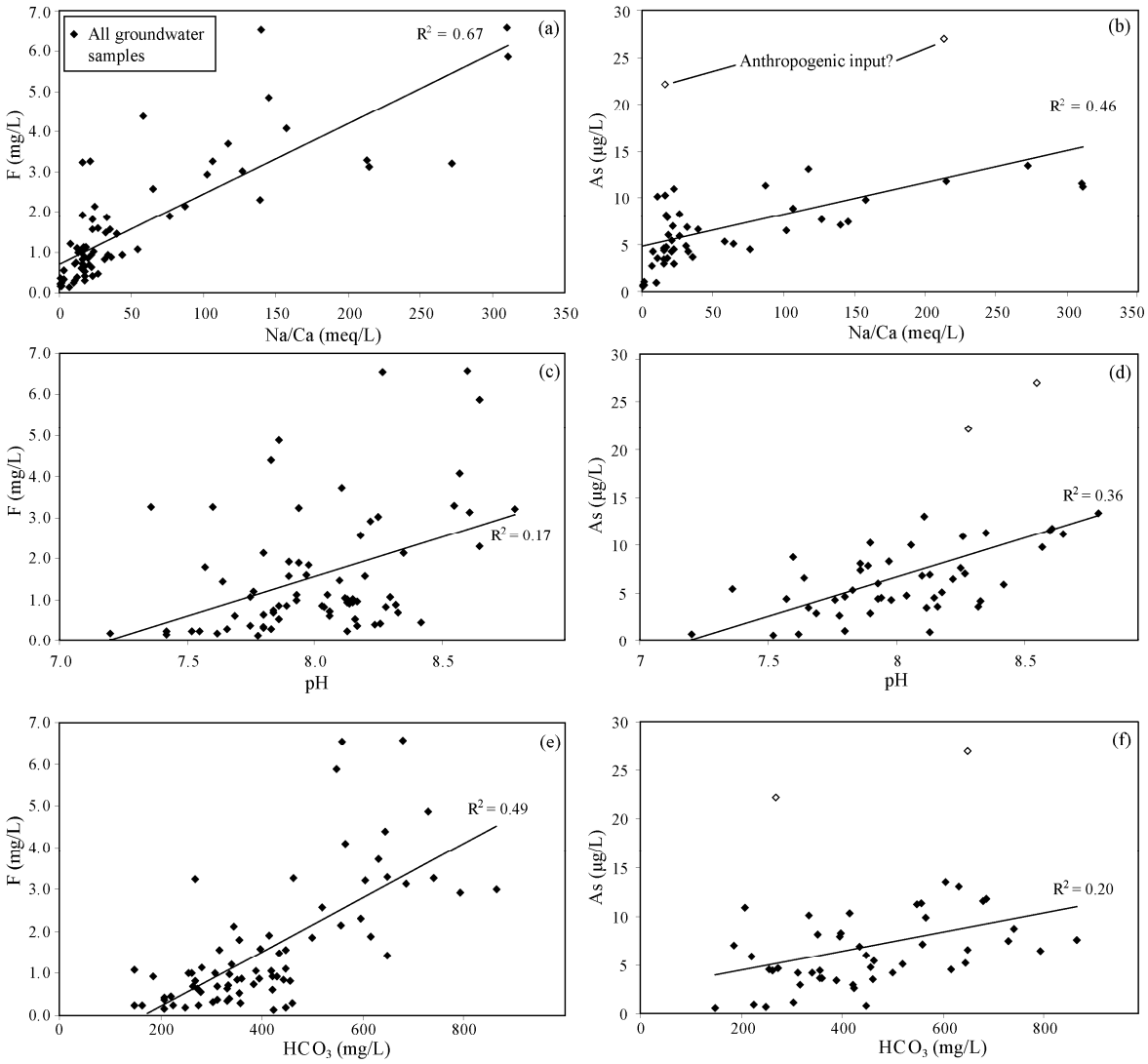

Fig. 8. Relationship between F and As concentrations with Na/Ca ratios (8a & 8b); pH values (8c & 8d) and HCO_3 concentrations (8e & 8f). Positive correlations between these parameters are consistent with mobilization of F and As occurring under particular geochemical conditions in the aquifer. Data in Table 1.

4.3.4 Sediment - solution experiments

The relationship between mobilisation of F and As and these aspects of water chemistry were explored further by means of experiments on five samples of sediment that were collected from the basin, including four loess samples from 2-3m below the ground surface and one clay (KL2) collected from 55m depth in a drill hole (Fig. 1b; Table 2). XRD analysis of the loess samples indicates that they are composed of approximately 40%

quartz, 20% albite, 15% calcite, 10 – 15% clay minerals (mostly illite), along with minor dolomite, chlorite and gypsum (Table 2). Aluminium oxides and iron oxides and oxyhydroxides such as ferrihydrite and goethite also are locally abundant in the loess, and particularly palaeosols, in the area (Liu, 1988). No common F-bearing minerals (e.g. fluorite, fluorapatite, hornblende) or As bearing minerals (e.g. arsenopyrite, realgar, orpiment) were detected in the XRD analysis. The loess samples were from the shallow subsurface, and hence may not fully represent the sediment compositions throughout the full depth of the aquifer, however from a mineralogical perspective they are broadly representative of loess in the region (e.g. Liu, 1988). The sediment samples were reacted with de-ionized water and two synthetic groundwater solutions in the laboratory. The two synthetic groundwater solutions have similar TDS and pH to deep groundwater in the quaternary aquifer, and the major difference between the solutions is the Na/Ca content (Table 3).

Mineral	**(LYL*)**	**(KL1)**	**(KL3)**	**(WGL)**
Quartz (%)	42.1	39.3	41.4	43.3
Albite	19.6	19.6	18.5	17.5
Orthoclase	-	3.1	2.3	3
Calcite	15.4	20.6	16	7.7
Dolomite	2.1	1.3	2.5	6.4
Aragonite	0.5	-	-	-
Low Mg Calcite	0.7	-	-	-
Gypsum	-	0.3	0.5	2.9
Chlorite	0.3	3.3	3.7	3.3
Illite/Muscovite	12.5	12.2	14.6	15.7
Kaolin	6.1	0.3	0.4	0.3

*Sample name, as shown on Fig. 1.

Table 2. Proportions of minerals identified by XRD analysis of loess samples

	Solution A	Solution B
Na (mmol/L)	5.0	12.7
Ca (mmol/L)	5.0	0.25
Mg (mmol/L)	0.52	0.49
HCO_3 (mmol/L)	5.0	5.0
Cl (mmol/L)	5.1	3.1
SO_4 (mmol/L)	2.9	3.0
EC (μS/cm)	1340	1390
Na/Ca (meq/L)	2.5	106
pH	8.1	8.7

Table 3. Composition of synthetic groundwater solutions

Different sediments released variable amounts of F and As. KL1 produced the highest F concentrations in solution (1.96 to 2.73 mg/L), while WGL produced the highest As concentrations in solution (13.5 to 16.7 μg/L). Sample KL2 (the clay sample) released the least F (0.49 to 0.95 mg/L) and the least As (0.51 to 1.58 μg/L), indicating either that there is less F and As present in the clay, or that it is less mobile compared to that which is in the loess. There was generally little difference (<13%) in the amounts of F or As that were released when the loess samples were reacted for 5 minutes compared to 6 hours (Table 3); although reacting the clay sample (KL2) for longer periods did result in a 23% increase in F and 54% increase in As, suggesting more gradual release of both elements occurs from clays. Reaction of sediments with de-ionized water and solution B (Na/Ca equivalents ratio of 106), generally resulted in similar amounts of F being released (Table 4). However, reaction of the sediments with the Ca-rich water (solution A) resulted in lower F concentrations in solution by between 12% and 45% (Table 4). Less As was also released from the sediments when the Ca-rich solution was used compared to the Na-rich solution (by between 12 and 35%), while similar amounts of As were released when the

Ca-rich solution and de-ionized water were used. The observation that greater amounts of both F and As were released into the high Na/Ca solution compared to the low Na/Ca solution are a further indication that the Na and Ca content of water have a control on the release of both elements from the loess.

Sample (Type)		**Solution / time of leaching**			
		DI / 5 mins	**DI /6 hrs**	**Sol A /6 hrs**	**Sol B /6 hrs**
KL1	F (mg/L)	2.71	2.71	1.96	2.73
(Loess)	As (μg/L)	1.51	1.74	1.97	3.01
KL2		0.49	0.64	0.85	0.93
(Clay)		0.51	1.12	1.04	1.58
KL3		1.08	0.99	0.71	1.3
(Loess)		1.93	1.81	1.88	2.86
WGL		1.89	1.85	1.46	1.89
(Loess)		13.6	16.7	13.6	15.7
LY1		1.23	1.41	1.21	1.38
(Loess)		4.12	4.26	4.18	4.74

Table 4. Concentrations of F (in mg/L, upper rows) and As (in μg/L, lower rows) that resulted after reaction of sediment samples from the Yuncheng Basin with de-ionized water and the synthetic groundwater solutions (A and B)

The observation that reaction of solutions with the loess for longer time periods generally did not result in an increase in F or As concentrations in solution indicates that these ions are more likely mobilized by desorption rather than dissolution of F- or As-bearing minerals. Minerals such as fluorite and arsenopyrite have low solubility in the temperature range of natural waters (e.g. Nordstrom and Jenne, 1977) and dissolution of fluorite under normal temperatures would be expected to produce gradual increases in F concentrations over time (e.g. Usunoff, 1990), which were not observed. On the other hand, desorption of $HAsO_4^{2-}$, F^- and certain other oxyanions from hydrous metal oxides can occur rapidly, and has been documented in a number of other semiarid, oxidising aquifer settings (Smedley and Kinniburgh 2002, Bhattacharya et al., 2006, Scanlon et al.,

2009). That no major F- or As-bearing minerals were detected in the sediments is consistent with this mechanism, as is the observation that the concentrations of F and As are correlated, as they are known to exhibit similar sorption-desorption behaviour in such environments (e.g. Smedley and Kinniburgh, 2002; Scanlon et al., 2009).

4.4 DISCUSSION

The correlations between groundwater major ion geochemistry and As and F concentrations, along with the results of the experiments with sediments, allow the sources and mobilisation mechanisms of F and As in the Yuncheng Basin groundwater to be better understood.

4.4.1 Source and mobilization of F and As in the Yuncheng Basin

The occurrence of high F and As concentrations over a wide area and in both shallow and deep groundwater with a large range of residence times indicates that enrichment of these elements is a broad-scale natural phenomenon. This widespread occurrence, and the relatively high concentrations of F and As in the solutions reacted with the loess samples compared to the clay (section 3.4) indicates that the source of F and As is probably the loess and/or palaeosols that make up much of the sedimentary aquifer matrix (with an additional possible anthropogenic source of As near Kaolao). Liu (1988) showed that aluminium oxides and iron oxides and oxyhydroxides are significant components of the Chinese loess. These are able to adsorb As oxyanions, and a number of other anions, probably including F^- (e.g. Smedley and Kinniburgh 2002). The bulk F/Cl ratios of the loess in China are relatively high (up to 0.4) and can be higher still in palaeosol layers (up

to 0.7, Liu 1988). Palaeosols generally contain greater amounts of secondary metal oxides and oxyhydroxides (and thus potential sorption sites for F and As) due to the high degree of microbial weathering associated with pedogenesis. Hence groundwater may derive a significant amount of F and As from these layers, although the palaeosols make up a much smaller volumetric proportion of the aquifer matrix than the loess itself (Liu 1988).

Mobilization of As and F anions in the groundwater is facilitated by high Na/Ca ratios, and possibly high pH values and HCO_3 concentrations (Section 4.3.3; 4.3.4, Fig. 8), that result from cation exchange and mineral weathering in the aquifer (e.g., section 4.3.1). Previous laboratory studies have demonstrated desorption of As oxyanions in response to a change from Ca-rich to Na-rich pore waters (Smith et al., 2002; Masue et al., 2007), which is termed the 'counter-ion effect'. This effect, as previously documented in soils (e.g. Smith et al. 2002) and locally observed in aquifers (e.g. Scanlon et al., 2009; McNab et al., 2009) probably relates to increased positive surface charge density around hydrous metal oxide sorption sites in the presence of Ca^{2+} (as opposed to Na^{+}), which facilitates sorption of anions such as $HAsO_4^{2-}$ and F^{-}. A change to Na-rich groundwater composition (e.g. due to cation exchange or mixing), therefore leads to mobilization of these sorbed anions (Smith et al., 2002; McNab et al., 2009; Scanlon et al., 2009). The substantial correlation between F and As concentrations with Na/Ca ratios is consistent with this being a major mechanism for mobilising these elements in the Yuncheng Basin, as is the fact that the solution with Na-rich, Ca-poor chemistry released greater amounts of F and As from the sediments compared to the Ca-rich solution, in all cases (Table 4). Cation exchange (e.g. in clay lenses and/or palaeosols) is therefore an important process that creates the geochemical conditions which facilitate As and F mobilization. In some aquifers, a

negative relationship between groundwater F and Ca concentrations can be explained by the fact that waters with high Ca contents reach saturation with respect to CaF_2 as F enrichment occurs, thereby limiting the amount of F^- in solution (e.g. Chae et al. 2007; Desbarats, 2009). However, groundwater in the Yuncheng Basin is undersaturated with respect to fluorite (saturation indices: -0.1 to -2.7, median -1.36, Table 1), indicating that fluorite saturation is never reached and fluorite precipitation does not limit the groundwater F concentrations.

High pH can also cause desorption of As oxyanions (and possibly F^-) from sediments. Generally, As in pore water desorbs more readily in oxidizing conditions at pH values of 8.5-9.0 than at circum-neutral pH (Smedley and Kinniburgh 2002). This is consistent with the observation that the Yuncheng Basin groundwater with high As concentrations (>10 μg/L) has pH values of 7.9 to 8.8 (Fig 5). While both the counter-ion effect and the high pH may be important controls, the strongest correlations in the data are between F and As concentrations and Na/Ca ratios, indicating that cation composition is likely the more important factor. However, it is difficult to completely separate the influence of cation composition and pH, as the Na-rich groundwater generally has higher pH. Similar amounts of F were released into the de-ionized water (pH = 7.0) and Na-rich solution (pH = 8.7), indicating that in the case of fluoride at least, pH had little effect on mobilization from the sediment samples.

Another possible factor that either causes de-sorption of F^- and $HAsO_4^{2-}$, or limits their capacity to be sorbed, is the presence of competitors for sorption sites, including HCO_3^- (e.g. Smedley and Kinniburgh 2002). Positive correlation between HCO_3 and both F and As concentrations (R^2 = 0.49 and 0.20, respectively) suggests that this may be an

additional control on F and As enrichment, although HCO_3 is generally considered a lesser competitor to As oxyanion sorption than other species such as PO_4 and VO_4 (e.g. Smedley et al., 2005). P and V were present below their detection limits (0.5 mg/L and 0.005 mg/L, respectively), meaning that links between F and As enrichment and these elements could not be investigated, although, in other settings where these elements appear to act as sorption competitors, they are present in much higher concentrations than these limits (e.g. Smedley et al., 2005; Scanlon et al., 2009), suggesting that they have little influence in the Yuncheng groundwater. Much of the HCO_3 in groundwater derives from weathering of carbonate minerals during recharge and to some extent in the aquifer matrix (Currell et al., 2010), meaning that pH and HCO_3 concentrations are also partly linked, as carbonate weathering increases both parameters, particularly under closed system conditions (e.g. Clark and Fritz 1997).

4.4.2 Primary source of F and As

The F and As in the aquifer sediments may have ultimately derived from rocks that are in the source regions of the loess, remaining in association with loess particles as they were transported to the basin. In this case, the relatively recent age of the sediments (Quaternary) may be a reason why there is still available F and As to be mobilized (e.g., Smedley et al., 2005). In the Yuncheng Basin, as in the broader Chinese Loess Plateau, loess mostly contains sedimentary quartz, feldspar, carbonate minerals, clays and mica. The Gobi and Badain Jaran deserts and alluvial fans draining the Qilian Mountains, which are all in northwest China, are the primary sources of this material, with the small size fraction (fine sand, silt and clay particles) transported to the east via dust storms (Liu 1988;

Derbyshire et al., 1998; Sun 2002; Guan et al., 2008). The fact that a number of regions in Inner Mongolia that lie along the transport path of the loess between northwest China and the Yuncheng Basin (e.g. the Hetao Plain, Alashan and Ba Men regions) also have groundwater with elevated As and F concentrations suggests that these elements are transported in association with loess to the region (e.g. Guo et al., 2001; Smedley et al., 2003; Guo et al., 2008) and/or that the loess is able to scavenge these elements during transport. Sediments in the Huhhot Basin to the north of the study area in Inner Mongolia, where groundwater contains high As and F concentrations, locally have elevated As contents (up to 29 mg/kg), although generally the sediments have concentrations from 3 to 9 mg/kg, which is within the range of world sediment averages (Smedley et al., 2003; Smedley et al., 2005). The As in these sediments is mostly associated with Fe-oxides, either as sorbed As anions and/or As incorporated into poorly ordered oxides via co-precipitation (Smedley et al., 2003), and this is likely also to be the case in the Yuncheng basin.

4.4.3 Global comparison with other basins.

Groundwater that has high Na/Ca ratios and/or pH values with elevated As and F concentrations is also found in basins containing Quaternary loess in several locations in Argentina, (La Pampa, Smedley et al., 2005; Rio Dulce, Bhattacharya et al., 2006; Cordoba, Gomez et al., 2009) and China (e.g. the Taiyuan Basin, Guo et al., 2007a; 2007b), as well as the Texas Southern High Plains aquifer (Scanlon et al., 2009). The primary As and F source in the basins in Argentina and the United States is likely volcanic ash and/or glass, (Bhattacharya et al., 2006; Gomez et al., 2009; Scanlon et al., 2009),

which is an important component of the loess in these basins and locally contains elevated As and/or F concentrations. In the Chinese loess, which comprises much of the sediment in the Yuncheng Basin (and the Taiyuan Basin); there is no volcanic ash or glass component and no known minerals enriched in As or F (Liu 1988; Yokoo et al., 2004). Despite many aquifers composed of loess having groundwater with high F and As concentrations globally, the sediments in these basins generally don't have greatly elevated bulk F and As concentrations compared to world sediment averages (e.g. As = 2-15 mg/kg, Smedley et al., 2005). Hence, rather than being related to source material containing particularly high As and F content, it may be that certain properties of loess (e.g. fine grain size, presence of palaeosols) and/or certain components common to loess in these different regions of the world, such as fine particles of hydrous Fe, Al and Mn oxides, facilitate sorption of anions of As and F under certain conditions, and release them into groundwater under other conditions (e.g. in the presence of high Na/Ca ratios and/or high pH). Anions of As, F and certain other elements (e.g. U, V, Mo, Se and B) exhibit similar sorption-desorption behaviour, particularly in the presence of metal oxides in oxidizing settings (Smedley and Kinniburgh, 2002; McNab et al., 2009). This explains the occurrence of both high As and F concentrations in these similar aquifer environments, irrespective of the primary source of the elements and the different sedimentary provenances.

Globally, groundwater containing high F and/or As concentrations from a variety of environments (not just in semi-arid areas) also has high Na/Ca ratios, and locally, high pH values and HCO_3 concentrations (e.g. Handa 1975; Welch et al., 2000; Jacks et al 2005; Chae et al. 2007; Desbarats 2009), which suggests that de-sorption of these anions as a result of these geochemical characteristics may be universally important. However, the

mechanism described appears to be particularly prevalent in semiarid regions in basins composed of terrestrial sediments. In the La Pampa and Rio Dulce regions of Argentina, pH is considered the most important factor causing mobilization of As (and possibly F) (Smedley et al., 2005; Bhattacharya et al., 2006), whereas in the Texas Southern High Plains aquifer (Scanlon et al., 2009), As and F mobilization appears to be more strongly linked to cation composition (Na/Ca ratios), as is the case in the Yuncheng Basin. It can be difficult to separate the influence of these factors, as there is a part causal link between low Ca content and high pH in the presence of HCO_3 (e.g. Smith et al., 2002; Bhattacharya et al., 2006), nevertheless, the correlations in the major ion data and laboratory experiments in this study indicate that F and As mobilization from the sediments from the Yuncheng Basin is most strongly influenced by the Na/Ca content of water.

In the Southern High Plains aquifer, a change from Ca-rich to Na-rich groundwater compositions is associated with mixing of saline, Na-rich water, whereas in the Yuncheng Basin, the high Na/Ca ratios likely result from cation exchange. A similar phenomenon was observed in an applied recharge site in California (McNab et al., 2009). In this case the introduction of recharge water that was out of equilibrium with minerals in the aquifer media led to enrichment of Na and K at the expense of Ca and Mg via cation exchange, along with mobilization of As and U (F concentrations were not measured in that study). This suggests that cation exchange and mobilization of As and F may relate to disturbance and/or transient conditions in an aquifer. In the Yuncheng Basin, and other similar basins in northern China, groundwater pumping is causing induced flow and mixing of water that may change its major ion geochemistry (by promoting mineral dissolution, ion exchange or other sorption-desorption reactions). Depending on the changes that occur, this may lead to

the further mobilization of F and As. Little is known about changes to groundwater chemistry caused by the water extraction in the Yuncheng Basin over the last 30 years; future monitoring should address such changes in order to predict whether F and As contamination may increase.

4.4.4 Migration of groundwater with high As and F concentrations

Given that groundwater pumping is causing significant disturbance to the natural flow system (Cao 2005; Currell et al., 2010), mixing between groundwater from regions with high F and As concentrations and groundwater with lower concentrations, where domestic supply wells are still used, is also a potential future concern. This is particularly relevant to the Kaolao region, where groundwater locally contains 4870 μg/L As and a number of wells have both elevated As and F concentrations (Fig. 1b & 1c). Most domestic supply wells have been abandoned near Kaolao village due to the very high incidence of fluorosis, however, there are many wells within 5-10 km of Kaolao that have not reported elevated F concentrations and are still used for irrigation and/or domestic supply. Deep groundwater pumping for irrigation is causing significant drawdown and a cone of depression to develop, west of Yuncheng city (Fig. 1c). This is already facilitating downward migration of saline, NO_3-rich water from shallow levels (Currell et al., 2010) and increasing rates of flow towards this area. Hence, there is a high probability that in the future, water with high As and F concentrations from the Kaolao region (and other areas) will migrate and mix both vertically and laterally in the aquifer to regions where groundwater is being pumped intensively.

4.5 CONCLUSIONS

High F and As concentrations in groundwater from the Yuncheng Basin result from desorption of $HAsO_4^{2-}$ and F^- from Fe, Al and Mn oxides in loess and palaeosols in the aquifer. Enrichment of As and F in groundwater is a broad-scale process affecting groundwater across a wide area and over a wide range of depths and residence times in the aquifer. Greater mobilization of As and F occurs in groundwater with high Na/Ca ratios, indicating the influence of cation exchange on As and F enrichment. This is probably due to decreased positive charge density around metal oxides sorption sites in the Na-rich, Ca-poor groundwater, reducing the capacity for sorption of As and F anions. Laboratory experiments indicate that relatively high Ca^{2+} content (e.g. Na/Ca equivalents ratio = 2) in solution results in the release of lesser amounts of F and As from sediments collected from the basin, compared to when water with a high Na/Ca equivalents ratio (106) is used, which is consistent with this interpretation. High pH values and the presence of competitors to sorption (especially HCO_3) may also facilitate mobilization. A local anthropogenic source is likely responsible for the very high As concentration in groundwater near Kaolao (4870 μg/L) and this source may also be affecting some nearby wells. Given that groundwater pumping is causing significant disturbance to the natural flow system in the basin, mixing of groundwater from this region with groundwater that is as yet unaffected by high As and F concentrations is a serious potential future health concern.

The strong similarity between the sediment types (e.g. Quaternary loess) and groundwater geochemical conditions associated with high As and F concentrations in the Yuncheng basin and other semiarid regions, such as Argentina and Texas, indicates that

certain properties of loess along with particular groundwater chemistry (Na-rich, high pH) favour the enrichment of F and As in groundwater in semiarid, oxidizing aquifer settings globally. It appears that the primary source of the elements is probably different in China than in Argentina and the US (as there is no volcanic ash in the Chinese loess). Hence, the capacity of loess to adsorb these elements and release them under particular geochemical conditions appears to be a critical factor leading to high groundwater F and As concentrations. The same mechanism and factors are probably responsible for elevated F and As concentrations in groundwater from other aquifers in northern China such as the Taiyuan Basin, located 350km north of the study area, which contains similar sediments and has similar groundwater chemistry.

Acknowledgments

This research was partly initiated and greatly supported by the Australia-China Water Resources Research Centre, including Dr. Deli Chen, Dr. Yongping Wei, Prof. Song Xianfang and Prof. Li Baoguo. Special thanks also to the Yuncheng City Water Resources Service Bureau, in particular Mr. Sun Xinzhong. Logistical support was also given by the Yongji, Linyi and Yuncheng county Water Resource Bureaus, and Dr. Wang Zhimin. We thank Dean Bradley for his logistical support in the field.

References

Andreae, M.O., 1980. Arsenic in rain and the atmospheric mass balance of arsenic. Journal of Geophysical Research 85(C8), 4512-4518.

Bhattacharya, P., Claesson, M., Bundschuh, J., Sracek, O., Fagerberg, J., Jacks, G., Martin, R.A., Stoniolo, A.R., Thir, J.M., 2006. Distribution and mobility of arsenic in the Rio Dulce alluvial aquifers in Santiago del Estero Province, Argentina. Science of the Total Environment 358, 97-120.

Brunt, R., Vasak, L., Griffioen, J., 2004. Fluoride in groundwater: Probability of occurrence of excessive concentration on global scale. International Groundwater Resource Assessment Centre report SP 2004-2, 20p.

Cao, X.H., 2005. Study of the intermediate and deep layers of the Sushui River Basin confined groundwater system. In: *Shanxi Hydrotechnics Bulletin No. 3.* China Academic Journal Electronic Publishing House. pp 41-43. (In Chinese)

Chae, G-T., Yun, S-T., Mayer, B., Kim, K-H., Kim, S-Y., Kwon, J-S., Kim, K., Koh, Y-K., 2007. Fluorine geochemistry in bedrock groundwater of South Korea. Science of the Total Environment 385, 272-283.

China Geological Survey, 2006. Groundwater resources and environmental issues assessment in the six major basins of Shanxi (in Chinese), China Geological Survey Special publication, Beijing. 98p.

Choubissa, S.L., 2001. Endemic fluorosis in southern Rajasthan, India. Fluoride 34(1), 61-70.

Clark, I., Fritz, P., 1997. Environmental Isotopes in Hydrogeology. Lewis Publishing, New York. 328p.

Currell, M.J., Cartwright, I., Bradley, D.C., Han, D.M., 2010. Recharge history and controls on groundwater quality in the Yuncheng Basin, north China. Journal of Hydrology 385, 216-229.

Datta, P.S., Deb, D. L., Tyagi, S.K., 1996. Stable isotope (^{18}O) investigations on the processes controlling fluoride contamination of groundwater. Journal of Contaminant Hydrology 24, 85-96.

Derbyshire, E., Meng, X., Kemp, R.A., 1998. Provenance, transport and characteristics of modern aeolian dust in western Gansu province, China, and interpretation of the Quaternary loess record. Journal of Arid Environments 39, 497-516.

Desbarats, A.J., 2009, On elevated fluoride and boron concentrations in groundwaters associated with the Lake Saint-Martin impact structure, Manitoba. Applied Geochemistry 24, 915-927.

Edmunds, W.M., 2003. Renewable and non-renewable groundwater in semi-arid regions. Developments in Water Science 50, 265-280.

Edmunds, W.M., Smedley, P.L., 2005. Fluoride in Natural Waters (Chapter 12) in: Selinus, O. (ed.) *Essentials of Medical Geology – Impacts of the Natural Environment on Public Health.* Elsevier, pp 301-315.

Fujita, S., Takahashi, A., Weng, J, Huang, L., Kim, H., Li, C., Huang, F.T.C., Jeng, F., 2000. Precipitation chemistry in East Asia. Atmospheric Environments 34, 525-537.

Gaciri, S.J., Davies, T.C., 1993. The occurrence and geochemistry of fluoride in some natural waters of Kenya. Journal of Hydrology 143, 395-412.

Gao, X., 2005. The distribution of fluoride in groundwater and nature of the processes causing high fluoride concentrations in groundwater in theYuncheng Basin. China Geological University Msc Thesis, 61p. (in Chinese)

Gao, X., Wang, Y., Li, Y., Guo, Q., 2007. Enrichment of fluoride in groundwater under the impact of saline water intrusion at the salt lake area of Yuncheng basin, northern China. Environmental Geology 53(4), 795 – 803.

Gomez, M.L., Blarasin, M.T., Martinez, D.E., 2009. Arsenic and fluoride in a loess aquifer in the central area of Argentina. Environmental Geology 57, 143-155.

Guan, Q., Pan, B., Gao, H., Li, N., Zhang, H., Wang, J. 2008. Geochemical evidence of the Chinese loess provenance during the Late Pleistocene. Palaeogeography, Palaeoclimate and Palaeoecology 270, 53-58.

Guo, H., Tang, X., Yang, S., Shen, Z. 2008. Effect of indigenous bacteria on geochemical behaviour of arsenic in aquifer sediments from the Hetao Basin, Inner Mongolia: Evidence from sediment incubations. Applied Geochemistry 23(12), 3267-3277.

Guo, Q., Wang, Y., Ma, T. and Ma, R., 2007(a). Geochemical processes controlling the elevated fluoride concentrations in groundwaters of the Taiyuan Basin, Northern China. Journal of Geochemical Exploration 93(1), 1-12.

Guo, Q., Wang, Y., Gao, X., Ma, T., 2007(b). A new model (DRARCH) for assessing groundwater vulnerability to arsenic contamination at basin scale: a case study in Taiyuan basin, northern China. Environmental Geology 52, 923-932.

Guo, X., Fujino, Y., Kaneko, S., Wu, K., Xia, Ya., Yoshimura, T., 2001. Arsenic contamination of groundwater and prevalence of arsenical dermatosis in the Hetao plain area, Inner Mongolia, China. Molecular Cell Biochemistry 222, 137-140.

Handa, B.K., 1975. Geochemistry and genesis of fluoride – containing ground waters in India. Ground Water 13, 275-281.

Jacks, G., Bhattacharya, P., Chaudhary, V., Singh, K.P., 2005. Controls on the genesis of some high-fluoride groundwaters in India. Applied Geochemistry 20, 221-228.

Liu, T.S., Zhang, S.X., Han, J.M., 1986. Stratigraphy and palaeoenvironmental changes in the loess of central China. Quarternary Science Reviews 5, 489-495.

Liu, T.S., 1988. Loess in China. China Ocean Press, Beijing.

Masue, Y., Loeppert, R.H., Kramer, T.A., 2007. Arsenate and arsenite adsorption and desorption behaviour on co-precipitated aluminium: iron hydroxides. Environmental Science and Technology 41, 837-842.

McNab Jr., W.W., Singleton, M.J., Moran, J.E., Esser, B.K., 2009. Ion exchange and trace element surface complexation reactions associated with applied recharge of low-TDS water in the San Joaquin Valley, California. Applied Geochemistry 24, 129-197.

Parkhurst, D.L., Apello, C.A.J., 1999. User's guide to PHREEQC (Version 2) – a computer program for speciation, batch-reaction, one-dimensional transport, and inverse geochemical calculations: US Geological Survey Water Resource Investigation Report 99-4259.

Rao, N.S. (2003) Groundwater quality: focus on fluoride concentration in rural parts of Guntur district, Andhra Pradesh, India. Hydrological Science 48(5), 835-847.

Saether, O.M., Andreassen, B.Th., Semb, A., 1995. Amounts and sources of fluoride in precipitation over southern Norway. Atmospheric Environment 29(15), 1785-1793.

Scanlon, B.R., Nicot, J.P., Reedy, R.C., Kurtzman, D., Mukherjee, A., Nordstrom, D.K., 2009. Elevated naturally occurring arsenic in a semiarid oxidizing system, Southern High Plains aquifer, Texas, USA. Applied Geochemistry 24, 2061-2071.

Smedley, P.L., Kinniburgh, D.G., 2002. A review of the source, behaviour and distribution of arsenic in natural waters. Applied Geochemistry 17, 517-568.

Smedley, P.L., Zhang, M., Zhang, G., Luo, Z., 2003. Mobilization of arsenic and other trace elements in fluviolacustrine aquifers of the Huhhot Basin, Inner Mongolia. Applied Geochemistry 18, 1453-1477.

Smedley, P.L., Kinniburgh, D.G., Macdonald, D.M.J., Nicolli, H.B., Barros, A.J., Tullio, J.O., Pearce, J.M., Alonso, M.S., 2005. Arsenic associations in sediments from the loess aquifer of La Pampa, Argentina. Applied Geochemistry 20, 989-1016.

Smith, E., Naidu, R., Alston, A.M., 2002. Chemistry of inorganic arsenic in soils: II. Effect of phosphorous, sodium and calcium on arsenic sorption. Journal of Environmental Quality 31, 557-563.

Sun, J., 2002. Provenance of loess material and formation of loess deposits on the Chinese Loess Plateau. Earth and Planetary Science Letters 203, 845-859.

Sun, J.X., 1988. Environmental geology in loess areas of China. Environmental Geology and Water Science 12(1), 49-61.

Tekle-Haimanot, R., Melaku, Z., Kloos, H., Reimann, C., Fantaye, W., Zerihun, L. and Bjorvatn, K., 2006. The geographic distribution of fluoride in surface and groundwater in Ethiopia with an emphasis on the Rift Valley. Science of the Total Environment 367, 182-190.

Usunof, E.J., 1990. Rate-limiting steps in the dissolution of fluorite. Journal of Hydrology 112, 319-326.

Walraevens, K., Cardenal-Escarcena, J., Van Camp, M., 2007. Reaction transport modelling of a freshening aquifer (Tertiary Ledo-Paniselian Aquifer, Flanders-Belgium). Applied Geochemistry 22, 289-305.

Wang, Q., Li, C., Tian, G., Zhang, W., Liu, C., Ning, L., Yue, J., Cheng, Z. & He, C., 2002. Tremendous change of the earth surface system and tectonic setting of salt-lake formation in Yuncheng Basin since 7.1 Ma. Science in China (Series D- Earth Sci.) 45(2), 110-122.

Welch, A.H., Westjohn, D.B., Helsel, D.R., Wanty, B., 2000. Arsenic in ground water in the United States: Occurrence and geochemistry. Ground Water 38(4), 589-604.

World Health Organisation, 1984. Guidelines for drinking water quality, Values 3; Drinking water quality control in small community supplies. WHO, Geneva.

World Health Organisation, 2001. Environmental Health Criteria 224: Arsenic compounds 2nd Edition. WHO, Geneva.

World Health Organisation, 2004. Fluoride in Drinking Water – Background Document for Development of WHO Guidelines for Drinking Water Quality. WHO, Geneva.

Xu, X., Ma, X., 1992. Geodynamics of the Shanxi Rift system, China. Tectonophysics 208, 325-340.

Yokoo Y., Nakano T., Nishikawa M. and Quan H. (2004) Mineralogical variation of Sr-Nd isotopic and elemental compositions in loess and desert sand from the central Loess Plateau in China as a provenance tracer of wet and dry deposition in the northwestern Pacific. Chemical Geology 204, 45-62.

Chapter 5

Groundwater iodine content and its relationship to palaeoclimatic variability: Evidence from palaeowaters in a semi-arid basin, northern China

Matthew J. Currell[1], Ian Cartwright[1], Massimo Raveggi[1]

[1] School of Geosciences, Monash University, Clayton VIC, Australia 3800

-----In preparation for submission to Chemical Geology-----

ABSTRACT

Total iodine concentrations were measured in groundwater from the Yuncheng Basin, an aquifer in semi-arid northern China containing palaeowaters with a range of ages up to ~22 k.a., that were recharged over a period characterized by significant changes in temperatures and rainfall amounts. Iodine concentrations are between 1.8 and 288 μg/L, and are generally highest in shallow groundwater (median 168 μg/L compared to 38 μg/L in deep and intermediate groundwater), largely due to the high degree of evapotranspiration of this water. However, molar I/Cl and I/Br ratios in the groundwater are also generally high (median ratios = $1.2*10^{-4}$ and 0.12, respectively) in comparison to typical groundwater from temperate climatic regions (I/Cl = ~$0.5*10^{-6}$ to $7.7*10^{-5}$). The high I/Cl and I/Br ratios indicate that rainfall from the East Asian summer monsoon delivers a large amount of marine I to the Asian continent, and/or that sorption of iodine in the soil zone is limited in this region compared to more temperate areas, due to the dry, alkaline soils. Positive correlation between $\delta^{18}O$ values and I/Br and I/Cl ratios (r^2 = 0.48 and 0.55, respectively), in groundwater that is unaffected by agriculture, indicates that

relatively large amounts of I have been delivered by precipitation during warm climates. This may be due to greater production of a range of gaseous iodine compounds (e.g. CH_3I, CH_2I_2 and I_2) by marine algae and cyanobacteria during warm periods that was incorporated into rainfall and groundwater. These data indicate that the I concentrations and ionic ratios of palaeowaters in basins of northern China have been responsive to past changes in climate and variable marine production of I over 1000s of years. As far as we are aware this is the first study to examine groundwater I concentrations as an indicator of palaeoclimatic variation.

Key words: Iodine, Groundwater, Palaeoclimate, China

5.1 INTRODUCTION

Iodine is rare in the Earth's crust but it is highly soluble and occurs in significant quantities in the oceans (55-60 μg/L) and to a lesser extent rainfall (~0.5 to 20 μg/L), surface water (~0.5 to 50 μg/L) and groundwater <0.5 to 100 μg/L (Lloyd et al., 1982; Fuge and Johnson, 1986; Truesdale and Jones, 1996; Moran et al., 2002; Neal et al., 2007). In natural water, inorganic iodine exists in two major forms as iodide (I^-) and iodate (IO_3^-). Most rainfall and surface water contain these species in approximately equal amounts (Truesdale and Jones, 1996), however in the normal pH and Eh range of groundwater (pH 5 to 9; Eh -100 to +400 mV), I^- is more stable than IO_3^- (Lloyd et al., 1982). Iodine can also occur in significant concentrations in natural waters as organo-iodine compounds (Andersen et al., 2002). Organic matter has a high affinity for iodine; for example, algae and other marine microorganisms assimilate it, concentrating it up to thousands of times above ambient levels (Dean, 1963; Andersen and Laurberg, 2009), while soils also commonly contain high concentrations because of iodine sorption by humic materials (Fuge and Johnson, 1986).

There are relatively few studies that have measured I in freshwaters, partly due to difficulties in measurement at the low concentrations that are often encountered (generally <10μg/L). I concentrations have been measured in rainfall and surface water (e.g. Campos et al., 1996; Truesdale and Jones, 1996, Moran et al., 2002; Neal et al., 2007, Gilfedder et al., 2010), and groundwater (e.g. Lloyd et al., 1982; Heathcote and Lloyd, 1985; Rosenthal and Mates, 1986), but in groundwater most studies have focused on iodine deficiency in drinking water (e.g. Rosenthal and Mates 1986) or constraining marine incursions into aquifers (e.g. Lloyd et al., 1982). Iodine has rarely been studied in groundwater from arid

or semiarid regions (with the exception of Rosenthal and Mates, 1986), or deep groundwater with long residence times.

Concentrations of I in the atmosphere and rainfall vary spatially and temporally with atmospheric and climatic conditions (Oram and Penkett, 1994, Campos et al., 1996, Saiz-Lopez and Plane, 2004; Smythe-Wright et al., 2006). Locally, greater production of I occurs during warm months (e.g. Oram and Penkett, 1994), probably due to greater biological productivity when the oceans are warmer. Kelp, other types of algae and photosynthetic picoplankton emit gaseous organic and inorganic I compounds that are converted to iodide and iodate via photolysis and incorporated into rainfall (Campos et al., 1996; Smythe-Wright et al., 2006; Küpper et al., 2008). This occurs both in inter-tidal areas and in the open ocean at tropical and sub-tropical latitudes, and may be a significant source of iodine in rainfall. There is also a relationship between the intensity of rain events and rainfall I concentrations due to washout and dilution of I during heavy rainfall (e.g. Duce et al., 1965; Truesdale and Jones, 1996). Recently, there has been speculation about the role of marine iodine production in the formation of atmospheric aerosols that are involved in cloud formation, and which may influence global climate (O'Dowd et al., 2002; McFiggans et al., 2004; Smythe-Wright et al. 2006; Intergovernmental Panel on Climate Change, 2007). So far, data presented in the literature has focused on seasonal variations (e.g. daily, monthly and yearly measurements) of I concentrations in the atmosphere and rainfall. However, little is known about long-term variations in concentrations of I in rainfall or the terrestrial hydrosphere, and their relationship to palaeoclimate.

Palaeowaters, such as those found in the groundwater basins in northern China, reflect the composition of recharging precipitation from the late Pleistocene to the present (e.g. Chen et al., 2003; Edmunds et al., 2006; Gates et al., 2008; Currell et al., 2010). Hence, variation in I concentrations in groundwater in these basins may reflect long term changes in climate, oceanic, atmospheric and terrestrial processes. In order to investigate these relationships, we examined total I concentrations and their relationship to $\delta^{18}O$ values and ^{14}C ages in groundwater from the Yuncheng Basin in northern China. The use of stable isotopes in this context is helpful, as these are also sensitive to climatic factors (e.g. temperature and rainfall amount). The Yuncheng Basin contains water with a wide range of ages, up to ~22 k.a. (Currell et al., 2010), and hence provides an ideal location for such an investigation. As far as we are aware, this is the first study to examine the I content in palaeowaters as an indicator of palaeoclimatic variation. Pennington and Lishman (1971) studied the I content of lake sediments, as far as we know this is the only other example where I has been used to examine palaeoenvironments.

This research may provide additional information that can aid in understanding past climates and help to delineate the complex geochemical relationships between the biosphere, oceans, atmosphere and continental hydrosphere.

5.2 SITE DESCRIPTION & BACKGROUND DATA

5.2.1 The Yuncheng Basin

The geology and hydrogeology of the Yuncheng Basin is summarised in Currell et al., (2010). The basin comprises a Quaternary aquifer of interlayered sediments that is up to 500m thick, and which includes a shallow unit (<70 m), a deep unit (>120 m), and an

intermediate unit (70 to 120m), although this unit is hydraulically connected to the deep unit (Cao 2005). The sediments of the Yuncheng Basin are mostly aeolian loess that is made up of quartz (~40%), feldspar (~20%), calcite (~20%), clays and mica (Liu, 1988) which is interlayered with alluvial sands and lacustrine clay lenses (China Geological Survey, 2006). In the south of the basin, the Quaternary aquifer sits above and adjacent to Archean basement metamorphic rocks that contain limited amounts of water in fractures.

The region has a semi-arid climate with annual rainfall averaging ~550 mm and potential evapotranspiration of ~1900 mm. Most rainfall (>65%) occurs between June and September during the East Asian summer monsoon, and in this period the rainfall amount can exceed evapotranspiration, facilitating groundwater recharge (China Geological Survey, 2006; Scanlon et al., 2006). Prior to development of the groundwater resource as a supply for agriculture, regional groundwater flow was from the eastern Yuncheng Basin to the west, towards the Yellow River (Fig.1; Currell et al., 2010). However, due to the large amount of pumping of deep groundwater for irrigation since the 1980s, horizontal groundwater flow in the deep aquifer is now towards a cone of depression to the west of Yuncheng City (Cao, 2005).

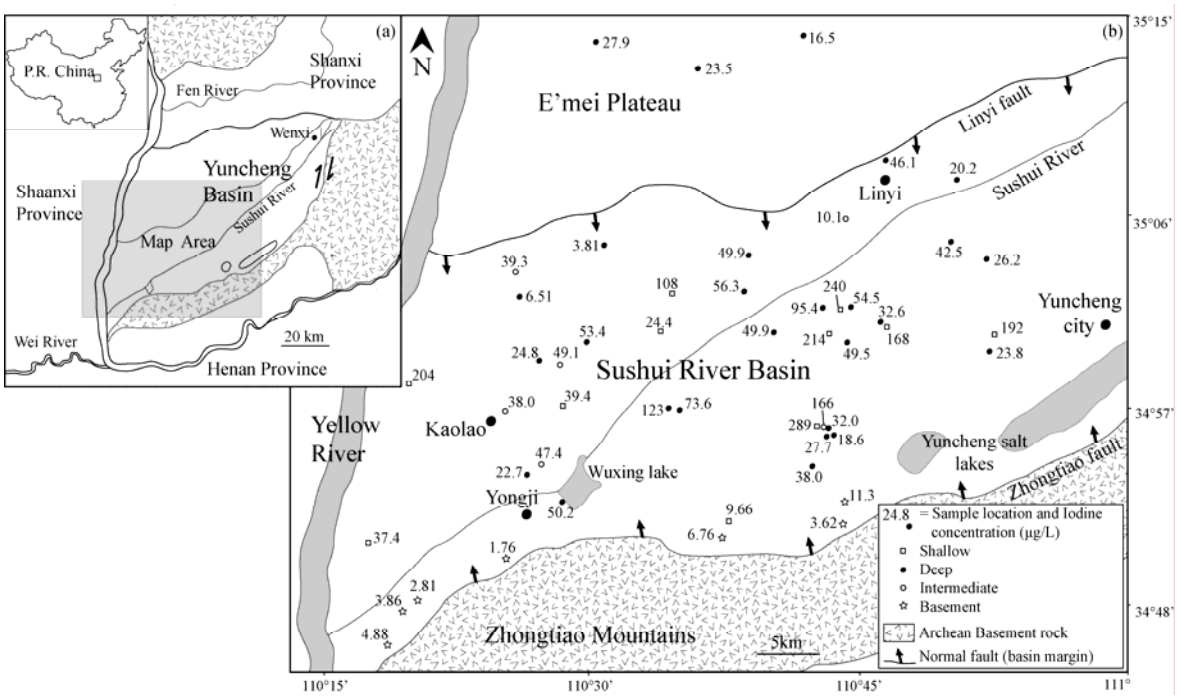

Fig. 1a. Location of the Yuncheng Basin. 1b. Detail of the study area, groundwater sampling sites and groundwater iodine concentrations (data from Table 1).

5.2.2 Groundwater quality

Shallow groundwater generally has high nitrate concentrations (up to 630 mg/L, median 31 mg/L) and high TDS concentrations (up to 8450 mg/L, median 1980 mg/L). Much of this nitrate is derived from synthetic fertilizers, while the high salinity is caused by evapotranspiration of shallow groundwater due to locally intensive flood irrigation (Currell et al., 2010). Generally, the deep groundwater is unaffected by these processes, and has lower TDS concentrations (median 1085 mg/L) and nitrate concentrations (median 1.8 mg/L). However, intensive pumping of the deep groundwater has caused large downwards vertical hydraulic gradients and locally, leakage of shallow groundwater into the deep aquifer occurs, as is indicated by elevated nitrate concentrations (>10 mg/L), particularly in the vicinity of the Linyi fault (Currell et al., 2010; Fig 1).

5.2.3 $\delta^{18}O$, $\delta^{2}H$ and ^{14}C

$\delta^{18}O$, $\delta^{2}H$ and ^{14}C data from the region are reported in Currell et al., (2010). The $\delta^{18}O$ and $\delta^{2}H$ values of groundwater mostly plot close to the global meteoric water line (GMWL) and local meteoric water line (LMWL) from Xi'an (Fig. 2a), indicating groundwater recharge via infiltration of meteoric precipitation. Most groundwater recharge occurs during the summer monsoon when precipitation is relatively intensive (>100 mm/month), producing groundwater with $\delta^{18}O$ and $\delta^{2}H$ values near the lower end of the LMWL (Currell et al., 2010). Groundwater residence times estimated using ^{14}C activities and a correction scheme based on major ion chemistry and $\delta^{13}C$ values (Currell et al., 2010) range from modern in shallow groundwater to between 3 and 22 k.a. in deep and intermediate groundwater (Table 1; Fig 2b). $\delta^{18}O$ values increase from old to young groundwater; groundwater recharged in the late Pleistocene has $\delta^{18}O$ values of ~-10‰ to -12‰, while groundwater recharged in the mid-Holocene has $\delta^{18}O$ values of ~-8.0‰ to -10‰ (Fig. 2b). This pattern is similar to that observed in groundwater from deep aquifers throughout northern China (Chen et al., 2003; Edmunds et al., 2006; Gates et al., 2008; Kreuzer et al., 2009), The $\delta^{18}O$ and $\delta^{2}H$ values in precipitation from the East Asian summer monsoon are sensitive to both changes in temperature and amounts of precipitation (e.g. intensity of rain events) (Yamanaka et al., 2004; Johnson and Ingram, 2004). However, the broad-scale increase in temperature from the Late Pleistocene to the early and mid-Holocene is likely the greatest factor responsible for the increase in $\delta^{18}O$ values over the period of groundwater recharge, both in the Yuncheng Basin (Currell et al., 2010) and in northern China generally (Edmunds et al., 2006; Gates et al., 2008).

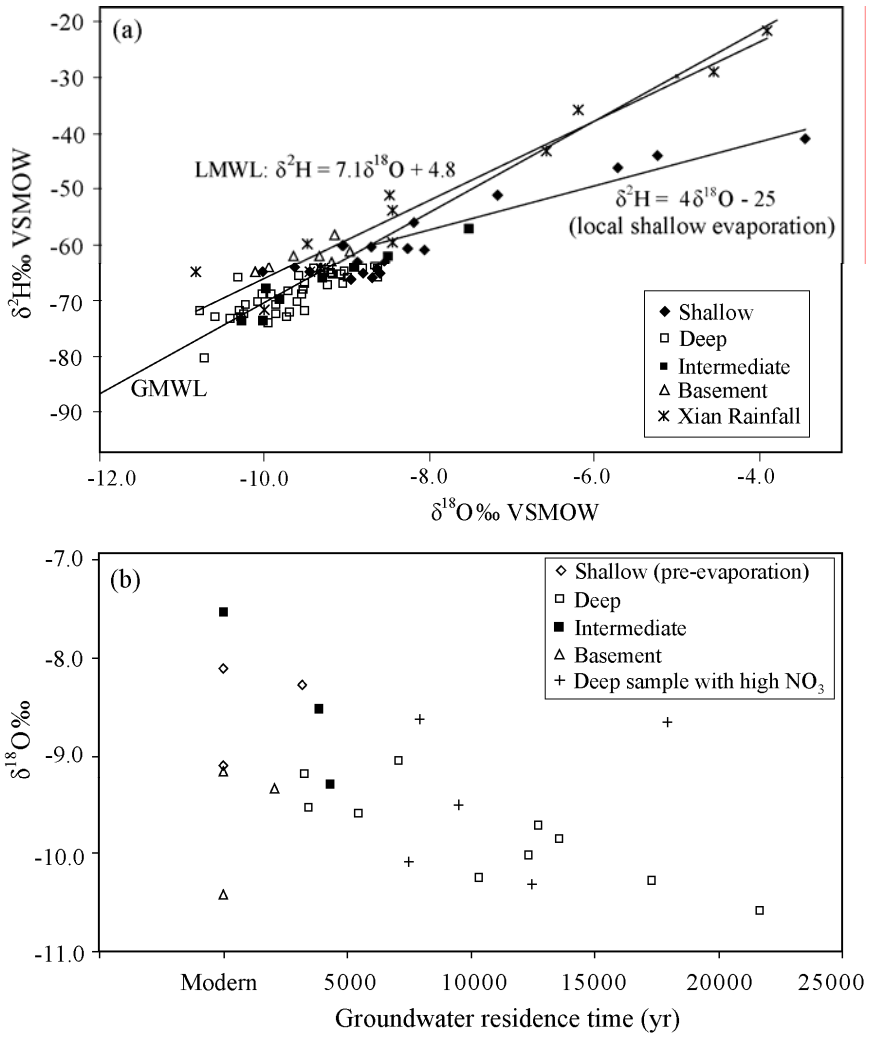

Fig. 2a. $\delta^{18}O$ and δ^2H values in groundwater samples. GMWL is the Global Meteoric Water Line (Rosanski et al., 1993) and LMWL is the Local Meteoric Water Line for Xian (IAEA/World Meteorological Organisation, 2007). **2b.** Relationship between $\delta^{18}O$ and residence times in groundwater from the Yuncheng Basin (Currell et al. 2010).

5.3 METHODS

Seventy-three groundwater samples were collected from the Yuncheng Basin during 2007 and 2008, from shallow, intermediate and deep wells in the Quaternary sediments and from the fractured basement rock, while two rain samples were also collected from Yuncheng City (Fig. 1; Table 1). The methods used for groundwater sampling and analysis of $\delta^{18}O$, δ^2H, a^{14}C and major anions are described in Currell et al., (2010). Total iodine concentrations were determined for 51 of the groundwater samples and two rain samples,

using a Thermo Finnigan X series II quadrupole ICP-MS at Monash University's School of Geoscience (Table 1; Fig 1). A series of calibration standards were prepared from a commercially available I stock solution diluted to the appropriate concentration with NH_4OH-Na-EDTA solution. This was also used to dilute the water samples, so that the pH of samples and calibration standards remained above 8.0, ensuring that iodide did not convert to I_2 and degas. The naturally high pH of the groundwater (pH 7.2 to 8.8) meant that loss of iodide by degassing during sample transport and preparation was minimal. Drift corrections were applied by the use of Te as an internal standard, and repeated analysis of standards throughout the analytical sessions. Internal precision is of the order of 3-6% (1σ) and external precision on repeat analysis of the unknowns was within this range. Accuracy was checked by analysing an in-house groundwater standard with similar TDS to the unknowns, spiked with a known concentration of I, which was in all cases correct within ±10% of the known values.

5.4 RESULTS

5.4.1 Iodine concentrations

Total iodine concentrations in groundwater from the Quaternary aquifer range from 1.8 to 288 μg/L, with a median concentration of 38 μg/L. In shallow groundwater the concentrations are generally the highest (median 168 μg/L); while they are lower in deep/intermediate groundwater (median 38 μg/L). Groundwater from the Quaternary aquifer generally has slightly higher Cl/Br ratios (median = 1070) than local rainfall (~300 to 800) indicating that a small amount of groundwater Cl is derived from a non-marine source, probably halite (Yokoo et al., 2004). Other than this, strong positive correlations

between TDS concentrations and both Br ($r^2 = 0.93$) and Cl ($r^2 = 0.90$) indicate that these halogens exhibit largely conservative behaviour in groundwater. Hence, groundwater I/Br and I/Cl ratios can be examined as an index of enrichment or depletion of I that is independent of the degree of evapotranspiration. I/Br ratios are similar in the shallow and deep groundwater (median 0.14 and 0.11, respectively; Fig. 3), indicating that the higher I concentrations in saline shallow water compared to deep groundwater are largely a result of high levels of evapotranspiration in the shallow groundwater. However, I/Cl (and likely also I/Br) ratios in groundwater from all depths; I/Cl = $7.3*10^{-6}$ to $1.1*10^{-3}$, median $1.2*10^{-4}$, are generally high relative to those in groundwater from other regions (I/Cl ratios typically $\leq 7.7*10^{-5}$; Table 2), indicating a naturally high input of I in the Yuncheng Basin that is not related to evapotranspiration. The groundwater I/Cl and I/Br ratios (I/Br ~0.05 to 0.30) are mostly slightly below the I/Cl and I/Br ratios in the local rainfall samples (e.g. I/Cl ~ $0.4*10^{-4}$ to $1.2*10^{-3}$; I/Br ~0.20 to 0.31, Fig. 3); this is probably due to sorption of I in the soil zone by humic material during recharge (Fuge and Johnson, 1986).

Sample No.	Unit*	GPS Latitude	GPS Longitude	Depth m	TDS mg/L	pH	O_2 mg/L	HCO_3 mg/L	Cl mg/L	Br mg/L	I µg/L	I/Br molar	I/Cl molar	NO_3 mg/L	Tot. Cations/Cl molar	δ^2H ‰	$\delta^{18}O$ ‰	Residence time +
1	S	350029.8	1104326.8	-34	5287	7.6	4	740	1335	1.96	215	0.069	4.49E-05	633	1.9	-63	-8.9	
2	S	350139.2	1104405.1	-20	3095	7.86	6	730	348	0.61	240	0.188	1.93E-04	36.2	4.8	-66	-8.7	
12	S	345153.5	1103748.1	-20	700	7.2	1	448	20.8	0.055	9.7	0.124	1.30E-04	0.1	12	-64	-9.6	
20	S	344630.5	1101738.2	-30	2165	7.66	3	460	388	0.58				56.8	2.6	-44	-5.2	
21	S	344641.6	1101653.9	-70	713	7.8	2	332	66.8	0.083				24.5	4.2	-60	-9.0	
25	S	345709.6	1102823.7	-58.5	858	8.65	2	596	15.4	0.11	39.4	0.210	7.14E-04	0.1	32	-56	-8.2	
29	S	345802.1	1102022.3	-35	1947	8.22	2	792	263	0.43				1.2	4.1	-46	-5.7	
30	S	345814.5	1101948.8	-40	2013	8.25	3	864	251	0.50	204	0.247	2.27E-04	1.2	4.6	-41	-3.5	Modern
31	S	345050.9	1101846.8	-50	1492	7.78	4	424	274	0.64				1.3	2.4	-51	-7.2	Modern
32	S	345046.4	1101727.6	-50	838	8.24	3	336	90.1	0.066	37.4	0.140	1.16E-04	0.1	4.5	-65	-10.0	
33	S	345037.8	1101536	-70	904	8.17	4	312	137	0.17				0.1	2.9	-60	-9.1	
42	S	345649.4	1104309	-17	6092	7.36	4.7	463	1130	2.22				69.4	2.7	-63	-8.5	
43	S	345612.9	1104240.5	-20	8455	7.94	6.4	269	1690	3.13	289	0.057	4.77E-05	54.5	2.1	-61	-8.1	
57	S	350036.6	1103355.4	-55	879	8.65	5	547	38.1	0.16	24.4	0.082	1.79E-04	36.5	12	-61	-8.3	3200± 1300
58	S	350223.3	1103435	-30	1478	8.6	5.5	680	115	0.30	108	0.200	2.62E-04	105	6.6	-65	-9.4	
62	S	350412.2	1103826.7	-40	1538	8.18	4.7	520	207	0.28				24.4	3.6	-66	-9.0	
65	S	350337.4	1104233.7	-40	2587	7.64	6	648	281	0.67				63.0	4.5	-64	-8.6	
71	S	350058.6	1104616.9	-27	2006	8.27	6	558	314	0.43	168	0.212	1.49E-04	27.0	3.1	-65	-8.6	
74	S	345934.5	1105241	-30	2488	7.83	4.3	644	375	0.91				103	3.4	-65	-8.8	
77	S	350029.4	1105233.2	-40	2534	8.11	5.1	630	487	1.36	192	0.094	1.10E-04	192	2.6	-60	-8.7	
24	I	345488.9	1102713.5	-120	1115	8.33	3	312	187	0.33	47.4	0.089	7.08E-05	0.7	2.9	-68	-10.0	
26	I	345655.8	1102513.4	-110	845	8.55	3	648	15.4	0.077	38.0	0.299	6.88E-04	0.1	33	-64	-8.9	
27	I	345909.1	1102819	-117	865	8.79	4	605	12.4	0.13	49.2	0.343	1.11E-03	0.1	40	-62	-8.5	3900± 1000
40	I	345610.2	1104258.7	-80	4673	7.76	4.8	340	850	1.51	166	0.066	5.45E-05	21.2	2.8	-57	-7.5	Modern
53	I	350334.7	1102309.7	-120	765	8.12	6	389	58.9	0.16				13.5	5.8	-70	-9.8	
55	I	350319.2	1102930.3	-120	5155	7.75	2	148	1510	1.72	39.3	0.017	7.28E-06	33.9	1.6	-74	-10.3	
66	I	350548.4	1104421.7	-100	1007	7.98	5.9	500	42.5	0.12	10.1	0.055	6.66E-05	22.3	11	-66	-9.3	4300± 1200
55a	I	350319.2	1102930.3	-120	3069	7.9	2	415	676	0.83				23.1	2.3	-74	-10.0	
3	D	350144.1	1104435.2	-240	1094	8.2	3	448	72.6	0.16	54.5	0.229	2.10E-04	2.2	7.0	-67	-9.0	7100± 1400
4	D	350140.5	1104301	-270	1313	8.13	4	308	154	0.32	95.4	0.168	1.73E-04	1.4	3.9	-71	-9.9	13600± 1100
6	D	350008.8	1104426	-220	957	8.03	7	444	59.2	0.14	49.5	0.246	2.34E-04	0.4	7.5	-65	-9.0	
7	D	345540.2	1104336.5	-300	1109	7.84	1	264	127	0.28				1.3	3.9	-72	-10.3	
8	D	345421.3	1104226.4	-230	774	8.06	4	332	96.5	0.15	38.0	0.164	1.10E-04	0.9	3.7	-73	-10.3	17400± 2000
22	D	345205.2	1102527.1	-240	733	8.13	2	224	116	0.22				0.3	2.9	-72	-10.8	
23	D	345400.6	1102629.6	-150	601	8.28	4	268	68.7	0.15	22.7	0.100	9.24E-05	0.2	4.1	-66	-10.3	12500± 1100
28	D	345913.7	1102713.8	-210	1808	8.35	5	556	164	0.28	24.8	0.051	4.23E-05	0.9	5.9	-66	-8.6	
35	D	345701.4	1103426.2	-210	1630	8.26	2	208	713	1.09	123	0.061	4.83E-05	2.3	1.6	-69	-10.0	12300±200

*S = Shallow, D = Deep, I = Intermediate, B = Basement

+Calculated using a ^{14}C data in Currell et al., (2010)

Continued..

36	D	345700.5	1103504.3	-250	1630	8.16	2	356	209	0.40	73.6	0.110	9.82E-05	0.6	3.6	-69	-9.9						
37	D	345235.6	1102832.6	-200	1036	8.42	3	220	193	0.35	50.2	0.088	7.26E-05	0.2	2.5	-73	-10.6	21700±600					
39	D	345550.4	1104301.7	-220	1088	7.93	5.5	262	131	0.24	27.7	0.071	5.88E-05	2.4	3.7	-71	-10.2						
41	D	345610.2	1104258.7	-270	1065	8.05	3.6	282	148	0.25	32.0	0.085	6.06E-05	1.7	3.1	-73	-9.9						
44	D	345552.9	1104324.1	-300	1109	8.15	6.2	255	131	0.23	18.6	0.050	3.96E-05	2.5	3.7	-73	-10.3	10400± 800					
46	D	351152.4	1104613.9	-210	667	7.8	6	344	27.9	0.096				29.5	11	-69	-9.5						
47	D	351412.9	1104157.2	-200	526	7.83	6	358	5.0	0.020	16.5	0.234	9.29E-04	11.3	48	-69	-9.7						
48	D	351129.2	1103943.3	-260	608	8.14	6.5	421	8.3	0.049				21.3	36	-64	-8.8						
49	D	351238.6	1103559.4	-260	579	7.9	5.5	316	30.7	0.10	23.5	0.242	2.14E-04	39.7	8.9	-70	-10.1	7500± 2800					
50	D	351008.8	1103346.9	-230	634	8.3	5.5	420	10.8	0.052				22.9	29	-66	-9.1						
51	D	351353.5	1103018.6	-224	561	8.32	6.9	360	12.5	0.046	27.9	0.298	6.22E-04	24.2	22	-66	-9.2						
52	D	350830.8	1102630.3	-280	623	8.15	6.2	430	11.4	0.050				18.0	27	-65	-9.2						
54	D	350211.5	1102601.5	-160	1294	7.94	2.3	615	52.9	0.150	6.5	0.027	3.44E-05	43.5	13	-64	-8.7	18000±1300					
56	D	350006.5	1102946.9	-220	1020	8.61	4.9	685	19.4	0.084	53.4	0.314	7.68E-04	7.1	27	-64	-8.6	8000± 800					
59	D	350710.5	1103303.4	-230	1289	7.8	5.5	272	154	0.23				12.2	3.7	-73	-10.4						
60	D	350435.9	1103049.3	-178	1273	8.57	5.9	566	76.9	0.34	3.8	0.006	1.38E-05	211	8.4	-67	-9.5	9500± 1200					
61	D	350409.8	1103804.7	-180	1236	8.04	6	456	119	0.18	49.9	0.157	1.17E-04	11.0	4.9	-66	-9.0						
63	D	350227.4	1103837.8	-220	1815	8.13	3	186	506	0.71	56.3	0.042	3.11E-05	3.9	1.6	-80	-10.7						
64	D	350029.2	1104016.1	-180	1102	8.1	5.5	434	88.5	0.15	49.9	0.186	1.57E-04	0.5	5.8	-73	-9.7	12800± 2000					
67	D	350731.4	1105031	-202	748	7.97	3.8	398	28.5	0.071	20.1	0.140	1.98E-04	0.3	13	-65	-9.2	3300±2100					
68	D	350540.1	1105145.9	-180	1267	7.93	6	448	117	0.22	42.5	0.107	1.01E-04	1.0	5.1	-64	-9.4						
69	D	350442.7	1105012.4	-200	1107	7.69	2	422	85.3	0.18	26.1	0.087	8.56E-05	1.3	6.0	-67	-9.2						
70	D	350829.2	1104633.9	-230	994	7.57	5.5	356	68.1	0.13	46.1	0.178	1.89E-04	20.5	6.8	-72	-9.5						
72	D	350058.6	1104616.9	-240	1085	7.89	3.3	396	93.0	0.15	32.6	0.117	9.80E-05	0.2	5.4	-70	-9.6	5500±1600					
73	D	350026.7	1104557.5	-180	1156	7.84	3.4	384	133	0.25				0.8	3.9	-72	-9.7						
75	D	345941.8	1105225.8	-320	821	8.17	6.2	336	64.9	0.16	23.8	0.094	1.03E-04	0.9	5.8	-68	-9.5	3500± 1700					
76	D	350041.4	1105214	-230	1251	7.86	4	352	164	0.29				1.8	3.5	-74	-9.9						
78	D	345645.5	1104529.3	-230	868	8.06	4	334	91.3	0.18				1.3	4.3	-66	-9.6						
9	B	345421.3	1104423.4	-347	406	7.55	6	276	5.4	0.040	11.3	0.191	5.90E-04	7.4	25	-64	-9.3	2100± 1000					
10	B	345143.5	1104404.4	-100	380	7.62	4	248	3.8	0.021	3.6	0.144	2.66E-04	0.0	32	-63	-9.2	Modern					
13	B	345109.3	1103719.8	-160	329	7.42	5	208	4.4	0.020	6.8	0.196	4.28E-04	0.0	24	-62	-9.7						
14	B	345041.6	1102620.1	-190	360	7.42	5	164	23.3	0.064				12.1	4.6	-65	-10.1						
15	B	345001	1102513.4	-254	261	7.52	2	148	4.1	0.016	1.8	0.074	1.20E-04	2.5	19	-64	-10.0						
17	B	344740.3	1101930	-75	504	7.8	5	304	9.6	0.047	3.9	0.052	1.12E-04	14.6	18	-62	-9.3						
18	B	344812.4	1102019.9	-130	335	7.75	6	208	5.3	0.013	2.8	0.124	1.49E-04	4.4	19	-58	-9.2	Modern					
19	B	344607.1	1101834.8	-115	440	7.86	5	280	14.5	0.067	4.9	0.063	9.44E-05	11.9	11	-61	-9.0						
R1	Rain	350119.6	1105858.5	na	26	5.78			0.4	0.004	1.7	0.309	1.15E-03	1.95									
R2	Rain	345941.8	1105225.8	na	227				5.1	0.02	7.5	0.198	4.08E-04	64.4									

Table 1. Sample locations, Iodine concentrations and results of various geochemical and isotopic analyses

Location	Groundwater I Concentration (range, µg/L)	I/Cl ratio range (molar)*10^6	Reference
Yuncheng Basin, China	1.8 to 288 (median 38)	7.3 to 1110 (median 116)	This study
Plynlimon Catchment, Wales	0.57 to 8.51		Neal et al., (2007)
Suffolk Chalk, UK	2.5 to 375	6.7 to 77	Heathcote and Lloyd, (1985)
Sussex Chalk, UK	2 to 65	1.2 to 9.7	Lloyd et al., (1982)
Lincolnshire Chalk	8 to 100		Lloyd et al., (1982)
Widnes area, Mersey valley UK		1.4 to 20	Lloyd et al., (1982)
Lincolnshire Limestone, UK	140 to 3200*	0.5 to 695*	Lloyd et al., (1982)
Northern Isreal	<2.5 to 25	≤ 18	Rosenthal and Mates, (1986)
Ocean water	55 to 60	0.7	Fuge and Johnson, (1986)

*High I concentrations attributed to fertilizer pollution

Table 2. I concentrations and I/Cl ratios in groundwater from various regions

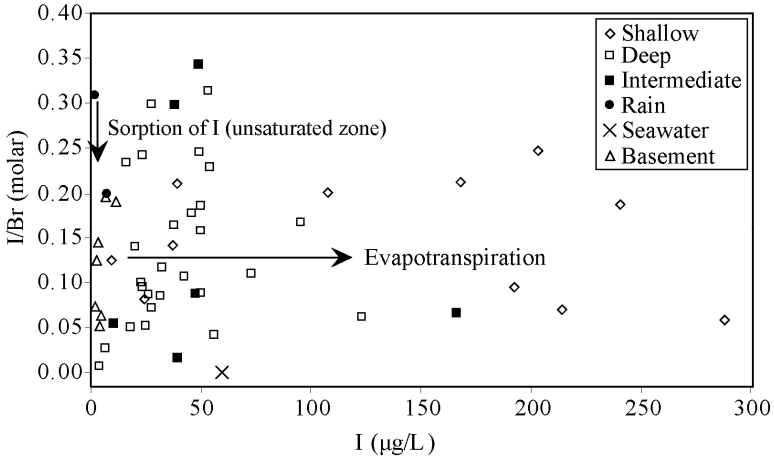

Fig. 3. I/Br ratios and I concentrations in groundwater and rainfall, indicating the influence of evapotranspiration and I sorption.

5.4.2 Iodine, stable isotopes & residence times

In groundwater that has nitrate concentrations <5 mg/L and TDS values <1500 mg/L, that is considered to be free of significant anthropogenic influences, I/Br and I/Cl ratios correlate positively with $\delta^{18}O$ values (r^2 = 0.48 and 0.55, respectively; Fig. 4).

Groundwater samples with NO_3 >5mg/L and/or TDS >1500 mg/L are affected by intensive evapotranspiration and/or contamination by chemical fertilizers; thus I concentrations in this water may not reflect natural delivery of I via rainfall. The deep and intermediate groundwater in the Yuncheng Basin has residence times of between 3 to 22 k.a., and is largely unaffected by anthropogenic disturbance; hence, the trend of increasing I/Br and I/Cl with increasing $\delta^{18}O$ in this groundwater may relate to variable delivery of I in rainfall due to changing atmospheric and/or climatic conditions over the period of groundwater recharge. Changes in soil conditions may also affect delivery of I to the saturated zone, although there is no clearly established link between soil conditions and the $\delta^{18}O$ values of groundwater. There is also a slight increase in I/Br ratios from older (e.g. late Pleistocene aged) to younger (e.g. Holocene aged) groundwater (Fig. 5); which also may relate to atmospheric/climatic changes over these periods.

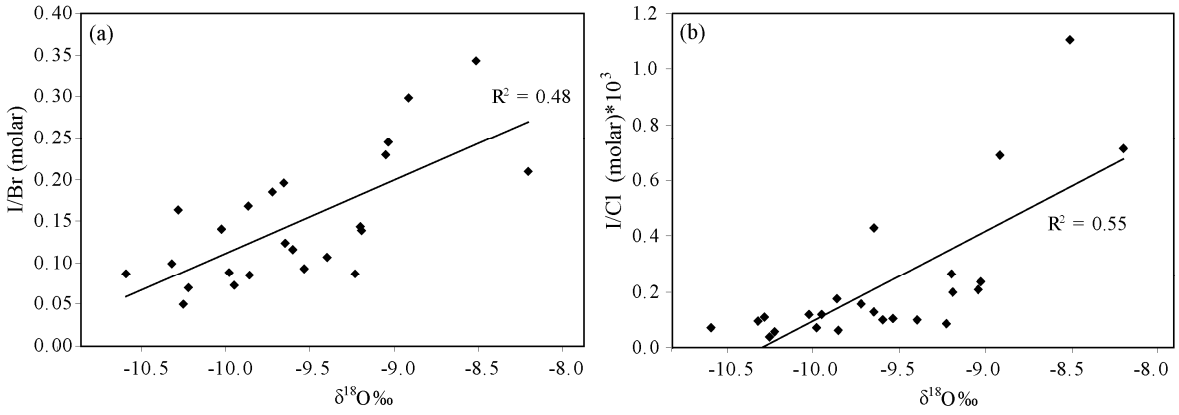

Fig. 4. Variation in I/Br (4a) and I/Cl (4b) ratios vs. $\delta^{18}O$ in groundwater with TDS <1500 mg/L and NO_3 < 5 mg/L.

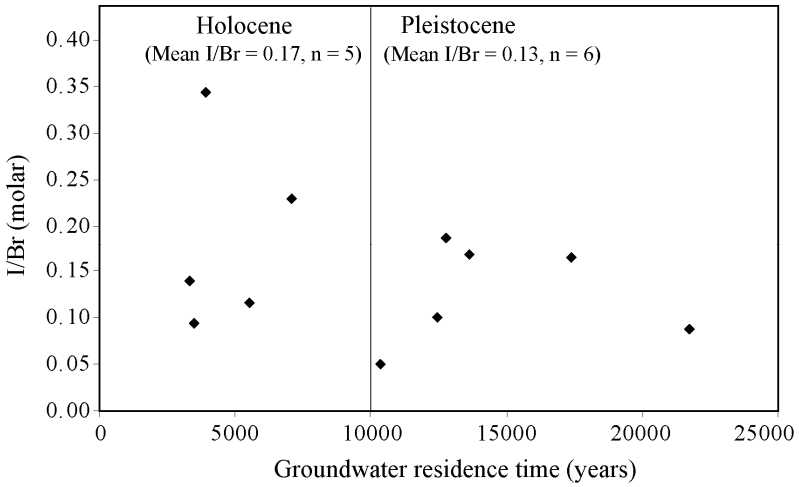

Fig. 5. I/Br vs. residence time in palaeowaters from the Yuncheng Basin

5.5 DISCUSSION

5.5.1 Sources of I in groundwater

In general, the most important source of iodine to groundwater is atmospheric precipitation (Fuge and Johnson 1986; Neal et al., 2007; Gilfedder et al., 2010) and this is probably the case in the Yuncheng Basin. Very few minerals or geological materials contain appreciable levels of iodine, hence weathering is not considered to be a source of I in groundwater except in unusual cases (Lloyd et al., 1982). Some organic-rich sediments, and limestone or chalk rich in marine fossils do contain elevated I (e.g. Lloyd et al., 1982), however, in the Yuncheng basin sediments there is very little organic material and the only fossils are sparse and of terrestrial origin (Liu, 1988). Some fertilizers are enriched in iodine, but this is not a common feature of fertilizer unless the materials used in the manufacture have elevated levels (Fuge and Johnson, 1986), and in any case, the palaeowaters in which I/Br and I/Cl data were examined (e.g. Fig. 4; Fig. 5) are free of any significant influence from fertilizers (Currell et al., 2010). Rainfall during the East Asian monsoon, which is the main source of groundwater and solutes in this basin, and in other

basins in northern China (e.g. Gates et al., 2008, Kreuzer et al., 2009), has thus probably been the main source of I in groundwater.

5.5.2 Iodine and climatic/environmental conditions in northern China

The relatively high I/Cl and I/Br ratios in the Yuncheng Basin compared to groundwater in other regions such as the temperate UK (e.g. Table 2; Lloyd et al., 1982; Heathcote and Lloyd, 1985; Neal et al., 2007) and the arid, continental climate in northern Israel (e.g. Rosenthal and Mates, 1986) may indicate that a relatively large amount of I is delivered by rainfall in this region, via the East Asian summer monsoon. This may relate to the relatively long transport path between the monsoon source regions and the Yuncheng area, which is located ~800 km inland, as I/Cl ratios in rainfall generally increase with distance from the coastline (Duce et al., 1965).

High I contents in rainfall relative to other elements could also relate to the fact that monsoon regions receive rain from relatively warm oceans, where biological productivity is high. The production of organo-iodine compounds by marine organisms such as *Prochlorococcus* is higher in tropical and subtropical regions in the Atlantic and Indian Oceans e.g. latitudes 10°N to 30°N (Smythe-Wright et al., 2006), and this can also be expected to apply to the South China Sea, which is the major source region for the East Asian monsoon (~10°N to 25°N; cf. Yihui and Chan, 2005). If this iodine is converted into soluble forms and incorporated into rainfall (e.g. after photo-oxidation), then rain from these regions would be expected to be relatively I-rich.

Additionally, the high groundwater I/Cl and I/Br ratios relative to other regions may relate to soil characteristics, in particular the sorption capacity of soils. Iodine sorption in

the soil zone by humic material generally removes a significant proportion of the I from infiltrating rain (Fuge and Johnson, 1986; Neal et al., 2007, Fig. 3), however it might be limited in the Yuncheng Basin compared to more temperate areas (e.g. Lloyd et al., 1982; Neal et al., 2007) due to the arid, alkaline soil environment (e.g. Yuncheng regional Water Bureau, 1982). Alkaline conditions in soils (e.g. pH > 7.5) generally cause humus to break down quickly, and elevated pH can prevent I sorption by clay minerals (Fuge and Johnson 1986), which is otherwise highly favoured at near-neutral pH. The alkaline soil environment may also limit degassing of I as I_2 during recharge, conserving larger amounts of I as water reaches the saturated zone.

5.5.3 Iodine, $\delta^{18}O$ and palaeoclimatic variability

Assuming that the sorption capacity of the soils has remained relatively constant over time, the variable I/Br and I/Cl ratios in the palaeowaters from the Yuncheng Basin would reflect past changes in the delivery of I in meteoric precipitation over the past ~22 k.a., as groundwater recharge occurred. The considerable variation in temperatures and intensity of the monsoon over this period (An et al., 2000; Huang et al., 2007), have likely affected the delivery of I to the aquifer, due to the sensitivity of rainfall Iodine concentrations to changes in atmospheric and oceanic conditions (Fuge and Johnson, 1986; Campos et al., 1996; Truesdale and Jones, 1996, Neal et al., 2007). This is consistent with the fact that stable isotope values (which are also sensitive to climatic variables: Clark and Fritz, 1997) correlate with I/Br and I/Cl ratios in the groundwater that is unaffected by modern agriculture (Fig. 4 and Fig. 5).

As noted above, differences in groundwater $\delta^{18}O$ values in the Yuncheng Basin were largely controlled by variations in temperatures that were experienced during the late Pleistocene and Holocene (Chen et al., 2003; Edmunds et al., 2006; Currell et al., 2010). Temperature variations may also have affected marine production of I (e.g. Oram and Penkett, 1994; Smythe-Wright et al., 2006), which may be responsible for the higher I/Br and I/Cl ratios in groundwater with high $\delta^{18}O$ values. The concentration of I in mixed ocean water is relatively constant, between ~55 and 60 μg/L, however, I is concentrated relative to Cl in rainfall and atmospheric aerosols (e.g., Duce et al., 1965; Fuge and Johnson 1986; Table 2). In part, this is due to photolytic production of methyl iodide at the ocean surface and photooxidation of organoiodines (Carpenter, 2003). However, a substantial amount of I transferred into the atmosphere from the oceans also derives from emissions from a range of marine organisms such as algae (e.g. kelp), and plankton (e.g. *Prochlorococcus*), which produce gaseous iodine as methyl iodide, diiodomethane, iodide and I_2 (Whitehead, 1984; O'Dowd et al., 2002; Smythe-Wright et al., 2006; Küpper et al., 2008). This is probably a mechanism to defend against cell damage by oxidants such as ozone (Küpper et al., 2008). Greater amounts of methyl iodide are produced at the ocean surface seasonally, during warm months (e.g. Oram and Penkett, 1994; Campos et al, 1996), and biological production of iodine in all forms is greater over the warmer tropical and sub-tropical oceans than cooler regions (e.g. >40°N, Smythe-Wright et al., 2006). Hence, if this I is subsequently converted to soluble forms and incorporated in rainfall, then the correlations between groundwater I/Br, I/Cl and $\delta^{18}O$ data are consistent with variable biological production of I, mediated by ocean temperatures, being a control on the flux of I from the oceans to the continents. According to this mechanism, periods of warm

conditions would be expected to have increased the supply of Iodine into the atmosphere, rainfall and groundwater. This may apply not just to the regions affected by the East Asian summer monsoon, but potentially also the Indian monsoon and other tropical and subtropical regions, where gaseous I production by marine organisms is a significant process (Smythe-Wright et al., 2006). This has implications for global climate models, as there is evidence that marine iodine production may play a role in climate feedback mechanisms via the formation of cloud condensation nuclei and other aerosols in the atmosphere (O'Dowd et al., 2002; Smythe-Wright et al., 2006).

The broad increase in groundwater I/Br ratios from the late Pleistocene to mid-Holocene aged groundwater (Fig. 5) may also correspond to the increase in temperatures experienced in northern China in this period (e.g. Fig. 2; Edmunds et al., 2006; Huang et al., 2007). The correlation between groundwater ages and I/Br ratios (Fig. 5) is, however, relatively weak compared to the correlation between $\delta^{18}O$ and I/Br (and I/Cl) ratios (Fig. 4). This may reflect the fact the residence times lack precision beyond +/- hundreds of years (Table 1), and that there would have been numerous temperature variations on seasonal, decadal and century-long time scales over the period of recharge. If I production from biological sources was indeed increased during warm periods, as suggested, then temperature variations would have affected I/Br, I/Cl and $\delta^{18}O$ directly (hence the relatively strong positive correlations between these data; Fig. 4.), whereas the relationship between age and temperature (Fig. 2b) is indirect, relating to regional climatic variation over 1000s of years.

An additional control on I contents in rainfall may be the intensity of precipitation, as in some cases I concentrations decrease with increasing precipitation on a given day (e.g.

Truesdale and Jones, 1996). Hence, another factor that could explain the relationship between I/Br and $\delta^{18}O$ values is that heavier rain events (e.g. during a more intense monsoon) may have reduced both the $\delta^{18}O$ values (e.g. Kreuzer et al., 2009) and delivery of I from rainfall. This could occur via dilution of I in cloud water (which contains a relatively large amount of I, cf. Neal et al., 2007) by condensate water en-route to the ground, and/or washout of iodine from the atmosphere during prolonged rainfall (Fuge and Johnson, 1986). However, the relationship between rainfall intensity and I concentrations is not a linear one, above a certain threshold value of precipitation (~10mm/day) the relationship breaks down (Truesdale and Jones, 1996), suggesting that this effect is likely minimized in the Yuncheng Basin, as recharge generally only occurs during heavy rain events. Also, dilution of I by condensate water would not be expected to affect I/Cl and I/Br ratios, as heavy rainfall generally causes dilution of all species in rain, not just iodine (Truesdale and Jones, 1996). Hence, the effect of rainfall intensity on delivery of I into groundwater relative to other elements is probably relatively minor in comparison to the effect of temperature.

While the chemistry of I during transport from oceans to atmosphere and from atmosphere to rainfall is clearly complex and not yet fully understood (Carpenter, 2003), the correlations between I/Br, I/Cl and $\delta^{18}O$ values in the groundwater from the Yuncheng Basin are indicative of a link between I and palaeoclimate, particularly palaeo-temperatures. Further analysis of I data from groundwater with a range of residence times from a range of climatic/geographical settings may further clarify this relationship.

5.6 CONCLUSIONS

Total Iodine concentrations in groundwater from the Yuncheng Basin are generally high relative to other regions where iodine has been measured in groundwater. This partly reflects the large degree of evapotranspiration that the groundwater is subject to in the area, particularly shallow groundwater. However, additionally, I/Cl ratios are elevated in comparison to groundwater from other regions (e.g. temperate climatic zones). This indicates that a relatively large amount of I is delivered by the East Asian summer monsoon and/or that the degree of sorption of I that occurs in the unsaturated zone is limited due to the arid, alkaline soils in northern China.

In groundwater that is unaffected by anthropogenic influence (e.g. contamination by fertilizers), I/Br and I/Cl ratios increase with increasing $\delta^{18}O$ values. This indicates that a relatively large amount of I has been delivered during warm climates. This may relate to greater levels of biological production of gaseous iodine compounds when the oceans have been warmer by marine organisms such as algae and picoplankton, which has been delivered into rainfall and groundwater. The results of this study indicate that iodine concentrations, and in particular I/Br and I/Cl ratios, in groundwater recharged over thousands of years in the region are responsive to changes in past climatic conditions. If variations in the flux of biological iodine produced in the sub-tropical and tropical oceans have indeed varied under the influence of temperatures over 1000s of years, then there are significant implications for palaeoclimate reconstruction and present-day climate models. As far as we are aware, this is the first time that the iodine content of palaeowaters has been investigated as an indicator of palaeoclimatic variation.

Acknowledgements

We would like to thank the PlasmaChem community and specifically Greg O'Neill, from the Australian Water Quality Centre, for sharing their knowledge on the Iodine ICPMS analytical method. This research program was partly initiated through and greatly supported by the Australia-China Water Resources Research Centre, including Dr. Deli Chen, Dr. Yongping Wei, Prof. Song Xianfang and Prof. Li Baoguo. Special thanks also to the Yuncheng City Water Resources Service Bureau, in particular Mr. Sun Xinzhong. Logistical support was also given by the Yongji, Linyi and Yuncheng county Water Resource Bureaus, and Dr. Han Dongmei

References

An, Z., Porter, S.C., Kutzbach, J.E., Wu, X., Wang, S., Liu, X., Li, X., Zhou, W., 2000. Asynchronous Holocene optimum of the East Asian monsoon. Quaternary Science Reviews 19, 743-762.

Andersen, S., Petersen, S.B., Laurberg, P., 2002. Iodine in drinking water in Denmark bound in humic substances. European Journal of Endocrinology 147, 663-670.

Andersen, S., Laurberg, P., 2009. The nature of Iodine in drinking water. In: *Comprehensive handbook of Iodine* (V.R. Preedy, G.N. Burrow, R. Watson eds) Elsevier, pp 125 to 134.

Campos M.L.A.M., Nightingale, P.D., Jickells, T.D., 1996. A comparison of methyl iodide emissions from seawater and wet depositional fluxes of iodine over the southern North Sea. Tellus 48B, 106-114.

Cao, X.H., 2005. Study of the intermediate and deep layers of the Sushui River Basin confined groundwater system. In: *Shanxi Hydrotechnics Bulletin No. 3.* China Academic Journal Electronic Publishing House. pp 41-43. (In Chinese)

Carpenter, L.J., 2003. Iodine in the marine boundary layer. Chemical Reviews 103, 4953-4962.

Chen, Z.Y., Qi, J.X., Xu, J.M., Xu, J.M., Ye, H., Nan, Y.J., 2003. Palaeoclimatic interpretation of the past 30 ka from isotopic studies of the deep confined aquifer of the North China plain. Applied Geochemistry 18, 997-1009.

China Geological Survey, 2006. Groundwater resources and environmental issues assessment in the six major basins of Shanxi (in Chinese), China Geological Survey Special publication, Beijing. 98p.

Clark, I., Fritz, P., 1997. Environmental Isotopes in Hydrogeology. Lewis Publishing, New York. 328p.

Currell, M.J., Cartwright, I., Bradley, D.C., Han, D.M., 2010. Recharge history and controls on groundwater quality in the Yuncheng Basin, north China. Journal of Hydrology 385, 216-229.

Dean, G.A., 1963. The iodine content of some New Zealand drinking waters with a note on the contribution of sea spray to the iodine in rain. New Zealand Journal of Science 6**,** 206-214.

Duce, R.A., Winchester, J.W., Van Nahl, T.W., 1965. Iodine, bromine and chlorine in the Hawaiian marine atmosphere. Journal of Geophysical Research 70, 1775-1799.

Edmunds, W. M., Ma, J., Aeschbach-Hertig, W., Kipfer, R., Darbyshire, D. P. F., 2006. Groundwater recharge history and hydrogeochemical evolution in the Minqin Basin, North West China. Applied Geochemistry 21, 2148-2170.

Fuge, R., Johnson, C.C., 1986. The geochemistry of iodine – a review. Environmental Geochemistry and Health 8(2), 31-54.

Gates, J.B., Edmunds, W.M., Darling, W.G., Ma, J., Pang, Z., Young, A.A., 2008. Conceptual model of recharge to southeastern Badain Jaran Desert groundwater and lakes from environmental tracers. Applied Geochemistry 23, 3519 - 3534.

Gilfedder, B.S., Petri, M., Wessels, M., Biester, H., 2010. An iodine mass-balance for Lake Constance, Germany: Insights into iodine speciation changes and fluxes. Geochimica et Cosmochimica Acta 74, 3090-3111.

Heathcote, J.A., Lloyd, J.W., 1985. Groundwater chemistry in southeast Suffolk (U.K.) and its relation to Quaternary Geology. Journal of Hydrology 75, 143-165.

Huang, C.C., Pang, J., Zha, X., Su, H., Jia, Y., Zhu, Y., 2007. Impact of monsoonal climatic change on Holocene overbank flooding along Sushui River, middle reach of the Yellow River, China. Quaternary Science Reviews 26, 2247-2264.

Intergovernmental Panel on Climate Change (2007) Couplings Between Changes in the Climate System and Biogeochemistry (Chapter 7). In: Solomon, S., Qin, M., Manning, Z., Chen, Z., Marquis, M., Averyt, K.B., Tignor, M., Miller, H.L. (eds), *Climate Change 2007: The Physical Science Basis. Contribution of Working Group I to the Fourth Assessment Report of the Intergovernmental Panel on Climate Change.* Cambridge University Press, Cambridge, UK, pp 499-588.

International Atomic Energy Association/World Meteorological Organisation, 2007. Global Network of Isotopes in Precipitation. The GNIP database. Accessible at http://isohis.iaea.org.

Johnson, K.R., Ingram, B.L., 2004. Spatial and temporal variability in the stable isotope systematics of modern precipitation in China: implications for paleoclimatic reconstructions. Earth and Planetary Science Letters 220, 365-377.

Kreuzer, A.M., Rohden, C.V., Friedrich, R., Chen, Z., Shi, J., Hajdas, I., Aeschbach-Hertig, W., 2009. A record of temperature and monsoon intensity over the past 40 kyr from groundwater in the North China Plain. Chemical Geology 259, 168-180.

Küpper FC, Carpenter LJ, McFiggans GB, Palmer CJ, Waite TJ, Boneberg E-M, Woitsch S, Weiller M, Abela R, Grolimund D, Potin P, Butler A, Luther III GW, Kroneck PMH, Meyer-Klaucke W, Feiters MC., 2008. Iodide accumulation provides kelp with an inorganic antioxidant impacting atmospheric chemistry. Proceedings of the National Academy of Science 105, 6954-6958.

Liu T.S. (1988) Loess in China, 2nd Edition. China Ocean Press, Beijing. 224p.

Lloyd, J.W., Howard, K.W.F., Pacey, N.R., Tellam, J.H., 1982. The value of iodide as a parameter in the chemical characterization of groundwaters. Journal of Hydrology 57, 247-265.

McFiggans, G., Coe, H., Burgess, R., Allan, J., Cubison, M., Alfarra, M.R., Saunders, R., Saiz-Lopez, A., Plane, J.M.C., Wevill, D.J., Carpenter, L.J., Rickard, A.R., Monks, P.S., 2004. Direct evidence for coastal iodine particles from Laminaria macroalgae – Linkage to emissions of molecular iodine. Atmospheric Chemistry and Physics 4, 701-713.

Moran, J.E., Oktay, S.D., Santschi, P.H., 2002. Sources of iodine and iodine 129 in rivers. Water Resources Research 38(8), 1149-1158.

Neal, C., Neal, M., Wickham, H., Hill, L., Harman, S., 2007. Dissolved iodine in rainfall, cloud, stream and groundwater in the Plynlimon area of mid-Wales. Hydrology and Earth System Sciences 11(1), 283-293.

O'Dowd, C.D., Jimenez, J.L., Bahreini, R., Flagan, R.C., Seinfeld, J.H., Hameri, H., Pirjola, L., Kulmala, K., Jennings, S.G., Hoffmann, T., 2002. Marine aerosol formation from biogenic iodine emissions. Nature 417, 632-636.

Oram, D.E., Penkett, S.A., 1994. Observations in Eastern England of elevated methyl iodide concentrations in air of Atlantic origin. Atmospheric Environment 28, 1159-1174.

Rozanski, K., Araguas-Araguas, L., Gonfiantini, R., 1993. Isotopic patterns in modern global precipitation. In: Swart, P.K., Lohmann, K.C., McKenzie, J., Savin, S. (eds.), *Climate Change in Continental Isotopic Records. AGU Geophys. Monograph Series.* American Geophysical Union, Washington, DC, pp.1-36.

Rosenthal, E., Mates, A., 1986. Iodine concentrations in groundwater of northern Isreal and their relation to the occurrence of goiter. Applied Geochemistry 1, 591-600.

Saiz-Lopez A., Plane, J.M.C., 2004. Novel iodine chemistry in the marine boundary layer. Geophysical Research Letters 31, L04112.

Scanlon, B.R., Keese, K.E., Flint, A.L., Flint, L.E., Gaye, C.B., Edmunds, W.M., Simmers, I., 2006. Global synthesis of groundwater recharge in semiarid and arid regions. Hydrologic Processes 20, 3335-3370.

Smythe-Wright, D., Boswell, S.M., Breithaupt, P., Davidson, R.D., Dimmer, C.H., Diaz, L.B.E., 2006. Methyl iodide production in the ocean: Implications for climate change. Global Biogeochemical Cycles 20, GB3003.

Truesdale, V.W., Jones, S.D., 1996. The variation of iodate and total iodine in some UK rainwaters during 1980-1981. Journal of Hydrology 179, 67-86.

Whitehead, D.C., 1984. The distribution and transformations of iodine in the environment. Environment International **10**, 321-339.

Yamanaka, T., Shimada, J., Hamada, Y., Tanaka, T., Yang, Y., Zhang, W., Hu, C.S., 2004. Hydrogen and oxygen isotopes in precipitation in the northern part of the North China Plain: climatology and inter-storm variability. Hydrologic Processes 18, 2211-2222.

Yihui, D., Chan, J.C.L., 2005. The East Asian summer monsoon: an overview. Meteorology and Atmospheric Physics 89, 117-142.

Yokoo, Y., Nakano, T., Nishikawa, M., Quan, H., 2004. Mineralogical variation of Sr-Nd isotopic and elemental compositions in loess and desert sand from the central Loess Plateau in China as a provenance tracer of wet and dry deposition in the northwestern Pacific. Chemical Geology 204, 45-62.

Yuncheng Regional Water Bureau & Shanxi Geological Survey, 1982. Hydrological and Geological maps and explanations for the Yuncheng region, 1:100000, Shanxi Geological Survey Special Report (In Chinese). 80p.

Chapter 6

Conclusions, Major findings & Implications

6.1 OVERVIEW

This thesis represents the first comprehensive geochemical study of groundwater in the Yuncheng Basin, and one of few such studies to be carried out in northern China, where groundwater is one of the most important resources supporting people's livelihoods. The findings of this work have implications for the local area and the broader north China region, where 100s of millions of people depend upon groundwater to supply domestic and irrigation water. This work has provided information on groundwater recharge, including timing, rates & mechanisms; controls on groundwater quality, including understanding hydrogeochemical evolution, sources of contamination and causes of enrichment of toxic elements; and relationships between groundwater and regional and global palaeoclimate.

6.2 MAJOR FINDINGS OF THIS RESEARCH

6.2.1 Recharge history and controls on groundwater quality:

- Deep groundwater in the Quaternary aquifer of the Yuncheng Basin is palaeowater, with residence time ranging between ~3,500 and 22,000 years. Shallow groundwater has modern residence time or contains a significant component of modern water.

- Shallow groundwater $\delta^{18}O$ and $\delta^{2}H$ values are similar to precipitation during the East Asian summer monsoon, indicating recharge via direct infiltration. Deep groundwater $\delta^{18}O$ and $\delta^{2}H$ values are lower than modern precipitation, implying recharge during a cooler and/or wetter climate than the present. $\delta^{18}O$ and $\delta^{2}H$ values increase from old to young groundwater, due to increasing temperatures from the late Pleistocene into the Holocene.
- The vertical recharge rate calculated using age/depth relationships is ~1 to 10mm/year. This is lower than the recharge rate estimated using tritium in soil profiles nearby (~60 mm/yr; Lin and Wei, 2006). This may indicate that vertical infiltration has increased in recent decades compared to historic times due to land-use changes (e.g. land clearing).
- Regional groundwater flow was historically from east to west, towards the Yellow River. Groundwater flow directions have been changed by pumping; deep groundwater now flows towards a cone of depression to the west of Yuncheng city.
- Shallow groundwater quality is heavily influenced by agriculture; it has high nitrate and TDS concentrations. The main source of nitrate is synthetic fertilizer; elevated TDS contents likely result due to intensive transpiration in the shallow subsurface below irrigated areas.
- Deep groundwater (>180m depth) also locally contains high concentrations of agricultural nitrate, particularly near the Linyi fault, where preferential leakage occurs via fractures. Intermediate depth groundwater (80 to 120m) has TDS and nitrate concentrations that are intermediate between shallow and deep groundwater,

indicating gradual vertical mixing and homogenization of chemistry, due to high rates of deep groundwater pumping.

6.2.2 Major ion chemistry, $\delta^{13}C$ and $^{87}Sr/^{86}Sr$ and hydrochemical evolution:

- Based on comparison of Br and Cl concentrations in rainfall and groundwater, evapotranspiration in shallow groundwater has concentrated solutes by factors of >100. Natural evapotranspiration during recharge also concentrated solutes in the deep groundwater by factors of ~5 to 50 prior to agricultural development. Rainfall has thus always been an important source of solutes in groundwater in the region.
- $^{87}Sr/^{86}Sr$, $\delta^{13}C$ and major ion data indicate that carbonate weathering is also a significant process and source of groundwater solutes. Both congruent and incongruent weathering of calcite and dolomite occur; dissolution occurs both during recharge (under an open system) and in the aquifer under a closed system.
- Despite the evidence of carbonate dissolution, groundwater is generally Ca-poor and Na-rich. This indicates substantial modification of major ion chemistry by cation exchange (between Ca and Na). This may occur in clay lenses that are layered throughout the aquifer.

6.2.3 Fluoride and Arsenic in groundwater

- Groundwater from a range of locations and depths in the Yuncheng Basin has fluoride and/or arsenic concentrations that are above World Health Organisation drinking water guidelines (1.5 mg/L and 10 μg/L, resepectively), posing a health risk in areas where groundwater is used for domestic supply.

- Groundwater F and As concentrations correlate positively, the correlation is strongest when normalized for salinity (e.g. F/Cl vs. As/Cl). This indicates a common source or common enrichment mechanism for F and As.
- The mechanism of enrichment is likely desorption of F^- and $HAsO_4^{2-}$ from Fe, Al and Mn oxides in the aquifer matrix. Groundwater major ion composition plays an important role in mobilisation; F and As concentrations correlate positively with Na/Ca ratios, pH values and HCO_3 concentrations. Experiments with sediments from the basin show that more F and As were mobilized when sediments are reacted with Na-rich, Ca-poor water compared to Ca-rich water.
- Groundwater with high F and As concentrations is found in analogous environments globally, in basins with similar sediments (Quaternary loess) and similar groundwater chemistry (e.g. high Na/Ca ratios and pH). The enrichment mechanism described may thus be important globally.

6.2.4 Palaeoclimate and groundwater Iodine contents

- Iodine concentrations and I/Cl ratios in groundwater from the Yuncheng Basin are generally high compared to other regions. This could be because the East Asian Summer monsoon delivers large amounts of marine Iodine to the Asian continent; and/or that sorption of I in the soil zone is limited in the Yuncheng region due to the arid, alkaline soils.
- In deep palaeowaters that are unaffected by agriculture, I/Cl and I/Br ratios correlate positively with $\delta^{18}O$ values. This indicates that relatively large amounts of

I were delivered in rainfall during warmer climates and that this I has been preserved in the palaeowaters of the Yuncheng Basin.

- Greater amounts of marine I incorporated into rainfall during warm climates may reflect increased biological production of gaseous I compounds (e.g. I_2, CH_3I and CH_2I_2) by marine algae and cyanobacteria in warmer oceans.

6.3 IMPLICATIONS FOR GROUNDWATER MANAGEMENT

The findings of this research have significant implications for the management of groundwater and agriculture in the Yuncheng Basin and many of these apply to other regions in northern China:

- Deep groundwater in the Yuncheng Basin is being extracted at rates that far exceed the natural recharge rate. A decrease in yields, and/or drying up of wells will result if pumping rates are not reduced, and the cone of depression will increase in size.
- Recharge of the shallow aquifer is occurring, but the water quality is heavily impacted by agriculture; it has high nitrate and TDS concentrations due to over-use of chemical fertilizers and evapotranspiration of water used in flood irrigation. To alleviate this, levels of fertilizer application should be reduced; this applies to many agricultural areas in China. Alternative irrigation practices (e.g. using covered irrigation channels, reducing irrigation volumes) and planting of different crop types may reduce nitrate contamination and salinisation of shallow groundwater (e.g. Li et al., 2007; Hu et al., 2008; Wei et al., 2009).
- Deep groundwater quality is threatened by vertical mixing; mixing has already affected deep groundwater quality near the Linyi fault and E'mei Plateau, and will

likely affect deep groundwater throughout the basin in future. Pumping may need to be restricted to prevent declining quality in the deep palaeowaters, particularly in the vicinity of fault/fracture zones.

- The use of groundwater for domestic supply is already limited in areas (e.g. Kaolao) due to high F concentrations. Use of groundwater for drinking in the Yuncheng Basin will be less feasible in the future as agriculture continues to impact groundwater quality, and as groundwater with high F and As concentrations spreads to new areas under the influence of pumping. If groundwater TDS and concentrations of toxic elements continue to increase, then use of groundwater for irrigation may soon be jeopardised, meaning that alternative water supplies and/or types of agriculture will need to be adopted.

6.4 FUTURE MONITORING AND RESEARCH

6.4.1 The need for monitoring

- This research was based largely on two groundwater sampling campaigns in 2007 and 2008. It is thus not possible to provide information on changes over time in groundwater chemistry or physical hydrogeology in the Yuncheng Basin. Given the issues that have been identified and the dependence of the region on groundwater, periodic monitoring of groundwater geochemical data is warranted.
- The most pressing concerns that warrant monitoring are high groundwater nitrate, fluoride and arsenic concentrations, which given the risks to health, should be continually monitored. As such, there is no publicly available data on the spatial

distribution of concentrations of these toxic elements in the Yuncheng Basin, or changes in concentrations over time; this is a major deficiency.

- Monitoring and reporting of basic chemical data (e.g. TDS, pH, DO) and groundwater levels would also aid agricultural management decisions and allow further research to be carried out to address local issues within the basin (e.g. water supply and quality issues).

6.4.2 Future research questions:

- At what rate is mixing of shallow and deep groundwater occurring in different regions? What is the extent of preferential leakage near the Linyi fault; can groundwater management be modified to reduce leakage? To what extent and at what rates are nitrate concentrations changing over time; is there natural attenuation of nitrate via de-nitrification in the soil? Further major ion data and stable isotope analysis (e.g. $\delta^{18}O$; $\delta^{15}N$) of groundwater and soil water in nested bore sites would allow these questions to be addressed.
- Can the process of shallow groundwater salinisation be characterised in more detail? Is transpiration the dominant process, as is broadly indicated by the groundwater $\delta^{18}O$ data, or does a combination of evaporation and transpiration occur? What are the critical depths of water table at which transpiration becomes intensive and does this vary depending on crop/plant type? Can planting different crop types lead to a reduction in evapotranspiration? These questions could be answered by stable isotope analysis of soil water along depth profiles (e.g. Barnes and Allison, 1988), and crop planting trials.

- Are recharge rates calculated using ^{3}H by Lin and Wei, (2006) and ^{14}C in this study representative of modern and historic recharge rates in the region? Additional estimates of recharge from a range of localities, using the same and/or additional techniques (e.g. chloride mass balance), could clarify this (e.g. Wood and Sanford, 1995; Scanlon et al., 2002). Study of the timing and extent of land-use changes, irrigation practices and rainfall patterns may also help to delineate reasons for increased recharge in modern times and factors that control recharge rates.
- Can the sources of carbon in the Yuncheng Basin and other aquifers in northern China be further constrained? Blaser et al., (2010) put forward a ^{14}C age correction model accounts for variations in pCO_2 related to palaeoclimatic fluctuations; if past climate can be better defined and greater characterisation of C sources can be achieved, then better age estimates may be able to be attained.
- Can groundwater F and As enrichment processes be better characterised? Questions remain as to the exact primary source of F and As in the aquifer sediments, e.g., are certain horizons or types of loess richer/poorer in these elements? Do characteristics of loess and palaeosols (e.g. mineralogy, grain size) influence the amounts of F and As that are mobilized? More targeted sampling of sediments from a range of depths and detailed geochemical analysis (e.g. sequential leaching) could address these questions.
- Are changes in groundwater chemistry that affect F and As mobilization (e.g. Na and Ca contents; pH) related only to natural processes, or is groundwater chemistry affected by pumping? For example, transient conditions or mixing may be favourable to cation exchange, increasing Na/Ca contents and mobilizing F and As

into groundwater (e.g. McNab et al., 2009). Monitoring changes in these chemical parameters over time could resolve this and help predict future spatial and temporal trends in groundwater F and As concentrations. Based on understanding the factors that lead to F and As enrichment, vulnerability modeling could be applied, taking into account relevant risk factors (e.g. Guo et al., 2007)

- What can Iodine concentrations I/Cl and I/Br ratios in groundwater reveal about palaeoclimate? Is the increase in I/Cl and I/Br ratios along with increasing $\delta^{18}O$ a widespread phenomenon in palaeowaters globally? What does this indicate about links between temperature, biological productivity in the oceans and atmospheric processes? How do cloud forming processes and rainfall intensity affect delivery of I in rainfall in different regions? Sampling of rainfall and groundwater from a range of climatic regions and analysis of I concentrations, along with $\delta^{18}O$ and residence times could help to answer these questions and refine the relationships between iodine, palaeo-hydrology and climate.

References

Barnes, C.J., Allison, G.B., 1988. Tracing of water movement in the unsaturated zone using stable isotopes of hydrogen and oxygen. Journal of Hydrology 100, 143-176.

Blaser, P.C., Coetsiers, M., Aeschbach-Hertig, W., Kipfer, R., Van Camp, M., Loosli, H.H., Walraevens, K., 2010. A new groundwater radiocarbon correction approach accounting for palaeoclimate conditions during recharge and hydrochemical evolution: The Ledo-Paniselian Aquifer, Belgium. Applied Geochemistry 25, 437-455.

Guo, Q., Wang, Y., Gao, X., Ma, T., 2007. A new model (DRARCH) for assessing groundwater vulnerability to arsenic contamination at basin scale: a case study in Taiyuan basin, northern China. Environmental Geology 52, 923-932.

Hu, K.L., Li, B, Chen, D., Zhang, Y., Edis, R., 2008. Simulation of nitrate leaching under irrigated maize on sandy soil in desert oasis in Inner Mongolia, China. Agricultural Water Management 95, 1180-1188.

Li, Y., White, R., Chen, D., Zhang, J., Li B., Zhang, Y., Huang, Y., Edis, R., 2007. A spatially referenced water and nitrogen management model (WNMM) for (irrigated) intensive cropping systems in the North China Plain. Ecological Modelling 203, 395-423.

Lin, R., Wei, K., 2006. Tritium profiles of pore water in the Chinese loess unsaturated zone: Implications for estimation of groundwater recharge. Journal of Hydrology 328, 192-199.

McNab Jr., W.W., Singleton, M.J., Moran, J.E., Esser, B.K., 2009. Ion exchange and trace element surface complexation reactions associated with applied recharge of low-TDS water in the San Joaquin Valley, California. Applied Geochemistry 24, 129-197.

Scanlon, B.R., Healey, R.W., Cook, P.G., 2002. Choosing appropriate techniques for quantifying groundwater recharge. Hydrogeology Journal 10, 18-39

Wei, Y., Chen, D., Hu, K., Willett, I.R., Langford, J. 2009. Policy incentives for reducing nitrate leaching from intensive agriculture in desert oases of Alxa, Inner Mongolia, China. Agricultural Water Management 96, 1114-1119.

Wood, W.W., Sanford, W.E., 1995. Chemical and isotopic methods for quantifying ground-water recharge in a regional, semiarid environment. Ground Water 33, 458-468.

[This page is intentionally left blank]

Appendix A

List of publications & conference abstracts

The following is a list of first author and co-authored publications that arose directly or indirectly from this research, including 3 peer-reviewed journal articles (Currell et al., 2010a; Han et al., 2010a; Han et al., 2010b); two peer-reviewed conference papers (Currell et al., 2008a; Bradley et al., 2008), and four conference abstracts (Currell et al., 2008b; Currell et al., 2009a; Currell et al., 2009b; Bradley et al., 2009). Electronic copies of these publications are included on the attached data DVD (see Appendix B)

References

Currell, M.J., Cartwright, I., Bradley, D.C., Han, D.M., 2010. Recharge history and controls on groundwater quality in the Yuncheng Basin, north China. Journal of Hydrology **385**, 216-229.

Han, D.M., Liang, X., Jin, M.G., **Currell, M.J.,** Song X.F., Liu, C.M., 2010a. Evaluation of groundwater hydrochemical characteristics and mixing behavior in the Daying and Qicun geothermal systems, Xinzhou Basin. Journal of Volcanology and Geothermal Research **189**, 92-104.

Han, D.M., Liang, X., **Currell, M.J.**, Chen, Z., Song, X., Han, Y. 2010b. Environmental isotopic and hydrochemical characteristics of groundwater systems in Daying and Qicun Geothermal fields, Xinzhou Basin, Shanxi, China. Hydrologic Processes, *in press* doi: http://dx.doi.org/10.1002/hyp.7742

Currell, M.J., Cartwright, I., Bradley, D.C., 2008a. Environmental isotopes as indicators of groundwater age, recharge environment and sustainability in the Yuncheng Basin, north China. Proceedings of the 36th IAH Congress, Toyama Japan. 8p.

Currell, M.J., 2008b. Geochemistry of groundwater with high fluoride concentrations in the western Yuncheng Basin, north China. Victorian Universities Earth and Environmental Sciences conference abstracts, University of Melbourne, Australia.

Bradley, D., Cartwright, I., **Currell, M.**, Chen, D., Liang, S., 2008. Nitrate pollution associated with recent agricultural development in Northern China. Proceedings of the 36th IAH Congress, Toyama Japan. 9p.

Currell, M.J., Cartwright, I., Bradley, D.C., Han, D. 2009a. $\delta^{13}C$, $\delta^{34}S$, $^{87}Sr/^{86}Sr$ and major ion chemistry as indicators of groundwater geochemical evolution in the Yuncheng Basin, China. 8th International Symposium on Applied Isotope Geochemistry abstracts, 21.

Currell, M.J., Cartwright, I., Bradley, D.C., Han, D., 2009b. Groundwater age, recharge history, quality, and vertical interaction in the Yuncheng Basin, north China. Victorian Universities Earth and Environmental Sciences conference abstracts, Monash University, Australia

Bradley, D., Cartwright, I., **Currell, M.J.,** Chen, D., Liang, S. 2009. Use of $\delta^{15}N$, $\delta^{18}O$ and $\delta^{13}C$ to determine the source of nitrate pollution in Inner Mongolia, China. 8th International Symposium on Applied Isotope Geochemistry abstracts, 13.

Appendix B

Supplementary data DVD notes

The DVD attached with this thesis contains data supplied by the Shanxi branch of the China Geological Survey, including the following:

- Groundwater elevation contour map (shallow unit)
- Groundwater elevation contour map (deep unit)
- Climate data from 1980 to 2004 (rainfall, potential evaporation)
- Drill logs from selected groundwater bores
- Location map of bores where drill logs were completed

The data are largely in mandarin Chinese; an English translation of relevant terms is provided where possible.

The DVD also contains the electronic copies of publications and conference abstracts listed in Appendix A.